Faculty of Medicine and Health Sciences

School of Medicine

Investigating the Role of Cten in Metastatic Colorectal Cancer

Hannah Thorpe

May 2016

Thesis submitted to the University of Nottingham for the

Degree of Doctor of Philosophy

Declaration

This report entitled 'Investigating the Role of Cten in Metastatic Colorectal Cancer**'** has been composed by Hannah Thorpe, and I confirm that the work presented in this thesis is my own, unless otherwise mentioned. No part of this thesis has been submitted for any degree, diploma or any other type of qualification at any other institution.

Hannah Thorpe

May 2016

Acknowledgements

Abbreviations

5-FU	Fluorouracil
ABD	Actin binding domain
ALDH1A2	Aldehyde dehydrogenase 1 family, member A2
ANOVA	Analysis of variance
APC	Adenomatous polyposis coli
AR	Androgen receptor
ARPC1B	Actin-related protein 2/3 complex subunit 1B
ASCL2	Achaete-scute family bHLH transcription factor 2
BCA	Bicinchoninic acid
β-Trcp	Beta-Transducin Repeat Containing E3 Ubiquitin Protein
BSA	Bovine serum albumin
BLAST	Basic local alignment search tool
C1	Protein kinase C conserved region 1
Cas9	CRISPR-associated nuclease 9
CHX	Cycloheximide
CIMP	CpG island methylator phenotype
CIN	Chromosome instability
CNKSR3	CNKSR Family Member 3
Co-IP	Co-immunoprecipitation
CRC	Colorectal cancer
CRISPR	Clustered regularly interspaced short palindromic repeats
CRM1	Chromosomal maintenance 1
cRNA	Complementary RNA
crRNA	CRISPR RNA
CSC	Cancer stem cell
CT	Computerised tomography

Cten$^{\Delta C1300\text{-}2313}$	Cten with deletion of nucleotides 1300-2313
Cten$^{\Delta N165\text{-}1289}$	Cten with deletion of nucleotides 165-1289
DAB	Diaminobenzidine
DDR	DNA damage response
DLC1	Deleted in liver cancer 1
DMEM	Dulbecco's Modified Eagle's Medium
DSB	Double strand break
ECM	Extracellular matrix
EGF	Epidermal growth factor
EGFR	Epidermal growth factor receptor
EMT	Epithelial to mesenchymal transition
EST	Expressed sequence tag
EV	Empty vector
FAK	Focal adhesion kinase
FAP	Familial adenomatous polyposis
FBS	Foetal bovine serum
FBXW1	F-box/WD repeat-containing protein 1
FBXL18	F-box and leucine-rich repeat protein 18
FBXO27	F-box protein
FGF2	Fibroblast growth factor 2
GAK	Cyclin G associated kinase
GFP	Green fluorescent protein
gRNA	Guide RNA
GSK3β	Glycogen synthase kinase-3 beta
HDR	Homology directed repair
HER2	Human epidermal growth factor
HNPCC	Hereditary non-polyposis colorectal cancer

HPRT	Hypoxanthine guanine phosphoribosyl transferase
HRM	High resolution melting
HRP	Horseradish peroxidase
IGF1	Insulin-like growth factor 1
IHC	Immunohistochemistry
IL-13	Interleukin 13
IL-6	Interleukin 6
ILK	Integrin-linked kinase
IMS	Industrial methylated spirits
Indel	Insertion or deletion
iPSC	Induced pluripotent stem cells
JAK	Janus kinase
Klf4	Kruppel-like factor 4
Kras	Kirsten rat sarcoma viral oncogene homolog
LATS2	Large tumour suppressor 2
LEF	Lymphoid enhancer factor
LOH	Loss of heterozygosity
LV	Leucovorin
MAPK	Mitogen activated protein kinase
MAT	Mesenchymal amoeboid transition
MET	Mesenchymal to epithelial transition
MLH1	MutL Homolog 1
MLH2	MutL Homolog 2
MLH6	MutL Homolog 6
MMP	Matrix metalloproteases
MRI	Magnetic resonance imaging
MSI	Microsatellite instability

MSI2	Musashi RNA-binding protein 2
Nanog	Nanog homeobox
NES	nuclear export sequence
NGF	Nerve growth factor
NHEJ	Non-homologous end joining
NLS	Nuclear localisation signal
NLS-Cten	NLS tagged Cten
PAK1	p21 activated kinase
PAK1	P21 protein (Cdc42/Rac)-activated kinase 1
PBS	Phosphate buffered saline
PBS-T	Phosphate buffered saline-tween
PCA	Principal components analysis
PCR	Polymerase chain reaction
PDGF	Platelet-derived growth factor
p-EMT	Partial EMT
PI3K	Phosphatidylinositol 3-Kinase
PKD1	Protein kinase D1
PMS2	PMS1 Homolog 2
PTB	Phosphotyrosine binding
PTEN	Phosphatase and tensin homolog
qRT-PCR	Quantitative reverse transcription PCR
RIPA	Radio immunoprecipitation assay
RCas9	RNA-targeting Cas9
RhoA	Ras homolog family member A
RhoGAP	Ras homology-GTPase-activating
RIN	RNA integrity number
RISC	RNAi induced silencing complex

RLC	Regulatory light chain
ROCK	Rho-associated, coiled-coil containing protein kinase
RT-	Reverse transcriptase negative
SAGE	Serial analysis of gene expression
SAM	Sterile alpha motif
SCF	Skp, Cullin, F-box containing complex
SCP1	C-terminal domain phosphatase 1
SH2	Src homology 2
siRNA	Small interfering RNA
Sox2	Sex determining region Y-Box 2
Sox4	Sex determining region Y-Box 4
START	Steroidogenic acute regulatory protein-related lipid transfer
Stat3	Signal transducer and activator of transcription factor 3
SW620^{CtenKO}	SW620 Cten knockout cell line
TALENs	Transcription activator-like effector nucleases
TBS	Tris buffered saline
TBS-T	Tris buffered saline-tween
TCF	T-cell factor
TGFβ	Transforming growth factor beta
Tm	Melting temperature
TMA	Tissue microarray
TP53	Tumour protein p53
TPM	Transcripts per million
UBE2D4	Ubiquitin-conjugating enzyme E2D 4
UBE2R2	Ubiquitin-conjugating enzyme E2R 2
VEGF	Vascular endothelial growth factor

Wt.	Wild type
X-gal	5-Bromo-4-chloro-3-indolyl β-D-galactopyranoside
ZFNs	Zinc finger nucleases

Abstract

Cten is upregulated in a number of tumour types and in colorectal cancer (CRC), expression is associated with advanced stage, poor prognosis and distant metastasis. Cten appears to regulate cell motility and it can confer features of stemness although, the knowledge of underlying signalling mechanisms is sparse. Cten is localised at focal adhesions and in the nucleus. It may promote cell motility through the regulation of cell adhesion and it may confer stemness through gene activation. To determine the biological activity of Cten in CRC, this thesis investigated three areas of Cten signalling.

Nuclear expression of Cten is more prevalent in liver metastasis than the primary tumour. In the nucleus, Cten binds to β-catenin, however, the relevance of this is not known. To investigate the function of Cten in the nucleus, CRC cell lines were transfected with nuclear targeted Cten (NLS-Cten) and cell proliferation, migration and colony formation efficiency assessed. Expression profiling was performed to identify the underlying molecular mechanisms and additionally, the effect of Cten on β-catenin transcriptional activity was explored. Nuclear localised Cten was associated with increased cell migration and colony formation efficiency however it was found likely that Cten did not induce this activity through the regulation of β-catenin transcriptional activity.

Activation of Epidermal growth factor receptor (EGFR) signalling in breast cell lines stimulates cell motility and upregulates Cten expression whilst simultaneously downregulating the expression of Tensin 3, known as the Tensin switch. Activity is mediated through signalling downstream to Deleted in liver cancer 1 (DLC1). This pathway was tested in CRC. Stimulation of CRC cell lines with recombinant Epidermal growth factor

(EGF) and knockdown of Kirsten rat sarcoma viral oncogene homolog (Kras) resulted in up and downregulation of Cten respectively. A Tensin switch was not observed and, unexpectedly, Tensin 3 was stabilised by Cten signalling. Additionally, DLC1 was not expressed in the majority of cell lines investigated. It is possible that these mechanisms are either tissue dependent or different pathways operate in normal and cancer cell lines.

Since Cten mediated cell migration was not regulated by a Tensin switch mechanism in CRC, other mechanisms of cell migration were sought. In CRC, Cten signalling downregulates E-cadherin expression. This prompted the investigation of Cten's role in epithelial to mesenchymal transition (EMT) signalling. An EMT marker panel was investigated following the manipulation of Cten expression. Snail was identified as a novel target of Cten signalling and additionally, Cten was shown to promote the stabilisation of Snail protein. Furthermore, this signalling was functionally relevant and contributed to increased cell invasion and migration.

To investigate Cten signalling, expression was manipulated using a dual approach of Cten forced expression using a plasmid expression construct and siRNA mediated knockdown. To develop more refined models, the novel, Clustered regularly interspaced short palindromic repeats – CRISPR associated nuclease 9 (CRISPR-Cas9) genome editing technology was utilised to create a Cten knockout SW620 cell line (SW620^{CtenKO}) thus providing an alternative or supplementary method to interrogate Cten signalling in CRC.

This study adds to the ongoing discussion of the role of Cten in cancer. It was confirmed that Cten was regulated by EGFR and Kras signalling but without a Tensin switch, however Cten did promote cell motility through

the stabilisation of Snail suggesting that Cten may play a role in EMT processes. Finally, Cten displays enhanced oncogenic activity in the nucleus which may further promote metastasis. Further refinement of these pathways will increase the understanding of the invasion-metastasis cascade.

Thesis-related Publications and Conference Communications

    A. Peer-reviewed Publications

H Thorpe, M Akhlaq, D Jackson, S Ghamdi, S Storr, S Martin and Ilyas M. (2015), Multiple pathways regulate Cten in colorectal cancer without a Tensin switch. International Journal of Experimental Pathology, 96: 362–369

M Akhlaq*, **H Thorpe*** and M Ilyas. (2014), Tensins in health and disease. Recent Advances in Histopathology, 23:169-180 (*co-authorship)

    B. In process publications

M Akhlaq, **H Thorpe**, D Jackson, and M Ilyas. Cten forms an SH2 domain-dependent complex with Focal Adhesion Kinase to induce cell motility in colorectal cancer (submitted for publication)

H Thorpe, M Akhlaq, A Asiri and M Ilyas. Cten promotes colonic tumour development through the stabilisation of Snail (manuscript in preparation)

    C. Presentations and Conference Communications

H Thorpe, M Akhlaq, A Asiri and M Ilyas. (2016), The stabilisation of Snail by Cten regulates tumourigenicity in the colon. Midlands Academy of Medical Sciences Research Festival – oral presentation

H Thorpe, M Akhlaq, A Asiri and M Ilyas. (2015), The stabilisation of Snail by Cten regulates tumourigenicity in the colon. 20th World Congress on Advances in Oncology and 18th International Symposium on Molecular Medicine - poster presentation

H Thorpe, M Akhlaq, A Asiri and M Ilyas. (2015), Cten regulates cell motility through Snail in colorectal cancer. 8th Joint Meeting of the British Division of the IAP and the Pathological Society - oral presentation

H Thorpe, M Akhlaq and M Ilyas. (2015), Does Cten regulate cell stemness in colorectal cancer? EMBL Frontiers in Stem Cells and Cancer - poster presentation

H Thorpe, S Al Ghamdi and M Ilyas. (2014), The regulation of Cten in colorectal cancer, 26th European Congress of Pathology - oral presentation

H Thorpe, M Akhlaq, S Al Ghamdi and M Ilyas. (June 2014), Nuclear Cten as a regulator of cancer cell stemness, 26th European Congress of Pathology - poster presentation

Contents

Index of Figures

Index of Tables

1 General Introduction

1.1 Colorectal Cancer

CRC is a major health issue, it is the third most commonly diagnosed malignancy in the UK and worldwide 1.2 million people are diagnosed yearly. The number of patients diagnosed with the disease has increased, likely due to improvements in screening and detection methods. Despite this, mortality rates have gradually fallen to 600,000 deaths per year worldwide which may also be attributed to earlier detection and better treatment options. CRC is more prevalent in men and as with most cancers, the prevalence increases with age. The incidence is greater in western countries, namely Europe, United States and Oceanic countries but it is on the increase in other counties as they adopt a more westernised lifestyle (Center et al., 2009, Brenner et al., 2014). Patient prognosis has seen a recent improvement in developed countries although there is still an imperative need to understand the stages in malignant transformation to circumvent the high mortality associated with CRC (Brenner et al., 2014).

1.1.1 Molecular Pathogenesis and Classification

Almost all CRC is adenocarcinoma and arises from the uncontrolled proliferation of epithelial cells of the colon and rectum. CRCs are generally sporadic and develop from a benign precursor lesion known as an adenoma. This may progress into a malignant cancer which can invade through the bowel wall and into surrounding tissues, namely the abdomen and pelvis. With further progression, tumour cells will metastasise to the local lymph nodes and then to distant sites such as the liver.

Genetic instability underpins the development of CRC. Progression from normal epithelium through to adenoma, cancer and ultimately metastasis is driven by gene mutations that correspond to histologic changes

(Armaghany et al., 2012). Approximately 70-85% of cases arise as a result of chromosome instability (CIN) (Worthley and Leggett, 2010). Comprising the majority of cases, CIN is characterised by deletions or amplifications of chromosomal regions. The classical multi-hit model for this process states that sequential Adenomatous polyposis coli (*APC*), *KRAS*, chromosome region 18q and Tumour protein p53 (*TP53*) mutations, among others, allows for progression from adenoma to advanced metastatic disease (figure 1-1) (Fearon and Vogelstein, 1990).

The microsatellite instability (MSI) route to carcinogenesis is characterised by mutations or loss of function in the DNA mismatch repair enzymes including MutL homolog 1 (*MLH1*), MutL homolog 2 (*MLH2*), MutL homolog 6 (*MLH6*) or PMS2 postmeiotic segregation increased 2 (*PMS2*). Alterations of these genes leads to defective repair of insertional or deletional mutations (Indels) occurring at microsatellite sequences which, causes the accumulation of mutations in these regions (Montazer Haghighi et al., 2009). Approximately 15% of CRCs follow this route to carcinogenesis (Boland and Goel, 2010). CRCs may also arise through the CpG island methylator phenotype (CIMP) pathway in which methylation of the promoter regions of tumour suppressor genes encourages uncontrolled cell growth. The CIMP pathway is often associated with MSI, for example, MLH1 is often inactivated through promoter hypermethylation (Nazemalhosseini Mojarad et al., 2013). In addition to those discussed, a number of other classifications and molecular subtypes of CRC have been proposed (Guinney et al., 2015, Chan et al., 2001).

Although most cases of CRC are sporadic, hereditary disease forms also occur. Familial adenomatous polyposis (FAP) is characterised by CIN

(Groden et al., 1991). Hereditary non-polyposis colorectal cancer (HNPCC) follows the MSI route to carcinogenesis (Leach et al., 1993, Bronner et al., 1994). However, colorectal carcinogenesis is complex with additional genes and molecular pathways further implicated in disease progression.
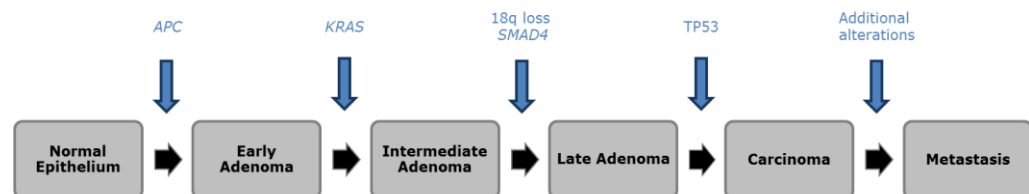
Figure 1-1: *The classical CIN adenocarcinoma sequence. Progression from normal epithelium to metastasis is driven my gene mutations. The classical CIN adenocarcinoma sequence states that sequential genomic alterations in APC, KRAS, chromosomal region 18q and TP53 drive carcinogenesis.*

1.1.2 Tools for Diagnosis

Diagnosis of CRC often comprises a sigmoidoscopy, colonoscopy or barium enema to identify any abnormalities in the colon or rectal wall and to allow for biopsies to be taken for further analysis. Following diagnosis, assessment of spread (i.e. tumour staging) may be investigated by x-ray, computerised tomography (CT) scanning or magnetic resonance imaging (MRI). Tumour stage is now more commonly assessed by the TNM classification system which is considered more precise than the previously used Dukes' staging system. This method assesses tumour penetration, nodal involvement and metastatic spread, which is used to assign the tumour a stage depending on the extent of spread (figure 1-2). Four

stages are used to define tumour penetration into the layers of the bowel wall (T1-T4). A T1 tumour is confined to the submucosa and penetrates with increasing stage, through the muscalaris propria, serosa and peritoneal surface. The extent of lymph node involvement is classified as 1 of 3 stages (N0-N2) to describe the tumour as having no lymph node involvement, tumour cells in 1-3 lymph nodes or the involvement of over 3 lymph nodes. The absence or presence of metastatic spread to distant organs is classified as M0 or M1 respectively. These are then categorised as an overall stage depending on the severity from carcinoma in situ (stage 0) through to metastatic cancer (stage 4) (Perston, 2011). This, together with the histological assessment of tumour grade, allows patient prognosis to be predicted and treatment routes to be followed accordingly.
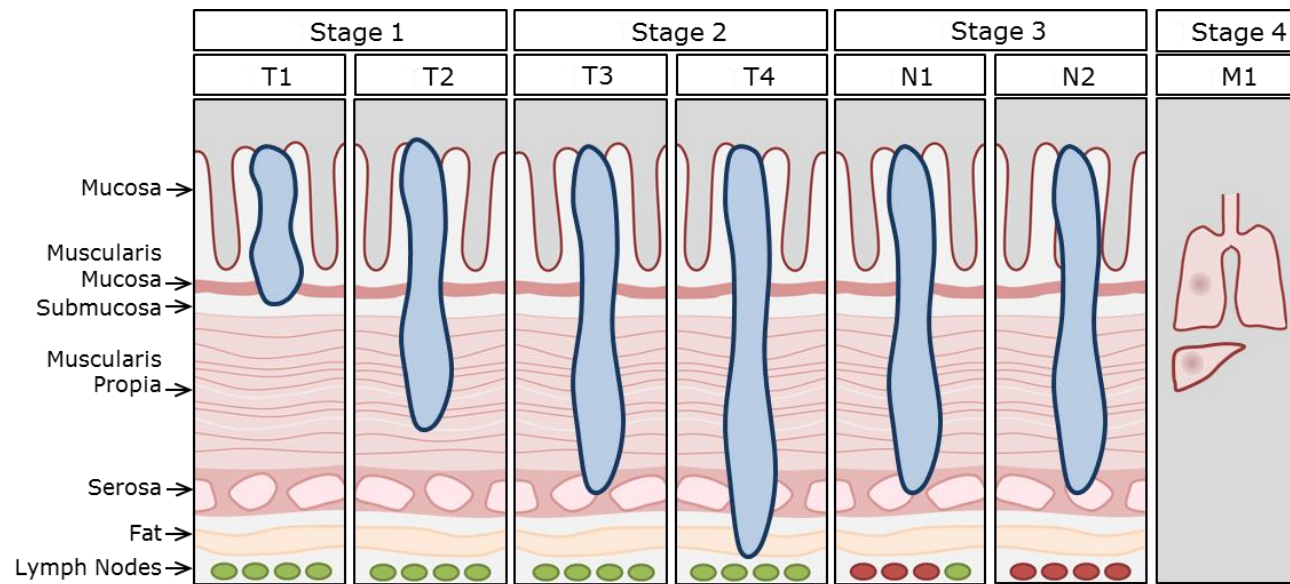
Figure 1-2: *TNM staging of CRC. The TNM staging system assesses the extent of tumour penetration (T1-4), lymph node involvement (N0-2) and the occurrence of distant metastasis (M0 or M1), which are combined to give an overall stage (1-4). The TNM stage can be used to predict patient prognosis and guide treatment.*

1.1.3 Therapeutic Intervention

The management of CRC is dependent on the tumour stage and in addition, the molecular classification may also direct therapy. Treatment for early CRC commonly comprises complete tumour removal although adjuvant chemotherapy or radiation therapy may be required for locally advanced disease. Fewer therapeutic options exist for metastatic disease. Surgery together with neoadjuvant and/or adjuvant therapy may be used to eradicate the tumour.

Chemotherapy traditionally targets DNA replication and transcription processes and hence cell growth. Five-fluorouracil (5-FU) is a uracil analogue, metabolites of which can be incorporated into RNA and also act to inhibit thymidylate synthase, crucial for thymidine synthesis. It is often administered alongside bio-modulating agent Leucovorin (LV) to increase potency. Sensitivity may depend on the mutation spectrum as deletion of *TP53* has been shown to reduce sensitivity to 5-FU (Bunz et al., 1999). In CRC, there is a 10-15% patient response rate to 5-FU but rates can be improved by combination with other chemotherapies (Longley et al., 2003). Newer chemotherapies include Irinotecan, which targets Topoisomerase I. Irinotecan binds to and increases the stability of the DNA-Topoisomerase complex thereby preventing continuation of DNA replication (Fuchs et al., 2006). Combinations of 5-FU/LV with Irinotecan increased disease free and overall survival compared to 5-FU/LV alone (Saltz et al., 2000). Alternatively, Oxaliplatin may be administered. Oxaliplatin is a platinum agent that prevents DNA replication through the induction of DNA crosslinking. Response rates can be improved when used

in conjunction with 5-FU (Rothenberg, 2000). In some circumstances, chemotherapy may be administered alongside targeted therapies.

Unlike chemotherapies that non-specifically target proliferating cells, targeted therapies such as monoclonal antibodies and molecular inhibitors interfere with specific molecules to help prevent and reduce tumour growth. Cetuximab and Panitumumab monoclonal antibodies both target the extracellular domain of EGFR, competitively inhibiting the binding of EGF and thus prevent downstream pathway activation. These therapies however are rendered ineffective in patients with mutated downstream target genes such as *KRAS* and *BRAF* which are commonly mutated in CRC (Misale et al., 2012). Thus anti-EGFR therapies are only administered to those with wt. *KRAS*, spurring an era of personalised medicine. Bevacizumab and Ramucirumab monoclonal antibodies both target VEGF signalling to prevent blood vessel growth (Ferrara et al., 2004). These therapies are used in the treatment of advanced, metastatic CRC. Regorafenib, a kinase inhibitor is also administered to prevent angiogenic processes in addition to other pathways promoting tumour growth. Although therapies may show initial success, resistance often prevails through downstream mutation in the targeted pathways, eventually rendering these therapies ineffective. Furthermore, treatment options for more advanced metastatic disease are limited and palliative rather than curative treatment is often the only option. Considering this, it is important that improved therapies are made available for late stage CRCs.

1.2 Cancer Metastasis

1.2.1 A multi-step process

The majority of cancer related deaths are attributed to metastatic disease. Consequently, it is imperative that the pathways involved in metastatic spread are understood (Spano et al., 2012). For a cell to establish tumour growth at a secondary site it must successfully undergo a sequential, coordinated series of events accomplished by the acquisition of molecular alterations. Metastasis is an inefficient process that is completed by only a minority of cells but, once achieved, it has a dramatic, negative impact on patient prognosis.

1.2.1.1 Cancer Cell Dissemination

Cancer metastasis is the spread of cancer cells to distant tissues of the body and broadly comprises the processes of cancer cell dissemination from the primary tumour followed by adaptation and growth at the distant site. Cancer cell metastasis involves the acquirement of migratory capabilities to permit cell movement to the secondary tissue. Further to increased cell migration, invasion is the passage of a cell through the tissue extracellular matrix (ECM), characterised by increased proteolytic activity and ECM breakdown. Cell invasion is an initial step in cancer metastasis. Both are closely linked processes and together are termed the invasion-metastasis cascade.

As the primary tumour grows, it breaches tissue boundaries and spreads into adjacent tissues. In attempt to reach the vascular system, the tumour cells may invade collectively, without losing contact with the initial tumour, or as sheets of epithelia. Alternatively, single cells may break away from

the primary tumour in an amoeboid or mesenchymal fashion. Amoeboid movement of single cells is characterised by squeezing through matrix barriers whereas mesenchymal migration is characterised by ECM breakdown (Yilmaz and Christofori, 2010). Tumours arising in different tissues tend to invade using a particular mode of migration however, it is likely that cells undergo mesenchymal amoeboid transition (MAT) and vice versa to adapt to variations in the microenvironment (Taddei et al., 2014).

Epithelial cell architecture is maintained by cell to cell junctions namely adherens junctions, tight junctions, gap junctions and desmosomes. Furthermore, epithelial cells are anchored to the underlying ECM via focal adhesions and hemidesmosomes (figure 1-3). During mesenchymal movement, cells may detach from the primary tumour by undergoing EMT, a process whereby epithelial cells display phenotypic plasticity by adopting a mesenchymal phenotype. This endows the cell with greater invasive capabilities. During EMT, the loss of adhesion is governed by changes in the expression of cell adhesion molecules that make up these cell junctional complexes. Epithelial cells experience loss of basolateral to apical polarity and adopt front to back polarity, as displayed by mesenchymal cells. Furthermore, cytoskeletal rearrangements induce morphological cell changes to form cell protrusions including lamellopodia and filopodia to aid cell motility (Lamouille et al., 2014). EMT pathways promote the formation of invadopodia that secrete proteolytic enzymes including matrix metalloproteases (MMPs) to facilitate ECM degradation (Bravo-Cordero et al., 2012). Further actin structural rearrangements promote stress fibre formation to facilitate cell migration. Interaction with the surrounding stroma is postulated to aid the invasion-metastasis cascade (Provenzano et al., 2006).

Following local invasion, cancer cell intravasation into nearby blood vessels and lymphatics is facilitated by the 'leaky' neovasuclar system (Weidner, 2002). Extravasation into the distant tissue is aided by the expression of growth factors and cytokine signalling. Cytokines may act as chemoattractants, for example, the chemokine receptor CXCR4 is expressed by cells derived from numerous tumour types and promotes migration towards target tissues that secrete its cognate ligand (Mukherjee and Zhao, 2013, Murakami et al., 2013). Moreover, the cell must undergo this obstacle of events whilst evading the immune responses.
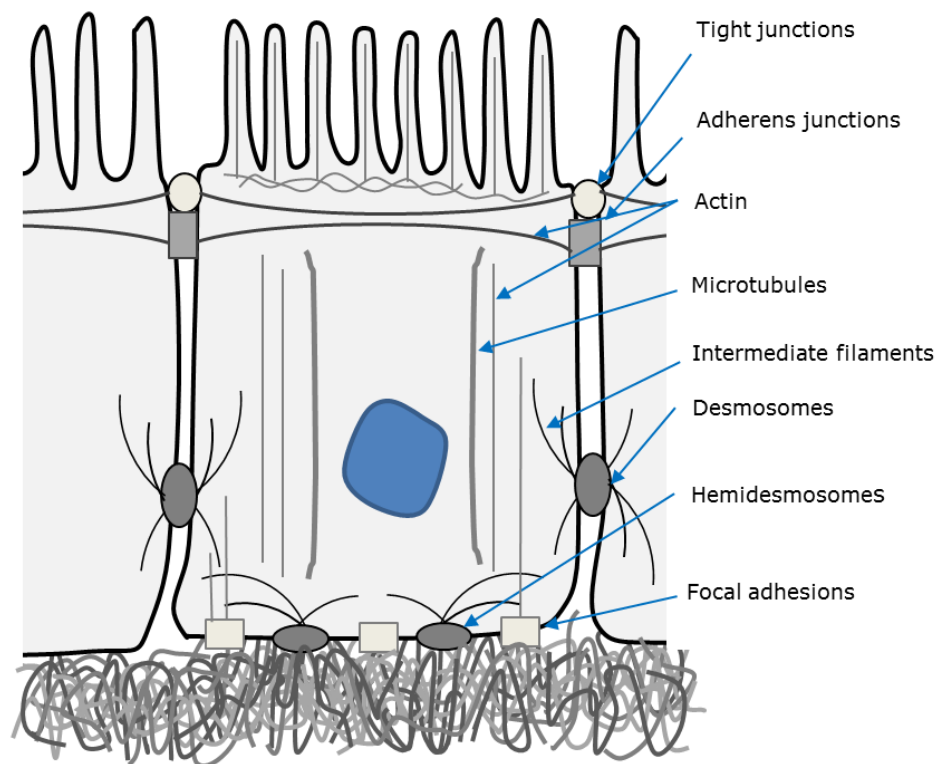
Figure 1-3: *Epithelial cell junctions. Epithelial cell structure is maintained by cell-cell and cell-ECM junctions. Tight junctions form regions of cell-cell attachment near the apical surface and are maintained by Claudins, Occludin and ZO proteins. Adherens junctions mediate cell-cell attachment via cadherin molecules which link via catenins to the actin cytoskeleton. Desmosomes form strong attachments to the intermediate filaments of neighbouring cells. Focal adhesions and hemidesmosomes mediate cell-ECM adhesion.*

1.2.1.2 Metastatic Colonisation

Upon reaching the target site, survival in a new, hostile environment is the next obstacle for the tumour cell to overcome. Initially, cells may form micrometastasis under these unfavourable conditions before progression to clinically detectable tumour growth. It is postulated that the reversal of EMT, mesenchymal to epithelial transition (MET), may occur to seed metastasis. This is demonstrated by the re-expression of epithelial markers and the loss of mesenchymal markers in metastatic tumours. EMT transcription factors can supress cell proliferation and reversal of this may promote tumour cell proliferation at the secondary site (Brabletz et al., 2001, Tsai et al., 2012). Together with the stimulation of angiogenic processes, clinically detectable macroscopic tumour metastases may prevail.

Metastases have a tendency to form in particular tissues dependant on the tumour type. This could just be a passive process dependent on tissue proximity to the primary tumour but accumulating evidence suggests that biological mechanisms permit secondary tumour growth at particular sites. The 'seed and soil' hypothesis states that tumour cells establish secondary tumour growth in particular distant tissues dependent on the environment of that tissue and its compatibility (Paget, 1889). Theories also suggest that the cell can secrete factors that prime the new environment ready for the cell's arrival (Kaplan et al., 2005).

1.2.2 The Role of Cancer Stem Cells in Metastasis

It has been proposed that only a subset of cells have the ability to establish clinically detectable metastasis and, those that have this ability, have attributes of stem cells, or cancer stem cells (CSCs). Stem cells have

self-renewal property and therefore can establish secondary growth at the distant site however it is likely that further attributes of stem cells promote metastatic growth. Cells in primary tumours that display high expression of stem cell markers show a higher tendency to metastasise and depletion of these cell pools abrogates metastasis (Pang et al., 2010, Hermann et al., 2007). Furthermore, the induction of EMT has been linked to the CSC concept. EMT programmes co-induce stem-cell pathways and those cells that are able to metastasise are coined 'migrating stem cells'. (Brabletz et al., 2005). In CRC, cells at the invasive tumour front were shown to have reduced expression of epithelial cell junction marker E-cadherin, and therefore thought to have undergone EMT. These cells were in an undifferentiated state, a feature of stem cells. Additionally, they displayed nuclear expression of β-catenin which is a feature of active Wnt signalling that maintains the stem cell compartment in the normal intestinal epithelium. These were phenotypically distinct from the cells in the centre of the tumour that displayed high expression of E-cadherin and an absence of β-catenin in the nucleus. Interestingly, differentiated cells were present in the corresponding liver metastasis suggesting that MET had occurred at the metastatic site (Brabletz et al., 2001). Further evidence supports the involvement of CSCs in EMT. The induction of EMT in human mammary epithelial cells was associated with the expression of mesenchymal markers. In addition, the induction of EMT also gave rise to a population of cells with properties of breast stem cells defined by $CD44^{high}/CD24^{low}$ marker expression. Cells that had undergone EMT were also more efficient at mammosphere growth, another property of stem cells (Mani et al., 2008).

Recent evidence supports the view that CSCs may be involved in EMT processes however, it is not known whether pathways promoting metastasis are always linked to stem cell properties. Using alternative models, others have shown the uncoupling of EMT and cell stemness (Ocana et al., 2012). It is clear that advances have been made in trying to determine the molecular pathways associated with metastatic spread however the complexity of events it entails precludes full understanding. It is evident that EMT processes play a central role and it is likely that this is driven by the induction of stem cell pathways.

1.2.3 Targeting metastasis

It is estimated that 90% of deaths arising from cancer do so as a result of metastasis (Spano et al., 2012). Thus, there is a critical need to use the knowledge of molecular mechanisms to develop therapies to target this process. Additionally, as many of the steps in metastasis are common among cancers, it would seem a logical and a worthwhile process to target. However, despite its clinical relevance, the current success of antimetastatic drugs is poor.

As discussed, there are some therapies targeted at molecules involved in metastatic spread in routine use, including inhibitors of angiogenic processes. Moreover, therapies against other metastatic pathways are under investigation, including inhibitors of Axl (a tyrosine kinase involved in EMT signalling), which reduced the metastatic burden of breast tumours in animal models and is demonstrating success in a number of tumour types (Holland et al., 2010, Myers et al., 2015). It is clear that despite the clinical significance of metastasis, the development of therapies targeting these pathways is limited. The drug discovery process may be facilitated

by further understanding of the complex series of molecular events involved. The molecular changes that may contribute to metastasis are next reviewed.

1.3 Focal Adhesions

1.3.1 The Structure of Focal Adhesions

Focal adhesions are large molecular assemblies that form an attachment between the cell and the ECM and consequently play crucial roles in cell migration. Focal adhesions are centred around membrane bound integrin receptors. Integrins are heterodimeric proteins comprising non-covalently associated α and a β subunits. In total there exist 18 α and 8 β subunits that combine to give 24 different integrin heterodimers. Externally, Integrins bind to ECM components including collagen, laminin and fibronectin (Knight et al., 2000, Huveneers et al., 2008, Belkin and Stepp, 2000). Internally, Integrins link to the actin cytoskeleton via large dynamic protein complexes. The proteins that bind to the cytoplasmic domain of the β-integrin subunit often do so via phosphotyrosine binding (PTB) domains that link to 1 of 2 conserved NXXY motifs in the integrin cytoplasmic tail. Integrin binding proteins link to the cytoskeleton either directly or indirectly through the binding of other proteins found in complex at focal adhesions (figure 1-4) (Zaidel-Bar et al., 2007, Campbell and Humphries, 2011).
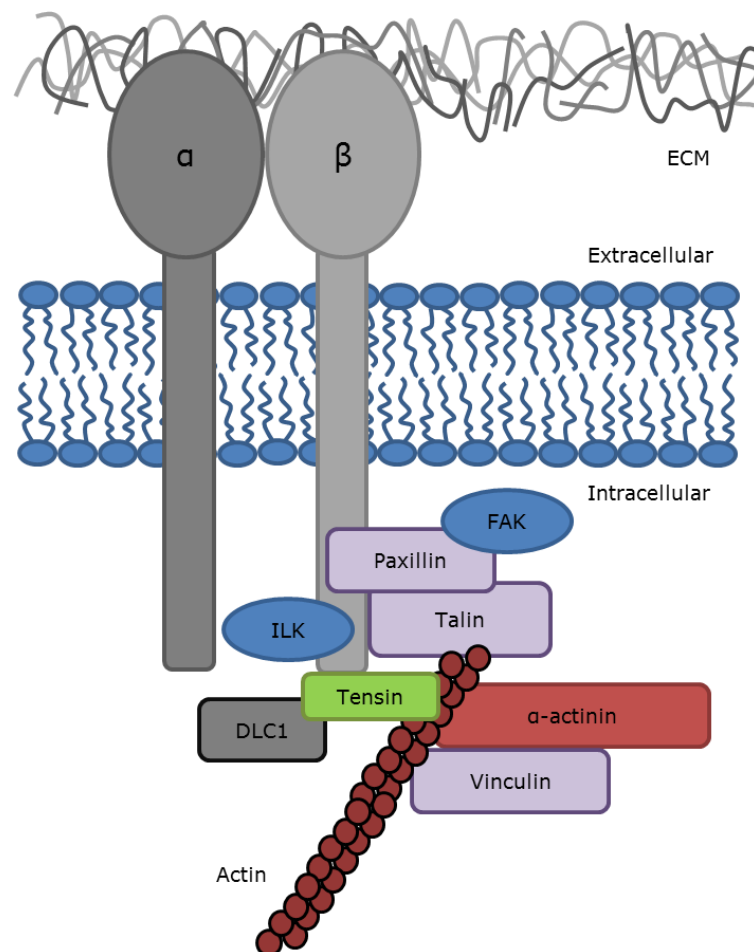
Figure 1-4: *The structure of focal adhesions. Focal adhesions are centred around integrin receptors. They bind externally to ECM components and link internally to the actin cytoskeleton via large dynamic molecular protein complexes comprising protein kinases, phosphatases and adaptor molecules.*

1.3.2 Focal Adhesion Signalling Regulates Cell Migration

Focal adhesions provide a mechanical linkage from the cell interior to the ECM, and in addition, serve as signalling platforms to regulate a range of cellular processes concerned with cell motility, differentiation and proliferation (Lo, 2006). Focal adhesions are critical for cell migration with continuous cycles of cell protrusion and attachment to the substratum at the leading edge followed by detachment and retraction at the cell posterior, regulated by focal adhesion dynamics and the associated coupling of actin filaments. The tension generated is able to promote changes in cell morphology and generate traction to pull the cell body. In actively migrating cells, focal adhesions are continuously forming, maturing and disassembling to regulate cell attachment to the underlying ECM (Wehrle-Haller, 2012). Adaptor proteins such as Talin, Paxillin and Vincullin provide links between Integrins and the cytoskeleton whilst kinases such as Src and FAK transmit downstream intracellular signals through phosphorylation events (Westhoff et al., 2004, Fukumoto et al., 2015, Legate and Fassler, 2009).

Focal adhesions form at lamellopodia of a migrating cell and mature as the migrating cell moves over them. The different stages of the focal adhesion life cycle are associated with the sequential recruitment of different proteins (Partridge and Marcantonio, 2006). Primitive focal adhesions, or nascent adhesions, are initially formed by the activation of Integrins, which expose binding sites and recruit adaptor proteins to the intracellular membrane surface. This action promotes further activation of nearby Integrins. Eventually, this leads to a cluster of integrin receptors at the site of cell-ECM contact. The recruitment of Talin in the early stages of formation stabilises this structure and provides binding sites to facilitate

the recruitment of additional protein complexes. This action initialises a link between Integrins and the actin cytoskeleton (Nayal et al., 2004).

Since Integrins do not possess any intrinsic catalytic activity, signal transduction is mediated by the proteins in complex at focal adhesions. Focal adhesion kinase (FAK) plays a central role in focal adhesion dynamics. It is recruited to Integrins and undergoes auto-phosphorylation at position Y397 (Toutant et al., 2002). This enables the binding of Src which in turn promotes further FAK phosphorylation and the binding of additional proteins (Mitra and Schlaepfer, 2006). FAK reinforces focal adhesion formation by the further recruitment of Talin protein (Lawson et al., 2012). The recruitment of Paxillin and subsequent recruitment of Vinculin further stabilises these complexes (Pasapera et al., 2010).

Under conditions of increased traction, the maturation of focal adhesions may occur. Maturation is initiated by Ras homology family member A (RhoA) activity and downstream signalling to Rho-associated protein kinase (ROCK), myosin II regulatory light chain (RLC) and mDia (Chrzanowska-Wodnicka and Burridge, 1996, Cao et al., 2012). Mature focal adhesions are associated with the formation of thick actin stress fibres (Zaidel-Bar et al., 2007). Mature focal adhesions recruit further proteins including Tensin and Zyxin. Rapid formation and disassembly of focal adhesions is a feature of actively migrating cells. In some cases, further maturation to fibrillar adhesions maintains firm cell-ECM attachment and this stage is generally associated with non-motile cells (Clark et al., 2010, Yoshigi et al., 2005).

Dissolution of focal adhesions usually occurs following retraction at the cell rear and is associated with further signal transduction events. In addition to focal adhesion formation, FAK has been shown to play a central role in disassembly. FAK recruits Dynamin which promotes focal adhesion turnover through microtubule mediated integrin internalisation by endocytosis (Ezratty et al., 2009, Ezratty et al., 2005). The cysteine protease Calpain is recruited to focal adhesions and mediates the cleavage of multiple focal adhesion substrates including FAK, Paxillin Tensin and Talin (Chan et al., 2010, Chen et al., 2000). This cycling of focal adhesions and associated formation and detachment of actin stress fibres drives cell migration.

As focal adhesion signalling is central to cell migration, dysregulation of such events is commonly associated with increased cell motility and consequently cancer metastasis (Lark et al., 2003). The altered expression of a number of focal adhesion localised proteins have been identified to contribute towards cancer progression (Lark et al., 2003, Cao et al., 2012). Amongst these is the Tensin family of proteins.

1.4 The Tensin Gene Family

1.4.1 Tensin Structure

Tensins are among the proteins clustered on the cytoplasmic side of focal adhesions and comprise Tensin 1, Tensin 2, Tensin 3 and Tensin 4 (also known as Cten). The Tensin family of proteins, with the exception of Cten, have extensive sequence and structural homology sharing common actin binding, Src homology 2 (SH2) and PTB domains yet with divergent central regions (figure 1-5) (Lo and Lo, 2002).

The first in the family to be identified was Tensin 1, which maps to chromosome 2q35-36 and translates into a 1735 amino acid protein with a molecular mass of 185 kDa. There are an additional 13 Tensin 1 protein coding splice variants. Tensin 1 was found to be present in most tissues investigated with elevated levels found in the heart, skeletal muscle, kidney and lung (Chen et al., 2000). Tensin 1 comprises of 2 actin binding domains located at the N terminus and also an additional actin binding domain in the central region of the protein. The central actin binding region has high sequence homology to Insertin, an actin capping protein which retards actin polymerisation (Lo et al., 1994, Chuang et al., 1995). Tensin 1 also links to the cell exterior through Integrin binding via its PTB domain located at the C terminal end of the protein. Although PTB domains are known for binding phosphorylated tyrosines, binding to integrins has been shown to be independent of phosphorylation (McLeverty *et al.* 2007). Further to Tensin 1's actin and Integrin binding capabilities, the cloned fragment of Tensin cDNA revealed an SH2 domain also located at the C-terminus, capable of binding phosphotyrosine proteins. Furthermore, the protein was shown itself to contain phosphorylated tyrosine residues (Davis *et al.* 1991). This finding was of marked significance as it made Tensin the first cytoskeletal protein to be identified with a SH2 domain thus, linking signal transduction to the actin cytoskeleton. Tensin 1 also shares homology to other protein domains including those of Auxillin, Cyclin G associated kinase (GAK) and Phosphatase and tensin homolog (PTEN). Knockout mice revealed that Tensin 1 was not essential for embryonic development however, focal adhesion biology and many of the proteins that interact with Tensin 1 are essential for embryonic development. Therefore, it was suggested that another related protein may be able to

compensate in the absence of Tensin 1 expression, which led to the identification of additional Tensin family members (Lo et al., 1997, Chen et al., 2002).

Tensin 2, located on chromosome 12 was identified as a protein related to Tensin 1 through homologous N and C terminal regions sharing 60% and 67% sequence similarity respectively. It maps to chromosome 12q13 and encodes a protein comprising 1410 amino acids with a molecular mass of 170 kDa. In total, there are 7 protein coding splice variants. Tensin 2 lacked the Insertin-like region in its centre and therefore may not serve the same actin remodelling role as Tensin 1 (Chen et al., 2002). Although it has similar actin binding, SH2 and PTB domains, Tensin 2 is the only member of Tensin family that has a Protein kinase C conserved region 1 (C1) at the N terminus. The C1 domain of Protein kinase C is known to bind to phospholipids (Johnson et al., 2000) (Hafizi et al., 2002). Tensin 2 was found to be present in most tissues investigated but particularly abundant in the heart, skeletal muscle, liver and kidney, similar to Tensin 1 further supporting the suggestion of a similar function (Chen et al., 2002).

Subsequent to this, Tensin 3 was identified as a 1445 amino acid protein with a molecular mass of 155 kDa (Cui et al., 2004). Tensin 3 has a further 8 protein coding splice variants. The gene maps to chromosome 7p12 and has similar domain structure to Tensin 1 and Tensin 2. Tensin 3 was found to contain 32 tyrosine residues, 13 of which are predicted to be potential sites of phosphorylation and possible candidates for signal transduction. Localisation was again revealed to be at focal adhesions and it was expressed in most tissues studied. Tensin3 was particularly prevalent in

the placenta and kidney with the spleen, lung, skeletal muscle and heart showing lower expression (Cui et al., 2004).

Unlike the previously identified Tensin family members, Cten, the most recently identified Tensin, is a more distant relative bearing homology to Tensins 1-3 but lacking the actin binding domain (Chen et al., 2013). The *CTEN* gene maps to chromosome 17q21 and encodes a 715 amino acid protein with a molecular mass of 77 kDa. Cten only has 1 additional splice variant consisting of only 33 amino acids. *CTEN* comprises 12 exons although only exons 4-11 share high sequence homology to the c-terminus of the other Tensins (Lo and Lo, 2002). In addition to localisation at focal adhesions, Cten also localises to the nucleus but the relevance of Cten in this localisation is unknown (Liao et al., 2009). Moreover, in contrast to the other Tensins, the expression of Cten was restricted to the placenta and prostate however expression has since been noted in other tissues (Lo and Lo, 2002, Martuszewska et al., 2009). The *CTEN* gene is restricted to mammals consistent with its expression mainly in the prostate and placenta. A total of 22 different mammalian species were found to have protein sequence similar to human Cten. The other Tensins however, are found in a greater diversity of species for example, Tensin 1 is present in the nematode, zebrafish and hydrozoan (Chen et al., 2013). Interestingly, Cten still contains the SH2 and PTB signalling component of the other Tensins but lacks the actin binding capability and thus may play a novel role in cellular processes.
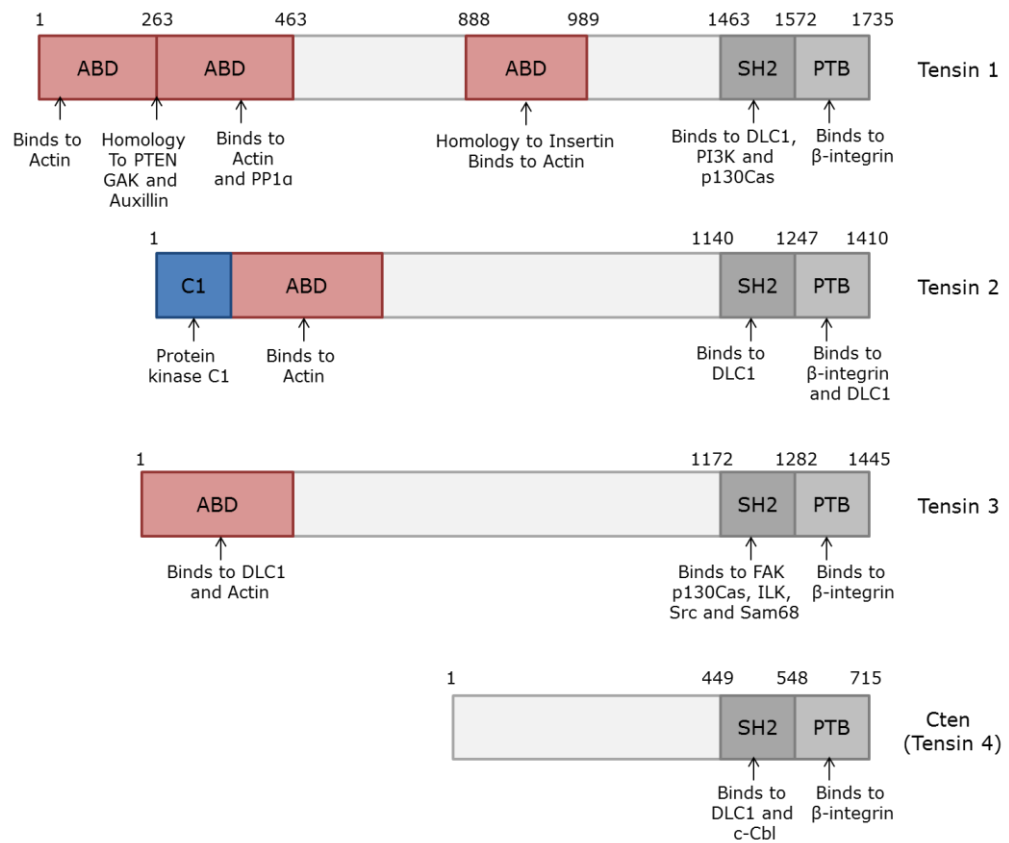
Figure 1-5*: Tensin domain structure. Tensins 1-3 comprise an actin binding domain (ABD) in addition to the SH2 and PTB domains present in Cten allowing a connection from the ECM to the actin cytoskeleton.*

1.4.2 The Role of the Tensin Proteins

Members of the Tensin family play pivotal roles in key cellular processes including proliferation, adhesion, migration, and apoptosis (Lo and Lo, 2002). The Tensins have each been linked to upstream and downstream signalling pathways, and have been shown to differentially interact with components to aid in mediating their responses (Cao et al., 2012, Clark et al., 2010). However, knowledge of Tensin signalling remains sparse. They share extensive sequence homology and the lack of embryonic lethality in mice suggests functional redundancy of the Tensins but divergent regions also suggests that they may, to some extent, have distinct roles (Chiang et al. 2004).

Tensins, not surprisingly due to their localisation at focal adhesions, interact with a number of other focal adhesion localised proteins including p130cas, FAK, ILK, DLC1, Src and Calpain (Thorpe et al., 2015, Albasri et al., 2011a, Al-Ghamdi et al., 2013, Cao et al., 2012, Zhao et al., 2016). It is likely that the Tensins coordinate cell function through the regulation of focal adhesion dynamics and actin remodelling. There are contradictory reports, however, on how Tensin 1 achieves this, with some suggesting an actin capping role whereas others suggest actin monomer insertion (Lo et al., 1994, Chuang et al., 1995). Investigations into the other Tensin family members has found that they promote actin structural rearrangements, but how this is regulated and contributes to focal adhesion turnover has not been intensively studied (Cao et al., 2012). Tensins 1-3 are generally associated with the later stages of focal adhesion maturation. Tensin 1 is absent from nascent adhesions but is recruited to mature focal adhesions and may play a role in the maturation to fibrillar adhesions (Zaidel-Bar et al., 2007, McCleverty et al., 2007). Tensin 3 is also associated with fibrillar

adhesions. The Tensins may localise to different areas of the migrating cell, Tensin 2, for example, was found to be located predominantly at the leading edge of the cell whilst, in contrast, Tensin 3 was found to be located towards the cell rear (Chen et al., 2002, Clark et al., 2010). Additionally, Tensins are cleaved by Caspase 3 and therefore possibly involved in the loss of cell attachment during apoptosis (Lo et al., 2005).

The dysregulation of Tensin signalling has been implicated in carcinogenesis, but how the Tensins contribute to disease progression remains a topic of debate. Whether the Tensins have oncogenic or tumour suppressive activity may be dependent on the Tensin member and may also be tissue or context dependant (Martuszewska et al., 2009, Qian et al., 2009, Albasri et al., 2011a).

1.5 Cten

1.5.1 The Expression of Cten in Cancer

Despite being one of the most recently identified members of the Tensin family, the role of Cten in cancer has been more extensively investigated. Cten was originally identified as a tumour suppressor in prostate cancer and is also down regulated in kidney tumours. However, its role as an oncogene in other tissues is now becoming increasingly apparent (Lo and Lo, 2002, Martuszewska et al., 2009). Cten expression was shown to be increased at both the mRNA and protein level in cancer cell lines in comparison to normal cells (Liao et al., 2009). Although not normally present in most tissues, elevated levels have been discovered in tumours of the lung, thymoma, colon, breast and pancreas and in most tissues investigated, Cten appears to be associated with late stage disease (Sasaki

et al., 2003a, Sasaki et al., 2003b, Albasri et al., 2009, Albasri et al., 2011b, Al-Ghamdi et al., 2013).

In melanoma tissues, Cten expression increased with tumour progression with 7%, 24%, 41% and 46% positivity in normal, dysplastic, primary melanoma and metastatic melanoma tissue respectively. Additionally, Cten expression was associated with advanced stage, tumour thickness and poor patient prognosis (Sjoestroem et al., 2013). In lung cancer, a lack of significant difference in Cten expression between tumour and normal lung tissue was found, however, the ratio of Cten in tumour to normal tissue was significantly higher for stage II-IV than stage I, suggesting that Cten expression is upregulated during the progression of established lung cancer (Sasaki et al., 2003a). Similarly, in thymomas, *CTEN* mRNA expression was significantly greater in tumour stage IV than stage I (Sasaki et al., 2003b).

In breast and CRC, Cten expression is generally associated with metastatic disease. Immunohistochemical analysis of breast carcinomas for Cten revealed no association between its expression and tumour size, however, there was for high EGFR and Human epidermal growth factor receptor (HER2) expression, low oestrogen receptor expression, lymph node metastasis and tumour grade (Katz et al., 2007). A larger scale study investigated Cten expression using immunohistochemistry in 1,409 invasive breast tumours. Cten staining was found in 90% of tumours and shown to be associated with tumour size, grade, nodal involvement and poor Nottingham prognostic index. Tumours with high Cten expression had a poorer prognosis in comparison to those expressing low levels and also had increased likelihood of developing metastasis (Albasri et al., 2011b).

Taken together, these studies suggest that Cten is involved in breast cancer metastasis.

Cten expression has been extensively investigated in colorectal tumours and overall suggests a role for Cten in metastasis. Investigation of mRNA expression in tumours and normal mucosal cells demonstrated that the majority of tumours experience upregulation, with 5 cell lines showing greater than a 35 fold increase in *CTEN* (Albasri et al., 2009). Interestingly, these cell lines were derived from metastatic deposits, highlighting further association of Cten with metastasis. Expression has been found by some to be upregulated in all stages of disease implicating a role for Cten in tumour formation and progression (Liao et al., 2009). Conversely, others have shown its involvement with metastasis consistent with other tumour types suggesting that Cten is concerned with late stage disease. Again, Cten expression was investigated on a much larger scale involving 462 clinical samples. Here, Cten expression was shown to correlate with advanced Duke's stage, poor prognosis and distant metastasis in CRC (Albasri et al., 2011a). The latter study utilised a larger sized cohort and therefore may be considered more representative than the former study. Further to this, analysis of the expression of Cten in paired cases of matched primary colorectal tumours and liver metastasis revealed that Cten nuclear expression was more prevalent in metastatic deposits (Albasri et al., 2011a). This implies that Cten in the nucleus is possibly involved in metastatic disease.

Serial analysis of gene expression (SAGE) data accessed through Unigene (NCBI) corroborates some of these findings. The expressed sequence tag (EST) profile for the Cten transcript (NM_032865.5) quantifies expression

in a number of normal and tumour tissues (Table 1-1 and 1-2). Cten expression is downregulated in tumours of the prostate and kidney, whilst upregulation of Cten expression is seen in colorectal, pancreatic, breast and lung tumours. Cten SAGE profiles were comparable to the expression of the other Tensins in the colon (Tensin 1 normal 146, tumour 186, Tensin 2 normal 51, tumour 26 and Tensin 3 normal 107, tumour 151 transcripts per million (TPM)) but to a lesser extent than β-catenin, known to be highly expressed in colorectal tumours (normal 241, tumour 355 TPM). In comparison, Cten appears to be considerably upregulated and moderately expressed in CRC (normal 68, tumour 106 TPM) however in other tissues such as the breast, the expression is much lower and the change in expression appears to be negligible (normal 19, tumour 21 TPM). Although in comparison, the expression of Cten in normal prostate is relatively low (31 TPM), the expression is completely lost in prostate tumours (0 TPM).

The role of Cten in carcinogenesis is, at present, not well defined and in part controversial, although evidence clearly implicates a role in advanced disease and in most tissues studied, expression is associated with metastasis. Since Cten is associated with aggressive disease, there is an imperative need to determine the underlying signal transduction mechanisms governing this process.

Tissue	Transcript/ million (TPM)	Spot intensity based on TPM	Gene EST/Total EST in the pool
Adipose tissue	0		0/12866
Adrenal gland	0		0/32940
Ascites	50		2/39834
Bladder	133		4/29860
Blood	0		0/122252
Bone	0		0/71618
Bone marrow	0		0/48737
Brain	7		8/1092688
Cervix	0		0/48486
Connective tissue	0		0/149072
Ear	0		0/16100
Embryonic tissue	0		0/212896
Eye	23		5/208840
Heart	0		0/89524
Intestine	68		16/231981
Kidney	14		3/210778
Larynx	42		1/23466
Liver	0		0/205291
Lung	41		14/334815
Lymph	0		0/44302
Lymph node	0		0/89748
Mammary gland	19		3/151230
Mouth	105		7/66150
Muscle	9		1/106371
Nerve	0		0/15535
Oesophagus	49		1/20154
Ovary	0		0/101488
Pancreas	37		8/213440
Parathyroid	0		0/20594
Pharynx	0		0/40725
Pituitary gland	0		0/16526
Placenta	84		24/283019

Prostate	31		6/189536
Salivary gland	0		0/20265
Skin	56		12/210759
Spleen	0		0/53397
Stomach	41		4/95679
Testis	0		0/435204
Thymus	0		0/79697
Thyroid	85		4/46583
Tonsil	0		0/17021
Trachea	19		1/51780
Umbilical cord	0		0/13764
Uterus	51		12/232093

Table 1-1*: The expression of Cten by EST in normal body tissues* (UniGene).

Tumour	Transcript/ million (TPM)	Spot intensity based on TPM	Gene EST/Total EST in the pool
Adrenal tumour	0		0/12655
Bladder carcinoma	170		3/17584
Breast tumour	21		2/93090
Cervical tumour	0		0/34484
Chondrosarcoma	0		0/82838
Colorectal tumour	106		12/112517
Gastrointestinal tumour	42		5/118498
Germ cell tumour	3		1/263230
Glioma	65		7/107194
Head and neck tumour	82		11/133826
Kidney tumour	0		0/68872
Leukaemia	0		0/94479
Liver tumour	0		0/96023
Lung tumour	58		6/102765
Lymphoma	0		0/72196
Non-neoplasia	31		3/96623
Normal	15		52/3328811
Oesophageal tumour	57		1/17245
Ovarian tumour	0		0/76185
Pancreatic tumour	76		8/105004
Primitive neuroectodermal tumour	0		0/127001
Prostate cancer	0		0/103844
Retinoblastoma	0		0/46439
Skin tumour	7		1/125373
Soft tissue/muscle tissue tumour	0		0/125265
Uterine tumour	122		11/90107

Table 1-2: *Gene expression of Cten by EST in tumours* (UniGene).

1.5.2 Cten Signalling and Function

Consistent with its focal adhesion localisation, Cten has been shown to regulate cell migration and invasion. Using *in vitro* models, Cten was shown to give increased cell migration and invasion through basement membrane extract following gene expression manipulation. This functional effect has been repeatedly observed (Liao et al., 2009, Albasri et al., 2011a, Albasri et al., 2009). In an investigation of Cten's role in metastasis, intrasplenic injection of CRC cells stably transfected with Cten into nude mice revealed that a similar number of tumours were formed in the liver and spleen however, these tumours were larger than the tumours formed in the control mice. The mice that stably expressed Cten also had a shorter overall survival (Albasri et al., 2011a).

Mechanisms underlying Cten's role in migration and invasion have, to an extent, been described but the full elucidation of pathways and additional layers of complexity remain to be resolved.

1.5.2.1 Cten and Focal Adhesion Signalling

Consistent with the other Tensins, Cten signals to other focal adhesion localised proteins. FAK is a tyrosine kinase that plays a critical role in the regulation of focal adhesion dynamics. FAK is recruited to focal adhesions where it is phosphorylated and induces cell migration in complex with Src (Mitra and Schlaepfer, 2006). FAK expression is upregulated in a number of cancers including CRC (Lark et al., 2003). The forced expression and knockdown of Cten in pancreatic cancer cell lines resulted in the upregulation and downregulation of FAK protein respectively (Al-Ghamdi et al., 2013). FAK is able to bind SH2 domain containing proteins and it has previously been found to co-immunoprecipitate with Tensin 1 and it could

therefore also be possible that this molecule directly binds Cten (Yamashita et al., 2004, McLean et al., 2000). Cten expression was associated with the expression of p-FAK suggesting that it may be possible that Cten promotes FAK activation in addition to expression levels (Albasri et al., 2014).

Integrin-linked kinase (ILK) is another non-receptor protein kinase found in complex with Integrins at focal adhesions and serves both scaffold and signal transduction functions. ILK is involved in the regulation of a number of cell processes including cell migration and invasion and is often upregulated in cancers including CRC (Yan et al., 2014, Bravou et al., 2003). Manipulation of Cten expression identified ILK as a downstream signalling target. Furthermore, this interaction was found to promote cell motility as assessed by *in vitro* migration and invasion assays. Whether Cten forms a complex with ILK was not investigated (Albasri et al., 2011a).

All the Tensins, including Cten, have been shown to directly interact with DLC1, a known tumour suppressor that regulates cell adhesion and actin stress fibre assembly through downstream inactivation of RhoA and ROCK (Cao et al., 2012). The binding to DLC1 has been mapped to the PTB, SH2 and actin binding domains of the Tensin proteins (Qian et al., 2007, Cao et al., 2012). The interaction between DLC1 and Cten occurs via an S/TIYXXI/V motif in the SH2 domain of Cten. The mechanism of interaction between DLC1 and Tensin family members is well understood and is required for DLC1's focal adhesion localisation and tumour suppressive activity (Liao et al., 2007).

DLC1 comprises a sterile alpha motif (SAM), steroidogenic acute regulatory protein-related lipid transfer (START) and a catalytic Ras homology-

GTPase-activating (RhoGAP) domain. DLC1 when active, hydrolyses RhoA-GTP to RhoA-GDP thus preventing RhoA downstream signalling. DLC-1 contains an autoinhibitory mechanism in which the SAM domain binds to the RhoGAP domain preventing its suppression of RhoA. It is proposed that in resting, non-migrating cells, Tensin 3 is highly expressed and binds to DLC1 via both its SAM domain and central region via Tensin 3 actin binding domain (figure 1-6). Binding of the Tensin 3 actin binding domain to the SAM domain prevents DLC1's autoinhibitory mechanism thus, DLC1 is active and hence RhoA signalling is inhibited. However, in migrating cells, Cten expression is high and Tensin 3 expression is suggested to be low enabling Cten to displace Tensin 3 from DLC1 binding. As Cten lacks an actin binding domain, the SAM domain of DLC1 is able to bind and inhibit the Rho-GAP domain and inactivates DLC1. In its inactive state, DLC1 can no longer interact with downstream substrates exerting its tumour suppressive activity. RhoA in its active GTP bound form is able to transduce signals to downstream ROCK, thus, focal adhesion turnover and actin stress fibre remodelling is induced, promoting cell motility (Cao et al., 2012). These investigations were performed in untransformed breast cell lines however, DLC1 is often deleted in cancer and it remains to be investigated whether this mechanism also occurs in cancer (Seng et al., 2007, Ng et al., 2000).
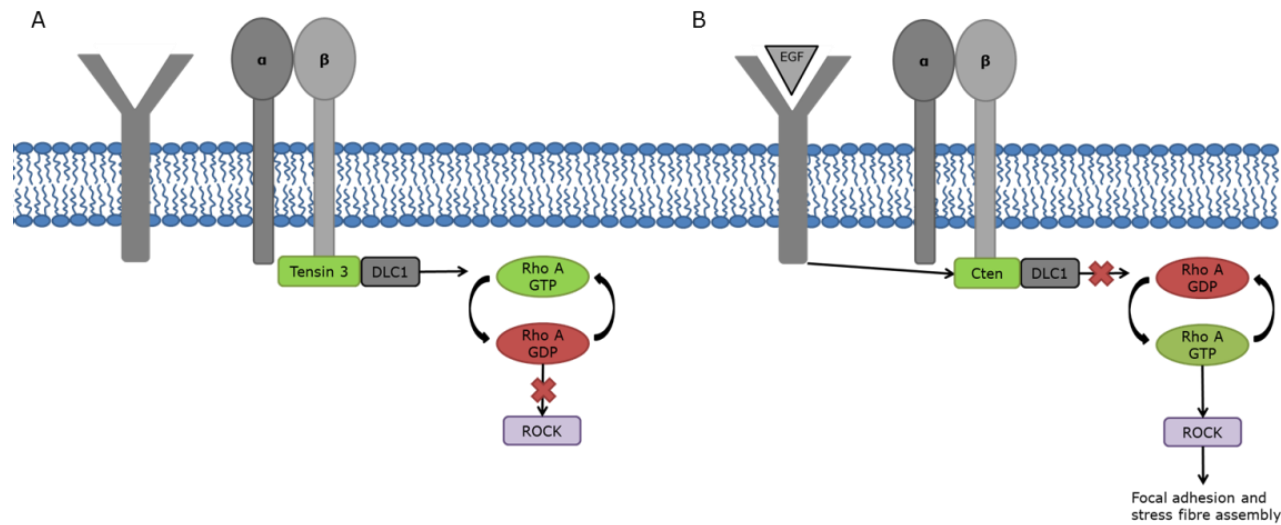
Figure 1-6: *The antagonistic regulation of cell migration by Cten and Tensin 3. A) In absence of EGFR stimulation, the ABD of Tensin 3 binds the SAM domain of DLC1 thus preventing its association and inhibition of the Rho-GAP domain. The Rho-GAP domain in its active state hydrolyses RhoA-GTP to its inactive GDP bound form, inhibiting migratory processes. B) Following EGF stimulation, Cten displaces Tensin 3 from focal adhesion sites and binds DLC1. As Cten lacks an ABD, the SAM domain of DLC1 is able to bind and inhibit the Rho-GAP domain. Since DLC1 is not active, this prevents the inactivation of RhoA thereby promoting actin remodelling through downstream ROCK (Cao et al., 2012).*

1.5.2.2 Focal Adhesion and Adherens Junction Crosstalk

In addition to the regulation of focal adhesion turnover, Cten has been linked to the regulation of components of adherens junctions. Manipulation of Cten expression revealed negative regulation of E-cadherin protein (Albasri et al., 2009). E-cadherin is a membrane receptor that links to cadherin molecules on adjacent cells to form strong cell-cell attachments. Internally, E-cadherin links to the actin cytoskeleton via p120-catenin, α-catenin and β-catenin. It is possible that Cten mediated loss of E-cadherin leads to the disruption of adherens junctions causing loss of cell attachment to surrounding cells, in addition to the loss of cell-ECM adhesion at focal adhesions. This suggests crosstalk of focal adhesions and adherens junction signalling pathways. Integrin signalling via FAK has been linked to a reduction in E-cadherin (Avizienyte et al., 2002). Additionally, ILK signalling is known to repress E-cadherin through the induction of the transcription factor Snail (Tan et al., 2001). However, Snail regulates E-cadherin at the mRNA level whereas Cten represses E cadherin at the protein level only (Albasri et al., 2009, McPhee et al., 2008). It is therefore more likely that Cten regulates the protein synthesis or degradation of E-cadherin. Cten may signal through other focal adhesion localised proteins to carry out this action including Calpain, a protease concerned with regulating motility, and shown to cleave E-cadherin (Ye et al., 2013). Alternatively, it is proposed that E-cadherin downregulation may occur through encapsulation in endocytic vesicles transporting the adhesion molecule away from the cell surface with subsequent degradation via the lysosomal pathway, a process induced upon Src expression (Palacios et al., 2005). How Cten downregulates E-cadherin remains to be investigated. Considering that the downregulation of E-cadherin is also a molecular

event associated with EMT, it is possible that Cten could regulate these pathways to promote cell migration and invasion.

E-cadherin sequesters β-catenin at adherens junctions. Following E-cadherin downregulation, release of β-catenin generates free cytoplasmic pools to cooperate in additional molecular pathways (Howard et al., 2011). β-catenin is a main component of the Wnt signalling pathway. Following activation of Wnt signalling, β-catenin translocates to the nucleus where it binds T-cell factor/Lymphoid enhancer factor (TCF/LEF) promoting transcription of target genes, which in the gastrointestinal epithelium are involved with stem cell maintenance and crypt homeostasis. Wnt signalling is frequently aberrant in CRC (Palacios et al., 2005). β-catenin had previously been found to undergo cellular redistribution on knockdown of Cten and furthermore, these two proteins were found to co-immunoprecipitate. Binding of β-catenin to Cten only occurred in the nucleus and not the cytoplasm (Barbieri et al., 2010, Liao et al., 2009). Cten and β-catenin confer increased colony formation and anchorage independent cell growth suggesting these proteins may act together to increase tumourigenicity, however, whether nuclear localised Cten promotes Wnt signalling remains to be investigated (Liao et al., 2009).

Many other focal adhesion proteins translocate to the nucleus and some are known to act as co-regulators of transcription. It is possible Cten may have a similar role regulating β-catenin/TCF/LEF activity (Dong et al., 2009, Sen et al., 2012, Liao et al., 2009). Since β-catenin is concerned with the maintenance of the normal intestinal stem cell epithelium, it is possible that Cten-β-catenin signalling could be involved in the regulation of CSC networks. CSCs are suggested to be responsible for metastatic

spread and, in addition, are associated with patient relapse and cancer recurrence following therapy (Hermann et al., 2007, Li et al., 2015). It is therefore, of upmost importance that the mechanisms regulating this cell phenotype are understood.

1.5.2.3 The Regulation of Cten

It is probable that Cten is under the regulation of a number of different cell signalling pathways. The regulation of Cten, shown in part through several different studies, appears to be under the control of the canonical EGFR-Kras-mitogen activated protein kinase (MAPK) signalling pathway. Activation of EGFR by its cognate ligand can lead to the activation of a variety of cellular processes including cell migration and this may indeed be mediated downstream by Cten and other members of the Tensin protein family. It was noted in breast cell lines that stimulation with EGF led to an increase in Cten levels and this effect was abolished by inhibition of MAPK signalling. EGF stimulation induced actin stress fibre reorganisation however, depletion of Cten disrupted actin fibre networks despite the presence of EGF suggesting that Cten acts downstream of EGF to regulate actin dynamics. EGF-Cten signalling was also associated with cell scattering. (Katz et al., 2007). The regulation of Cten by EGF and MAPK signalling was confirmed by others in hepatocellular carcinoma. Stimulation with EGF induced Cten expression which was subsequently abolished following the inhibition of MAPK signalling (Chan et al., 2015).

Kras, which is often located downstream of the EGFR, was also shown to be a regulator of Cten in colorectal cell lines. Downregulation of Cten was shown after Kras knockdown. Cten levels were not affected by Kras knockdown in cells containing mutant *BRAF* but Braf knockdown gave a

reduction in Cten expression suggesting that a Kras-Braf-Cten pathway exists (Al-Ghamdi et al., 2011). *EGFR* mutations are not common in CRC but *KRAS* and *BRAF* mutations occur in approximately 50% of tumours (Vaughn et al., 2011). A direct functional relevance between Kras and Cten was also demonstrated as ectopic expression of Cten following Kras knockdown was able to restore any loss in cell motility. Similar effects were also observed upon repetition of these experiments in pancreatic cancer cell lines, selected on the basis of high *KRAS* mutation. Other mechanisms of regulating Cten must exist as some *KRAS/BRAF* wild type cell lines also show high levels of Cten expression (Al-Ghamdi et al., 2011).

Phosphatidylinositol 3-Kinase (PI3K) signalling is activated by receptor tyrosine kinases and can be mediated dependently or independently of Kras signalling. Signalling downstream to Akt can regulate a number of cellular pathways. PI3K signalling was shown to be another main signalling pathway inducing Cten expression. The stimulation of cells with a number of growth factors and cytokines including EGF, Fibroblast growth factor 2 (FGF2), Insulin-like growth factor 1 (IGF-1), Transforming growth factor beta (TGF-β), Nerve growth factor (NGF), Platelet-derived growth factor (PDGF), Interleukin 13 (IL-13) and Interleukin 6 (IL-6) induced Cten expression in a CRC and an untransformed prostate cell line. Stimulation together with inhibition of PI3K inhibition prevented the upregulation of Cten through all of these pathways except through IGF-1 which may signal independently of the PI3K pathway (Hung et al., 2013). How PI3K signalling influences Cten function remains to be studied.

Signalling through the Signal transducer and activator of transcription factor 3 (Stat3) is reported to be involved in inducing Cten expression.

Stat3 was first shown to upregulate Cten expression levels in mouse breast models. This led to an earlier onset and more invasive tumours in knock in mice displaying constitutively active Stat3. Induction of Cten expression could be stimulated by EGFR activation or by the cytokine IL-6 via Stat3 (Barbieri et al., 2010). Stat3 also acts downstream of Src and although at present Src has not been linked to Cten, it is implicated in the regulation of the other Tensin proteins (Davis et al., 1991). This has also been confirmed in lung cancer cell lines whereby inhibition of Stat3 signalling abrogated EGFR induced Cten expression (Bennett et al., 2015). Furthermore, inhibition of Janus kinase (JAK) signalling was shown to downregulate Cten expression. JAK signalling through to Stat3 may also regulate Cten expression (Hung et al., 2013).

A number of Cten regulatory factors have been described. Those pathways identified are commonly overexpressed or mutated to a constitutively active form in many tumour types. In particular, *KRAS*/*BRAF* mutations are prevalent in colorectal tumours as is PI3K pathway signalling and, thus, in turn may be responsible for elevated levels of Cten since no mutations in the *CTEN* gene or epigenetic mechanisms of upregulation have been described (Davies et al., 2002, Salhab et al., 1989).

1.6 Aims and Hypothesis

It is evident that Cten plays a role in CRC progression, possibly through the promotion of metastasis, however, the underlying signalling mechanisms are largely unknown. The aims of this present study were to investigate the mechanisms of Cten signalling and how this contributes to CRC progression.

1. Ascertain the significance of nuclear localised Cten.

Cten localises to the nucleus and this localisation was more prevalent in liver metastases. It was therefore hypothesised that Cten in the nucleus may enhance the oncogenic activity of Cten. Cten binds to β-catenin in the nucleus, and aberrant β-catenin signalling is common in CRC, thus, it was further hypothesised that Cten could act as a β-catenin transcriptional co-factor to mediate this effect. Since β-catenin regulates the stem cell compartment in the intestinal epithelium, the ability of Cten to interact with β-catenin to induce the transcription of stem cell related genes was investigated.

2. Determine whether Cten is a target of EGFR signalling and promotes cell motility through a Tensin switch mechanism in CRC.

CRCs display high levels of *KRAS* mutations, rendering EGFR targeted therapies ineffective. Cten is a target of Kras signalling in CRC and since Cten is regulated by EGFR signalling in other tumour types, it was hypothesised that Cten could be regulated by EGFR-Kras signalling in CRC. Cten lies downstream of Kras signalling and therefore could be a putative therapeutic target against CRC.

3. Decipher Cten's role in EMT signalling.

Due to Cten's localisation at focal adhesions and interaction with other focal adhesion localised proteins, it is likely that Cten regulates focal adhesion dynamics to induce cell motility. In addition, Cten regulates E-cadherin. It was hypothesised that Cten could induce cell migration through EMT pathways and that this could promote metastasis in CRC.

2 Materials and Methods

2.1 Cell Culture

All work was undertaken in CRC cell lines RKO, HCT116, SW480, SW620, Caco-2, DLD1 and C32, which were a kind gift from Prof Ian Tomlinson (table 2-1). The identity of these cell lines was validated by high resolution melting (HRM) analysis of mutation profiles (table 9-1 and figures 9-1 – 9-7).

2.1.1 Cell Maintenance

Cells were maintained at 37°C in a 5% CO_2 environment and cultivated in Dulbecco's Modified Eagle's Medium (DMEM) (Thermo Fisher Scientific) supplemented with 10% foetal bovine serum (FBS) (Sigma) and penicillin (0.1 mg/ml) and streptomycin (100 units/ml) (Sigma) under sterile conditions. Microscopic examination of the cells was used to assess cell viability and ensure cultures remained free of bacterial and fungal infections. Cells were fed twice weekly by discarding the media and replacing with fresh DMEM (containing FBS and penicillin/streptomycin).

2.1.2 Passaging Cells

Cells were passaged when 70-80% confluency was reached. Media was removed and cells washed twice with phosphate buffered saline (PBS). Cells were incubated for up to 5 minutes with 1 ml of trypsin EDTA (Sigma) until they were completely detached from the flask surface. The trypsin was neutralised by the addition of 9 ml of DMEM (containing FBS and penicillin/streptomycin). Cells in suspension were pelleted by centrifugation at 1,500 rpm for 5 minutes, the media discarded and the cells resuspended in a volume of media dependent upon the split ratio (i.e. 10 ml for a 1:10

split ratio). One ml cell suspension was transferred to a new flask containing 12 ml of DMEM (containing FBS and penicillin/streptomycin).

Cell Line	Dukes' Stage	Differentiation	Origin	MSI Status	CIN	*KRAS*	*BRAF*	*PIK3CA*	*PTEN*	*TP53*
HCT116	D	Well	Colon	MSI	No	G13D	wt.	H1047R	wt.	wt.
RKO	C	Poor	Colon	MSI	No	wt.	V600E	H1047R	wt.	wt.
Caco-2	B	Well	Colon	MSS	Yes	wt.	wt.	wt.	wt.	E204X
SW620	C	Moderate	Lymph node	MSS	Yes	G12V	wt.	wt.	wt.	R273H;P309S
DLD1	C	Moderate	Colon	MSI	No	G13D	wt.	E545K;R233X	wt.	S241F
SW480	B	Moderate	Colon	MSS	Yes	G12V	wt.	wt.	wt.	R273H;P309S
C32	C	Well	Colon	MSS	Yes	wt.	wt.	wt.	wt.	wt.

Table 2-1: *CRC cell line characteristics.*

2.2 Plasmid Preparation

2.2.1 Plasmid Transformation

Plasmid expression vectors were used to forcibly express the required protein. The pEGFP-C1 plasmid (CLONETECH laboratories Inc.) inserted with Cten was kindly donated by Prof Su Hao Lo and the pEGFP-N1 plasmid containing NLS-Cten was kindly provided by Dr Maham Akhlaq. The TOP-flash, FOP-flash and Renilla expression constructs were kindly donated by Dr Abdolrahman Shams Nateri. The Cten targeting CRISPR construct was purchased from Sigma.

Plasmids were transfected into NEB 5-alpha Competent E. coli cells (New England Biolabs) using the heat shock method. Five µl of plasmid was incubated with 50 µl of competent cells and placed on ice for 30 minutes. Following this, the cell/plasmid mix was placed in the water bath for 45 seconds at 42°C before being placed back on ice for 2 minutes. One ml of SOC Outgrowth Medium was added and the cells incubated on a shaker (200 rpm) for 1 hour at 37C°. The cells were then centrifuged at 13,000 rpm for 2 minutes, 700 µl of the supernatant removed and the cells resuspended in the remaining 300 µl. The cells were transferred to agar plates (20 ml of LB agar containing 50 µg/ml kanamycin or ampicillin) using aseptic technique and colonies allowed to grow overnight at 37°C.

Following incubation, 1 colony was picked by dipping a 10 µl pipette tip into the colony and the bacteria seeded into 5 ml of LB broth supplemented with 50 µg/ml kanamycin (called minipreps). This was incubated overnight at 37°C on a shaker (200 rpm) to allow the bacterial colony to expand. The miniprep was transferred into a midiprep mix of 100 ml LB broth (containing kanamycin or ampicillin, 50 µg/ml) and incubated

overnight at 37°C on a shaker (200 rpm). The following morning, the bacterial cells were pelleted by centrifugation at 5,000 x g for 15 minutes.

2.2.2 Plasmid Purification

Midiprep plasmid purification was performed using the Genelute Plasmid Midiprep kit (Sigma) in accordance with the manufacturer's instructions. The bacterial cell pellet was resuspended in 4 ml of chilled Resuspension/RNase A Solution followed by alkaline lysis by the addition of 4 ml of Lysis Solution. The contents were inverted 6 times and incubated for 4 minutes. Four ml of chilled Neutralisation Solution was added, inverted 6 times and subsequent to this 3 ml of binding solution was added and inverted twice. The lysate was transferred to the barrel of the filter syringe and left to sit for 5 minutes at room temperature. To prepare the Midi-Prep column, 4 ml of Column Preparation Solution was added, centrifuged at 3,000 xg for 2 minutes and the eluate discarded. Following this, half of the cell lysate was expelled into the Midi-Prep column, centrifuged at 3,000 xg for 2 minutes and the eluate discarded. This process was repeated with the remainder of the cell lysate. Columns were then washed by the addition of 4 ml of Wash Solution 1 to the column followed by centrifugation at 3,000 xg for 2 minutes and the eluate discarded. This process was then repeated with Wash Solution 2. To elute the plasmid, the binding column was transferred to a new collection tube, 1 ml of Elution Solution added followed by centrifugation at 3,000 xg for 5 minutes. The DNA was quantified using the NanoDrop system (Thermo Fisher Scientific).

Following quantification, 0.5 µg of each DNA sample in a volume of 10 µl together with DNA loading buffer (Promega) were run alongside 5 µl of 1kb

DNA ladder (Promega) on a 1% agarose gel containing SYBR Safe at 100 V for 50 minutes. Products were viewed using a gel documentation viewing system.

2.3 Mammalian Cell Transfection

2.3.1 Gene Forced Expression

Lipofectamine 2000 (Thermo Fisher Scientific) was used to transfect the plasmid into the target cell. To optimise the transfection process, Lipofectamine 2000 volumes of 5-20 µl were incubated together with 2-8 µg of the expression construct. The transfection efficiency was assessed by flow cytometry according to Green fluorescent protein (GFP) expression. The condition that gave the greatest protein expression for plasmid transfection was considered optimal. For NLS-Cten, Cten and empty vector constructs, 5 µg of plasmid DNA together with 10 µl Lipofectamine 2000 was considered optimal. For the CRISPR-Cas9 construct, 4 µg of plasmid was added to cells together with 5 µl of Lipofectamine 2000.

The transfection procedure was performed according to the manufacturer's protocol using the optimised conditions determined. Transfection was usually performed in a 6-well plate in a total volume of 2 ml. For plasmid forced expression, cells were transfected at 60-70% confluency. Twenty four hours post seeding in the usual DMEM growth media, the media was replaced with 1.5 ml of Opti-MEM reduced serum media and cells incubated at 37ºC for 1 hour. For each condition, the optimised volume of Lipofectamine 2000 was added to 250 µl of Opti-MEM and incubated for 5 minutes. The optimal plasmid concentration was added to 250 µl of Opti-MEM. Following this, the diluted Lipofectamine 2000 and plasmid mixes

were combined to give a total volume of 500 µl. These were incubated for 20 minutes at room temperature and following this, added dropwise to the cells. The cells were incubated with the transfection reagents for 6 hours, the media replaced and experimentation performed 24 hours post transfection.

The transfection of TOPflash, FOPflash and Renilla plasmids was performed in a 24 well plate in a total volume of 500 µl. Twenty four hours post seeding, DMEM was replaced with 300 µl of Opti-MEM and incubated for 1 hour at 37°C. Following this, 2.5 µl of Lipofectamine 2000 was diluted in 100 µl of Opti-MEM and incubated for 5 minutes. Either 1.25 µg of Cten or empty vector plasmids together with 0.4 µg of TOPflash or FOPflash plasmids and 0.05 µg of Renilla plasmid were diluted in 100 µl of Opti-MEM. Lipofectamine 2000 and plasmid mixes were combined to give a total volume of 200 µl and incubated for 20 minutes. Following incubation, the transfection reagents were added dropwise to the cells. Transfection reagents were replaced with DMEM after 6 hours and experimentation performed 36 hours post transfection.

2.3.2 Gene Knockdown

siRNA duplexes (Thermo Fisher) were used for gene knockdown and transfection was performed according to the protocol for plasmid transfection. To optimise, Lipofectamine 2000 volumes of 5-20 µl were incubated together with 50-200 nM of siRNA duplexes (table 2-1). The transfection efficiency was assessed by western blot and the condition that gave the greatest reduction in protein, whilst using the minimal siRNA concentration, was considered optimal. For FAK knockdown, 50 nM of

siRNA was transfected together with 5 µl of Lipofectamine 2000. For the knockdown of Kras, Cten and Snail 100 nM of siRNA was transfected together with 5 µl of Lipofectamine 2000. Luciferase targeting siRNA was used as a control and transfected at the same concentration as the target siRNA.

Transfection was performed in a 6-well plate in a total volume of 2 ml. For siRNA knockdown, cells were transfected at 40-50% confluency. Twenty four hours post seeding in DMEM, the cells were incubated with 1.5 ml of Opti-MEM at 37ºC for 1 hour. For each condition, the optimised volume of Lipofectamine 2000 was added to 250 µl of Opti-MEM and incubated for 5 minutes. The optimised concentration of siRNA was added to 250 µl of Opti-MEM. Following this, the diluted Lipofectamine 2000 and siRNA mixes were combined to give a total volume of 500 µl. These were incubated for 20 minutes and following this, added dropwise to the cells. The cells were incubated with the transfection reagents for 6 hours and experimentation performed 48 hours post transfection.

siRNA target	Sequence
Cten	UUCUCAUUGACAUGGUGCUCUGGGC
Snail	CCUUCUCUAGGCCCUGGCUGCUACA
FAK	GAUGUUGGUUUAAAGCGAU
Kras	CAGGGUGUUGAUGAUGCCUUCUAUA
Luciferase	CGUACGCGGAAUACUUCGA

Table 2-2: siRNA sequences.

2.3.3 Co-transfection

For co-transfection, in which both forced expression and knockdown were required in the same experiment, cells were transfected at 50% confluency. For each condition, 10 µl of Lipofectamine 2000 was added to 250 µl of Opti-MEM and incubated for 5 minutes. The optimal plasmid and siRNA concentrations were added together to 250 µl Opti-MEM. Following this, the diluted Lipofectamine 2000 and plasmid/siRNA mixes were combined to give a total volume of 500 µl. These were incubated for 20 minutes at room temperature and following this, added dropwise to the cells. The cells were incubated with the transfection reagents for 6 hours and experimentation performed 48 hours post transfection.

2.4 Cell Treatments

2.4.1 EGF Stimulation

Cells were treated with EGF to stimulate signalling through the EGFR. Cells were seeded and allowed to adhere for 3 hours. Following this, the cells were starved in serum free DMEM (supplemented with penicillin/streptomycin) for 24 hours prior to stimulation. Cells at 60-70% confluency were treated with 0-80 ng/ml recombinant EGF (Thermo Fisher Scientific) under serum free conditions. Cells were harvested after incubation for 24 hours.

2.4.2 Cycloheximide

Cycloheximide (CHX) is an inhibitor of protein translation. Cells were treated with CHX to assess changes in protein stabilisation. Twenty four hours post cell transfection, the media in all wells was replaced with fresh DMEM (supplemented with FBS and penicillin/streptomycin). Cells were

incubated with DMEM containing 100 µg/ml CHX for 0-16 hours dependent upon the half-life of the protein. Cells were harvested at the same time point following incubation and western blotting performed.

2.5 Western Blotting

2.5.1 Protein Extraction and Quantification

Western blotting was performed to quantify protein expression. To prepare cell lysates, the media was removed from the cells and following this, the cells were washed with PBS. Cell lysates were prepared using ice-cold radio immunoprecipitation assay (RIPA) buffer (Thermo Fisher Scientific) supplemented with phosphatase and protease inhibitor (Thermo Fisher Scientific), added to the cells and incubated on ice for 15 minutes. Following this, cell lysates were centrifuged at 13,000 rpm at 4^0C for 30 minutes and the supernatant retained.

The bicinchoninic acid (BCA) assay (Thermo Fisher Scientific) was used for protein quantification and performed according to manufacturer's protocol. One hundred µl of BCA reagent was added to 12.5 µl of either the protein or albumin standard in a 96 well plate and incubated for 30 minutes at 37ºC. The absorbance was measured at 550 nm using the Multiskan EX plate reader (Thermo Fisher Scientific). Protein concentrations were determined from a standard curve of protein standards of known concentrations.

2.5.2 SDS-PAGE Gel and Western Blot

NUPAGE LDS Sample Buffer (Thermo Fisher Scientific) containing 5% β-mercaptoethanol was added to 50 µg of protein. The protein samples were

heated at 90^{0}C for 5 minutes, incubated on ice for 5 minutes and following this, centrifuged at 13,000 rpm for 2 minutes. Proteins were run on pre-cast 4-12% NUPAGE Bis-Tris-HCl buffered (pH 6.4) polyacrylamide gel (Thermo Fisher Scientific) using the NUPAGE gel electrophoresis system with NUPAGE MOPS SDS Running Buffer (Thermo Fisher Scientific) at 125 V for 90 minutes. PVDF membrane (GE Life Sciences) was activated in methanol for 10 seconds. Proteins were transferred onto the PVDF membrane using the NUPAGE Transfer Buffer (Thermo Fisher Scientific) and the Trans Blot semi-dry transfer system (Biorad) at 20 V for 30 minutes.

Membranes were blocked for 40 minutes with gentle rotation at room temperature in solutions of 5% milk or 5% bovine serum albumin (BSA) in 0.1% tween PBS (PBS-T) or 0.1% tween TBS (TBS-T) (dependent on the antibody diluent). Following blocking, the membrane was incubated with the primary antibody overnight with gentle rotation at 4°C (table 2-2). Membranes were washed 3 times in PBS-T or TBS-T for 5 minutes at room temperature and following this, they were incubated with the appropriate horseradish peroxidase (HRP) labelled anti-rabbit or anti-mouse secondary antibody (Sigma) for 1 hour at room temperature. Following this, the membranes were washed twice in PBS-T/TBS-T and once in PBS/TBS each for 5 minutes at room temperature.

To enable detection of the bound antibody, the membrane was incubated for 5 minutes with ECL Prime detection solution (GE Life Sciences). The membrane was exposed to film (GE Life Sciences) for 1 second to 1 minute depending on the signal strength and passed through the developer solution (Sigma), fixer (Sigma) and then rinsed in water.

Antibody	Supplier	Primary dilution	Secondary dilution	Diluent
Actin	Sigma	1:50,000	1:30,000	Milk PBS
Cten	Sigma	1:20,000	1:10,000	Milk PBS
E-cadherin	Cell Signalling	1:1,000	1:10,000	BSA TBS
FAK	Cell Signalling	1:5,000	1:10,000	BSA TBS
KLF4	Cell Signalling	1:1,000	1:10,000	BSA TBS
Kras	Abcam	1:250	1:10,000	Milk PBS
N-cadherin	Abcam	1:500	1:10,000	BSA TBS
Snail	Cell Signalling	1:1,000	1:10,000	Milk TBS
Tensin 3	Sigma	1:1,000	1:10,000	Milk PBS
Vimentin	Cell Signalling	1:1,000	1:10,000	BSA TBS
β-catenin	Enzo	1:200	1:10,000	Milk PBS

Table 2-3: *Optimised antibody conditions for western blotting.*

2.6 Co-immunoprecipitation

Binding interactions between proteins were investigated using co-immunoprecipitation (co-IP). Cell lysates were first subjected to a pre-clearing stage to reduce non-specific binding. The protein (1 ml) was incubated with 20 µl of Protein G/A agarose beads (Calbiochem IP05) at 4°C with gentle rotation for 30 minutes. The lysate was centrifuged at 4°C at 13,000 rpm for 5 minutes to pellet the beads and the supernatant retained. 1 µg of β-catenin (10 µl), Snail (4 µl) or Cten (2 µl) antibody was added to 300 µg of the pre-cleared lysate and incubated rotating overnight at 4°C. In addition, 300 µg of pre-cleared lysate (without antibody) was also incubated with the pre-cleared beads for the negative control.

Following incubation, 30 µl of the Protein A/G beads were added to the reactions and incubated on a rotator for a further 24 hours at 4°C. The beads were pelleted by centrifugation at 13,000 rpm at 4°C for 5 minutes and washed twice in ice cold PBS. The sample was resuspended in 10 µl 3X NUPAGE loading Buffer and heated at 95° for 5 minutes, kept on ice for 5 minutes and centrifuged for 2 minutes at 13,000 rpm before loading onto an SDS gel for western blot analysis. Fifty µg of protein was loaded for the input.

2.7 qRT-PCR

2.7.1 Primer Design

Primers for qPCR were designed where possible to cover exon boundaries and amplify all protein coding transcript variants using the Universal Probe Library software (Roche, http://www.universalprobelibrary.com) or, if there were no suitable primer sets, Primer Basic local alignment search tool (BLAST) (NCBI, http://www.ncbi.nlm.nih.gov/tools/primer-blast) was used (table 2-3). Tensin 3 primer sequences were those used previously by Cao and colleagues (Cao et al., 2012). Primer specificity was checked against the Refseq mRNA database using Primer BLAST. Melting temperature (Tm), GC content and self-complementarity were also assessed using Primer BLAST.

Target Gene	Forward Primer Sequence	Reverse Primer Sequence
HPRT	AAATTCTTTGCTGACCTGCT	TCCCCTGTTGACTGGTCATT
CTEN	GCGTCTGCTCAGAATCGAC	GATGAGGAAGTGTCGGATGG
KLF4	GGGAGAAGACACTGCGTCA	GGAAGCACTGGGGGAAGT
LGR5	CCCTTCATTCAGTGCAGTGTT	ATTCTGATCAGCCAGCCATC
SOX4	CCAACTCCTTAGTGCCGATT	CCTCTCCTACAATGCAAAGCA
NANOG	CCAGCTGTGTGTACTCAATGATAGAT	TGTTGGAGAGTTCTTGCATCTG
SOX2	AAGGGGGAAAGTAGTTTGCTG	AGCCTGGGGCTCAAACTT
OCT4	AGCGACTATGCACAACGAGA	CCAGAGGAAAGGACACTGGT
TENSIN 3	GTTGAAAGGGTGCTCGAATGA	GAACTTTCTGCTATTTCCTCCAATG

Table 2-4*: qPCR primer sequences.*

2.7.2 RNA Extraction

RNA extraction was performed using the Mammalian Total RNA Mini-prep kit (Sigma) according to the manufacturer's recommended protocol. Two hundred and fifty µl of Lysis buffer containing 1% β-mercaptoethanol per well was added to cells grown in a 6 well plate. The lysate was collected and homogenised in a filtration column for 2 minutes at 13,000 rpm and following this 250 µl of 70% ethanol was added to the lysate and mixed by pipetting. The sample was transferred to a binding column, centrifuged at 13,000 rpm for 15 seconds and the flow through discarded. The spin column was placed back in the collection tube and 250 µl of Wash 1 buffer was added. The sample was centrifuged at 13,000 rpm for 15 seconds, the flow through discarded and the collection tube replaced. A master mix of DNaseI (10 µl per column) and buffer (70 µl per column) was prepared and

mixed by inversion. Eighty µl of this was added directly to the column and incubated at room temperature for 15 minutes. Two hundred and fifty µl of Wash 1 buffer was added to the column, centrifuged at 13,000 rpm for 15 seconds, the flow through discarded and the collection tube replaced. Five hundred µl of Wash 2 buffer (containing ethanol) was added to the column, centrifuged at 13,000 rpm for 15 seconds and the flow through again discarded and the collection tube replaced and repeated again with 500 µl of Wash 2 buffer and centrifuged for 2 minutes. The column was then centrifuged at 13,000 rpm for 1 minute and following this placed in a 1.5 ml collection tube. Fifty µl of RNase free H_2O was added directly to the spin column membrane and centrifuged at 13,000 rpm for 1 minute to elute the RNA. The RNA was quantified using the NanoDrop system.

2.7.3 Reverse Transcription

For cDNA synthesis, 0.5 µg of random hexamers (Thermo Fisher Scientific) and 1 µg of RNA was made up to a total volume of 15 µl with nuclease free H_2O. This was incubated at 70°C for 5 minutes to remove secondary structure and immediately placed on ice for a further 5 minutes. Following this, each RNA sample was incubated with M-MLV RT Buffer (Thermo Fisher Scientific), dNTPs (0.5 mM) (Thermo Fisher Scientific) and M-MLV Reverse Transcriptase (200 U) (Thermo Fisher Scientific) made up to 25 µl and prepared as a master mix. Reverse transcriptase negative (RT-) samples, in which the enzyme was omitted, were also prepared for each sample. Reactions were incubated at 37°C for 1 hour to allow strand synthesis, followed by 95°C for 10 minutes. cDNA was diluted 1:10 with nuclease free H_2O prior to gene quantification.

2.7.4 qPCR

The annealing temperature was optimised for each primer set using gradient PCR. The reaction comprised Go Taq DNA Polymerase (Promega), 250 nM of the forward and reverse primers (Eurofins) and 10% cDNA in a total volume of 10 µl. The reaction comprised a run cycle of 95 °C for 2 minutes, 40x (95°C for 30 seconds, 60°C +/- 10°C for 30 seconds, 72°C for 30 seconds) and 72°C for 10 minutes using the Primus 96 thermocycler (MWG Biotech Inc.). The products were run on a 2% agarose gel containing SYBR Safe along with a 100 bp ladder (Promega). The temperature that gave the greatest specific product together with an absence of non-specific products was considered optimal.

Following annealing temperature optimisation, the efficiency of the reaction was determined using a standard curve. The reaction was prepared as before, using serial dilutions of cDNA template. qPCR was performed on the 7500 Fast Real-Time PCR System (Applied Biosystems) and the reaction cycle was as follows, a 95°C for 2 minutes holding stage followed by 40x (95°C for 3 seconds, optimised annealing temperature for 30 seconds). This was followed by the melt curve stage from 60-95°C. Reactions with efficiencies of 90-110% were deemed acceptable. If reaction efficiencies were obtained outside of this range, magnesium (2-4 mM) and primer concentrations (50-350 nM) were optimised until the reactions were displaying this range of efficiency.

Following optimisation, qPCR was performed by scaling the reaction up to a total volume of 30 µl. qPCR was performed on the 7500 Fast Real-Time PCR System and the reaction cycle was as follows, 95°C for 2 minutes holding stage followed by 40 X (95°C for 3 seconds, optimised annealing

temperature for 30 seconds). RT- controls were run for each sample and no template controls were run for each target gene. Each sample was run in triplicate. Since the reactions were determined to have similar efficiencies, the $2^{-\Delta\Delta Ct}$ method was used for gene quantification. The expression of Hypoxanthine phosphoribosyl-transferase (*HPRT*) was used for gene normalisation.

2.8 Fluorescence Microscopy

2.8.1 GFP-tagged Cten

Cells were seeded on coverslips in 6 well plates and harvested 24 hours post transfection. Cells were washed in PBS for 5 minutes on a shaker and fixed with 10% formalin for 5 minutes. The cells were subject to a further 2 wash stages and stained with DAPI (1 µg/ml) for 5 minutes and again washed with PBS. The treated coverslips were mounted with 10 µl of Fluorescein mounting media (Sigma) on glass slides. Cells were viewed under the Leica DMRB upright fluorescence microscope using the FITC (488 nm) and DAPI (405 nm) filters at x63 objective.

2.8.2 Phalloidin Staining

Cells were seeded on coverslips in 6 well plates and stained 24 hours post transfection. Cells were washed with PBS and following this fixed in 4% paraformaldehyde for 10 minutes. Cells were subjected to a further 3 washes in PBS then permeabilised in 0.1% Triton X-100 for 10 minutes at room temperature. The cells were washed a further 2 times in PBS and incubated with fluorescently labelled phalloidin (1:10,000) (Thermo Fisher) and Dapi (1 µg/ml) for 15 minutes at room temperature. Following this, the cells were washed a further 2 times in PBS and mounted on a glass

slide in 70% glycerol/PBS. The cells were viewed using the Zeiss LSM 710 confocal microscope using the FITC (488 nm), DS red (583 nm) and DAPI (405 nm) filters at x40 objective. Zen software (Zeiss) was used for image acquisition.

2.9   Flow Cytometry

Flow cytometry was used to quantify GFP expressing cells following transfection. Cells were harvested by trypsinisation (see 2.1.2) 24 hours post transfection and resuspended in 500 µl PBS. The quantification of Cten transfected cells was performed using the Coulter Altra Flow Cytometer (Beckman Coulter). The argon laser (488 nm) was used to detect GFP expressing cells. Weasel software (version 3.0.2) was used for data analysis. Cells were first gated to exclude any cell debris. Gates were applied to detect GFP expressing cells using untransfected cells as a negative control.

2.9.1 Cell Sorting

Both Cten and Cten targeting CRISPR-Cas9 transfected cells were sorted for downstream experiments based on the expression of a GFP tag. Following transfection, cells were trypsinised and resuspended in 500 µl of PBS. GFP expressing cells were sorted using the 488 nm argon laser of the MoFlo cell sorter (Beckman Coulter). As with standard flow cytometry, cells were gated to exclude any cell debris and then the expression of GFP in untransfected cells was used as a cut-off to gate the GFP expressing cells in the transfected samples. Weasel was used for data analysis.

2.10 CRISPR-Cas9 Gene Editing

2.10.1 Clonal Expansion of CRISPR Transfected Cells

CRISPR-Cas9 genome editing was used to create a Cten knockout SW620 cell line. The CRISPR-Cas9 construct targeted exon 3 of Cten (CCGCCAGATCAAGGTGCCACGA). Following transfection of the CRISPR-Cas9 construct in SW620 cells (see 2.3.1), single GFP expressing cells were sorted into 96 well plates (see 2.9.1) and clonally expanded over a 28 day period until cell growth was sufficient for passage into a T75 flask.

2.10.2 Confirmation of Gene Knockout

2.10.2.1   DNA Extraction

DNA was extracted from the CRISPR-Cas9 transfected cells using the Mammalian Genomic DNA Miniprep kit (Sigma), used according to the manufacturer's instructions. Briefly, $5x10^6$ cells were pelleted and resuspended in 200 µl of Resuspension solution followed by RNase treatment with 20 µl of RNase A Solution for 2 minutes at room temperature. Following this 20 µl of Proteinase K was added and 200 µl of Lysis solution to lyse the cells. Five hundred µl of Column Preparation Solution was added to a Genelute column and centrifuged at 12,000 xg for 1 minute and the flow through discarded. Two hundred µl of ethanol was added to the cell lysate and vortexed before loading onto the column. The sample was centrifuged at 12,000 xg for 1 minute and placed in a new collection tube. The sample was washed by adding 500 µl of Wash Solution and centrifuged at 12,000 xg for 1 minute and then was placed in a new collection tube. This was followed by a second wash with centrifugation for 3 minutes. The column was then centrifuged at 12,000 xg for 1 minute and

placed in a new collection tube. Two hundred µl of Elution Solution was added to the membrane and incubated for 5 minutes and then centrifuged for 1 minute at 12,000 xg. DNA was quantified using the NanoDrop.

2.10.2.2   PCR

The region of the Cten gene around the CRISPR-Cas9 target site was amplified by PCR using Hotshot Mastermix (Clent Life Science), 625 nM forward and reverse primers (table 2-4), 10% LC green (BioFire Defense) and 1 ng/µl of the DNA template. The run cycle was as follows: 95°C for 5 minutes followed by 45x (95^{0}C for 20 seconds, 70°C for 45 seconds, and 72^{0}C for 30 seconds) followed by an extension stage at 72^{0}C for 2 minutes and was performed using the Primus 96 thermocycler. The PCR products were run on a 2% agarose gel containing SYBR Safe and visualised using a gel documentation viewing system.

Target Gene	Forward Primer Sequence	Reverse Primer sequence
CTEN	AGGGAGGGTGACTGGAACTG	GAGAGACACGAAGCAGCAGT

Table 2-5: *PCR primer sequences used in the preparation of the Cten knockout SW620 cells.*

2.10.2.3   High Resolution Melting

Confirmation of mutation at the target region was determined using HRM. HRM identifies a change in the DNA sequences as a result of a shifted melting profile. Products were melted using the LightScanner (BioFire Defense) and HR1 High Resolution Melter (Idaho Technology Inc.)

instruments. Ten µl of PCR product was added to 10 µl of mineral oil and melted over a range of 68-95ºC with a temperature increase of 0.3ºC/second. The melt curves were analysed using the HR1 or LightScanner Instrument and Analysis software packages. Those cell populations displaying an altered melt curve profile compared to wild type SW620 cells (>4% change in fluorescence) were considered to contain a mutation.

2.10.2.4   TA Cloning and Blue White Screening

To isolate each Cten allele for subsequent sequencing, the PCR product was inserted into a plasmid expression vector using the TOPO TA cloning kit (Thermo Fisher Scientific), according to the manufacturer's instructions. Briefly, 4 µl of the PCR product was incubated with 1 µl of Salt Solution and 1 µl of the TOPO vector. The reaction was incubated at room temperature for 5 minutes and following this placed on ice.

Blue white screening was performed to select for recombinants. The plasmid transformation was carried out as described in section 2.2 however, the agar plates were coated with 40 µl of 5-Bromo-4-chloro-3-indolyl β-D-galactopyranoside (X-gal) (Sigma) at a concentration of 20 mg/ml. White colonies (recombinants) were picked for subsequent miniprep preparation and purification.

2.10.2.5   Sanger Sequencing

Sequencing was performed by the University of Nottingham Sequencing Facility using the 3130xl ABI PRISM Genetic Analyser (Thermo Fisher Scientific). Sequencing results were analysed using Chromas Lite and

compared to the Cten gene reference sequence (NC_000017.11) to determine whether a mutation in the Cten sequence had occurred.

2.11 Deletion Mapping

2.11.1 Primer Design

In order to map the region of Cten responsible for binding to β-catenin, deletion mapping of the Cten protein was planned. Initially large deletions of the N-terminus and the C-terminus were planned (figure 2-1). Primers were designed to enable the deletion of regions of the Cten sequence from the pEGFP-C1 plasmid which contained the Cten protein coding sequence (165-2313 of the Cten transcript sequence NM_032865.5) (table 2-5). Primers were designed to create a construct that comprised only the N-terminal region of Cten, with the deletion of amino acids 1300-2313, designated Cten$^{\Delta C1300-2313}$. The second construct comprised the C terminus of the Cten protein sequence with deletion of residues 165-1289 and designated Cten$^{\Delta N165-1289}$ (table 2-5).
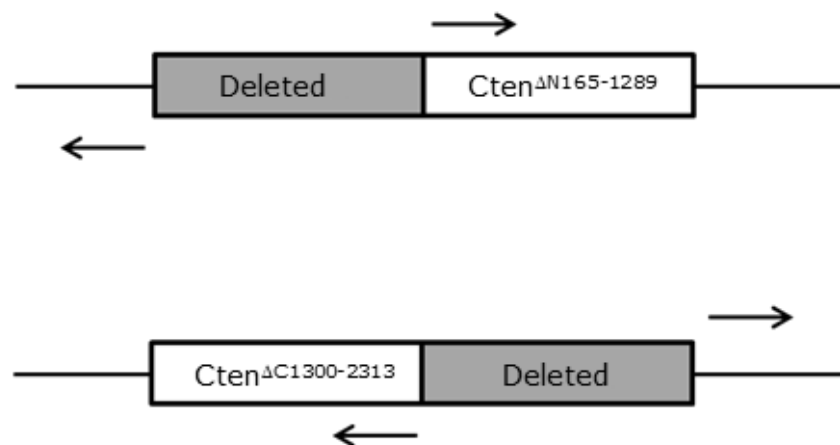
Figure 2-1: *Diagrammatic representation of the primer positions used to create the deletion mapping constructs.*

Primer	Forward sequence	Reverse sequence
Cten$^{\Delta C1300-2313}$	TTCGAATTCGATGTCCCAGG TGATGTCCAG	CCGTTGATCAGCACAATGG GTATGTCCACC
Cten$^{\Delta N165-1289}$	TGATCAACGGCTGCCCAGA ACCAGGGTCTT	CCTGCGTCTTTCCTACATCC CTAGGTGGGC

Table 2-6: *Deletion mapping primer sequences.*

2.11.2 PCR Deletion of Plasmid DNA and Gel Extraction

PCR was used to amplify the desired regions using 0.02 U/µl of Phusion Hot Start II Polymerase, 200 µM of dNTP's, 0.5 µM of forward and reverse primers and 0.02 ng/µl of Cten plasmid DNA. The reaction cycle comprised an initial denaturation stage for 2 minutes at 98°C followed by 35x (98°C for 1 minute, 52.3°C for 1 minute and 72°C for 4 minutes) and a final extension stage at 72°C for 10 minutes. Products were run on a 1% agarose gel at 100 V for 50 minutes and bands visualised using a blue light transilluminator.

Gel extraction was performed using the Genelute Gel extraction Kit (Sigma) according to the manufacturer's recommended instructions. The band was excised using a scalpel and weighed. Three hundred µl of solubilisation solution was added for every 100 mg of gel and incubated at 50-60°C for 10 minutes with occasional vortexing. Five hundred µl of Column Preparation Solution was added to the binding column, centrifuged for 1 minute at 13,000 xg and the flow-through discarded. One hundred µl of isopropanol for every 100 mg of gel was added to the solubilised gel and mixed. The solubilised gel solution was loaded onto the binding column, centrifuged at 13,000 xg for 1 minute and the flow-through discarded.

Seven hundred μl of Wash solution was added to the binding column, centrifuged at 13,000 xg for 1 minute and the flow-through discarded. The tube was centrifuged for a further minute. The column was transferred to a new collection tube, 50 μl of Elution solution was added and centrifuged at 13,000 xg for 1 minute. The eluate was retained.

Resulting plasmids were sequenced to confirm deletion of the targeted Cten regions. Plasmids were transfected into HCT116 cells to confirm the deleted construct was translated into protein (see 2.3.1).

2.12 Expression Profiling

2.12.1 Assessment of RNA Integrity

In order to test for downstream targets of Cten, expression profiling was performed. The NLS-Cten, Cten or empty vector plasmids were transfected into HCT116 and RKO cell lines (see 2.3.1). Transfected cells were enriched by cell sorting (see 2.9.1) and the cell RNA extracted (see 2.7.2). RNA integrity was assessed using the 2100 Bioanalyzer (Agilent). Two μl of each RNA sample was aliquoted and heated at 70°C for 2 minutes and placed on ice. One μl of Nano Dye Concentrate was added to an aliquot of gel (65 μl), vortexed thoroughly and centrifuged for 10 minutes at 13,000 xg. A chip was placed on the chip priming station, 9 μl of the gel dye mix was pipetted into the appropriate well and the chip priming station was closed. The plunger was pressed down until hooked underneath the clip and released after 30 seconds. Nine μl of gel dye mix was pipetted into the two indicated wells. Five μl of Nano Marker was pipetted into all the ladder and sample wells and 6 μl into all the unused wells. RNA samples were pulse centrifuged and 1 μl added to the appropriate well. One μl of size

ladder was also added to the indicated well. Following this, the chip was vortexed for 1 minute and placed in the analyser. 2100 Expert software (Agilent) was used for data acquisition.

2.12.2 cRNA Synthesis

The preparation of labelled complementary RNA (cRNA) was carried out using the GeneChip 3' IVT PLUS Reagent Kit (Affymetrix) used according to manufacturer's instructions. In the first strand synthesis step, RNA was reverse transcribed into cDNA with a T7 promoter sequence at the 5' end. Two hundred and fifty ng of RNA was made up to a volume of 3 µl and added to 2 µl of Poly-A RNA Control. Four µl of 3' First-Strand Buffer and 1 µl of 3' First-Strand Enzyme was added to each sample and incubated for 2 hours at 42°C followed by 2 minutes at 4°C.

The second cDNA strand was prepared by adding 13 µl of dH$_2$O, 5 µl of 3' Second-Strand Buffer and 2 µl of 3' Second-Strand Enzyme to the cDNA. Samples were incubated for 1 hour at 16ºC, 10 minutes at 65ºC followed by 2 minutes at 4ºC.

The double stranded cDNA was transcribed into cRNA using T7 RNA polymerase. Four µl of 3' IVT Biotin Label, 20 µl of 3' IVT Buffer and 6 µl of 3' IVT Enzyme were added to the double stranded cDNA. Samples were incubated for 16 hours at 40ºC.

RNA binding beads were used to purify the cRNA from inorganic phosphates and unincorporated nucleotides. One hundred µl of the purification beads were mixed with the cRNA sample, transferred into the well of a 96 well plate and incubated for 10 minutes to allow binding. The

plate was incubated for a further 5 minutes on a magnetic stand to pellet the beads and the supernatant was then removed. The beads were washed 3 times with 200 µl of 80% ethanol for 30 seconds and following this, air-dried for 5 minutes. After removal from the magnetic stand, the cRNA was eluted by incubation for 1 minute with 27 µl of preheated (65ºC) dH_2O. The plate was transferred back to the magnetic stand and the supernatant retained. The cRNA yield was determined using the NanoDrop system.

2.12.3 Fragmentation

The cRNA was fragmented by divalent cations and high temperatures. Fifteen µg of cRNA was added to 8 µl of 3' Fragmentation buffer and incubated for 35 minutes at 94ºC followed by 2 minutes at 4ºC. The fragmented cRNA size distribution was evaluated using the 2100 Bioanalyzer.

2.12.4 Hybridisation

Hybridisation Controls were incubated for 5 minutes at 65ºC. A hybridisation mix was prepared comprising 3.7 µl of Control Oligo B2, 11 µl of 20X Hybridisation Controls, 110 µl of Hybridisation Mix, 22 µl of DMSO and 43.9 µl of dH_2O. Two hundred µl of hybridisation mix was added to each GeneChip Human Genome U133 Array (Affymetrix) and incubated for 30 minutes in a preheated hybridisation oven at 45 ºC with 60 rpm rotation. Following this, 190.6 µl of the hybridisation mix was added to 29.4 µl (11 µg) of cRNA and incubated for 5 minutes at 99ºC followed by 5 minutes at 45ºC. The pre-hybridisation mix was removed from the array and replaced with the cRNA hybridisation mix. The arrays were incubated for 16 hours at 45ºC with rotation at 60 rpm. Following this, the arrays

were washed with Wash Buffer A and stained using 600 μl of Stain Cocktail 1, 600 μl of Stain Cocktail 2 and 800 μl of Array Holding Buffer in a fluidics station. The arrays were then scanned into the GeneAtlas software (Affymetrix).

2.12.5 Data Analysis

Partek Genomics Suite (version 6.6) was used for data analysis. Genes differentially expressed >2-fold from the control with $p<0.05$ were identified.

2.13 Mutation Profiling

2.13.1 PCR

Cell line identities were verified by HRM mutation profiling of commonly mutated genes in CRC. Nested PCR was first used to amplify the region around the targeted mutation. An initial multiplex PCR was performed comprising Hotshot Diamond mastermix, 188 nM of each outer primer (table 2-6) and 20 ng template in a 20 μl reaction. The reaction was run on the Primus 96 thermocycler with a run cycle comprising a holding step of 95ºC for 5 minutes, 30x (95˚C for 10 seconds/55˚C for 30 seconds/72˚C for 20 seconds). The PCR product was diluted 1:100 with nuclease free H_2O and used as template for the subsequent PCR reaction.

A second PCR reaction was performed using primers internal to the primers from the first reaction. PCR reactions were performed for each inner primer pair with a reaction comprising Hotshot Diamond mastermix, 10% Eva Green, 250 nM of forward and reverse primers and 20% template in a volume of 10 μl. The PCR was again performed on the Primus 96 thermocycler with a holding step of 95˚C for 5 minutes followed by 30x

(95˚C for 1 second/55˚C for 1 second) with an extension of 72ºC for 2 minutes for *PIK3CA*, TP53, *BRAF* and *PTEN*. The run cycle for *KRAS* comprised a holding step of 95˚C for 5 minutes followed by 30x (95˚C for 1 second/62˚C for 1 second) with an extension of 72ºC for 2 minutes.

Gene	Exon	Reaction	Forward Primer	Reverse Primer
KRAS	2	Outer	TGAATATAAACTTGT GGTAGTTGG	GCTGTATCGTCAAGG CACTCT
		Inner	ATATAAACTTGTGGT AGTTGGAG	TATCGTCAAGGCACT CTTGC
PIK3CA	20	Outer	TGAGCAAGAGGCTT TGGAGT	CCTATGCAATCGGTC TTTGC
		Inner	GCAAGAGGCTTTGG AGTATTTC	TTTTCAGTTCAATGC ATGCTG
BRAF	11	Outer	TGTTTGGCTTGACTT GACTTT	CTTGTCACAATGTCA CCACATTACATA
		Inner	GACGGGACTCGAGT GATGAT	TGTCACAATGTCACC ACATTACA
	15	Outer	ATCTACTGTTTTCCT TTACTTACTACAC	CAGCATCTCAGGGCC AA
		Inner	TGTTTTCCTTTACTT ACTACACCTCA	CCACAAAATGGATCC AGACA
PTEN	3	Outer	TCATTTTTGTTAATG GTGGCTTT	ACTCTACCTCACTCT AACAAGCAGA
		Inner	GGCTTTTTGTTTGTT TGTTTTG	CCTCACTCTAACAAG CAGATAACTTTC
TP53	6	Outer	AGGCCTCTGATTCC TCACTGAT	ACCCTTAACCCCTCC TCCCA
		Inner	CCTCTGATTCCTCAC TGATTGC	CTTAACCCCTCCTCC CAGAG

Table 2-7: *Mutation profiling primer sequences.*

2.13.2 High Resolution Melting

PCR products were melted using the LightScanner system. Ten µl of PCR product was added to 10 µl of mineral oil and melted over a range of 68-95^{0}C (68-98^{0}C for *TP53*) with a temperature increase of 0.3^{0}C/second. The melt curves were analysed using the LightScanner Instrument and Analysis software package (version 2.5.0.3057). A known wt. cell line was used as a reference sample and those melt curves displaying >4% change in fluorescence were considered to contain a mutation.

2.14 Functional Assays

2.14.1 Transwell Migration Assay

The Transwell system (Corning) was used to measure cell migration in 24 well plates (figure 2-2). The Transwell inserts (8 µm pore size) were incubated in DMEM at 37°C for 1 hour prior to use. Following this, 600 µl of DMEM (containing 20% FBS) was added to the outer wells of the Transwell plate and the Transwell inserts placed inside. Cells were harvested by trypsinisation and a total of 1 x10^5 cells in DMEM (containing 10% FBS) were seeded onto the Transwell insert. The plate was incubated at 37°C for 24 hours. Following this, the cells that had migrated through to the bottom of the outside well, using the higher FBS concentration as a chemoattractant, were manually counted. Triplicate wells were seeded for each experimental condition.
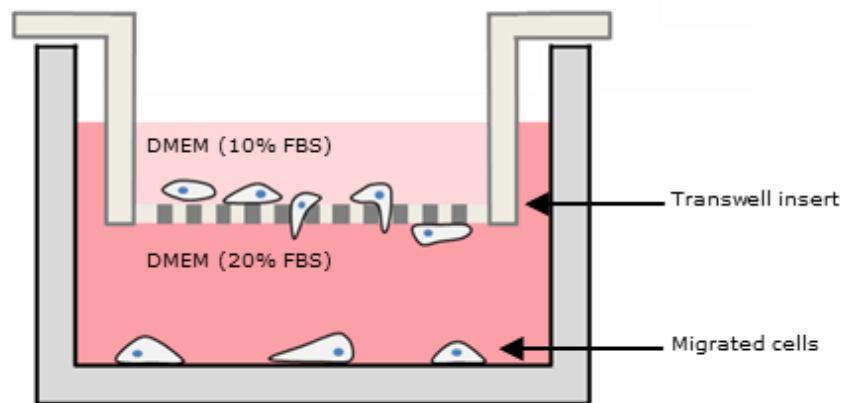
Figure 2-2: *The Transwell system. Cell migration and invasion experiments were performed using the Transwell system. FBS was used as a chemoattractant for migrating cells.*

2.14.2 Transwell Invasion Assay

To assess cell invasion, Transwell inserts were coated with 80 µl of Matrigel basement membrane extract (Corning) at a concentration of 3 mg/ml and incubated overnight at 37°C. The coated Transwells were incubated in DMEM at 37 °C for 1 hour prior to use. Six hundred µl of DMEM (containing 20% FBS) was added to the outer well of the 24 well plate and following this, the Transwell insert placed inside. Transfected cells were harvested by trypsinisation and 2×10^5 cells were seeded onto each Transwell insert. Cells were incubated at 37 °C for 48 hours and the migrated cells at the bottom of the outer well were manually counted. Wells were seeded in triplicate for each experimental condition.

2.14.3 Proliferation Assay

PrestoBlue Cell Viability Reagent (Thermo Fisher Scientific) was used to assess cell proliferation. The experiment was performed according to the manufacturer's protocol. Briefly, 2×10^4 cells were plated in triplicate in a 24 well plate and allowed to adhere for 3 hours. Following this, the cells were incubated with 200 µl of PrestoBlue Cell Viability Reagent for 1 hour at 37ºC. As a blank, 200 µl of PrestoBlue Cell Viability Reagent was also incubated without cells. One hundred µl of the PrestoBlue Cell Viability Reagent was removed from the cells and transferred to a 96 well plate. The fluorescence was measured using the BMG FLUOstar Optima Plate reader (excitation 569 nm/emission 586 nm). The PrestoBlue Cell Viability Reagent on the cells was replaced with fresh media. Further readings were taken at 24, 48 and 72 hour time points. The blank fluorescence reading was subtracted from each experimental fluorescence reading. The blank corrected values were then normalised to the 0 hour time point.

2.14.4 Colony Formation Assay

Colony formation in soft agar was used to assess anchorage independent cell growth. One ml of a 0.7% agarose layer (Sigma) containing 2,500 transfected cells in DMEM (supplemented with 10% FBS and penicillin/streptomycin) was plated in 6 well plates on top of 1 ml of a 1% agar layer (Sigma) containing DMEM (supplemented with 10% FBS and penicillin/streptomycin). Plates were incubated at 37°C for 3 weeks and fed with 0.5 ml of DMEM (supplemented with 10% FBS and penicillin/streptomycin). Following this, the plates were stained with 0.005% crystal violet and 4% formaldehyde for 1 hour. The number of

colonies were manually counted and the colony formation efficiency determined (number of colonies counted/number of cells seeded x 100).

2.15 TOPflash Reporter Assay

The TOPflash assay was used as a method to measure ß-catenin transcriptional activity. HCT116 cells were transfected with Firefly Luciferase expressing TOPflash or FOPflash plasmids in addition to a Renilla Luciferase expressing plasmid, in triplicate. Firefly and Renilla Luciferase were measured using the Dual-Luciferase Reporter Assay System (Promega) according to the manufacturer's instructions. Cells were lysed with 100 µl Passive Lysis Buffer with agitation at room temperature for 15 minutes. Ten µl of the cell lysate was transferred to a 96 well plate. An automated lumonitor was used to dispense 100 µl LAR II into each sample well and Firefly luciferase measured. Next, 100 µl Stop & Glo reagent was dispensed into the well and Renilla Luciferase measured. Firefly Luciferase was normalised to Renilla Luciferase (Firefly Luciferase/Renilla Luciferase x 1000) and the FOPflash subtracted from the TOPflash result. The fold change from the control condition was then determined.

2.16 Immunohistochemistry

Immunohistochemical staining was performed using the Novolink Polymer Detection Kit (Leica) on tissue microarray (TMA) sections (4µm thickness) mounted on glass slides. Briefly, slides were heated for 10 minutes at 60ºC, dewaxed in xylene and dehydrated in industrial methylated spirits (IMS) using the Autostainer XL (Leica) and following this citrate antigen retrieval was performed. Peroxidase Block was applied for 5 minutes and washed with TBS followed by Protein Block for 5 minutes and a TBS wash. Slides were then treated with either Cten (1:250), Tensin 3 (1:200) or

Snail (1:30) antibodies diluted in Antibody Diluent (Leica) for 1 hour. Slides were treated with β2-microglobµlin (1:2,000) (Dako) as a positive control or diluent alone as a negative control. Post Primary Block was applied for 30 minutes, washed and Novolink Polymer applied for 30 minutes followed by a further wash with TBS. Visualisation of bound antibody was achieved using Diaminobenzidine (DAB) prepared from DAB Chromogen and DAB Substrate Buffer. This was incubated for 5 minutes, washed with TBS and following this, the slides were treated with Haematoxylin for 6 minutes. Finally, the slides were cleared in xylene and rehydrated in IMS using the Autostainer XL before mounting in DPX.

Whole slides were scanned using the Nanozoomer digital slide scanner (Hamamatsu) and viewed using the associated NDP.view 2 viewing software (Hamamatsu). The TMA's were manually scored using the H score. The H score was calculated using the formula (3 x percentage of strongly stained cells) + (2 x percentage of moderately stained cells) + (percentage of weakly stained cells), which assigned a score of 0-300 for each core.

2.17 Statistical Analysis

Graphical representation of the results was performed using GraphPad Prism (version 6) with the error bars representing the standard deviation. The Shapiro-Wilk statistical test was performed to test for normality. Following this, for normally distributed data, either the unpaired t-test (for data sets containing 2 treatment groups) or the analysis of variance (ANOVA) (for more than 2 treatment groups) statistical tests were applied. Statistical analysis was performed using GraphPad Prism.

IBM SPSS Statistics (version 22) was used for the analysis of immunohistochemistry (IHC) TMA staining. The Chi squared test was used to test for associations between categorical data. The median H score was taken as the cut off to describe tumours as having low or high marker expression. The association of marker expression with tumour grade, tumour stage, nodal stage, vascular invasion, lymph node involvement and resection margin were investigated. If a small sample size invalidated the statistical test (>20% with a value <5), the Fishers exact test was performed.

The Shapiro-Wilk test was used to test for normality. The Wilcoxon signed ranks test was used to test for associations between marker expression in the tumour and normal colon for non-normally distributed, continuous data.

The Spearman's rank test was used to test for correlations between the expression of 2 different markers. This was applied to continuous data that did not follow a normal distribution pattern.

For all statistical tests used, $p < 0.05$ was considered significant.

3 Investigating the Role of

Cten in the Nucleus

3.1 Introduction

Cten localises to focal adhesions where it is possible it forms part of a large, dynamic molecular complex to regulate cell function. Cten has however also been found to localise to the nucleus but the relevance of Cten in this cell localisation is unknown. Nuclear localisation of Cten was found to be more prevalent in colorectal liver metastasis compared to the primary tumour which could suggest that Cten signalling in the nucleus further enhances cancer progression (Albasri et al., 2011a). Interestingly, Cten in the nucleus (but not in the cytoplasm) binds to β-catenin, a transcription factor in the canonical Wnt signalling pathway (Liao et al., 2009). The Wnt pathway is concerned with the maintenance of stem cells in the normal intestinal epithelium and is frequently dysregulated in colorectal tumours, usually through loss of APC function. Aberrant signalling leads to increased β-catenin transcriptional activity and hyper proliferation in the intestinal crypt arising from the stem cell compartment (Fodde, 2002).

Exactly how Cten is interacting with nuclear β-catenin and whether this is functionally relevant in tumour cell biology is currently unknown. Forced expression of Cten was shown to give increased colony formation in soft agar. This is an *in vitro* method to assess anchorage independent cell growth and measure a cells ability to undergo unlimited replication (both are features of stem cells) and this was suggested to occur in conjunction with β-catenin (Liao et al., 2009, Franken et al., 2006).

CSCs, which could arise from aberrant stem cell signalling or from cancer cells acquiring stem cell characteristics, are thought to comprise a sub-population of cells within the total tumour mass. CSCs have been shown to

be critical for tumour initiation, metastasis and therapeutic resistance (Li et al., 2007, Abdullah and Chow, 2013). Consequently, it is imperative that mechanisms regulating cancer cell stemness are determined.

It was hypothesised that nuclear localised Cten may play an important role in inducing the CSC phenotype. To investigate this, Cten was targeted to the nucleus and the functional activity and downstream signalling of Cten in this localisation was investigated. Additionally, the interaction between Cten and β-catenin was explored in order to try and determine how these proteins could interact.

3.2   Results

3.2.1 The Targeting of Cten to the Nucleus

3.2.1.1 Plasmid Preparation and Transfection

The targeting of Cten to the nucleus was used to investigate Cten signalling in CRC. A construct containing Cten tagged with a nuclear localisation signal (NLS-Cten) was generated by Dr Maham Akhlaq. Cten, NLS-Cten and empty vector control expression constructs were prepared and agarose gel electrophoresis performed to assess plasmid integrity prior to downstream use (figure 3-1). All three constructs revealed the presence of a heavy lower molecular weight band indicative of supercoiled DNA, a second band representative of linear DNA and a third just visible nicked plasmid band. There is an absence of single stranded circular plasmid which would be present if denaturation had occurred. NLS-Cten, Cten and empty vector constructs comprise 7,193 bp, 7,172 bp and 5,000 bp respectively. NLS-Cten and Cten constructs migrated a similar distance with supercoiled DNA in the region of 4,000-6,000 bp and the empty vector at 2,500-4,000 bp slightly lower than the expected sizes due to the migratory behaviour of this plasmid form.
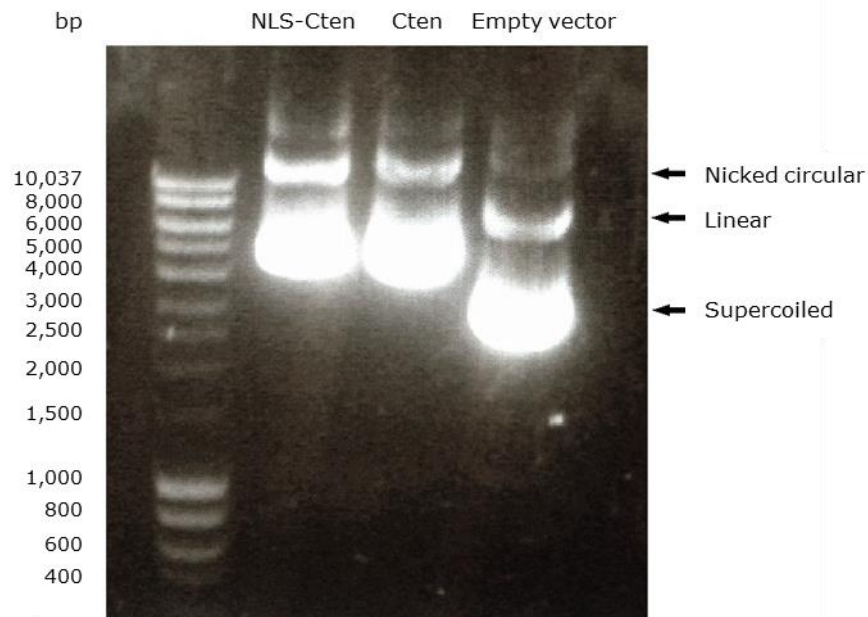
Figure 3-1: Analysis of plasmid integrity. NLS-Cten, Cten and empty vector plasmids run on a 1% agarose gel revealed the presence of supercoiled, linear and nicked circular plasmid DNA.

3.2.1.2 Sequencing of the Cten and NLS-Cten Constructs

The sequencing of both the NLS-Cten and Cten plasmids was performed to ensure that both the full and correct Cten sequence was present in both plasmids and confirm that the NLS sequence was present in the NLS-Cten construct (figure 3-2). A BLAST search confirmed that full length Cten was present in both the Cten and NLS-Cten plasmids. The NLS sequence (CCGAAACGGAGAAGGACATAC) was located at Cten N-terminus in the NLS-Cten plasmid.
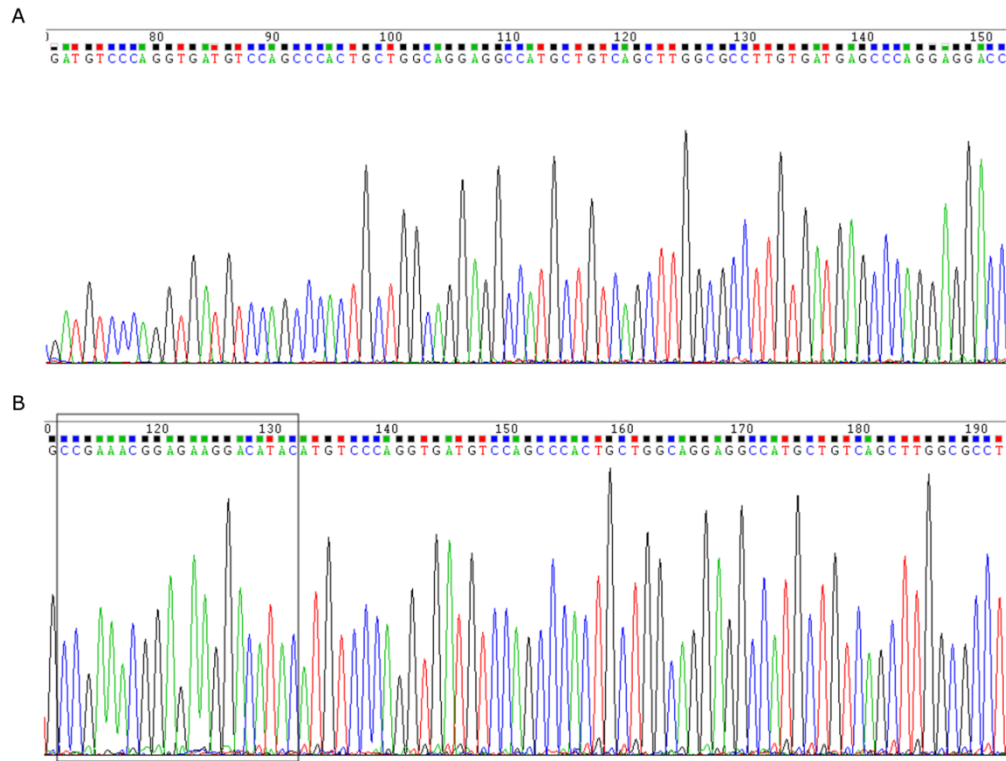
Figure 3-2: *Sequencing of the Cten and NLS-Cten plasmids. A) Sequencing of the Cten plasmid with the start codon of the coding region (ATG) from position 71. B) Sequence results of the NLS-Cten plasmid shows the NLS sequence (highlighted), followed by the Cten coding sequence from position 133.*

3.2.1.3 Transfection Optimisation

Optimal plasmid transfection conditions were next determined (table 3-1). Initial transfection experiments revealed that the NLS-Cten plasmid had lower transfection efficiency than the Cten plasmid and the empty vector control plasmid had the greatest transfection efficiency of all. The NLS-

Cten construct was used for optimisation experiments so that the minimum transfection efficiency was known. Plasmid concentration, Lipofectamine 2000 transfection reagent volume and cell density parameters were optimised in HCT116, a low expressing Cten cell line. Flow cytometry was used to measure the number of cells expressing GFP, present within the expression construct and tagged to NLS-Cten. The optimal concentration had a transfection efficiency of 26.61% using 5 µg of NLS-Cten plasmid together with 10 µl of Lipofectamine 2000 and cells at 70% confluency. This condition was used for transfection experiments using the NLS-Cten and Cten expression constructs.

Cell Density	3 µg Plasmid 10 µl Lipofectamine	4 µg Plasmid 10 µl Lipofectamine	4 µg Plasmid 10 µl Lipofectamine	6 µg Plasmid 20 µl Lipofectamine	8 µg Plasmid 24 µl Lipofectamine
70%	21.70	23.43	**26.61**	16.87	20.24
80%	21.84	24.10	21.85	19.49	15.41
90%	19.53	21.45	20.10	15.30	16.27

Table 3-1: Optimisation of NLS-Cten transfection efficiency in HCT116 cells.

Following optimisation, transfection of NLS-Cten, Cten and empty vector plasmids was performed in HCT116 and RKO cell lines and western blot used to verify protein expression (figure 3-3). Cten was present in both the NLS-Cten and Cten transfected cells in the region of 110 kDa (combined molecular weight of Cten and GFP) yet absent in the empty vector control. The transfection is more efficient in Cten transfected cells than those transfected with the NLS-Cten construct. Both Cten and NLS-Cten constructs transfected better in HCT116 than RKO. NLS-Cten was only weakly expressed in RKO cells. Multiple bands were occasionally observed on western blots following forced expression of Cten. As these were not seen following blotting for endogenous Cten, it is likely that the additional bands were a result of plasmid degradation, which was evident on longer exposures of the western blot.
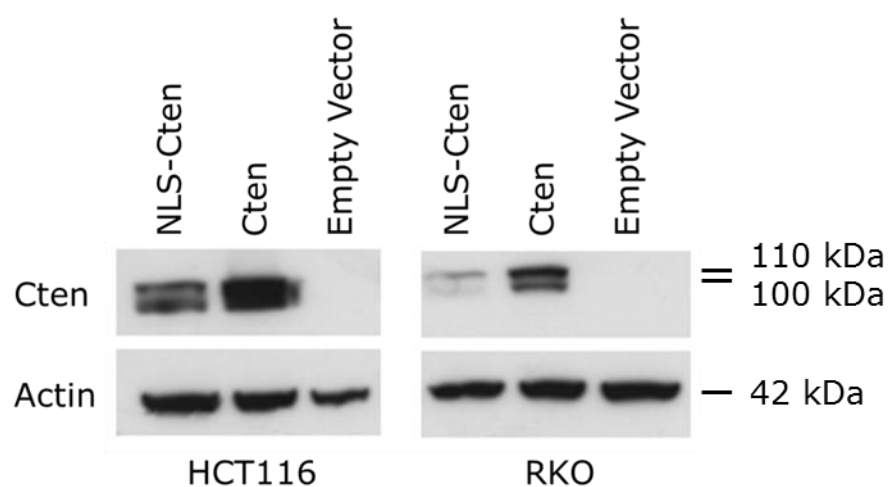
Figure 3-3: *Forced expression of Cten and NLS-Cten. Transfection of the NLS-Cten, Cten or the empty vector plasmids in HCT116 and RKO cell lines.*

3.2.1.4 Confirmation of Cten Nuclear Targeting

To verify that the NLS-Cten expression construct was targeting Cten to the nucleus, confocal microscopy was used following the transfection of NLS-Cten and Cten expression constructs in RKO cells (Figure 3-4). RKO cells transfected with NLS-Cten displayed both nuclear and cytoplasmic GFP expression but the localisation was predominantly nuclear. Cells transfected with wt. Cten also displayed both nuclear and cytoplasmic localised GFP however nuclear GFP was present to a lesser extent than in the NLS-Cten transfected cells. This suggests that although not highly efficient, the NLS signal is sending some of the Cten protein to the nucleus. The cells transfected with the empty vector control plasmid showed high levels of GFP expression. GFP was located both in the cytoplasm and nucleus of the cells as expected. GFP due to its small size can diffuse into the nuclear compartment.
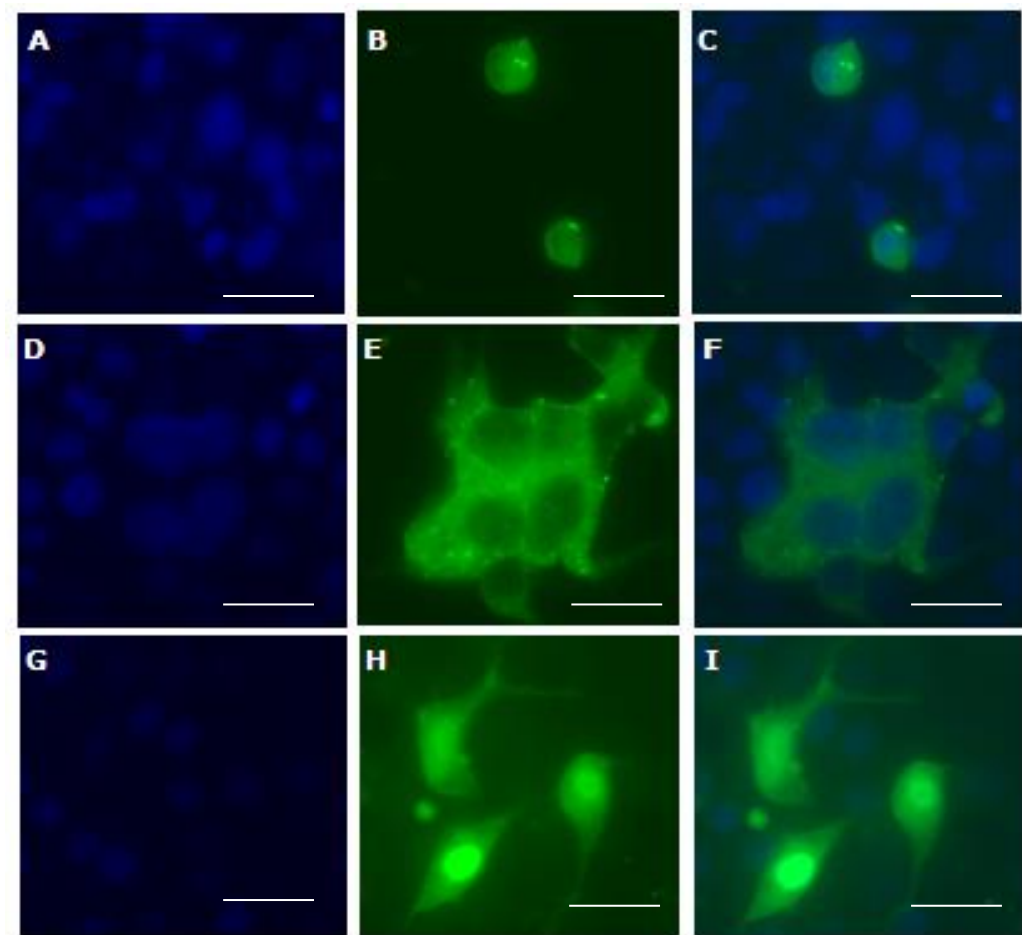
Figure 3-4: NLS-Cten targeted Cten to the nucleus. (A-C) The cellular localisation of Cten tagged with GFP following transfection with the NLS-Cten expression construct is mostly nuclear. (D-F) Cten is mainly localised to the cytoplasm following transfection with the Cten expression construct. (G-I) GFP is localised to both the nucleus and cytoplasm in the control cells (scale bar 25 μm).

3.2.2 The Functional Activity of Cten in the Nucleus

Little is known about the functionality of Cten in the nucleus. To investigate this, Cten was forcibly targeted to the nucleus using the NLS-Cten expression construct, together with Cten and the empty vector as controls in both HCT116 and RKO cell lines. Cell proliferation was assessed using the PrestoBlue assay which provides a measure of cell metabolic activity and therefore provides an indirect measure of cell viability (figure 3-5). In both HCT116 and RKO there was no difference in cell proliferation between the NLS-Cten, Cten and empty vector transfected cells at 72 hours.

The ability of Cten and nuclear localised Cten to induce colony formation in soft agar was investigated (figure 3-6). The colonies formed from single cells after 21 days of growth were all of a similar size but the number of colonies formed differed. Cten transfected HCT116 cells gave rise to a greater number of colonies than empty vector transfected cells and cells transfected with NLS-Cten gave a greater number of colonies than Cten transfected cells. This was also validated in RKO cells which showed a similar pattern of colony formation efficiency (figure 3-6). This suggests that nuclear localised Cten increases colony formation efficiency compared to wt. Cten.

Transwell migration assays were performed in HCT116 and RKO cell lines to determine whether nuclear localised Cten acts to increase cell migration (figure 3-7). In both cell lines, cell migration was increased when cells were transfected with Cten compared to the empty vector control. Transfection of cells with NLS-Cten increased cell migration further still, demonstrating that nuclear localised Cten acts to increase cell migration compared to wt. Cten.
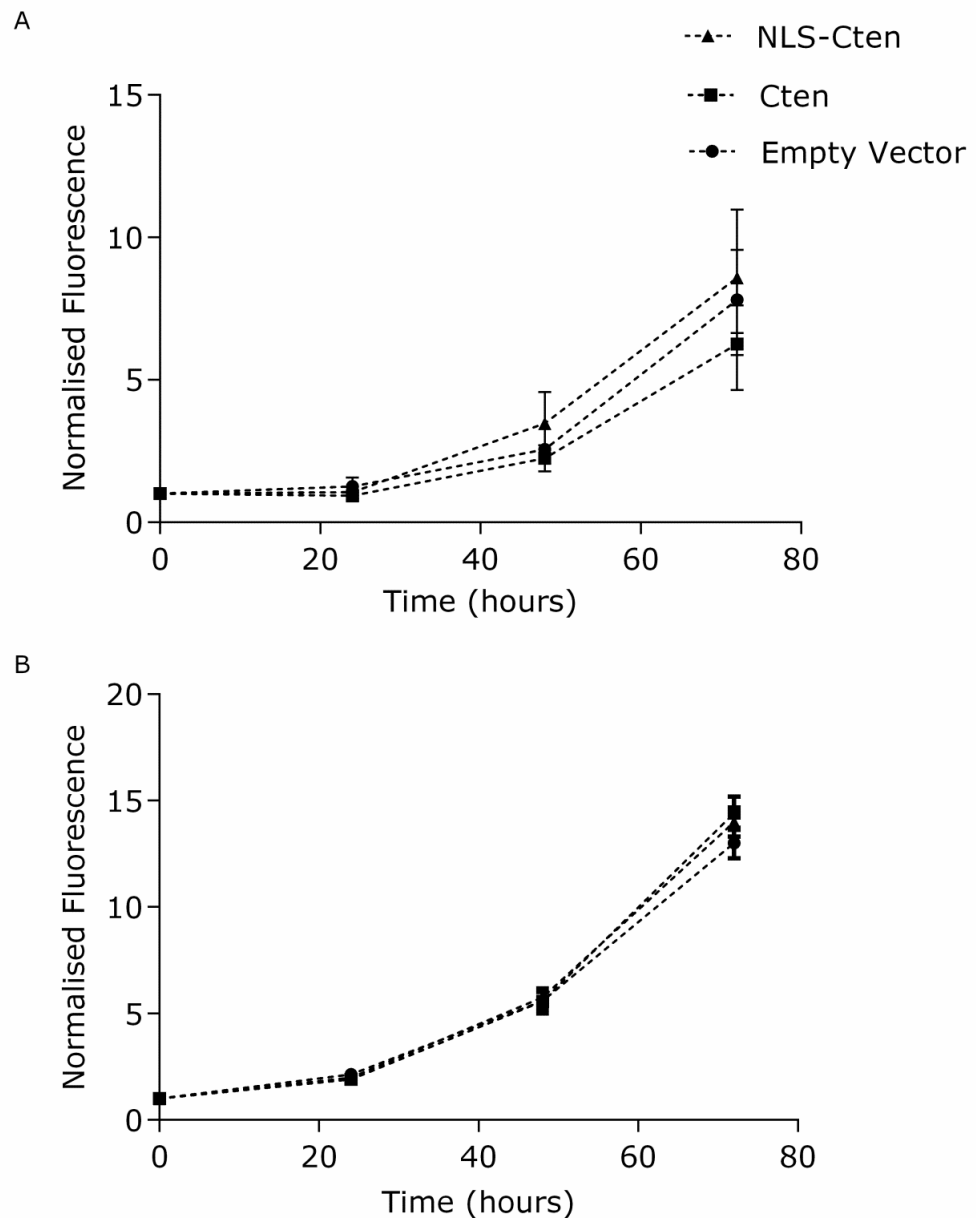
Figure 3-5: *Nuclear Cten does not affect cell proliferation. (A) In HCT116 there was no significant difference in proliferation between NLS-Cten and Cten (p=0.3651) and Cten and empty vector transfected cells (p=0.6151). (B) Similarly, in RKO there was a lack of difference in cell proliferation between NLS-Cten and Cten expressing cells (p=0.9175) and Cten and empty vector transfected cells (p=0.4250) (One-way ANOVA at 72 hour time point, n=3).*
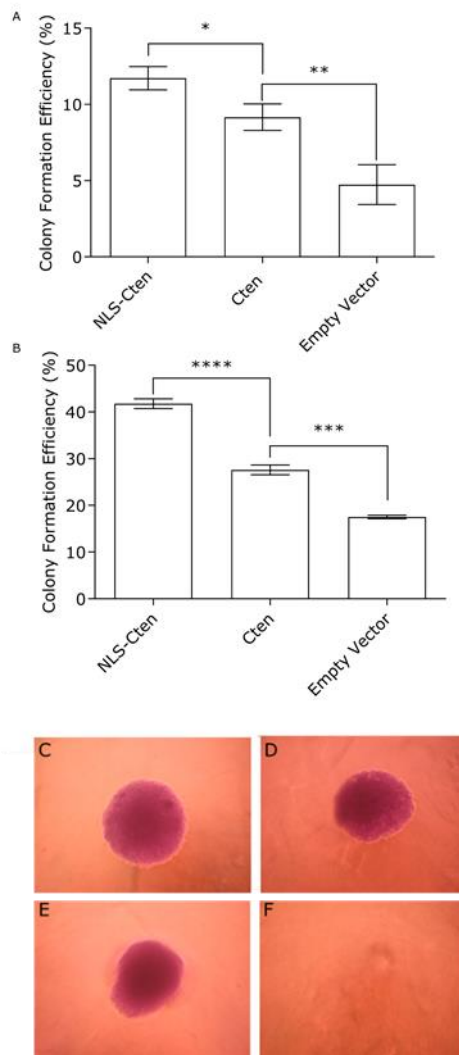
Figure 3-6: *Nuclear Cten increases colony formation efficiency. (A) Forced expression of Cten in HCT116 cells gave higher colony formation efficiency than the empty vector control (P=0.0041) and more colonies were formed when Cten was targeted to the nucleus (P=0.0473). (B) NLS-Cten transfected RKO cells gave a greater number of colonies than Cten transfected cells (P<0.0001) which produced more colonies than the control (P=0.0005) (One-way ANOVA, n=3). Colonies formed after transfection with (C) NLS-Cten, (D) Cten or (E) the empty vector constructs were all of similar size. (F) The blank control containing no cells was also included as a negative control.*
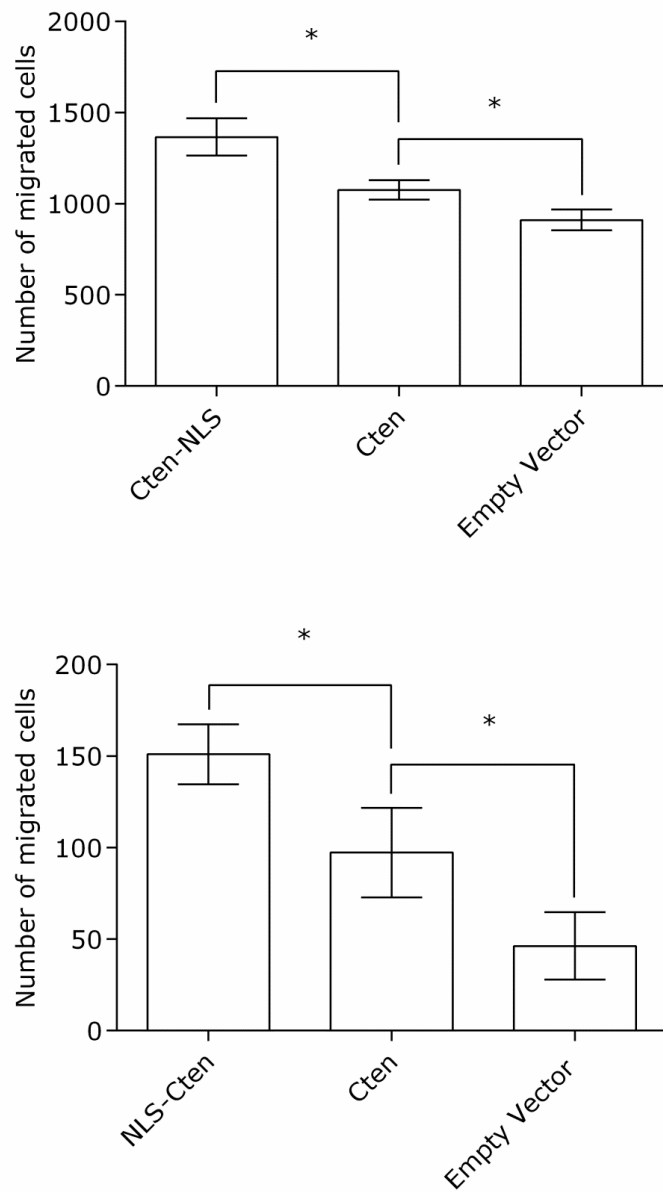
Figure 3-7*: Nuclear Cten increases cell migration. (A) Upon forced expression of Cten in HCT116, a greater number of cells migrated through the Transwell membrane (p=0.0218) and this migratory effect was furthermore increased upon the targeting of Cten to the nucleus (p=0.0122). (B) In RKO, there were a greater number of migrated cells for NLS-Cten transfected cells compared to Cten (p=0.0342) and Cten transfected cells migrated more than the empty vector transfected cells (p=0.0443) (One-way ANOVA, n=3).*

3.2.3 Cten's Role in the Regulation of Cancer Cell Stemness

Forced expression of Cten in the nucleus increased colony formation efficiency, which assesses the ability of a cell to undergo unlimited rounds of replication and hence is an indication of cell stemness. Additionally Cten binds to β-Catenin which regulates the intestinal stem cell compartment. It is possible that Cten in the nucleus acts to regulate genes associated with cell stemness. To investigate this, either the NLS-Cten, Cten or the empty vector control constructs were transfected into HCT116 cells and the changes in expression of a panel of CSC markers were investigated. *KLF4* was upregulated over 2-fold when cells were transfected with nuclear targeted Cten compared to wt. Cten but *NANOG*, *OCT4*, *SOX2* and *SOX4* were unaffected (figure 3-8). This effect of nuclear localised Cten was validated in RKO cells which showed over a 3-fold increase in *KLF4* expression following transfection of the NLS-Cten construct compared to wt. Cten. The expression of *LGR5* was also investigated but this marker wasn't highly expressed in the CRC cell lines investigated.

Cells expressing nuclear targeted Cten displayed an upregulation of *KLF4* mRNA. To determine whether KLF4 was also upregulated at the protein level, a western blot was performed following the transfection of NLS-Cten, Cten or empty vector control plasmids (figure 3-9). Lysates were harvested at both 24 and 48 hours post transfection to allow for any delays in protein translation. KLF4 protein expression remained consistent for all treatment conditions demonstrating that contrary to that seen at the mRNA level, Cten in the nucleus does not induce KLF4 expression.
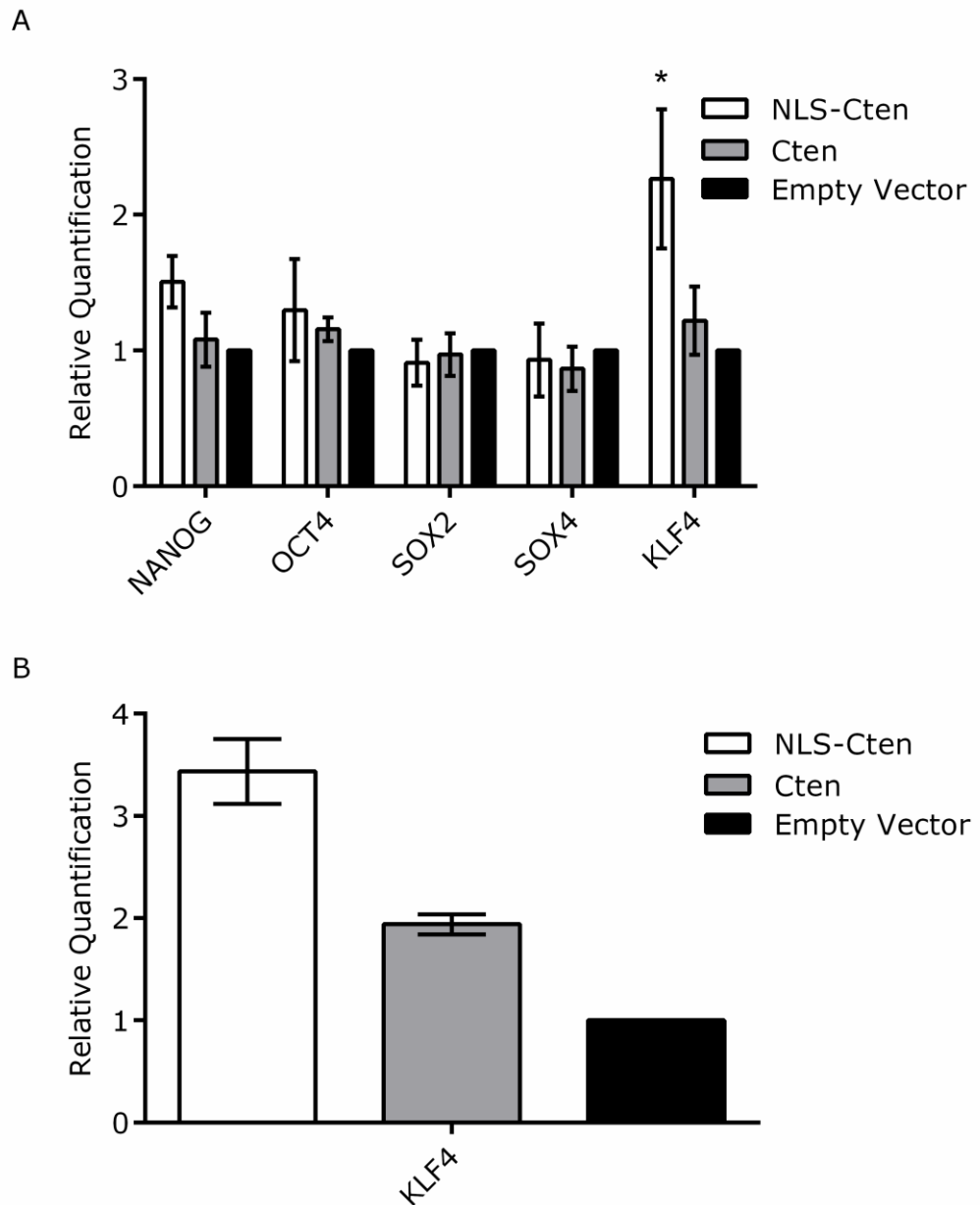
Figure 3-8: *Nuclear Cten upregulates KLF4 mRNA. A) The transfection of NLS-Cten in HCT116 cells did not affect the mRNA expression of NANOG (p=0.0551, n=3) OCT4 (p=0.5644, n=3) SOX2 (n=2), SOX4 (n=2) compared to transfection with Cten. NLS-Cten was associated with an increase in KLF4 expression in HCT116 (p=0.0341, n=3) and B) RKO cell lines (n=2) (One-way ANOVA).*
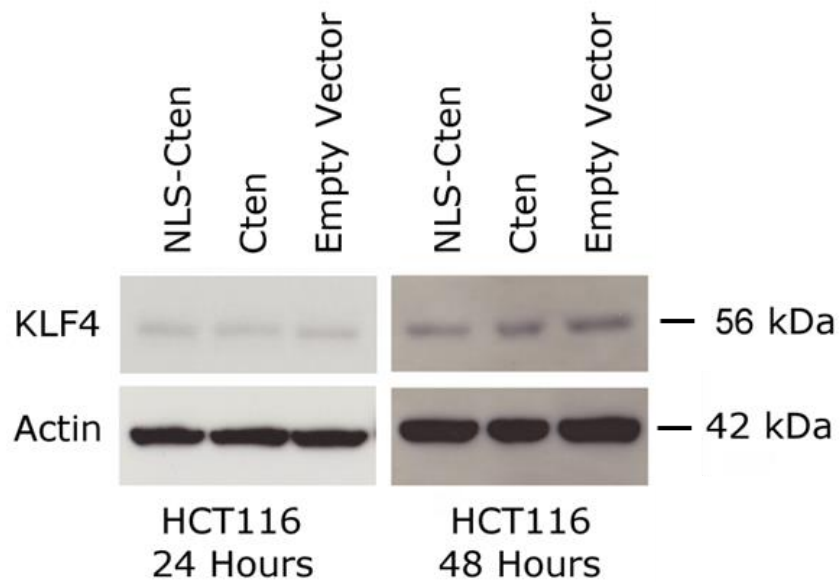
Figure 3-9: *Cten does not regulate KLF4 at the protein level. KLF4 protein expression was consistent following the transfection of NLS-Cten, Cten or the empty vector plasmids in HCT116 at both 24 and 48 hours post transfection.*

3.2.4 Identification of Cten Downstream Targets

3.2.4.1 Sample Preparation for Expression Profiling

Initial investigations of the ability of nuclear localised Cten to induce the expression of stem cell markers failed to identify any downstream targets. To widen the search for potential Cten target genes, expression profiling was performed following the transfection of NLS-Cten, Cten or the empty vector control plasmids in both HCT116 and RKO cell lines.

To allow comparison between Cten and NLS-Cten transfected cells, despite differences in transfection efficiencies and also to enrich for transfected cells, HCT116 and RKO cells were sorted based on the expression of the GFP tag contained within the plasmid following transfection. GFP positive cells were successfully sorted from untransfected cells to use for downstream analysis (figure 3-10).
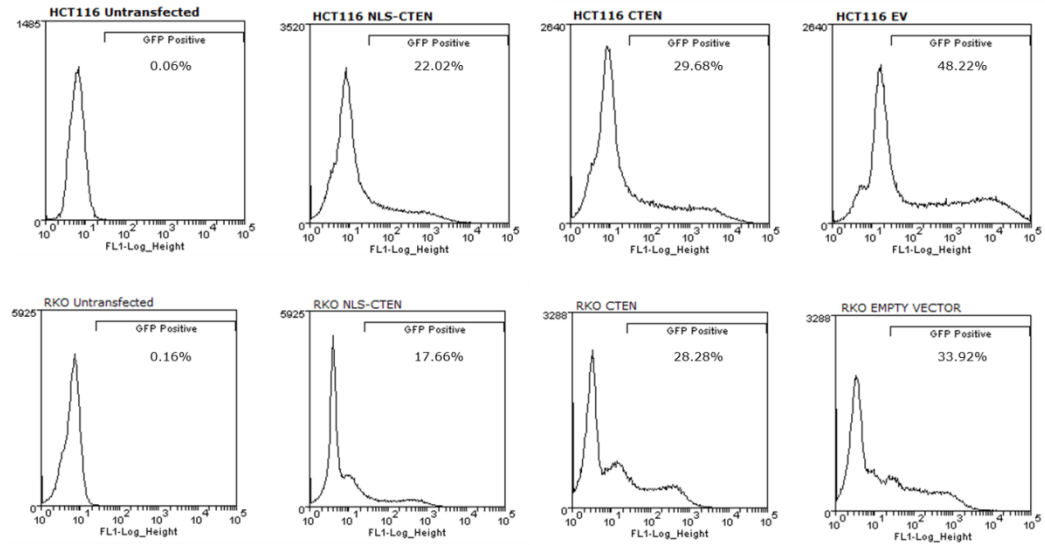
Figure 3-10: *Enrichment of Cten and NLS-Cten transfected cells for expression profiling. Cells were sorted based on GFP expression.*

Following cell sorting Cten protein expression was investigated by western blotting. It was expected that following sorting, the expression of Cten would be similar in both NLS-Cten and Cten transfected cells however this was not the case, possibly due to a lower stability of the NLS-Cten fusion protein (figure 3-11).
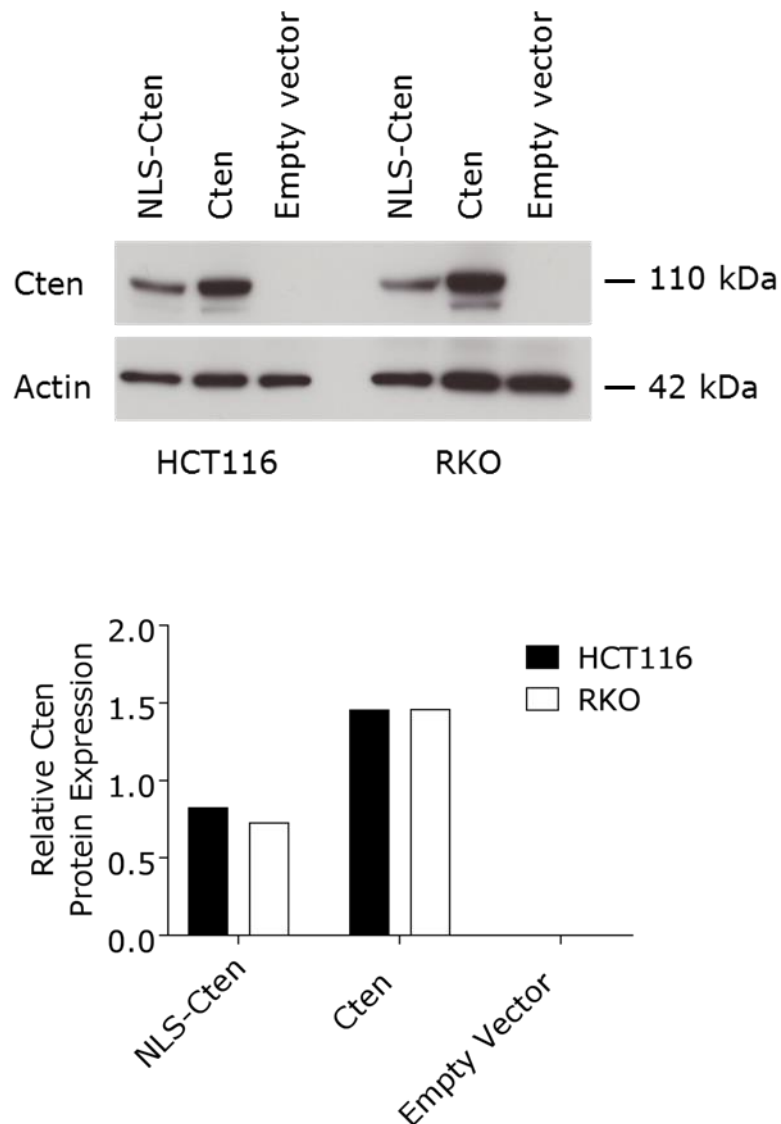
Figure 3-11: *The expression of NLS tagged and wt. Cten in HCT116 and RKO cells following cell sorting (n=1).*

RNA was extracted from the cells following cell sorting. Those RNA samples with acceptable purity, assessed by the 260/280 nm and 260/230 nm absorbances, were also assessed for RNA integrity. This was determined using the 2100 Bioanalyzer and the RNA integrity number (RIN) calculated

was used as an indication of the RNA quality (figure 3-12). The gel image showed that the RNA extracted was of good quality as the 28S and 18S rRNA bands could be clearly identified with band thickness approximately double for the 28S rRNA than the 18S band. Lanes were clear showing an absence of RNA degradation products. Graphical representation of the RNA also revealed 2 distinct peaks representative of rRNA. Those samples with a RIN >7 and within a similar range were accepted to use for expression profiling.
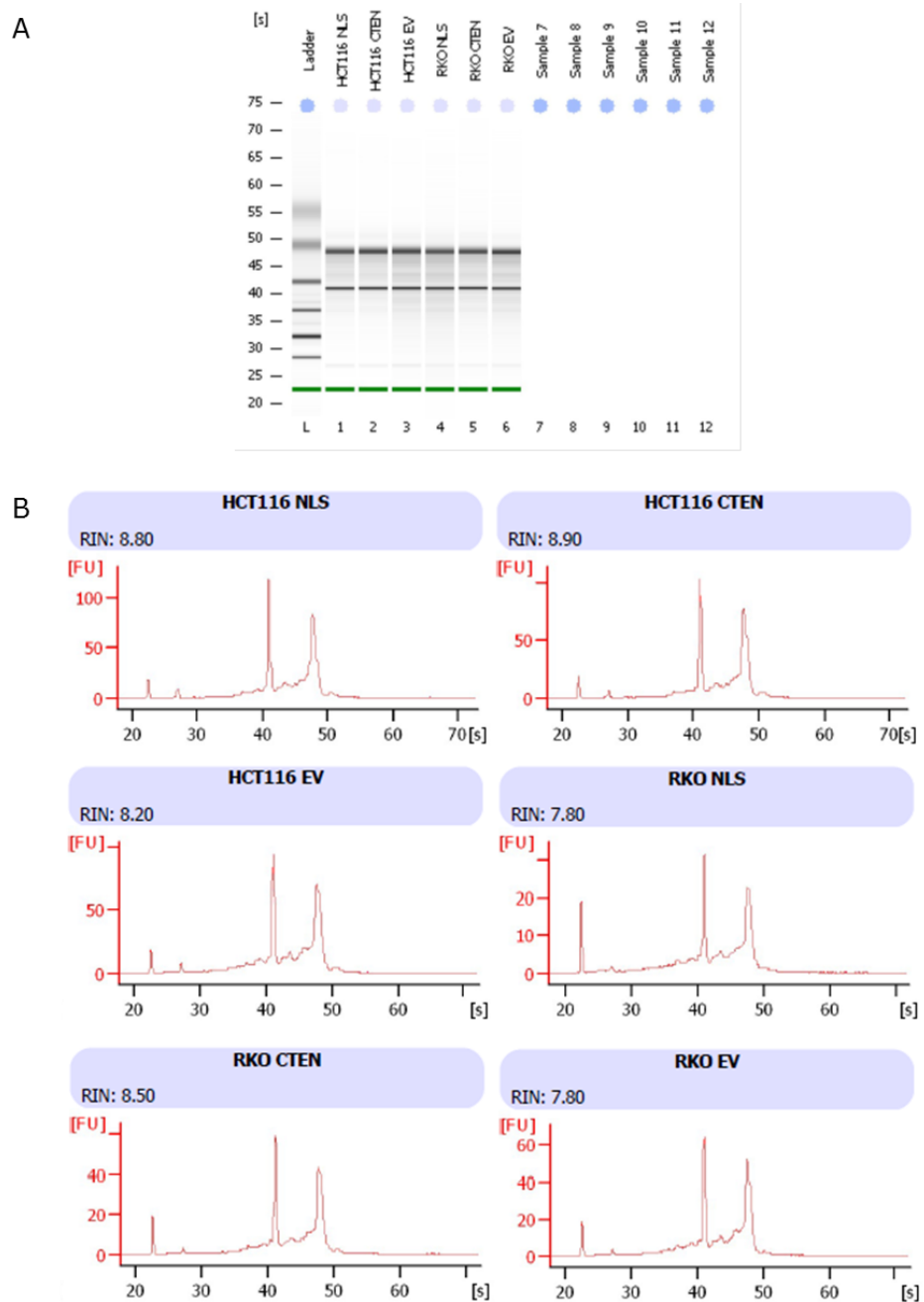
Figure 3-12: *Analysis of RNA integrity. A) The electrophoresis gel revealed clear 18S (lower) and 28S (upper) rRNA bands with minimal degradation products for RNA derived from Cten, NLS-Cten and empty vector transfected cells. B) Graphical representation of HCT116 and RKO RNA revealed 2 distinct rRNA peaks with acceptable RIN's (>7).*

3.2.4.2 Differentially Expressed Genes Identified by Expression Profiling

Affymetrix microarray expression profiling was performed by Prof Sean May, University of Nottingham. It was used to identify differentially expressed genes between NLS-Cten, Cten and empty vector transfected cells in both HCT116 and RKO cell lines. The principal components analysis (PCA) plot was used to explore the preliminary data and this showed that the biggest separation of samples, based on gene expression, was between the different cell lines (figure 3-13). Ellipsoids for all 3 HCT116 treatment groups do not overlap showing there is a difference in gene expression profiles between these groups. For RKO, both NLS-Cten and Cten expression profiles are different to the empty vector transfected cells but are not different to each other as the ellipsoids display an overlap.
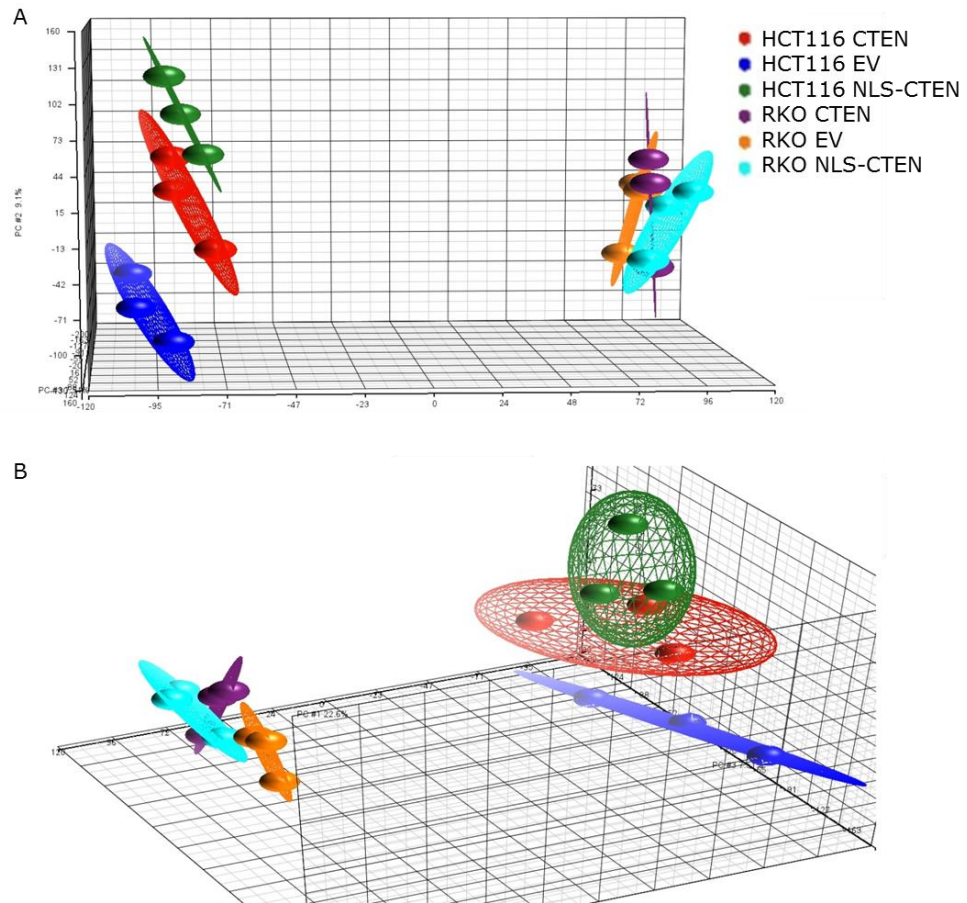
Figure 3-13*: Expression profiling PCA plot. A) The PCA plot displays both HCT116 and RKO data points but is positioned to show the clustering of HCT116 sample replicates with no overlap between NLS-Cten, Cten and empty vector samples. B) Rotation of this image reveals that RKO NLS-Cten and Cten ellipsoids overlap demonstrating that transcriptome expression levels are similar for these 2 samples.*

Partek uses ANOVA to identify differentially expressed genes. A concise list was created for each cell line displaying those genes showing >2 fold difference with $p<0.05$ (table 9-2 and 9-4). Using these criteria, in HCT116 there were 335 genes differentially expressed between Cten and empty vector control transfected cells whilst in RKO there were 31 genes differentially expressed between Cten and empty vector control transfected cells. There were considerably more differentially expressed genes in HCT116 than there were in RKO. To further narrow down the number of genes and to further ascertain that the genes identified were true downstream targets of Cten, 25 genes that were differentially expressed in both HCT116 and RKO where identified (figures 3-14 and 3-15, table 9-6). Of those genes, 17 could be identified whereas 8 of the differentially expressed genes were unknown. The genes identified have a range of cellular functions including the regulation of cell motility, DNA replication, membrane trafficking and many are implicated in cancer. There were no stem cell markers present in the group of 25 genes but there were a number of markers that were shown to be differentially expressed either in 1 cell line only or less than 2-fold, including Aldehyde dehydrogenase 1 family, member A2 (ALDH1A2) ($p=4.070 \times 10^{-5}$), Musashi RNA-Binding Protein 2 (MSI2) ($p=0.004$), and Achaete-scute family bHLH transcription factor 2 (ASCL2) ($p=0.006$), which were upregulated 5.420, 2.270 and 1.405 fold respectively in Cten transfected HCT116 cells compared to the empty vector. MSI2 expression was also upregulated in RKO ($p=0.010$).
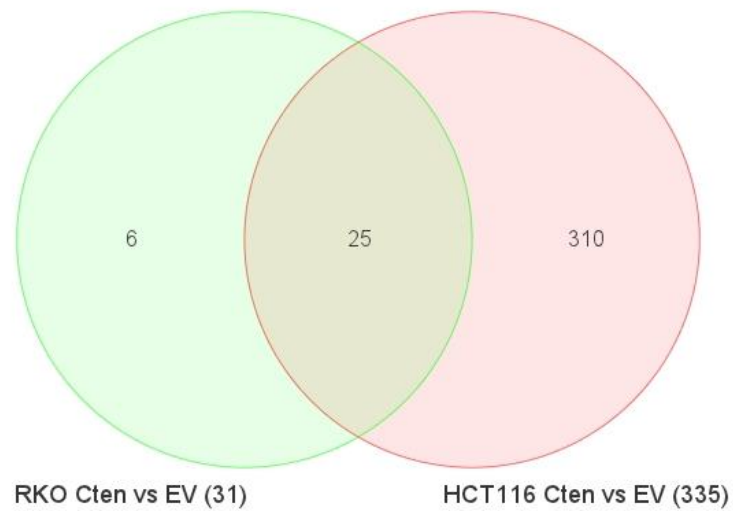
Figure 3-14: *Differentially expressed genes for Cten and empty vector transfected cells. Thirty one and 335 genes were identified as differentially expressed between Cten and empty vector transfected RKO and HCT116 cells respectively (>2-fold, p<0.05, ANOVA). Twenty five differentially expressed genes were common to both cell lines.*
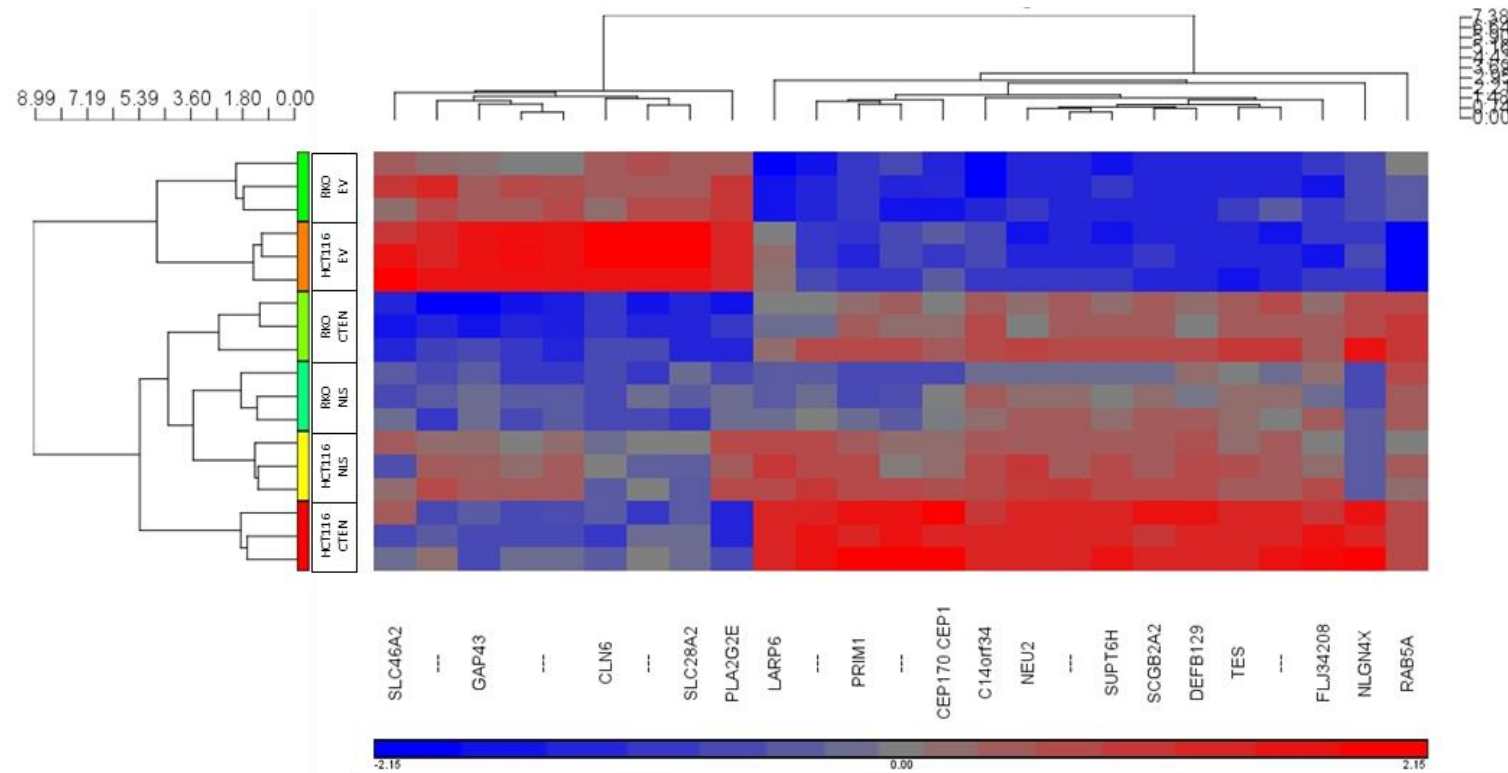
Figure 3-15*: Hierarchical clustering of differentially expressed genes. Genes differentially expressed (>2-fold, p<0.05, ANOVA) between Cten and empty vector transfected cells common to both HCT116 and RKO cell lines.*

To determine which pathways the differentially expressed genes between Cten and empty vector transfected HCT116 cells mapped to, Ingenuity Pathway Analysis (IPA) was performed (figure 3-16). Consistent with Cten signalling in breast cell lines, differentially expressed genes were concerned with Rho signalling. CXCR4 and tight junction signalling pathways were identified and are consistent with Cten's function in metastasis. Furthermore, additional pathways not previously linked to Cten function were identified including metabolic, semaphorin and Cdk5 signalling pathways.
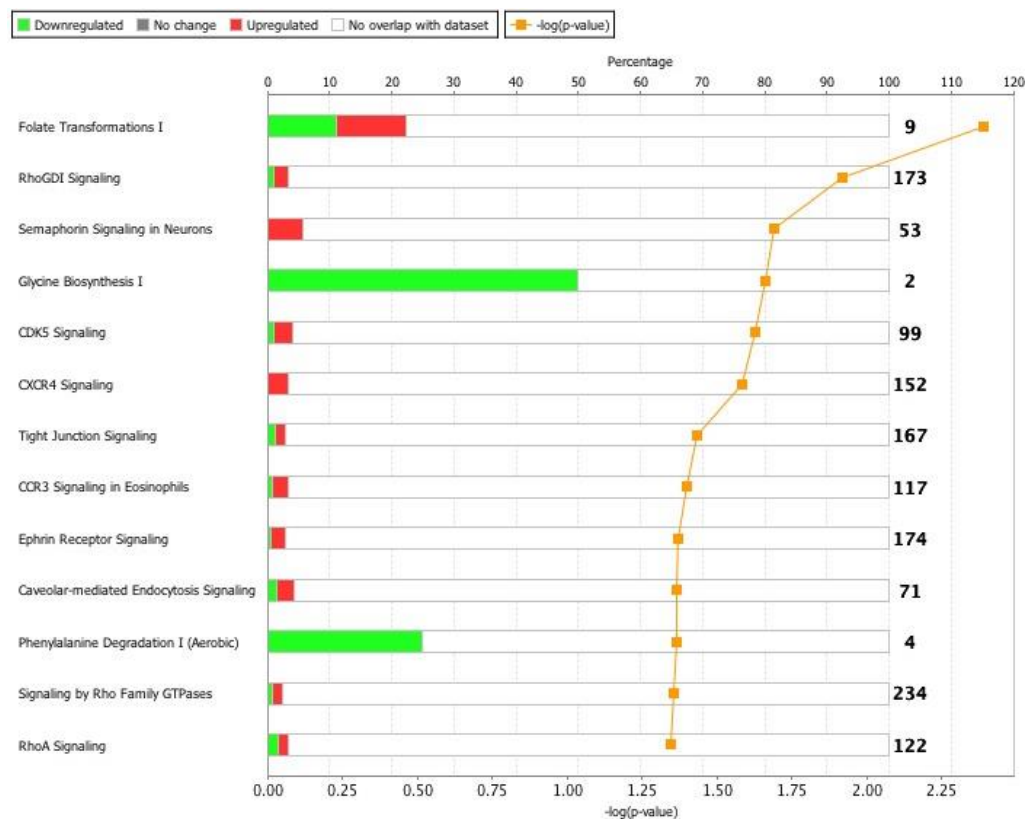
Figure 3-16: *Cten pathway analysis. Signalling pathways significantly altered in response to Cten transfection in HCT116 cells.*

The expression profiles of HCT116 and RKO cells transfected with NLS-Cten were also determined and compared to the expression of genes in wt. Cten transfected cells (figure 3-17, table 9-3 and 9-5). In HCT116, there were 8 differentially expressed genes identified between the 2 samples (> 2-fold, $p < 0.05$) however all of these genes were also differentially expressed when comparing Cten to empty vector transfected cells. It is possible that Cten in the nucleus does not affect the transcriptional activity of any genes and those genes that were identified were so due to a lower transfection efficiency of the NLS-Cten plasmid than wt. Cten. In RKO 2 genes were identified to be differentially expressed when comparing the expression profiles of NLS-Cten and Cten transfected cells. Of these 2 genes, 1 was not identified previously however the identification of this gene was unknown.
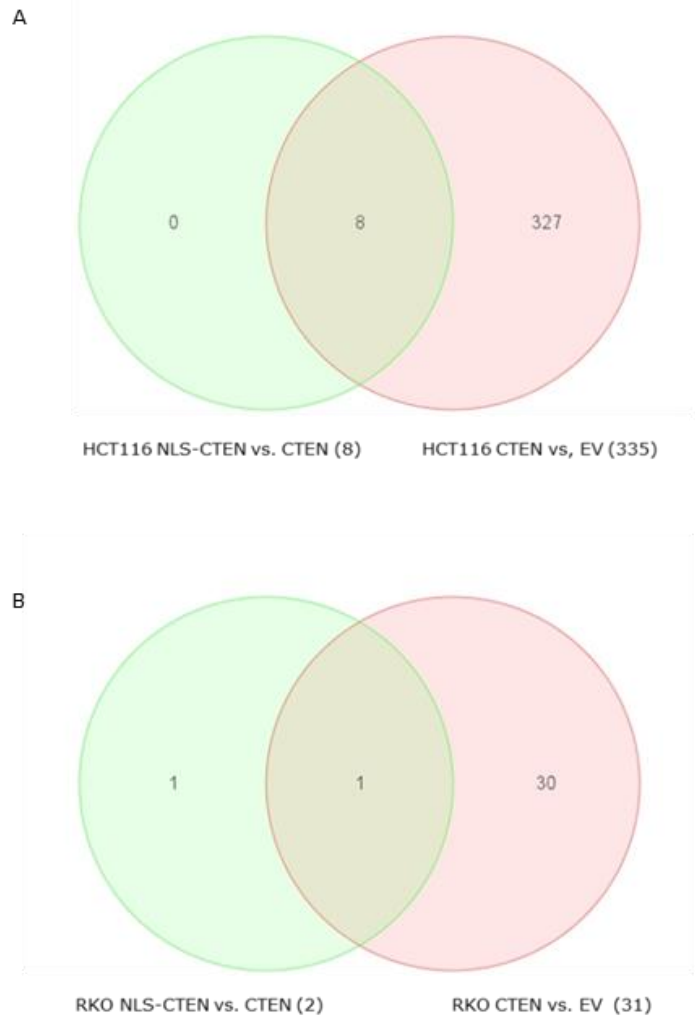
Figure 3-17: *Differentially expressed genes for Cten and NLS-Cten transfected cells. A) The 8 differentially expressed genes identified between NLS-Cten transfected and Cten transfected HCT116 cells were all differentially regulated between Cten and empty vector transfected cells. B) In RKO 2 genes were differentially expressed between NLS-Cten and Cten transfected cells, of these 1 was also differentially expressed when comparing Cten and empty vector transfected cells (>2-fold, p<0.05, ANOVA).*

3.2.5 Cten and β-catenin Interaction in the Nucleus

3.2.5.1 Mapping the Regions of Cten Binding

Cten has been shown to bind to β-Catenin in the nucleus however the relevance of this interaction is unknown. First, to confirm that Cten did bind to β-Catenin, a co-IP experiment was performed (Figure 3-18). A co-IP was performed in HCT116 as future experiments used forced expression of Cten in this cell line. Forcibly expressed Cten immunoprecipitated with β-Catenin in HCT116 cells. To confirm that this interaction occurs without manipulation of gene expression, a co-IP was performed in SW620. Here endogenous Cten immunoprecipitated with β-Catenin, thus confirming that these 2 proteins interact.
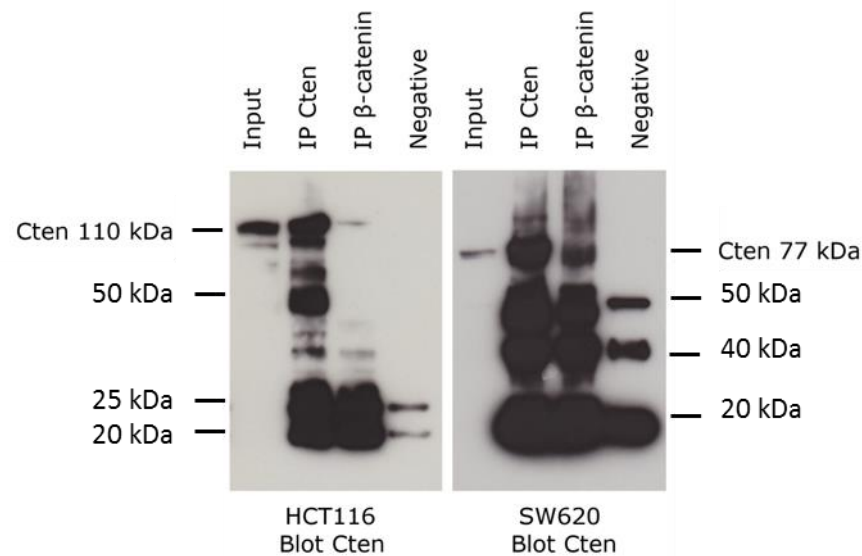
Figure 3-18*: Cten co-immunoprecipitated with β-Catenin. Cten co-immunoprecipitated with β-Catenin for both endogenous Cten in SW620 and forcibly expressed Cten in HCT116 cells.*

Following confirmation that Cten binds to β-catenin, the regions of Cten binding were investigated to gain further mechanistic detail. This was achieved through deletion mapping experiments in which PCR was used to amplify all but the required deletion region from the Cten plasmid. Two Cten deletion constructs were created. Cten$^{\Delta C1300\text{-}2313}$ comprised Cten N-terminus containing nucleotides 165-1300 of Cten with nucleotides 1301-2312 deleted. Cten$^{\Delta N165\text{-}1289}$ comprised Cten C-terminus and contained nucleotides 1290-2312 of Cten with nucleotides 165-1289 deleted. Following amplification of the required sequence from the wt. Cten expression vector, the products were run on a gel to confirm that the deletion constructs were of the predicted size (Cten$^{\Delta C1300\text{-}2313}$ 6031 bp and Cten$^{\Delta N165\text{-}1289}$ 5755 bp) (figure 3-19). Both constructs migrated to approximately 6,000 bp as expected. The resulting plasmids were transformed and purified. The deletion constructs were sent for sequencing to ensure that the correct sequences had been deleted as intended and that the remaining Cten sequence was present within the plasmid. Of those constructs sequenced, 1 contained the desired sequence for Cten$^{\Delta C1300\text{-}2313}$ and 2 constructs contained the correct sequence for Cten$^{\Delta N165\text{-}1289}$ (Cten$^{\Delta N165\text{-}1289}$(1) and Cten$^{\Delta N165\text{-}1289}$(2)).
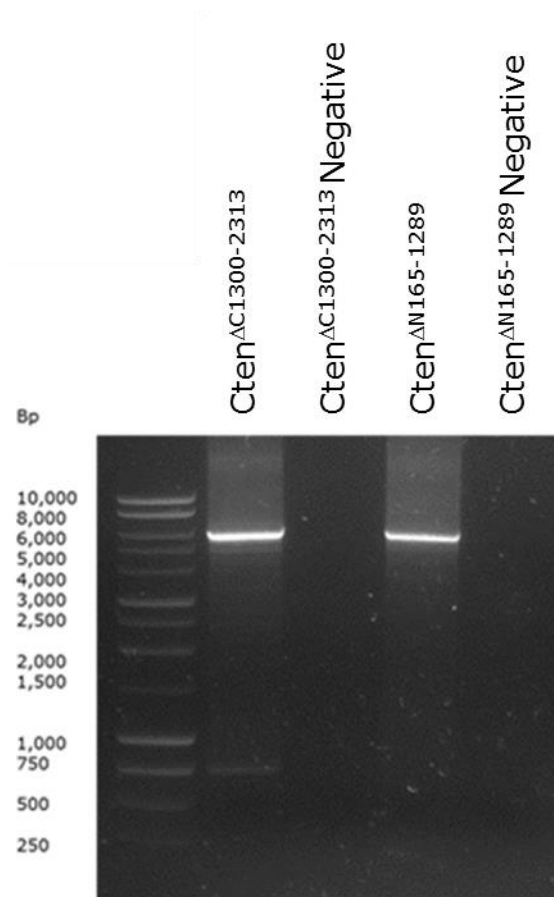
Figure 3-19*: Agarose gel of Cten deletion constructs. Cten deletion constructs were prepared by amplifying the desired region from the Cten expression construct and the products run on an agarose gel.*

Following confirmation that the plasmids contained the correct sequence, transfection into HCT116 cells and western blotting was performed to determine whether the deletion constructs were expressed at the protein level (figure 3-20). Cten$^{\Delta C1300\text{-}2313}$ was expressed as a 65 kDa protein (when fused to GFP). Neither of the 2 Cten$^{\Delta N165\text{-}1289}$ constructs that contained the correct sequence were expressed at the protein level following transfection in HCT116. To ensure that this wasn't a problem with loss of the antibody

binding site, flow cytometry was performed by counting the number of cells expressing GFP, also contained within the plasmid and expressed as a fusion protein tagged to Cten. Confirming the western blot results, 48.85% of Cten$^{\Delta C1300-2313}$ transfected cells expressed GFP was but there was only 0.51-0.57% GFP expression for Cten$^{\Delta N165-1289}$ transfected HCT116 cells.
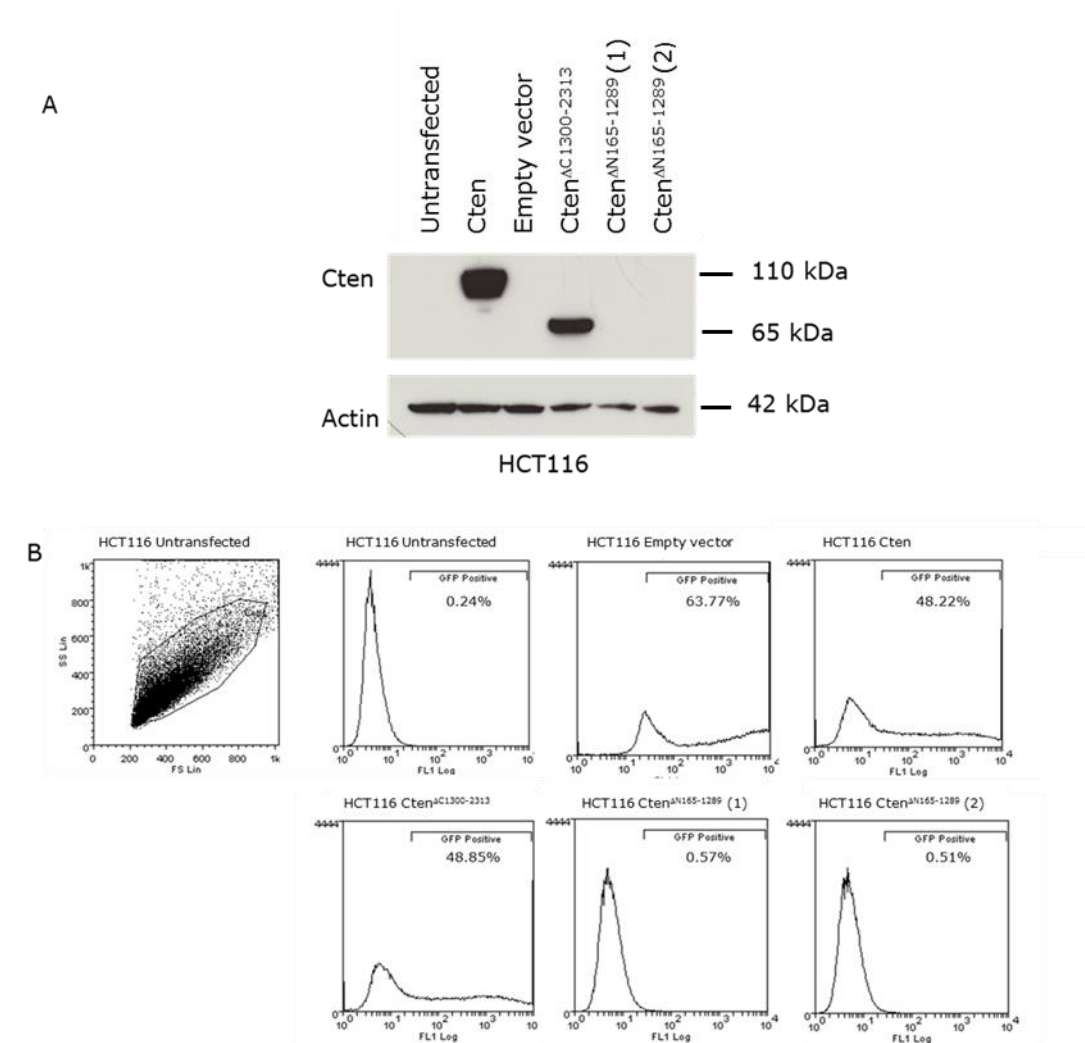
Figure 3-20: *The expression of the Cten deletion constructs. A) The expression of wt. Cten, the Cten deletion constructs Cten$^{\Delta C1300-2313}$, Cten$^{\Delta N165-1289}$(1) and Cten$^{\Delta N165-1289}$(2) in HCT116 cells by western blotting. B) The expression of the Cten deletion constructs by flow cytometry.*

The ability of Cten$^{\Delta C1300-2313}$, to retain binding to β-catenin was next investigated following transfection in HCT116 (figure 3-21). The lysates were immunoprecipitated with β-catenin and blotted with Cten to determine whether the interaction between these 2 proteins was maintained through the N terminal region of Cten. Weak Cten-β-catenin binding is present in the lysate from full length Cten and this binding is still present in the lysate derived from cells transfected with Cten$^{\Delta C1300-2313}$. This demonstrates that binding to β-catenin is at least partly through the N terminal region of Cten.

HCT116: Blot Cten
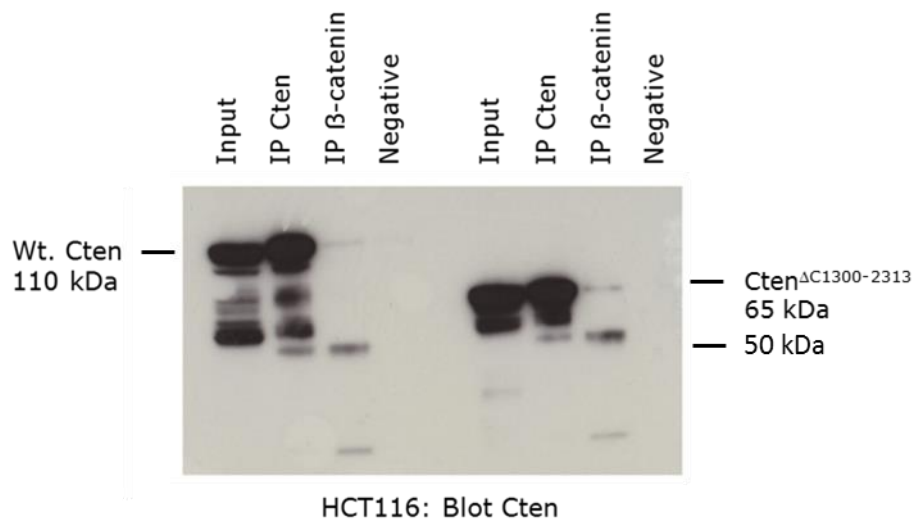
Figure 3-21: *Co-immunoprecipitation of Cten$^{\Delta C1300-2313}$ and β-catenin. Wt. Cten and Cten$^{\Delta C1300-2313}$ transfected HCT116 whole cell lysates immunoprecipitated with β-catenin.*

3.2.5.2 Investigating the Relevance of the Cten and β-catenin Interaction

It was hypothesised that nuclear Cten may retain β-Catenin in the nucleus thereby enhancing β-Catenin transcriptional activity and enabling the expression of target genes. To investigate this, a western blot of β-Catenin expression was performed following transfection of NLS-Cten, Cten or the empty vector control constructs (Figure 3-22). Firstly, β-Catenin protein expression was investigated in whole cell lysates derived from HCT116 and RKO transfected cell lines. β-Catenin protein expression increased slightly when cells were transfected with Cten compared to transfection with the empty vector control. β-Catenin protein expression however was not further increased when cells were transfected with the NLS-Cten construct, possibly due to the lower transfection efficiency of this plasmid. β-Catenin was not expressed, nor was it induced in RKO cells following Cten or NLS-Cten plasmid transfection. This demonstrates that Cten may increase β-catenin protein expression. A further western blot was performed to investigate β-Catenin expression in the nuclear lysate fraction of HCT116 cells. Taking into account the expression of actin, β-Catenin expression remained consistent in all transfection conditions. This implies that although Cten may increase β-catenin expression, it does not retain β-Catenin in the nucleus. There are however preliminary results and further repetition is required.
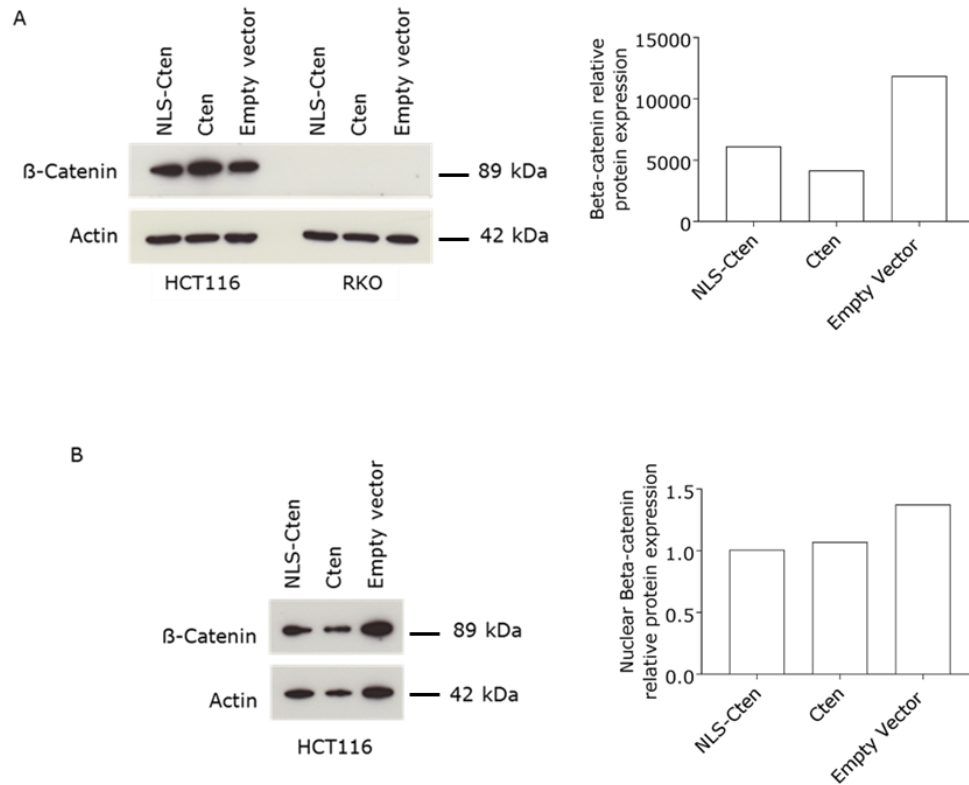
Figure 3-22*: β-Catenin expression following transfection of NLS-Cten, Cten or the empty vector control. A) β-Catenin expression in the whole cell extract and B) the nuclear extract (n=1).*

Despite showing that Cten does not retain β-Catenin in the nucleus, it is still possible that Cten may promote β-Catenin transcriptionally activity, perhaps by aiding binding to the TCF/LEF promoter regions or via other unknown mechanisms. The TOP-flash assay is a well described assay that can be used to measure β-Catenin transcriptional activity. HCT116 cells were transfected with either Cten of the empty control as with previous experiments however in addition, a Renilla Luciferase expressing plasmid, together with either a TOP-flash or FOP-flash plasmid were also

transfected. The TOP-flash plasmid contains a Firefly Luciferase reporter gene downstream of a TCF/LEF promoter region. The FOP-flash contains point mutations in the promoter region thereby acting as a negative control. The levels of normalised Luciferase were measured as an indication of β-Catenin transcriptional activity (figure 3-23). Cten expressing HCT116 cells expressed similar levels of Luciferase to the empty vector control transfected cells. This suggests that Cten does not induce β-Catenin transcriptional activity in HCT116 cells.
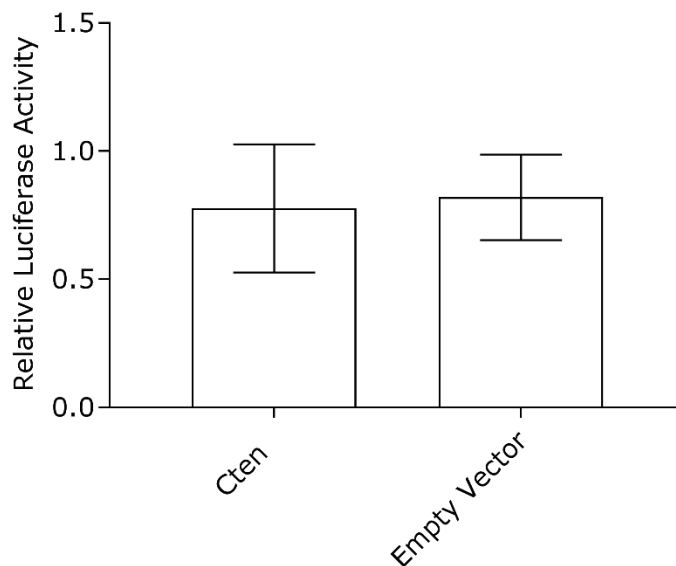
Figure 3-23: *The effect of Cten on β-catenin activity. TOPflash luciferase reporter activity remained consistent in both Cten and empty vector transfected HCT116 cells (p=0.6170, unpaired t-test, n=3).*

3.2.6 The Expression and Localisation of Cten in Colorectal Cancer Tissue

Cten protein is predominantly expressed in the cytoplasm but expression has also been found in the nucleus. The localisation of Cten in 84 colorectal cases was investigated by immunohistochemistry. The TMA was constructed from cores taken from the centre, invasive and luminal edges of the tumour. An area of normal colon adjacent to the tumour was also sampled for each patient.

Antibody optimisation was initially performed using kidney tissue, chosen as it expresses moderate levels of Cten protein and due to tissue availability. Initial antibody concentrations of 1:100, 1:500 and 1:1,000 were used and following this, further antibody dilutions enabled the optimum antibody concentration to be determined. Final optimisation was performed using colon tissue (figure 3-24). A concentration of 1:250 was chosen as a variation in staining could be observed across the different cases and had minimum background staining. Following this, the colon TMA was subject to staining (figure 3-25).

Cten staining was found to localise mainly to the cytoplasm with all cases showing positive cytoplasmic staining. Positive nuclear staining was observed but only in 4 of 84 cases. Cten staining was also localised to the membrane in 20 cases. The Wilcoxon signed ranks test was used to test for significant differences in Cten staining between the normal colon and tumour. There was no difference in Cten expression between tumour and normal colon (p=0.366) however Cten positivity was greatest in the tumour with all patients showing Cten positive staining however only 91% samples showed positive Cten staining of normal colon tissue. The Chi

squared test was used to test for associations between Cten staining and the clinical features. Cten staining in each cellular localisation was not associated with tumour grade, tumour stage, nodal stage, vascular invasion, Dukes stage, lymph node involvement or resection margin (table 3-2).
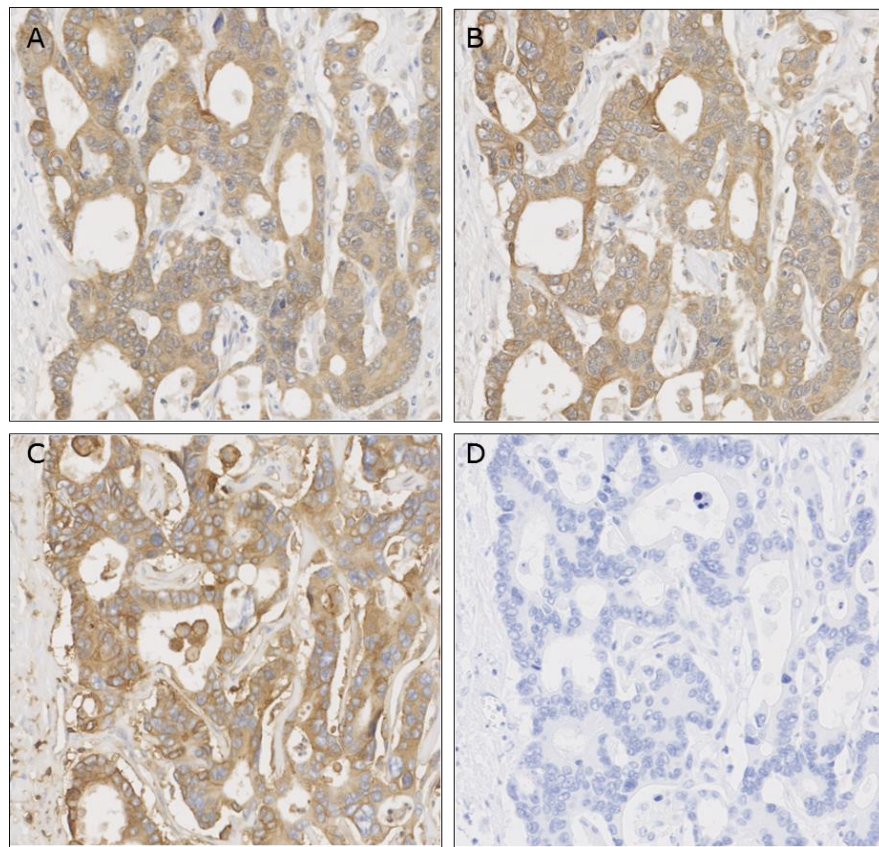
Figure 3-24: *Optimisation of Cten IHC staining. A) Cten was optimised in colorectal tissue at dilutions of 1:500 and B) 1:250. C) Staining of colon tissue with β2-microglobulin was used as a positive control. D) Colon stained without any antibody served as a negative control.*
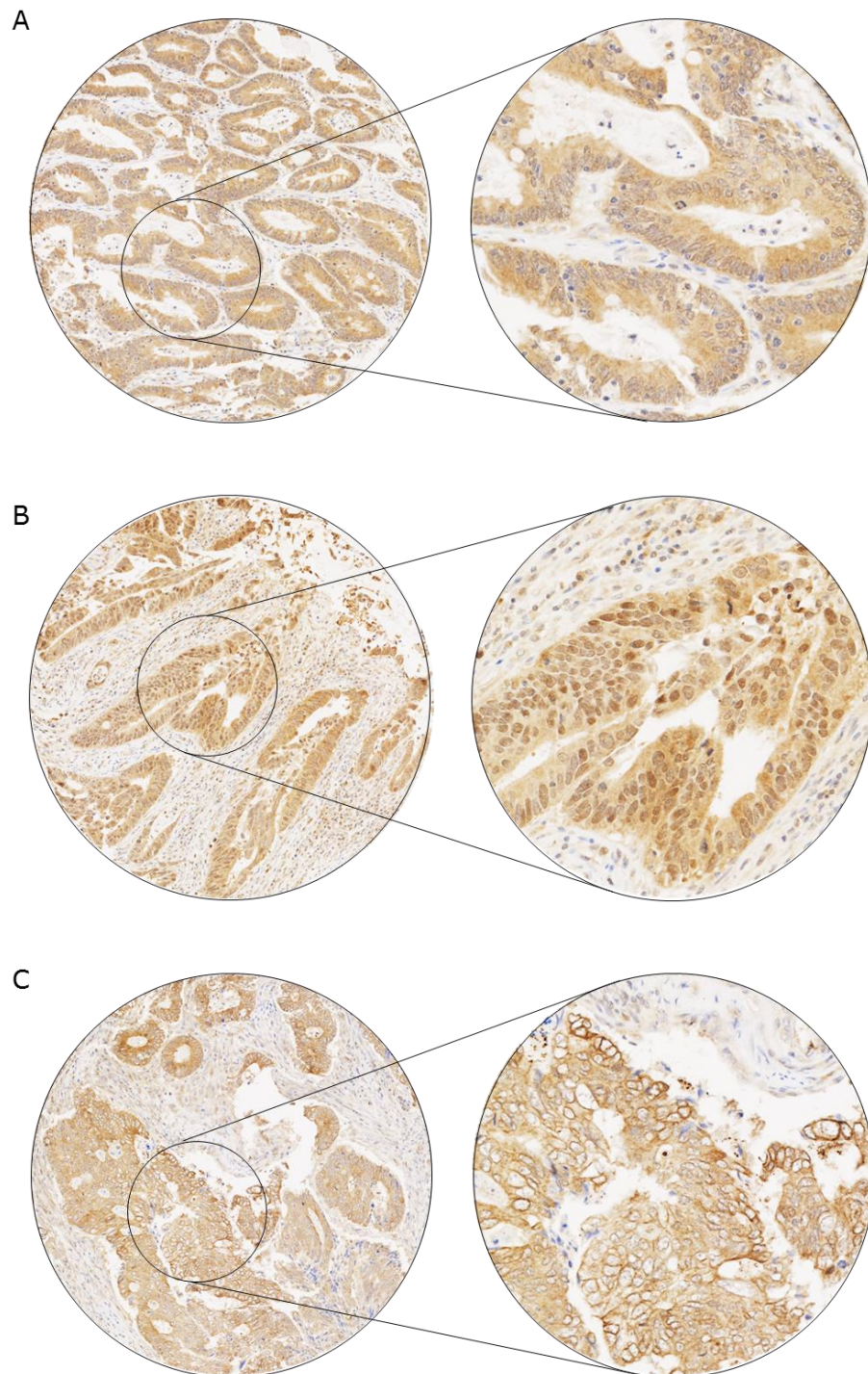
Figure 3-25: Cten staining of colorectal tumours. A) TMA cores of CRC revealed Cten staining in the cytoplasm B) cytoplasm and nucleus, and C) membrane and cytoplasm.

Parameter	Cytoplasmic Staining			Nuclear Staining			Membranous staining		
	Low	High	P	Low	High	P	Low	High	P
Tumour Grade			0.834			0.299			0.366
1	1	1		2	0		2	0	
2	37	40		74	3		54	23	
3	3	2		4	1		5	0	
Tumour Stage			0.544			0.671			0.886
1	1	2		3	0		2	3	
2	6	6		12	0		9	12	
3	20	26		44	2		32	46	
4	14	9		21	2		18	23	
Nodal Stage			0.105			0.360			0.256
0	23	30		51	2		38	15	
1	12	12		23	1		16	8	
2	6	1		6	1		7	0	
Vascular Invasion			0.344			1.000			0.804
0	19	23		40	2		29	13	
1	22	18		38	2		30	10	
2	0	2		2	0		2	0	
Dukes Stage			0.370			0.786			0.744
A	7	6		13	0		10	3	
B	16	22		37	1		26	12	
C1	17	11		26	2		20	8	
C2	1	3		4	0		4	0	
Lymph Nodes			0.618			0.241			0.842
0	23	30		51	2		38	15	
1+	18	13		29	2		23	8	
Resection margin			0.616			0.184			0.291
Free	38	40		75	3		58	20	
Involved	2	1		2	1		2	2	

Table 3-2: *Association of Cten staining in cytoplasmic, nuclear and membranous localisations and the clinicopathological features. Significance was tested using the chi squared test.*

3.3   Discussion

Cten localises to the nucleus however the relevance of Cten in this subcellular localisation in terms of cell signalling and cancer progression is unknown (Albasri et al., 2011a). Cten was successfully targeted to the nucleus in colorectal cell lines and Cten when localised to the nucleus was shown to further enhance cell migration and colony formation efficiency compared to wt. Cten, which is predominantly localised at focal adhesions.

Although there was a shift in Cten to the nucleus, the nuclear targeting was not 100% efficient as Cten was still observed in the cytoplasm of some cells. Cten localisation was assessed by confocal microscopy and may have benefited from cell fractionation to better assess the localisation of Cten following transfection with both constructs. Furthermore, despite optimisation, the expression of Cten using the NLS-Cten construct was consistently lower than forced expression of wt. Cten. The presence of multiple start codons within the primer used to create the NLS-Cten construct may have led to reduced translation of the full NLS tag and also Cten protein expression. Alternatively, the NLS-Cten construct may have undergone a change reducing its transfection efficiency in mammalian cells. In the former case, redesigning of the NLS-Cten construct may give increased Cten expression and nuclear localisation to better allow comparison between wt. Cten and nuclear localised Cten. Investigations could determine whether the NLS tag is more efficient placed at the N-terminus, C-terminus or at both Cten termini. In the latter case, testing more clones after the initial construction of NLS-Cten may have picked up plasmids with greater transfection efficiency. However, the increased functional changes were observed despite the reduced transfection efficiency of the NLS-Cten construct and Cten nuclear localisation

suggesting that nuclear localised Cten does strongly induced these cell properties. Tests for proliferation showed no difference compared to empty vector for either NLS-Cten or wt. Cten thereby confirming previous data showing that Cten does not affect cell number (Albasri et al., 2009).

The colony formation assay is often used as an *in vitro* method to assess cell stemness and this property was indeed increased when Cten was targeted to the nucleus. However, this assay alone is not sufficient to confirm that Cten promotes cancer cell stemness and other supplementary methods should be used. The gold standard method is serial transplantation in animal models to demonstrate the cell's unlimited replicative ability although there are other *in vitro* methods that could support this hypothesis (Schatton and Frank, 2010). These include spheroid formation and Aldefluor assays. Despite there being *in vitro* evidence of an effect of nuclear localised Cten on stemness, there was no convincing increase in the expression of stem cell markers. NLS-Cten transfected cells were compared to Cten transfected cells specifically for a panel of genes which have been used to create induced Pluripotent Stem Cells (iPSCs) (Okita et al., 2007). There was no change in the expression of these, other than in KLF4. This however was not seen at the protein level and thus remains of uncertain significance. A similar comparison was performed using Affymetrix expression profiling arrays which did not identify any downstream targets at the mRNA level. This would suggest that Cten in the nucleus is not acting as a transcription factor however it is possible that Cten is regulating protein expression or carrying out alternative functions in the nucleus that remain to be identified. It is possible that expression changes were missed due to the lower transfection efficiency of the NLS-Cten construct. Additionally, the level of

nuclear Cten in each experiment was not known. Experiments performed using the NLS tag may have benefited from cell fractionation to assess Cten localisation rather the immunoblotting the total cell lysate, to allow better interpretation of the results. However, it appears that the NLS tag did target Cten to the nucleus and unequivocally this altered cell function (when compared to wt. Cten) although the mechanism of this remains to be further investigated.

Although forcibly expressing Cten in the nucleus provides a way of investigating the role of Cten in this localisation, the NLS tag is not endogenous to Cten. Once mechanisms of Cten activity have been identified, these should be validated with experiments investigating endogenous Cten in the nucleus.

As others have shown, it was confirmed that Cten does bind to β-catenin and this binding was mapped to the N-terminus of Cten (Liao et al., 2009). Further work is needed to confirm that the Cten does not bind to the C terminus, as binding could be mediated via both regions and further work could also narrow down the binding region in Cten, which was not completed due to time constraints. Other focal adhesion localised proteins have been reported to translocate to the nucleus and act as transcriptional co-regulators (Sen et al., 2012). It was hypothesised that Cten binding could act to retain β-catenin in the nucleus thereby sustaining β-catenin transcriptional activity. The β-catenin reporter assay revealed that there were no changes in transcriptional activity following Cten transfection. β-catenin activity is however already high in HCT116 cells due to the deletion of a critical serine residue and it is possible that forced expression of Cten could not further increase this (Ilyas et al., 1997). Further experiments could investigate this relationship using alternative cells lines or assays.

Nuclear localised Cten did not increase β-catenin expression however, as mentioned there were issues with the expression and targeting of the NLS-Cten construct which may compromise this due to Cten being much more weakly expressed. It must also be noted that β-catenin signalling is not mutated in RKO cells yet increases in colony formation by nuclear Cten are seen in both HCT116 and RKO cell lines. It is possible that even though the transfection efficiency is lower in RKO, since RKO does not have stabilised β-catenin, the forced expression of NLS-Cten has a more marked effect than in HCT116.

There remain further points to address regarding the nuclear localisation of Cten. Firstly, Cten does not appear to contain a NLS and therefore it would be of interest to determine how Cten gets to the nucleus and whether it is co-transported along with any other proteins. It would also be interesting to determine whether Cten shuttles between the nuclear and cytoplasmic compartments by using inhibitors of the nuclear import and export processes. It would also be of interest to determine whether Cten forms part of a large complex in the nucleus and binds other proteins in the nucleus which might give further clues to its role in this localisation.

Despite not identifying downstream targets of forced expression in the nucleus, the expression profiling did identify a number of novel downstream targets on wt. Cten. These were involved in a number of cellular processes. Before proceeding with further investigation into these signalling pathways, validation of expression profiling results by qPCR and confirmation of expression changes at the protein level is required.

Others have shown Cten localisation in colon tumour tissue and this was here confirmed in a limited tumour set (Albasri et al., 2011a). However

expression was not associated with the clinicopathological status of this data set. There was no difference between the prevalence of Cten in the nucleus in the normal colon and the colorectal tumours. Previously nuclear Cten expression was upregulated in liver metastasis compared to the primary tumour (Albasri et al., 2011a). It is possible that increased nuclear Cten expression is associated with metastasis but not the primary tumour. Membrane expression of Cten was observed which has not been previously reported. However, Cten is localised at focal adhesions and it's possible that Cten localises to membrane junctions. Limitations of this experiment that may account for the discrepancies seen with previously published data include the limited size of the data set and that the scoring was not verified by a pathologist. Additionally, as during construction of the TMA, cores were taken from 3 different areas of the tumour, this may weaken any overall effect if Cten is only localised to a specific region of the tumour.

In conclusion, investigations have demonstrated that Cten has enhanced colony formation and migratory capabilities when targeted to the nucleus and although Cten does bind to β-catenin in this compartment, it has not been ascertained that Cten signalling to β-catenin and the induction of CSC pathways are responsible for this activity.

4. Investigating the Tensin Switch in Colorectal Cancer

4.1. Introduction

Cten is a potential biomarker in some cancers and in most tumour types it appears to be an oncogene, particularly associated with advanced disease (Sjoestroem et al., 2013, Albasri et al., 2011a, Albasri et al., 2011b, Lo, 2014). To date, no mutations of Cten have been documented, making it plausible that Cten is upregulated through the activation of upstream signalling pathways. Relatively little is known about the regulation of Cten however it is important that pathways that increase cell migration and consequently promote cancer metastasis are identified.

Previously, others have shown in breast cell lines that Cten is regulated by the EGFR signalling pathway. Stimulation of EGFR signalling caused an upregulation of Cten levels and this was associated with a Tensin switch, whereby Tensin 3 expression was simultaneously reduced. It was proposed that the upregulation of Cten by EGF displaced Tensin 3 from integrin binding sites at focal adhesions. When Tensin 3 is bound to integrins it also binds to the actin cytoskeleton. As Cten lacks the actin binding domain, actin structural rearrangements occur, focal adhesions are detached from the actin cytoskeleton which in turn promotes cell motility (Katz et al., 2007). In support of this, a further publication linked this Tensin switch activity to differential binding of Cten and Tensin3 to downstream DLC1, a tumour suppressor which regulates cell migration through a Rho-GAP domain. Upregulation of Cten induced an auto-inhibitory mechanism in DLC1, inhibiting its interaction with RhoA and preventing its tumour suppressive activity. Consequently, downstream pathways promoting cell migration were activated (Cao et al., 2012).

The regulation of Cten was further investigated in both a malignant CRC cell line and a non-malignant prostate cell line. Here Cten was found to be upregulated by a number of growth factors and cytokines namely EGF, FGF2, PDGF, NGF, IGF1, TGF-β IL-6 and IL-13. Cten has also been shown to be under the regulation of Kras in colorectal and pancreatic cancer cell lines and also regulated by Stat3 via IL-6 signalling (Hung et al., 2013, Bennett et al., 2015).

Despite the identification of a number of upstream regulators, the pathways that regulate Cten and how these cooperate are poorly understood. It appears that EGFR-Kras signalling may be a common mechanism however, Cten has been shown to be upregulated by EGFR signalling in the *KRAS* mutant cell line SW480 (Hung et al., 2013). Considering this, it is likely that signalling mechanisms are more complex and Kras-independent mechanisms of Cten induction could exist. To investigate this further, the regulation of Cten by EGFR and Kras signalling was explored and additionally, whether this caused a Tensin switch in CRC cell lines was investigated.

4.2. Results

4.2.1. EGF Stimulation Upregulates Cten Expression

The regulation of Cten by EGFR signalling was firstly investigated. Four CRC cell lines were selected based on their varying levels of Cten expression and *KRAS* mutation status. These cell lines were stimulated with EGF and the levels of Cten and Tensin 3 protein investigated (figure 4-1). Both SW480 and C32 cell lines initially express moderate levels of Cten and following EGF stimulation show a dose-dependent increase in Cten expression. Since SW480 harbours a *KRAS* mutation (G12V) and C32 is wt. for both *KRAS* and *BRAF*, the effect of EGF stimulation on Cten expression appears to be independent *of KRAS* mutation status. RKO cells do not express any detectable levels of endogenous Cten and although wt. for *KRAS*, RKO cells harbour a *BRAF* mutation (V600E). It was hypothesised that stimulation of RKO cells with EGF may induce Cten expression however, this was not the case. EGF stimulation was next investigated in a high Cten expressing cell line. SW620 cells are derived from the same patient as SW480 cells. Whilst SW480 are derived from the primary tumour, SW620 cells are derived from the metastatic tumour and display higher expression of endogenous Cten. Similar to SW480, SW620 cells harbour a mutation in the *KRAS* gene (G12V). Initially, under low EGF concentration conditions, Cten expression was increased however, stimulation with high concentrations of EGF caused a decrease in Cten expression. The data suggests that Cten expression is induced by EGFR signalling however, when Cten expression is high, expression cannot be further induced. It is possible that negative feedback mechanisms apply to prevent further Cten upregulation. Furthermore, the upregulation of Cten by EGFR signalling appears to be independent of *KRAS* mutation status.

EGFR signalling regulates Cten at the protein level. Next, to determine whether EGFR signalling is regulating *CTEN* at a transcriptional level, qRT-PCR was performed following stimulation with EGF (figure 4-2). In SW480, SW620 and C32 cell lines, *CTEN* mRNA levels remained consistent following stimulation. This suggests that EGFR signalling regulates Cten at the protein level only.

To investigate whether a Tensin switch process occurs in CRC, the levels of Tensin 3 protein and mRNA were investigated (figure 4-1 and 4-2). There was no consistent pattern of Tensin 3 protein expression following EGF stimulation but often, the expression reflected the changes in Cten expression. As with *CTEN*, the levels of *TENSIN 3* mRNA did not respond to EGF stimulation. It would therefore seem that there is no Tensin switch in these CRC cell lines investigated.
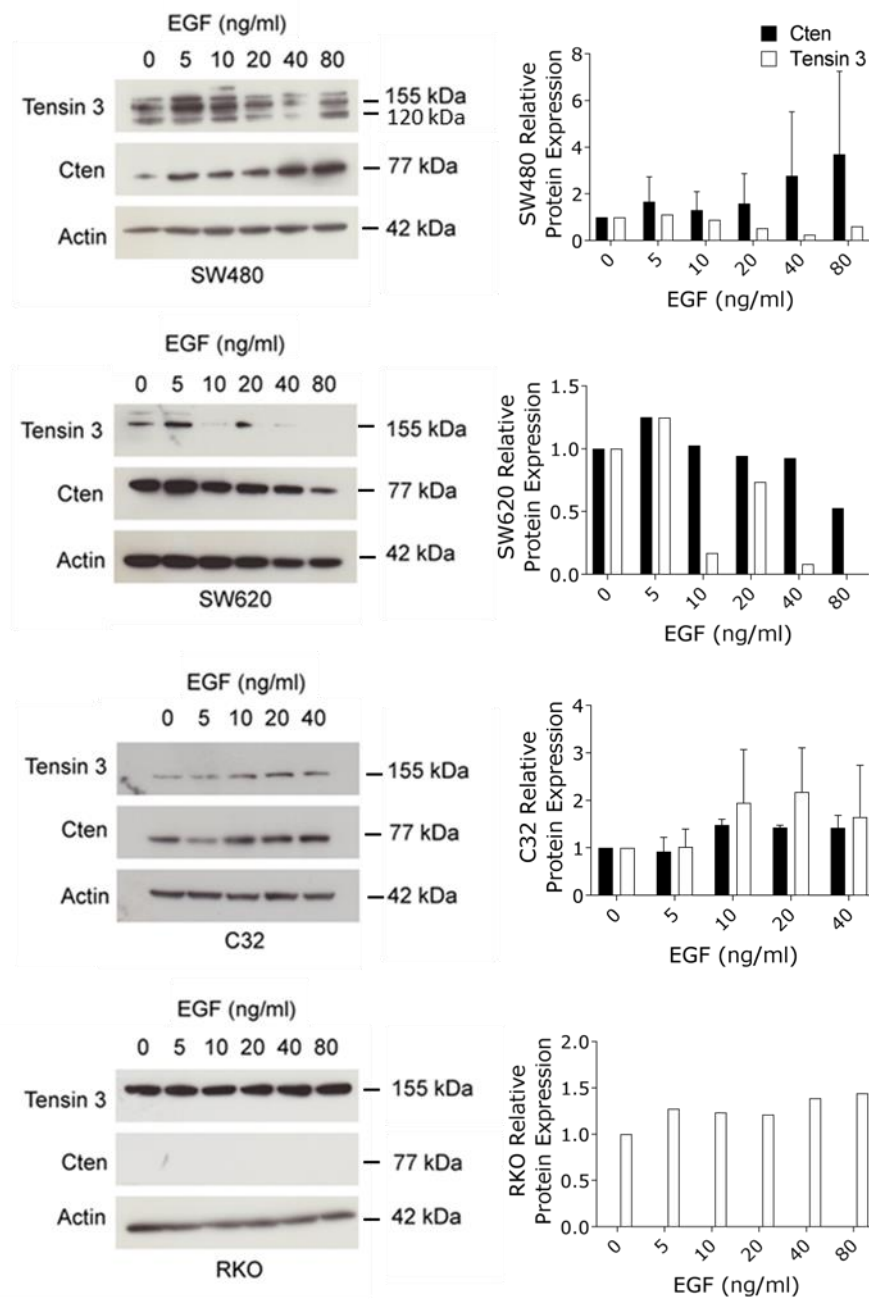
Figure 4-1: *The regulation of Cten and Tensin 3 protein by EGFR signalling. SW480, SW620, RKO and C32 cell lines were stimulated with EGF (0-80 ng/ml) and the changes in Cten and Tensin 3 protein expression were determined by western blotting (C32 and SW480 n=2, SW620 result is representative of 2 experiments, RKO n=1).*
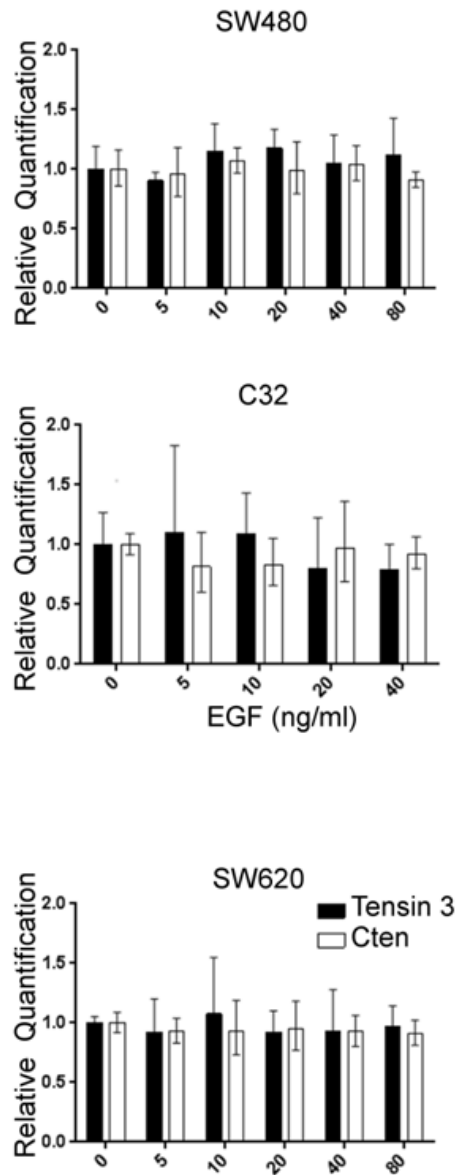
Figure 4-2: EGFR signalling does not regulate the transcription of CTEN and TENSIN 3. CTEN and TENSIN 3 mRNA expression levels were determined by qRT-PCR. In SW480, C32 and SW620 cell lines, CTEN and TENSIN 3 expression remained consistent following EGF stimulation (0-80 ng/ml) (all $p > 0.05$, one-way ANOVA, n=3).

4.2.2. Kras Regulates Cten and Tensin 3 Expression

Cten has previously been shown to be regulated by Kras-Braf signalling (Al-Ghamdi et al., 2011). To confirm these findings, and additionally, to extend this to Tensin 3 signalling, Kras expression was manipulated in SW620 and DLD1 cell lines, which both harbour *KRAS* activating mutations (G12V and G13D respectively) and high levels of Cten expression. Corroborating with earlier findings, siRNA mediated knockdown of Kras was associated with reduced Cten expression in both DLD1 and SW620 (figure 4-3). Additionally, knockdown of Kras was also associated with a reduction in Tensin 3 protein.

At the mRNA level, knockdown of Kras led to a reduction in *CTEN* expression suggesting that whilst EGFR signalling regulates Cten at the protein level, Kras signalling regulates *CTEN* at the transcriptional level. Knockdown of Kras was associated with an increase in *TENSIN 3* mRNA but a decrease at the protein level suggesting that post-transcriptional regulation of Tensin 3 may exist. Overall however, a Tensin switch did not occur through Kras signalling.
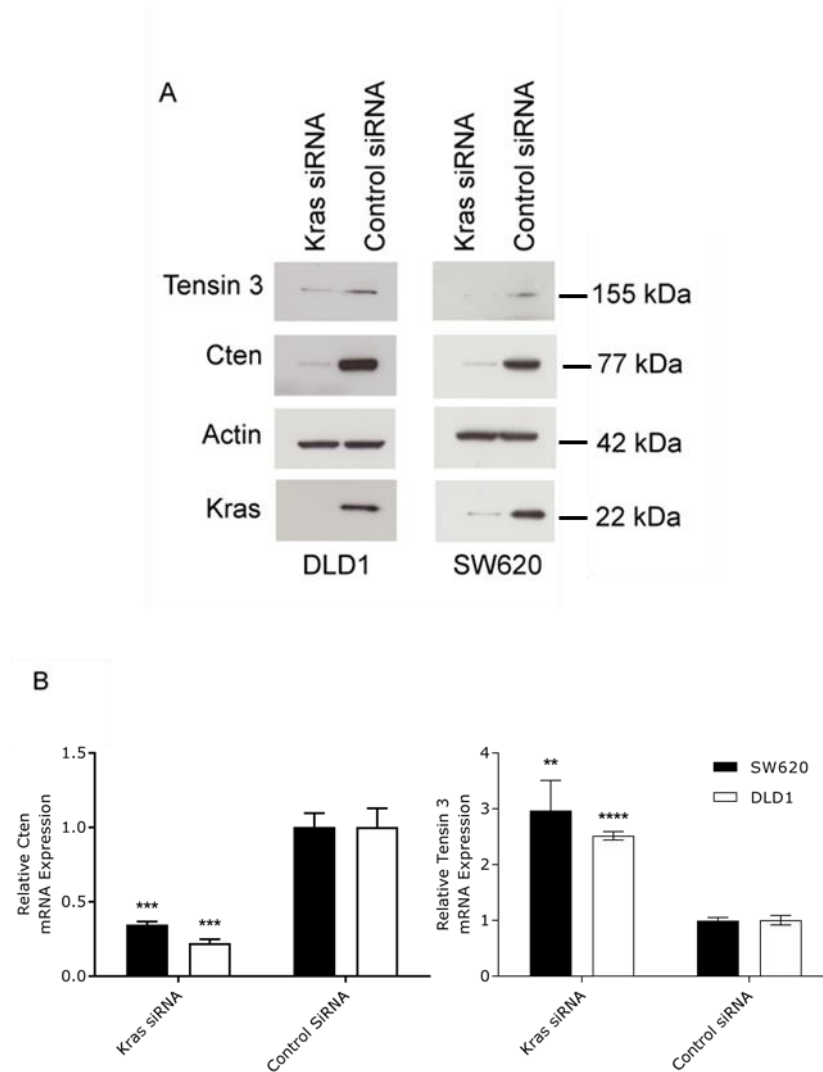
Figure 4-3*: Cten and Tensin 3 are regulated by Kras. A) Knockdown of Kras in DLD1 and SW620 led to a reduction of Cten and Tensin 3 protein expression. Results are representative of at least 2 experimental replicates. (B) The knockdown of Kras was associated with a reduction of CTEN mRNA expression in DLD1 (p=0.0004) and SW620 (p=0.0003) cell lines. An increase in TENSIN 3 mRNA expression was observed in DLD1 (p<0.0001) and SW620 (p=0.0033) cell lines (unpaired t-test, n=3).*

4.2.3. Cten Regulates Tensin 3 Expression

Following the manipulation of EGFR and Kras signalling, the expression of Tensin 3 protein often reflected the changes in Cten protein expression and it is therefore possible that they could be regulated in the same pathway. To investigate this, the levels of Cten expression were manipulated. Knockdown of Cten using siRNA was optimised in SW620 cells as this cell line expresses high endogenous levels of Cten (figure 4-4). A condition in which 100 nM of Cten targeting siRNA was transfected together with 10 μl of Lipofectamine 2000 was considered optimal. Following this, forced expression of Cten in HCT116 and knockdown using siRNA in SW620 cells was performed and the levels of Tensin 3 protein expression were determined (figure 4-5). Tensin 3 protein expression increased on forced expression of Cten and was reduced following Cten knockdown. Taken together, it appears that Cten positively regulates Tensin 3 protein expression.
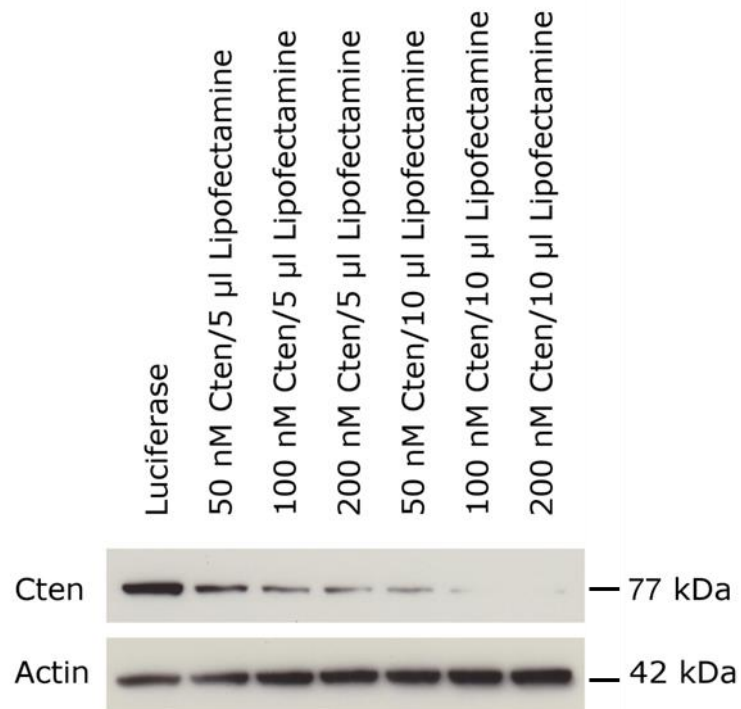
Figure 4-4: *The optimisation of Cten knockdown. The knockdown of Cten using Cten targeting siRNA duplexes was optimised in SW620 cells. A transfection condition using 100 nM of siRNA together with 10 µl of Lipofectamine 2000 was considered optimal.*
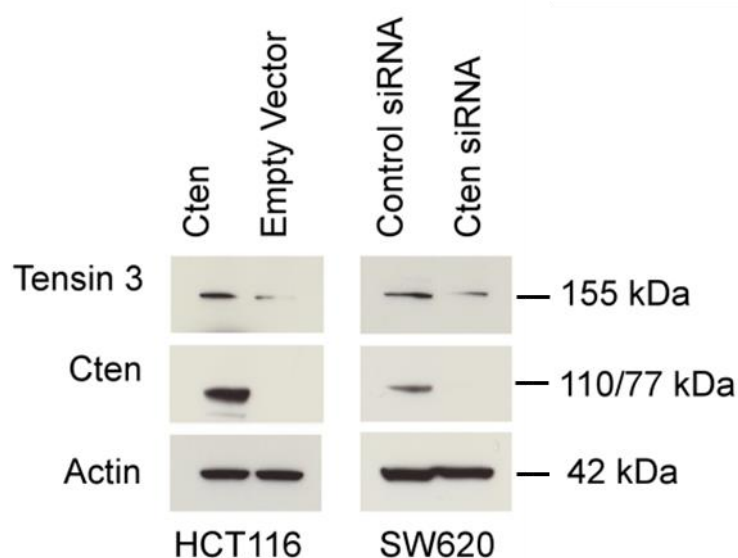
Figure 4-5: *Cten regulates Tensin 3 expression. Forced expression of Cten in HCT116 increased Tensin 3 expression. Knockdown of Cten in SW620 cells was associated with a decrease in Tensin 3 protein. Image representative at of least 2 experimental replicates.*

4.2.4. Cten Stabilises Tensin 3 Protein

As Cten positively regulated Tensin 3 protein, the ability of Cten to increase Tensin 3 protein stability was investigated. CHX inhibits protein synthesis by stopping the elongation of the peptide during translation. CHX was added to HCT116 cells following Cten or empty vector transfection and changes in Tensin 3 protein expression were investigated (figure 4-6). The results did indeed show that Tensin 3 protein is stabilised following Cten transfection when compared to cells transfected with the empty vector control. Following transfection of Cten, Tensin 3 protein is still expressed at 16 hours whereas Tensin 3 protein in the empty vector transfected cells has diminished after 4 hours.
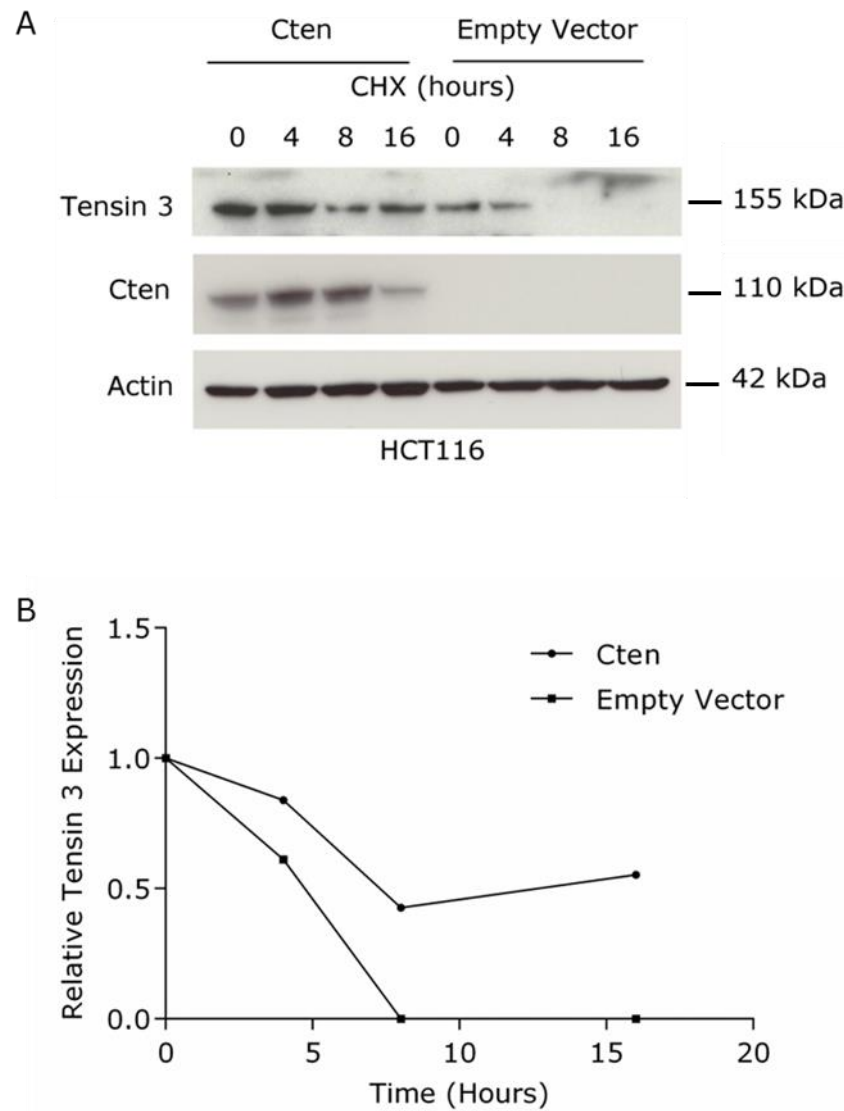
Figure 4-6: *Cten increases Tensin 3 protein stability. A) Tensin 3 protein was stabilised for much longer in HCT116 cells expressing Cten following treatment with CHX compared to HCT116 cells that did not express Cten. Image representative of at least 2 experimental replicates. B) The Tensin 3 decay curve following treatment with CHX. Tensin 3 protein expression was normalised to actin and then normalised to the 0 hour time point.*

4.2.5. DLC1 may not Contribute to Colorectal Cancer Metastasis

The Tensin switch between Cten and Tensin 3 has been shown to cause changes in cell migration through the activity of DLC1 in breast cell lines (Cao et al., 2012). As the results in CRC suggest that a Tensin switch does not occur and in fact Cten stabilises Tensin 3, it was of interest to determine whether Cten still signals to DLC1 to promote cell migration. Seventeen colorectal cell lines were screened for the expression of *DLC1* mRNA, of these, RKO, C32 and CACO2 had the highest expression (figure 4-7). To investigate whether this expression was detectable at the protein level these 3 cell lines, in addition to HCT116, LOVO, SW480 and SW620 were subject to western blot analysis. Only RKO expressed detectable levels of DLC1 at the protein level. As the majority of the cell lines investigated did not express DLC1, it was reasoned that Cten signalling to DLC1 may not play a prominent role in colonic tissue.

DLC1 maps to chromosome 8p22, a region that frequently undergoes loss of heterozygosity (LOH) in CRC. The SAGE profiles for *DLC1*, accessed through Unigene (NCBI), shows that there is low level *DLC1* expression in the intestine and even lower level expression in the tumour thus corroborating the findings that *DLC1* is not highly expressed in CRC.
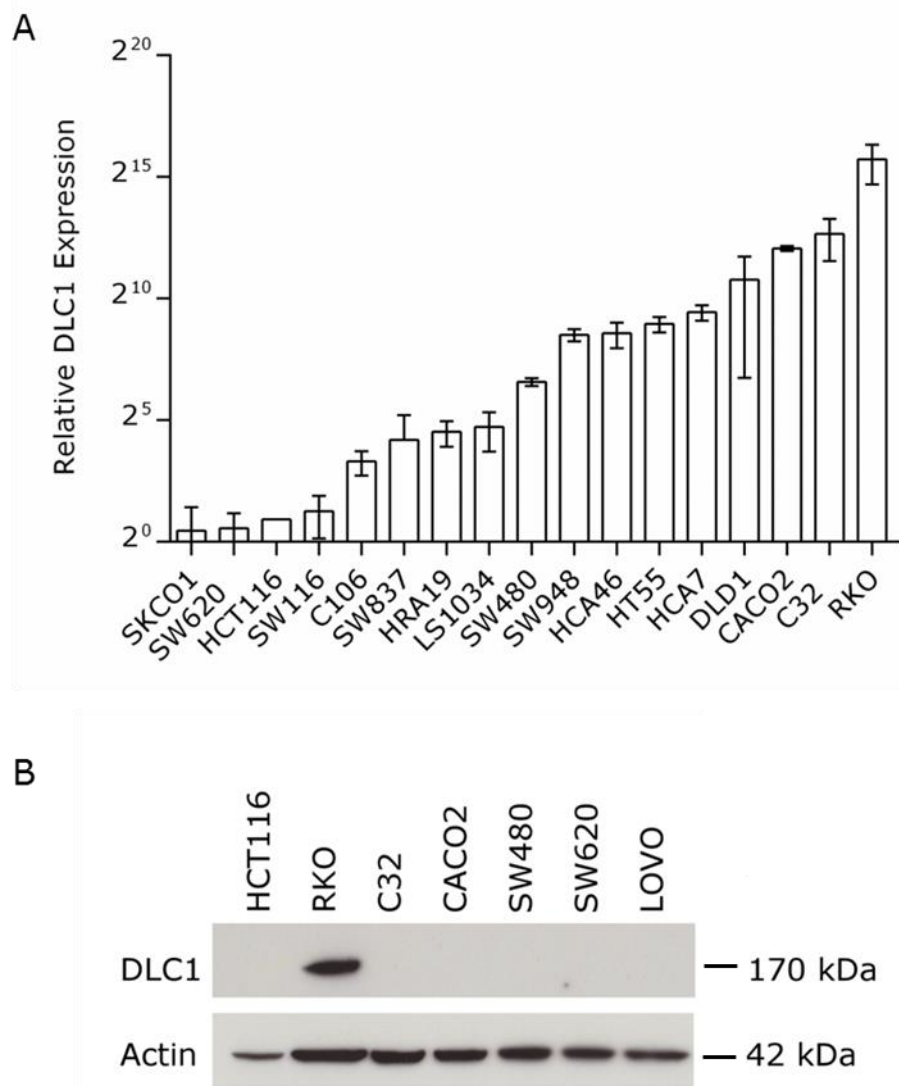
Figure 4-7: DLC1 is not widely expressed in CRC cell lines. A) The mRNA expression of DLC1 in a series of colorectal cell lines. Results were normalised to SKCO1, the lowest DLC1 expressing cell line. B) DLC1 protein expression in colorectal cell lines. Only RKO expressed a detectable level of DLC1 protein.

Tissue	Transcript/ million (TPM)	Spot intensity based on TPM	Gene EST/Total EST in the pool	
adipose tissue	621		8	/ 12866
adrenal gland	60		2	/ 32940
Ascites	0		0	/ 39834
Bladder	0		0	/ 29860
Blood	0		0	/ 122252
Bone	139		10	/ 71618
bone marrow	61		3	/ 48737
Brain	47		52	/ 1092688
Cervix	0		0	/ 48486
connective tissue	147		22	/ 149072
Ear	186		3	/ 16100
embryonic tissue	117		25	/ 212896
Eye	86		18	/ 208840
Heart	189		17	/ 89524
Intestine	25		6	/ 231981
Kidney	47		10	/ 210778
Larynx	42		1	/ 23466
Liver	58		12	/ 205291
Lung	173		58	/ 334815
Lymph	0		0	/ 44302
lymph node	0		0	/ 89748
mammary gland	52		8	/ 151230
Mouth	0		0	/ 66150
Muscle	65		7	/ 106371
Nerve	128		2	/ 15535
oesophagus	0		0	/ 20154
Ovary	19		2	/ 101488
pancreas	32		7	/ 213440
parathyroid	0		0	/ 20594
Pharynx	49		2	/ 40725
pituitary gland	0		0	/ 16526
Placenta	56		16	/ 283019
Prostate	26		5	/ 189536

salivary gland	0		0	/	20265
Skin	123		26	/	210759
Spleen	93		5	/	53397
Stomach	41		4	/	95679
Testis	82		36	/	435204
Thymus	25		2	/	79697
Thyroid	128		6	/	46583
Tonsil	0		0	/	17021
Trachea	154		8	/	51780
umbilical cord	0		0	/	13764
Uterus	77		18	/	232093
Vascular	212		11	/	51649

Table 4-1*: The expression of DLC1 by EST in normal body tissues*

(Unigene).

Tumour	Transcript/ million (TPM)	Spot intensity based on TPM	Gene EST/Total EST in the pool	
adrenal tumour	0		0	/ 12655
bladder carcinoma	0		0	/ 17584
breast tumour	21		2	/ 93090
cervical tumour	0		0	/ 34484
chondrosarcoma	229		19	/ 82838
colorectal tumour	8		1	/ 112517
gastrointestinal tumour	33		4	/ 118498
germ cell tumour	34		9	/ 263230
Glioma	37		4	/ 107194
head and neck tumour	44		6	/ 133826
kidney tumour	43		3	/ 68872
leukaemia	0		0	/ 94479
liver tumour	93		9	/ 96023
lung tumour	0		0	/ 102765
lymphoma	0		0	/ 72196
non-neoplasia	51		5	/ 96623
Normal	89		298	/ 3328811
oesophageal tumour	0		0	/ 17245
ovarian tumour	26		2	/ 76185
pancreatic tumour	19		2	/ 105004
primitive neuroectodermal tumour	39		5	/ 127001
prostate cancer	28		3	/ 103844
retinoblastoma	21		1	/ 46439
skin tumour	79		10	/ 125373
soft tissue/muscle tissue tumour	31		4	/ 125265
uterine tumour	33		3	/ 90107

Table 4-2*: Gene expression of DLC1 by EST in tumours (Unigene).*

4.2.6. Tensin 3 Expression in Colorectal Cancer Tissue

The role of Tensin 3 in cancer is currently debated and the expression of Tensin 3 protein in CRC tissue has yet to be determined. Staining for Tensin 3 in 83 cases (1 core case could not be analysed) of CRC was performed (see 3.2.6). Following initial optimisation in kidney tissue, selected as it is a moderate expresser of Cten and due to tissue availability, the determined antibody concentration was then used for optimisation in colon tissue (figure 4-8). An antibody dilution of 1:200 was selected as it gave a good intensity of staining and showed variability between different colon tissues.

Following optimisation, the colon TMA was subject to staining for Tensin 3 (figure 4-9). Tensin 3 expression was localised to the cytoplasm which is consistent with its localisation at focal adhesions. Of the 83 tumour cases stained 81 (98%) were positive for cytoplasmic Tensin 3 staining. Surprisingly, Tensin 3 was also localised to the nucleus. Nuclear localisation of Tensin 3 was present in 15/83 (18%) tumour cases stained. Tensin 3 positivity in the normal colon was present in 42/49 (86%) and 0/49 (0%) cases for cytoplasmic and nuclear localisations respectively (some normal colon cores were unsuitable for analysis). The Wilcoxon signed ranks test was used to test for significant differences in Tensin 3 expression in the normal colon and tumour. Although there were a greater number of positive cases in the tumour than normal colon, cytoplasmic Tensin 3 staining was not significantly greater in the tumour compared to normal colon (p=0.831). Nuclear Tensin 3 staining was however greater in the tumour compared to the normal colon (p=0.003). Tensin 3 positivity was also detected in the stroma. The Chi squared test was used to test for associations between Tensin 3 staining and the clinical features. Tensin 3

expression was not associated with tumour grade, tumour stage, nodal stage, Dukes stage, vascular invasion, resection margin or lymph node status (table 4-3). Additionally, Tensin 3 expression did not correlate with Cten staining as determined by the Spearman's rank statistical test (figure 4-9 and table 4-4).
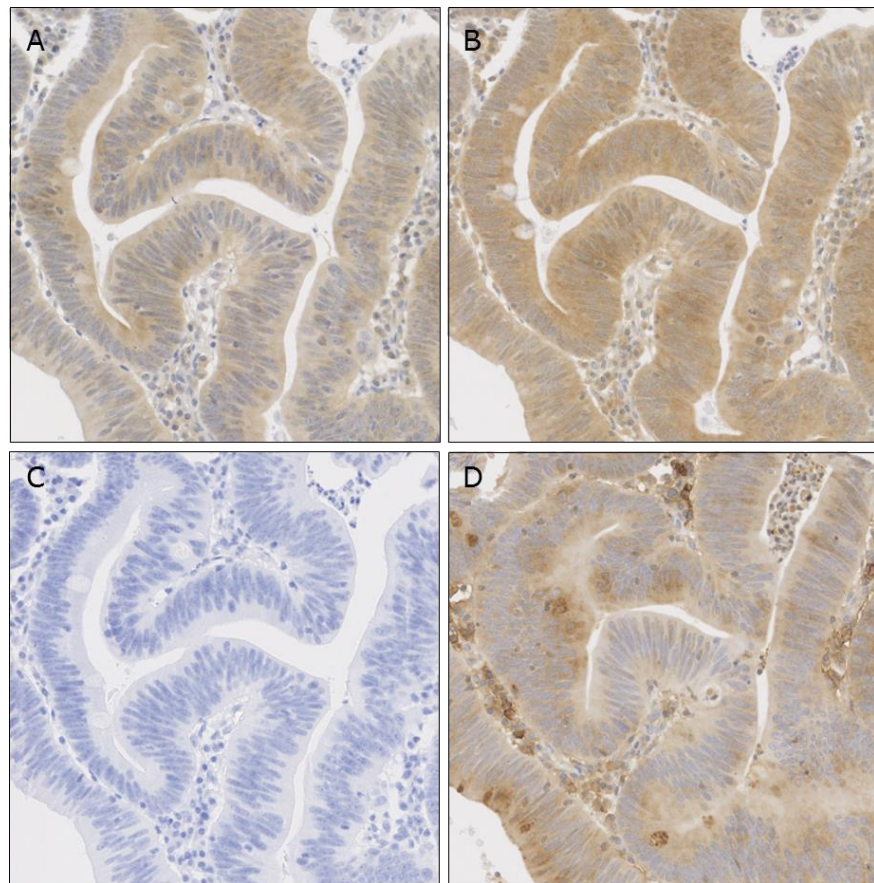
Figure 4-8: *Optimisation of Tensin 3 IHC antibody staining. A) Tensin 3 staining of colon tissue with antibody concentrations of 1:300 B) and 1:200. C) Colon tissue was incubated in absence of primary antibody as a negative control. D) Colon tissue was probed for β2-microglobulin as a positive control*
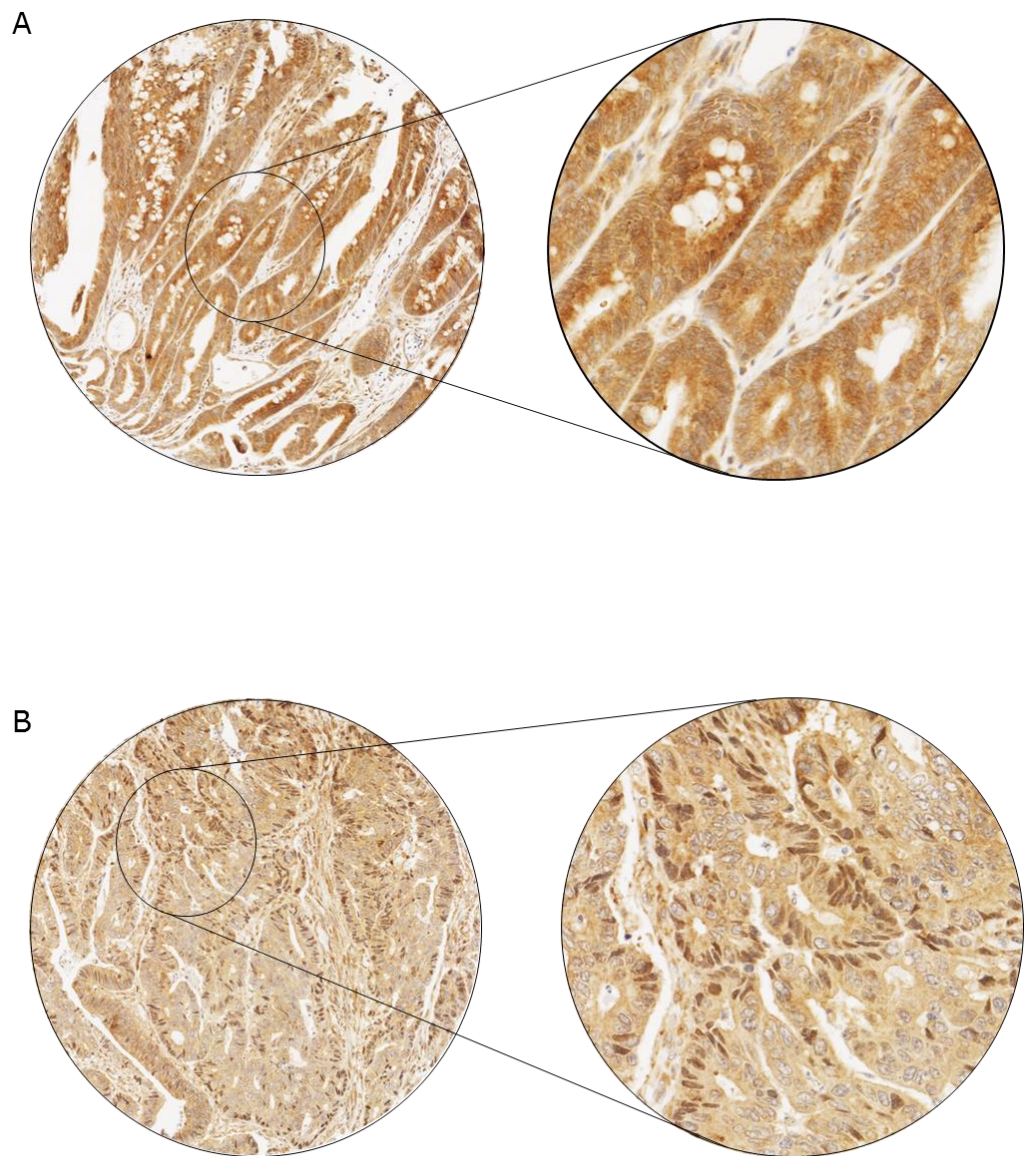
Figure 4-9: Tensin 3 staining of colorectal tumours. A) Tensin 3 staining was mainly localised to the cytoplasm. B) Nuclear Tensin 3 was observed in some of the TMA cores.

Parameter	Cytoplasmic Staining			Nuclear Staining		
	Low	High	P	Low	High	P
Tumour Grade			0.683			0.475
1	0	2		1	1	
2	36	40		57	19	
3	2	3		3	2	
Tumour Stage			0.454			0.154
1	2	1		2	1	
2	3	9		10	2	
3	22	23		29	16	
4	11	12		20	3	
Nodal Stage			0.787			0.922
0	24	28		39	13	
1	10	14		17	7	
2	4	3		5	2	
Vascular Invasion			0.751			0.483
0	21	21		30	12	
1	16	23		30	9	
2	1	1		1	1	
Dukes Stage			0.343			0.399
A	4	9		11	2	
B	19	18		27	10	
C1	11	17		18	10	
C2	3	1		4	0	
Lymph Nodes			1.000			0.798
0	24	28		39	13	
1+	14	17		22	9	
Resection margin			0.598			0.559
Free	36	42		56	22	
Involved	2	1		3	0	

Table 4-3: *Association of Tensin 3 staining of the colorectal tumours and the clinicopathological features (chi-squared statistical test applied).*
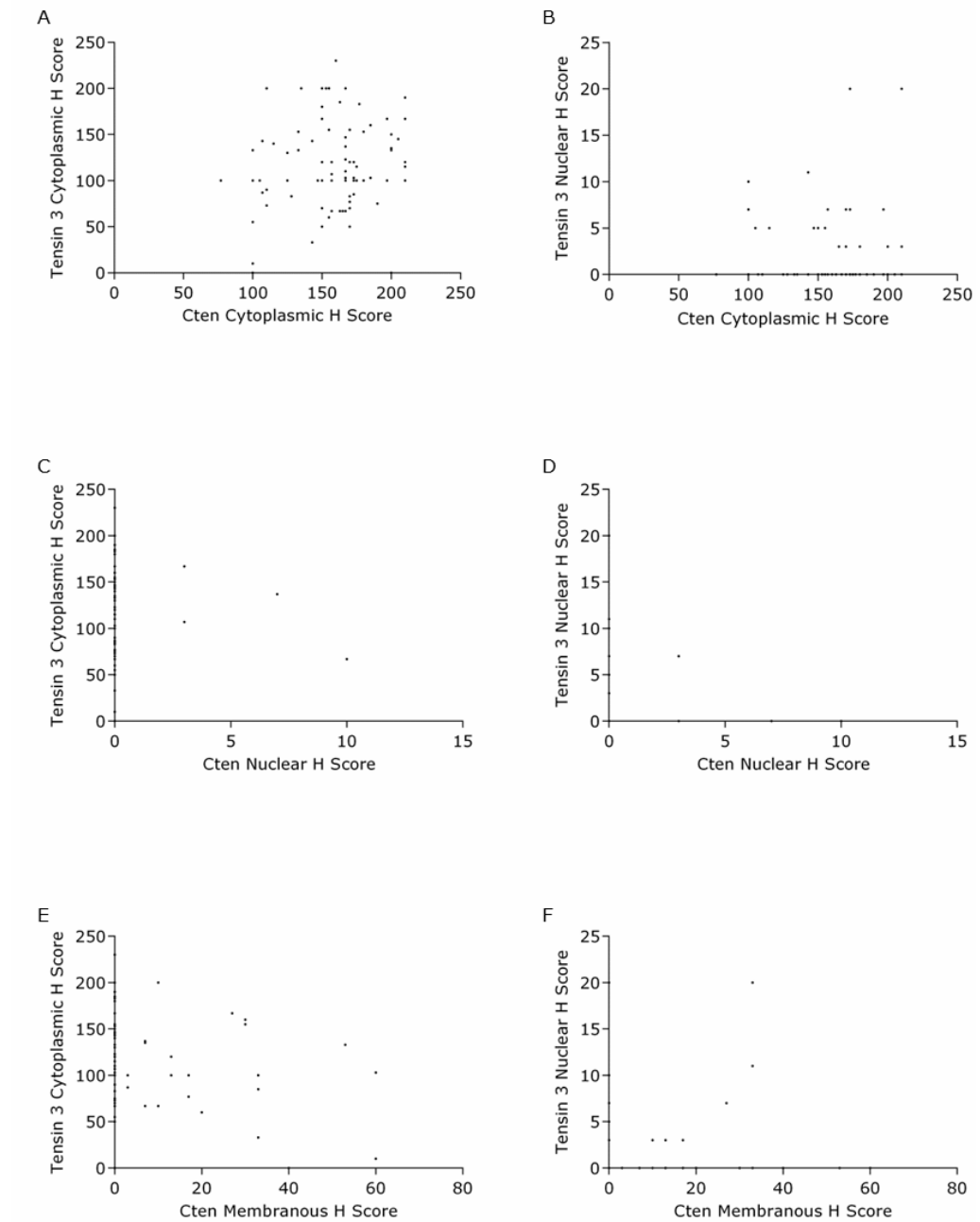
Figure 4-10: *The correlation of Cten and Tensin 3 staining. A) The graphs display the correlations of cytoplasmic Cten and cytoplasmic Tensin 3 H score, B) cytoplasmic Cten and nuclear Tensin 3 H score, C) nuclear Cten and cytoplasmic Tensin 3 H score, D) nuclear Cten and nuclear Tensin 3 H score, E) membranous Cten and cytoplasmic Tensin 3 H score and F) membranous Cten and nuclear Tensin 3 H score.*

	Cytoplasm Cten Staining		Nuclear Cten Staining		Membranous Cten Staining	
	r_s	p	r_s	p	r_s	p
Tensin 3 Cytoplasmic Staining	0.156	0.160	0.030	0.786	-0.181	0.101
Tensin 3 Nuclear Staining	0.073	0.514	0.001	0.991	0.008	0.944

Table 4-4: *The correlation of Cten and Tensin 3 staining of colorectal tumours* (Spearman's rank)*.*

4.3.Discussion

Cten expression is upregulated in tumour tissues however the knowledge of mechanisms that regulate Cten expression are sparse (Albasri et al., 2011b, Sasaki et al., 2003a, Sasaki et al., 2003b). It is here shown that Cten is under the regulation of both EGFR and Kras signalling however no Tensin switch occurs at the protein level in CRC cell lines.

Others have shown that Cten is regulated by EGFR signalling in breast cell lines and it was of interest to determine whether this mechanism of regulation also occurred in CRC (Katz et al., 2007). Stimulation with EGF did indeed upregulate Cten expression but only at the protein level whereas others have found that *CTEN* is upregulated by the EGFR at the transcript level (Cao et al., 2012). Reasons for this discrepancy are not known however, this was seen across multiple cell lines. It is possible that transcriptional changes are not apparent at the longer EGF stimulation periods here used. Additionally, previous experiments were performed in non-tumourigenic cell lines derived from different tissues and it is possible that different signalling pathways apply. Earlier reports that Cten was regulated by Kras signalling were also confirmed (Al-Ghamdi et al., 2011). Unexpectedly, Cten expression was upregulated by EGF stimulation in the Kras mutant cell line SW480. If Kras was downstream of the EGFR with regard to the regulation of Cten, this should not be the case as Kras activity would already be high thus rendering signalling from the EGFR ineffective. This suggests that the EGFR could also signal through a Kras independent pathway to upregulate Cten, possibly through the JAK-Stat pathway, as others have shown that Stat3 is another regulator of Cten expression (Barbieri et al., 2010, Bennett et al., 2015). There are many downstream targets of the EGFR which could possibly be upregulating Cten

and this could be further investigated. In SW620, a cell line that expresses high endogenous levels of Cten, expression was overall decreased on EGF stimulation which suggests that negative feedback mechanisms may prevent further upregulation of Cten. It was also found that EGF stimulation could not induce Cten expression in those cell lines that did not already express Cten. It is possible that epigenetic mechanisms may be overriding the EGFR signalling pathway to prevent the expression of Cten in these cell lines and this remains to be investigated.

In addition to investigating possible regulators of Cten, regulators of Tensin 3 were also determined, to investigate whether a Tensin switch occurred in CRC, and this was shown not to occur. The knockdown of Kras did cause differential regulation of Cten and Tensin 3 at the mRNA level however this did not translate to the protein level. Only approximately 40% of transcriptional data translates to protein as many post transcriptional regulatory mechanisms exist, including the regulation of protein synthesis and protein degradation (Vogel and Marcotte, 2012). This is the first report of Tensin 3 regulation by Kras.

Tensins 1 and 2 in breast cell lines were unaffected by EGF stimulation however since in CRC the Tensin switch did not occur through Tensin 3, and as Tensin 1 and Tensin 2 have a similar domain structure to Tensin 3, it would be of interest to see if these were affected by EGFR signalling in CRC (Cao et al., 2012). Despite levels of Tensin 3 increasing through EGFR signalling, it may still be of interest to determine which Tensin member is bound to Integrins following pathway activation. It is possible that Cten and Tensin 3 compete for Integrin binding regardless of total protein levels. However, together with the fact that DLC1 expression is often lost

in CRC, it is likely that Cten does not promote cell migration through the Tensin switch as was shown to be the case in breast cell lines (Cao et al., 2012). It is possible that the mechanisms of Cten regulation and downstream signalling are tissue specific. It should be noted that as Kras regulates Tensin3 at the mRNA level yet stimulation with EGF does not see a change in Tensin3 mRNA this suggests that Kras-independent mechanisms of Tensin 3 EGFR regulation could also exist.

Further to finding an absence of a Tensin switch in CRC cell lines, Cten was shown to positively regulate Tensin 3 expression. It is not known whether this interaction is functionally relevant, this remains to be investigated. The role on Tensin 3 in cancer is debated with both oncogenic and tumour suppressive activity reported. Prior to the identification of a Tensin switch in breast cell lines, others showed that stimulation with EGF did not cause a decrease in Tensin 3 protein expression but did increase Tensin 3 phosphorylation and this activity was via Src family kinase (Cui et al., 2004). EGF also caused dissociation of Tensin 3 from FAK and dephosporylation of FAK has been shown to promote cell migration however, a defined role for Tensin 3 is yet to be demonstrated in CRC (Cui et al., 2004, Lu et al., 2001). Analysis of microarray expression data revealed a downregulation of Tensin 3 in CRC. In a separate study the expression profiles of SW480 and SW620 were compared (GSE1323). Tensin 3 expression was upregulated in SW620 and since this cell lines is derived from the metastatic tumour, it is possible that Tensin 3 could play a role in metastasis (Muharram et al., 2014, Provenzani et al., 2006). However we have shown that in CRC, Tensin 3 mRNA and protein levels do not correlate and analysis of Tensin 3 expression at the protein level was required. Analysis of 83 cases of CRC revealed that in addition to a

cytoplasmic localisation, Tensin 3 also localises to the nucleus and nuclear localisation was more prevalent in the tumour than the normal colon. This is the first report of Tensin 3 in the nucleus and this finding should be further investigated to ensure that this is not due to poor antibody specificity. Despite showing that Cten stabilises Tensin 3 *in vitro*, Cten staining of colorectal tumours did not correlate with staining for Tensin 3. The reasons for this may lie at the experimental level; the study may benefit from a larger sample size and scoring verification by a pathologist. Additionally as previously mentioned, cores were taken from 3 different regions of the tumour in the construction of the TMA, This may dilute the score if Tensin 3 is only expressed in a particular area of the tumour. At the biological level, it is likely that many other pathways also regulate Tensin 3 *in vivo*, including interactions with the ECM, and it is the interplay between these pathways that regulate the overall Tensin 3 expression. Other pathways could compensate for the upregulation of Tensin 3 by Cten.

It can be concluded that mechanisms of Cten migration are complex and most likely tissue dependant. A Tensin switch does not occur in CRC and it is probable that the EGFR does not signal through Kras to upregulate Cten but these are independent events. Since in CRC the Tensin switch does not explain increased cell motility function by Cten, further signalling mechanisms need to be explored.

5. The Stabilisation of Snail by Cten Increases Cell Tumourigenicity

5.1. Introduction

Cten plays a role in cancer progression, particularly in metastatic disease and it is thought that Cten achieves this by increasing cell migration and invasion. This has been demonstrated by *in vitro* studies using cell lines derived from colon, pancreas, lung, and breast tumours in addition to untransformed cell lines derived from breast tissue (Al-Ghamdi et al., 2011, Bennett et al., 2015, Cao et al., 2012, Katz et al., 2007). Investigations of Cten's role in promoting cell motility *in vivo* are sparse although Cten transfected cells were found to give larger metastatic deposits in mice (Albasri et al., 2011a). Further to this, Cten expression in colon and breast tumours was associated with metastatic disease which supports the notion Cten is increasing cell motility (Albasri et al., 2011a, Albasri et al., 2011b).

It is now of interest to determine how Cten promotes motility and so far only a small number of Cten downstream targets have been identified. Since in the colon, it is likely that Cten doesn't increase cell motility via the Tensin switch mechanism, other pathways downstream of Cten responsible for Cten induced cell motility are sought (Thorpe et al., 2015). In the colon, Cten does signal to focal adhesion localised proteins ILK and FAK which are known to regulate cell motility. (Albasri et al., 2011a, Al-Ghamdi et al., 2013) Additionally Cten downregulates E-cadherin; downregulation of this gene is a hallmark characteristic of EMT (Albasri et al., 2009). Further pathway elucidation and mechanistic details regarding Cten mediated cell migration in CRC is warranted.

EMT is a process whereby epithelial cells acquire a mesenchymal cell phenotype to allow cell migration and invasion and is a process native to

embryonic development, wound healing and of interest here, cancer metastasis. Epithelial cells usually have fixed sheet–like structures held together by cell to cell junctions. The main feature of EMT is the downregulation of adherens junction marker E-cadherin thus allowing the breakdown of cell-cell attachment (Cano et al., 2000). EMT may involve the downregulation of other junctional markers including Claudins, ZO1 and Occludin further promoting cell detachment allowing the cell to escape from the primary site. Simultaneous to the loss of epithelial markers, during EMT, the cell epithelium acquires expression of a host of mesenchymal cell markers including N-cadherin and Vimentin (Lamouille et al., 2014). These proteins provide key molecular markers to experimentally investigate EMT processes. Additionally transcription factors that regulate these expression changes are also markers of EMT and include Zeb, Twist and Snail. Snail is a zinc finger transcription factor that regulates transcription through binding E box sequences in the promoter regions of target genes. Snail acts to repress epithelial genes whilst activating mesenchymal genes thereby facilitating cell invasion and migration (Lamouille et al., 2014). E-cadherin is a well described target of Snail signalling (Cano et al., 2000).

Since Cten regulates E-cadherin, and additionally Cten regulates ILK and FAK that have also been linked to EMT processes, it was hypothesised that Cten may be increasing cell motility through the targeting of EMT pathways (Tan et al., 2001, Cicchini et al., 2008). The ability of Cten to regulate EMT processes and the functional relevance of this was investigated in this chapter.

5.2. Results

5.2.1. Cten Promotes Changes associated with EMT

To investigate Cten's role in EMT, Cten (or the empty vector control) was forcibly expressed in HCT116 and Caco-2 cell lines, neither of which express any detectable levels of endogenous Cten, and the protein expression of a panel of EMT markers was determined (figure 5-1). Confirming earlier reports, forced expression of Cten was associated with a decrease in E-cadherin expression, although only a small change was observed (Albasri et al., 2009). Snail expression increased in both HCT116 and Caco-2 cell lines following transfection of the Cten expression construct when compared to the empty vector control transfected cells. Although Snail protein was clearly increased on Cten expression, this did not reach significance at the protein level due to the variation of the increased level of expression on replicate western blots. There was however a clear trend of Snail protein induction. Levels of N-cadherin, the mesenchymal adherens junction marker although induced slightly in Caco-2, generally remained consistent following forced expression of Cten. Vimentin expression was also investigated but found not to be expressed in either of these cell lines. To validate that these observations are not experiment or cell line specific, Cten was knocked down in SW620 using Cten targeting siRNA duplexes and western blotting was again performed to look at the changes in expression of proteins associated with EMT (figure 5-2). Confirming the Cten forced expression results, knockdown of Cten was associated with a decrease in Snail protein expression. Additionally, Cten knockdown was associated with an increase in E-cadherin expression and N-cadherin and Vimentin remained unchanged from the luciferase targeting control.
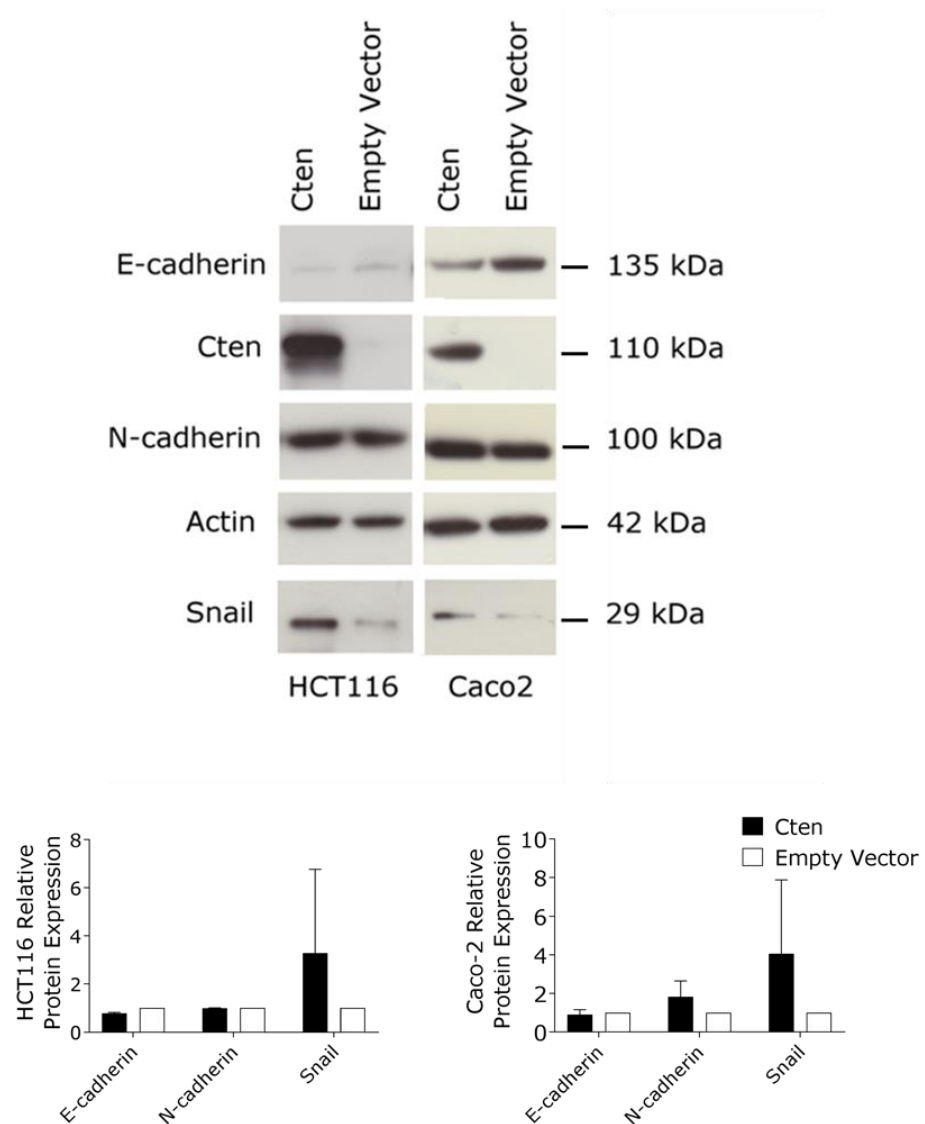
Figure 5-1: *Cten forced expression induces changes associated with EMT. Forced expression of Cten in HCT116 and Caco-2 cell lines was associated with a slight decrease in E-cadherin protein expression (n=2) and an increase in Snail expression (p=0.3206, n=3, unpaired t-test). N-cadherin expression was not consistently altered (n=2).*
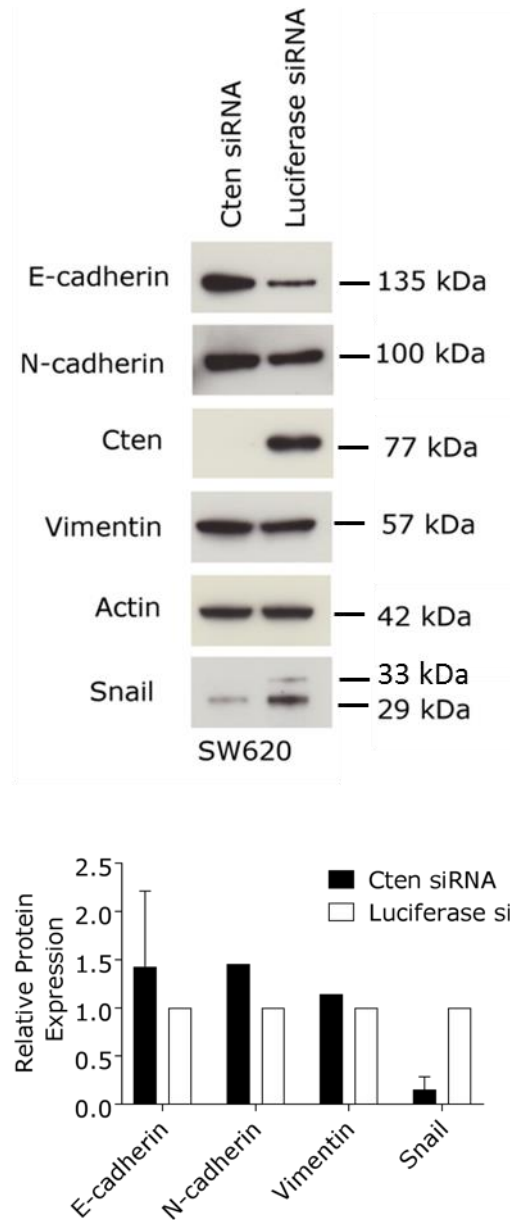
Figure 5-2*: Cten promotes changes associated with EMT. Knockdown of Cten in SW620 cells was associated with an increase in E-cadherin protein expression (n=2) and a decrease in Snail expression (n=2). N-cadherin and Vimentin remained unchanged (n=1).*

Cten expression results in a decrease in E-cadherin expression and increase in Snail expression, both of which are molecular changes associated with EMT to enable detachment from the substratum. As a consequence of these molecular changes, during EMT cells may also adopt morphological changes to assist cell invasion and migration. To investigate whether Cten was associated with a change in cell morphology, HCT116 cells were stained with fluorescently labelled phalloidin which targets the actin cytoskeleton, thus allowing changes in cell morphology to be observed (figure 5-3). In the control cells transfected with the empty vector, HCT116 cells had a rounded appearance and were tightly clustered together. Phalloidin staining was mainly present around the cell periphery. Cten transfected cells generally appeared to be more scattered and less adhered to surrounding cells. However, there were some cells not transfected with Cten that also showed a similar morphology. This shows that in addition to the molecular changes observed, Cten may also induce cell morphological changes associated with EMT however, further study is required.
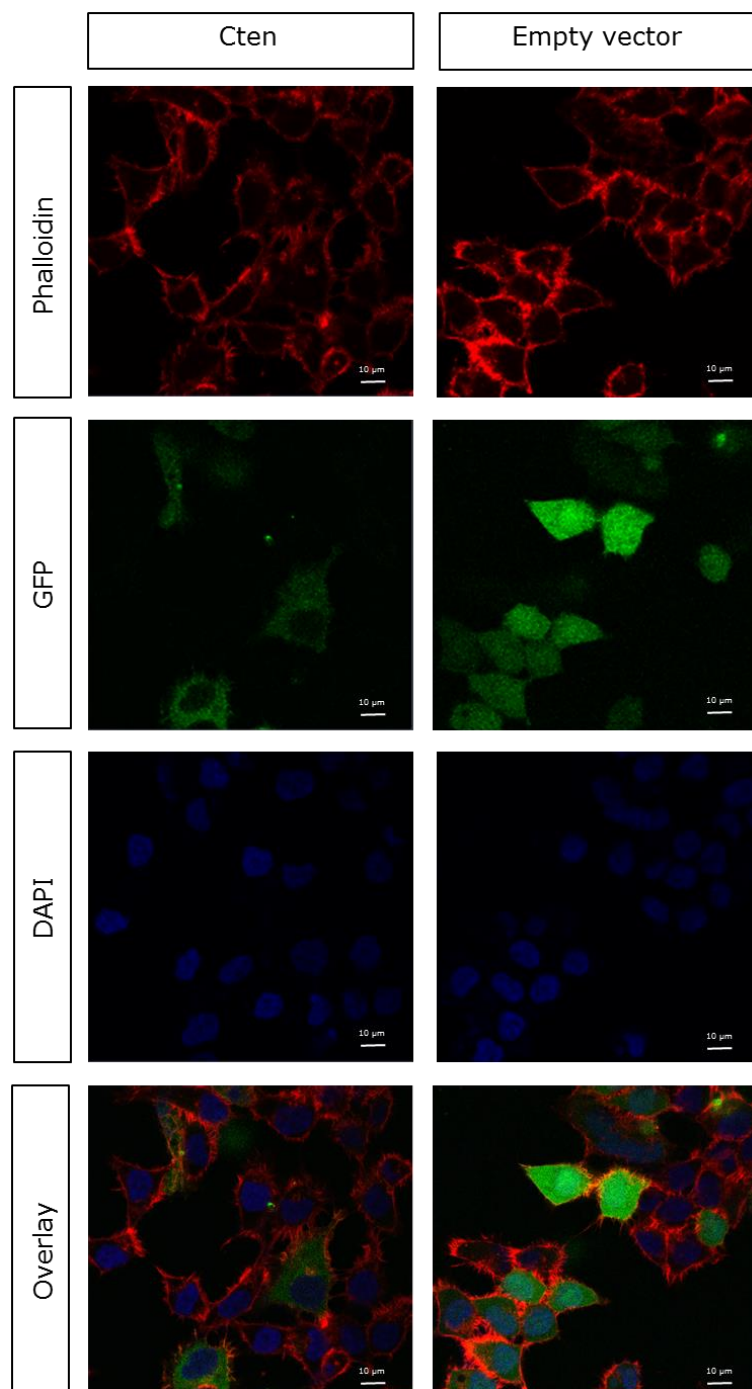
Figure 5-3*: Assessment of cell morphology. Cten transfected HCT116 cells were more loosely arranged than empty vector transfected cells.*

5.2.2. Cten Stabilises Snail Protein Expression

It has been demonstrated that Cten regulates Snail protein expression, next it was of interest to determine the mechanistic detail of this pathway. It is possible that Cten is regulating Snail at a transcription or protein level, or both. To investigate this, Cten was forcibly expressed in HCT116 cells and qRT-PCR performed to quantify changes in *SNAIL* mRNA (figure 5-4). *SNAIL* message level remained consistent following the expression of Cten compared to the empty vector control. This suggests that Cten regulates Snail at the protein level only. It is possible that Cten regulates the rate at which Snail protein is translated following transcription, or it could prevent the degradation of Snail protein. To investigate this, Cten was again transfected into HCT116 cells and following this, cells were treated with CHX, an inhibitor of protein translation (figure 5-5). Inhibiting translation allows the tracking of protein degradation since no new protein is being synthesised. In the control cells, Snail protein had mostly been degraded after 1 hour. In Cten expressing HCT116 cells, Snail protein is stabilised for 2 hours, suggesting that Cten acts to prevent the degradation of Snail protein.

Cten and Snail localise to both the cytoplasm and nucleus and therefore it's possible that that these 2 proteins form part of a complex which prevents Snail degradation. A co-IP was performed to investigate binding interactions (figure 5-6). In this experiment, Cten did not immunoprecipitate with Snail which implied that these 2 proteins do not physically interact.
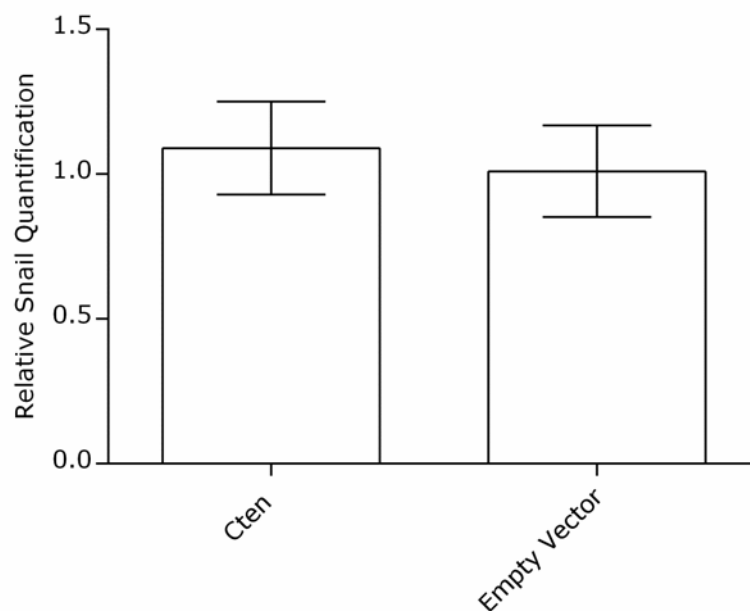
Figure 5-4: *Cten does not regulate SNAIL at a transcriptional level. SNAIL mRNA was unchanged following transfection of Cten in HCT116 cells compared to empty vector control transfected cells (P=0.5730) (unpaired t-test, n=3).*
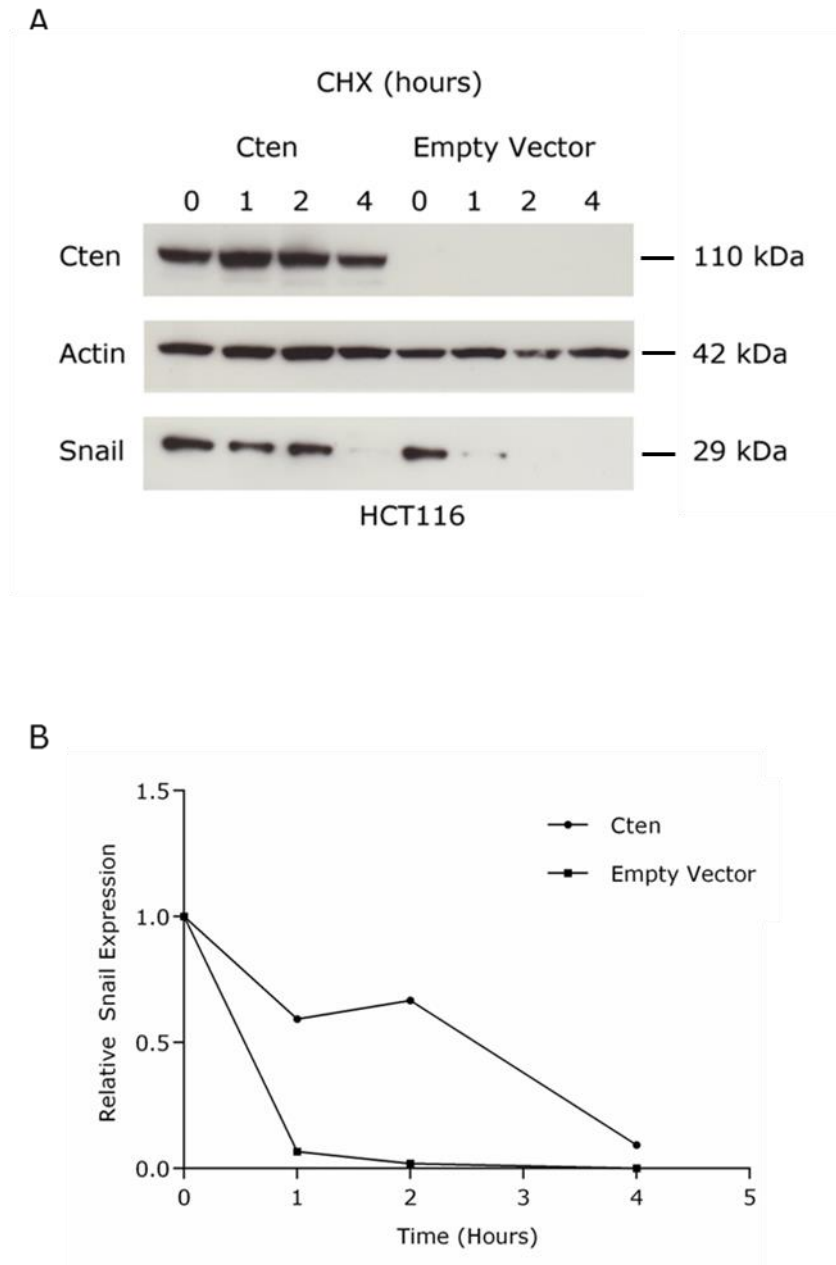
Figure 5-5: *Cten stabilises Snail protein. A) Following the treatment of HCT116 cells with CHX, Snail protein was stabilised for longer in Cten transfected HCT116 cells compared to empty vector transfected cells. Image is representative of 2 experimental replicates. B) The Snail decay curve following treatment with CHX. Snail protein expression was normalised to Actin and then normalised to the 0 hour time point.*
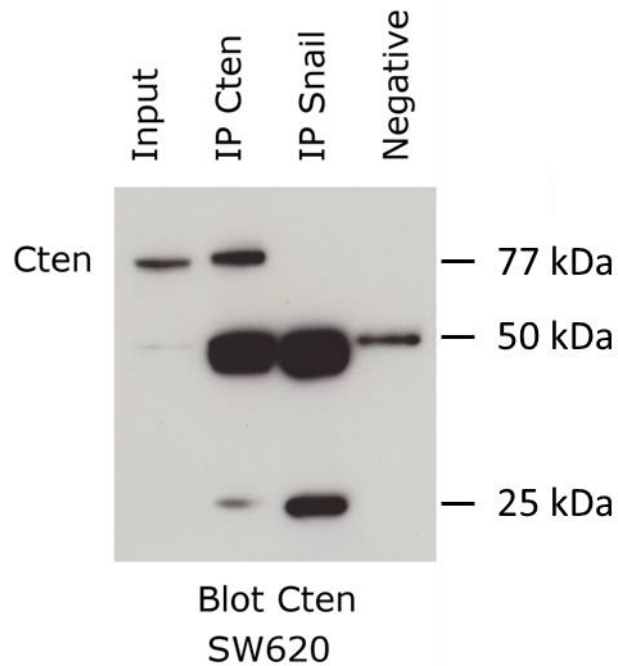
Figure 5-6: *Cten does not co-immunoprecipitate with Snail. Endogenous Cten does not co-immunoprecipitate with Snail in SW620 cells.*

5.2.3. Cten does not Signal through FAK to Stabilise Snail

Cten increases Snail protein stability, next it is of interest to determine how Cten elicits this activity. Cten signals downstream to focal adhesion localised protein FAK and since FAK is linked to EMT, it was hypothesised that it could be a signalling intermediate in the Cten-Snail pathway (Cicchini et al., 2008). To investigate this, overexpression of Cten in HCT116 cells was investigated together with knockdown of FAK to interrogate Snail signalling. Transfection of the Cten expression construct was optimised previously (see 4.2.3). siRNA duplexes targeting FAK were first optimised using 50-200 nM of siRNA together with 5-10 µl of

Lipofectamine 2000 (figure 5-7). The condition that gave the greatest knockdown of FAK protein was considered optimal. Transfection of 50 nM of siRNA together with 5 μl of Lipofectamine 2000 gave the greatest reduction in FAK protein. This condition was considered optimal for future transfection experiments.

Following optimisation, Cten was forcibly expressed in HCT116 cells and FAK subsequently knocked down (figure 5-8). Knockdown of FAK was associated with a reduction in Snail protein expression and forced expression of Cten was associated with a small increase in Snail protein. Forced expression of Cten however was not associated with an increase in FAK expression. In this experiment is seems that Cten is not regulating FAK. It is therefore unlikely that Cten is signalling to Snail through FAK. Further repeats of this experiment are required before firm conclusions can be drawn.
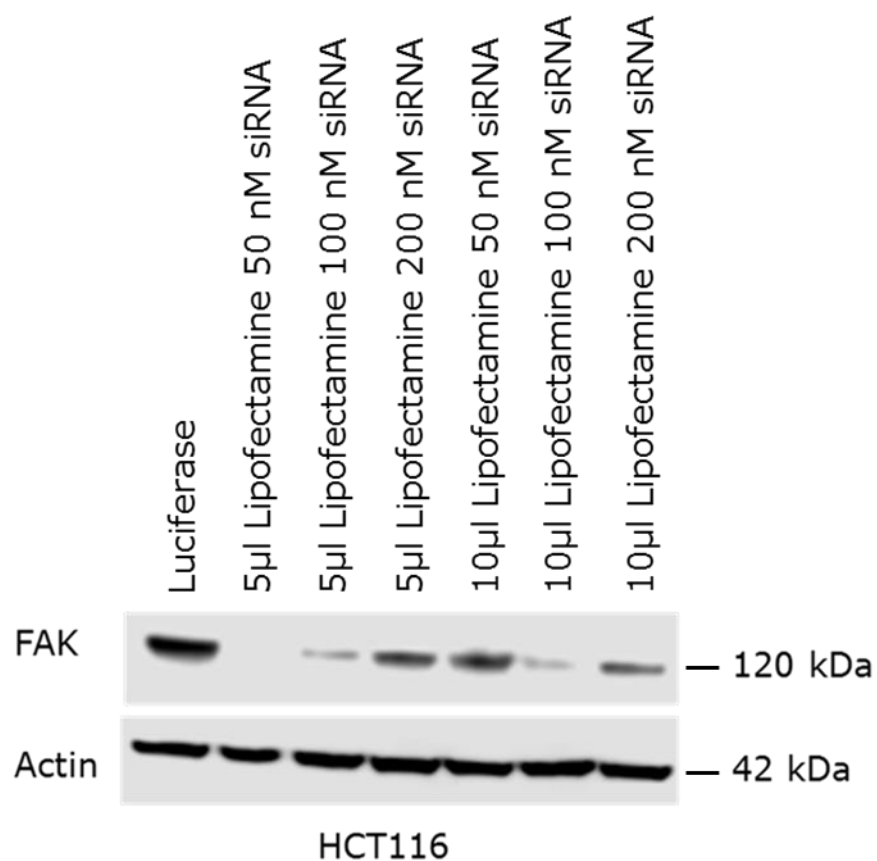
Figure 5-7*: The optimisation of FAK knockdown. The knockdown of FAK using siRNA duplexes was optimised in HCT116. Transfection of 50 nM of siRNA together with 5 µl of Lipofectamine 2000 was considered optimal.*
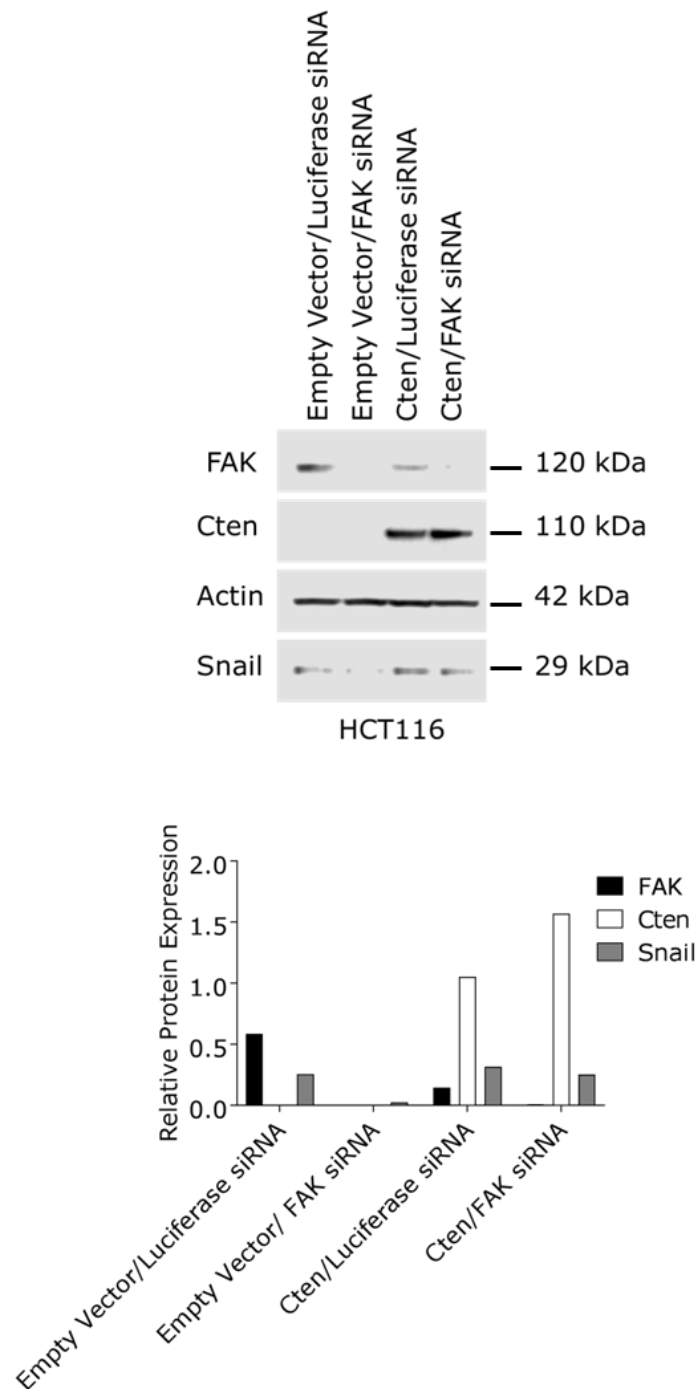
Figure 5-8: Cten may not regulate Snail through FAK signalling. *Forced expression of Cten induced Snail protein expression and this was reduced on knockdown of FAK, but Cten did not induce FAK expression (n=1).*

5.2.4. Cten Regulates Cell Function by Signalling to Snail

Snail has been identified as a downstream target of Cten signalling, next it was of interest to determine whether this signalling axis was functionally relevant. To investigate this, it was necessary to forcibly express Cten in low expressing cell line HCT116 followed by knockdown of Snail and the changes in cell function assessed. The knockdown of Snail using siRNA in HCT116 cells was first optimised (figure 5-9). Snail targeting siRNA duplexes were transfected at a concentration range of 50-200 nM together with 10 µl of Lipofectamine 2000. The optimal condition giving the greatest reduction in Snail protein was by using 100 nM siRNA together with 10 µl Lipofectamine. This transfection condition was used for subsequent Snail knockdown experiments.
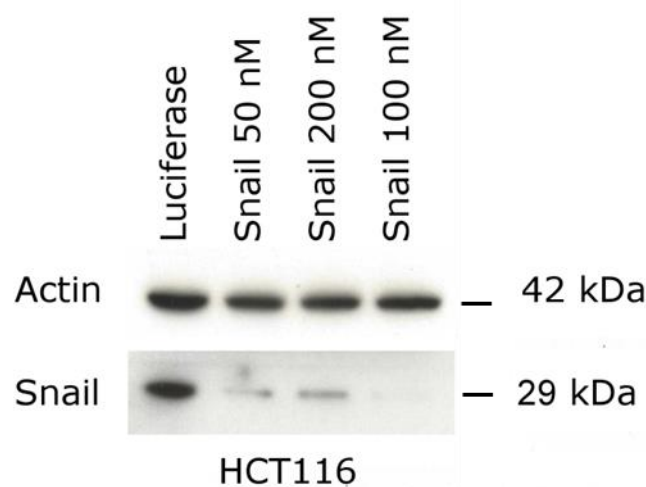
Figure 5-9: The optimisation of Snail knockdown. Cells were transfected with a final concentration of 50, 100 or 200 nM of Snail siRNA together with 10 µl of Lipofectamine 2000. Control cells transfected with 200 nM of Luciferase siRNA together with 10 µl of Lipofectamine.

Both Cten and Snail play roles in regulating cell invasion and migration. Since Cten regulates Snail, it is possible that Cten signals through Snail to increase both of these cell functions. To investigate this hypothesis, Cten was forcibly expressed in HCT116 cells together with knockdown of Snail expression (figure 5-10). The ability of Cten to regulate cell migration was investigated using the Transwell migration assay. Forced expression of Cten in HCT116 was associated with an increase in cell migration however when Snail was subsequently knocked down, this increase in cell migration was lost. This implies that Cten regulates cell motility via Snail signalling. The Transwell invasion assay, which is similar to the Transwell migration assay with the exception that the cells must migrate through a layer of basement membrane extract, was next performed. Forced expression of Cten in HCT116 cells resulted in an increase in cell migration compared to the empty vector and luciferase transfected control cells. The number of invading cells was reduced with subsequent knockdown of Snail, suggesting that Cten and Snail regulate cell invasion by signalling through the same pathway. As an *in vitro* method to assess cell tumourigenicity, the colony formation assay was next performed. The forced expression of Cten in HCT116 cells increased colony formation efficiency and this was lost when Cten was forcibly expressed together with Snail targeting siRNA. These results indicate that Cten could signal through Snail to regulate cell migration, invasion and colony formation efficiency.
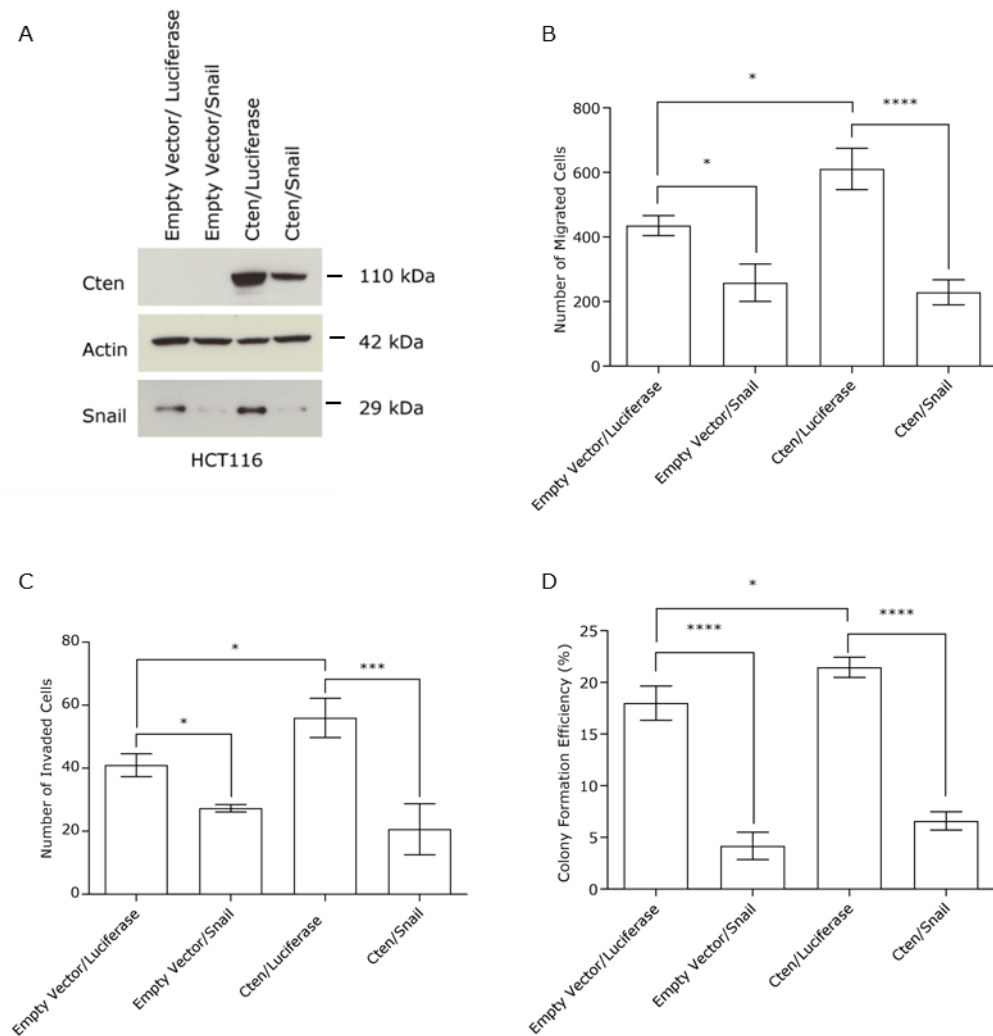
Figure 5-10: *Cten signals through Snail to increase cell function. A) Simultaneous forced expression of Cten and siRNA mediated Snail knockdown. B) Forced expression of Cten in HCT116 increased cell migration (p=0.0110) which was lost with subsequent Snail knockdown (p<0.0001). C) Forced expression of Cten increased cell invasion (p=0.0289) which was lost on Snail knockdown (p=0.0001). D) Forced expression of Cten was associated with an increase in colony formation efficiency (p<0.0380) and this was reduced when Snail was subsequently knocked down (p<0.0001) (one-way ANOVA).*

5.2.5. Snail Expression in Colorectal Cancer Tissue

The expression of Cten in colorectal tumours was previously investigated and here, the expression of Snail was investigated in 84 cases of CRC following antibody optimisation (see 3.2.6). Snail antibody staining was first optimised in kidney tissue, selected as it expresses Snail and as the availability of colon tissue for optimisation was lacking (figure 5-11). After narrowing down the antibody concentration range, Snail optimisation was performed in colon tissue. Antibody dilutions of 1:50 and 1:100 were used with 1:50 giving a greater staining intensity.

Following antibody optimisation, the TMA was stained (figure 5-12). Snail expression was localised to the cytoplasm in 81/84 (96%) of the tumours and nuclear localisation was observed in 55/84 (65%) of the cases (averaged over 3 cores). Staining in the cytoplasm was often granular in appearance. In the normal colon, Snail expression was localised to the cytoplasm in 39/44 (89%) of the cases and nuclear localisation was observed in 12/44 (27%) of the cases (based on 1 core). The Wilcoxon signed ranks test was used to test for significant differences in Snail staining between the normal colon and tumour. The expression of Snail in the nucleus was greater in colorectal tumours compared to the normal colon (p=0.013) whilst cytoplasmic expression was greater in the normal colon than the tumour (p=0.007). Snail staining was not associated with tumour grade, tumour stage, nodal status, vascular invasion, lymph node involvement, Dukes stage or resection margin as determined using the Chi squared statistical test (table 5-1). The Spearman rank test revealed that Snail staining did not correlate with staining for Cten (figure 5-12 and table 5-2).
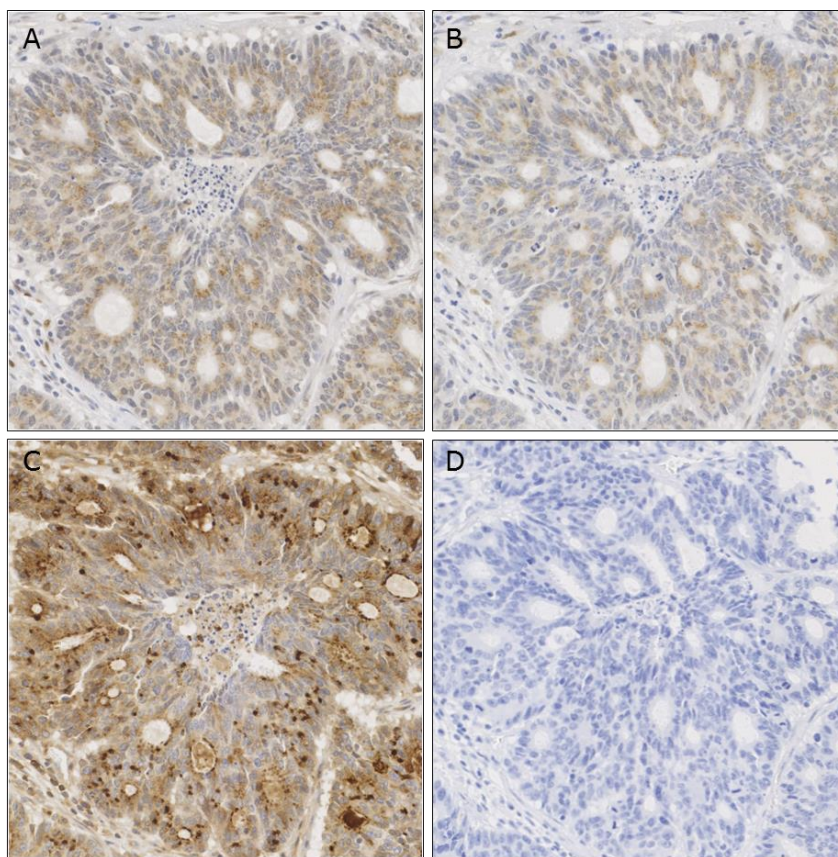
Figure 5-11: Optimisation of Snail IHC *staining.* A) Snail antiodiy staining was optimised in colon tissue at using dilutions of 1:50 B) and 1:100. C) Colon tissue was probed for β2-microglobulin as a positive control. D) Colon tissue was incubated without antibody as a negative control.
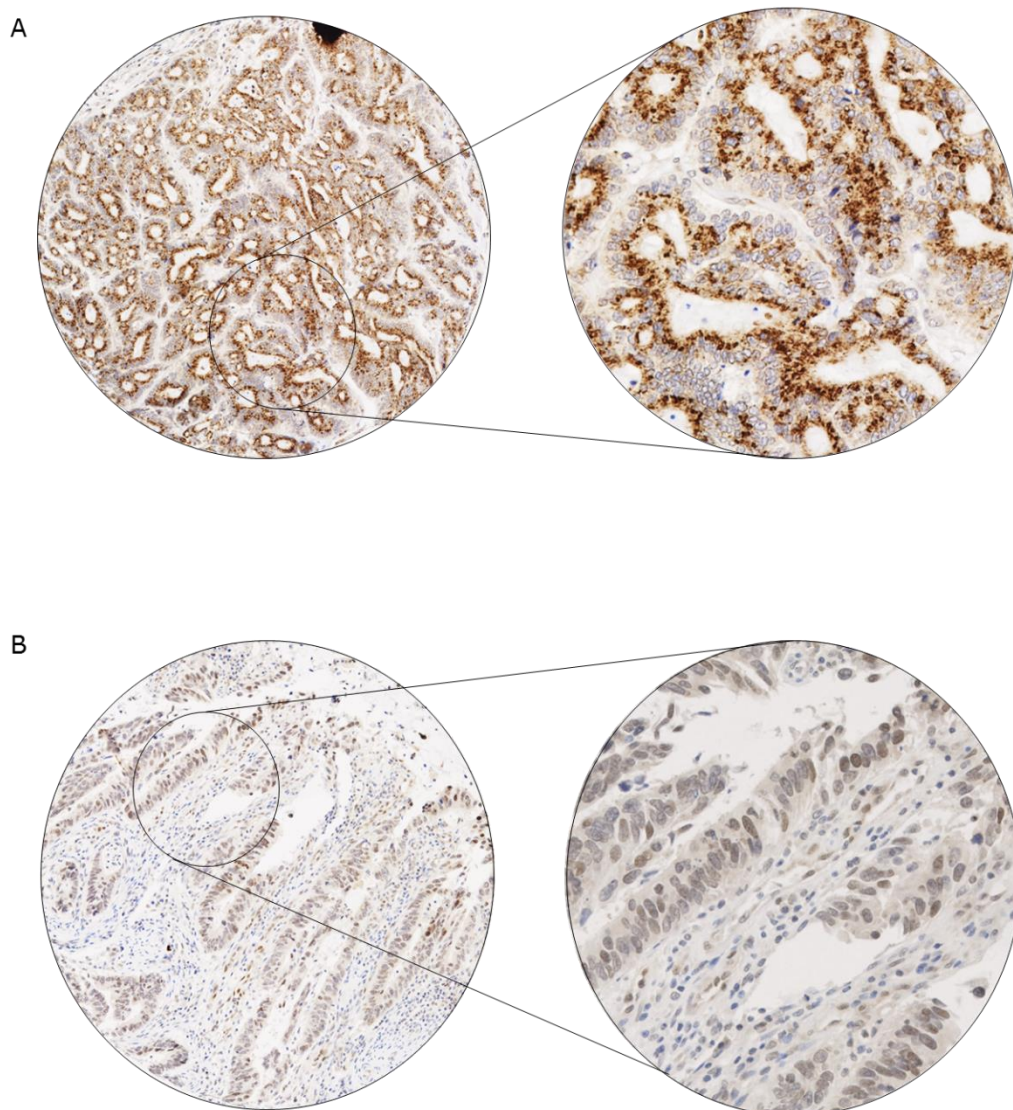
Figure 5-12: *Snail staining of colorectal tumours. A) TMA cores of CRC revealed strong, granular Snail staining of some cores localised to the cytoplasm. B) Snail staining was also localised to the nucleus.*

Parameter	Cytoplasmic Staining			Nuclear Staining		
	Low	High	P	Low	High	P
Tumour Grade			1.000			0.594
1	1	1		1	1	
2	39	38		39	37	
3	2	3		1	4	
Tumour Stage			0.206			0.544
1	0	3		2	1	
2	8	4		8	4	
3	24	22		21	24	
4	10	13		10	13	
Nodal Stage			0.695			
0	25	28		27	25	
1	14	10		12	12	
2	3	4		2	5	
Vascular Invasion			0.912			0.248
0	22	20		23	18	
1	19	21		18	22	
2	1	1		0	2	
Dukes Stage			0.683			0.111
A	6	7		9	4	
B	19	19		17	20	
C1	16	12		14	14	
C2	1	3		0	4	
Lymph Nodes			0.651			0.651
0	25	28		27	25	
1+	17	14		14	17	
Resection margin			1.000			0.616
Free	40	38		39	38	
Involved	2	2		1	3	

Table 5-1*: The association between Snail expression in colon tumours and the clinicopathological features using the chi-squared statistical test.*
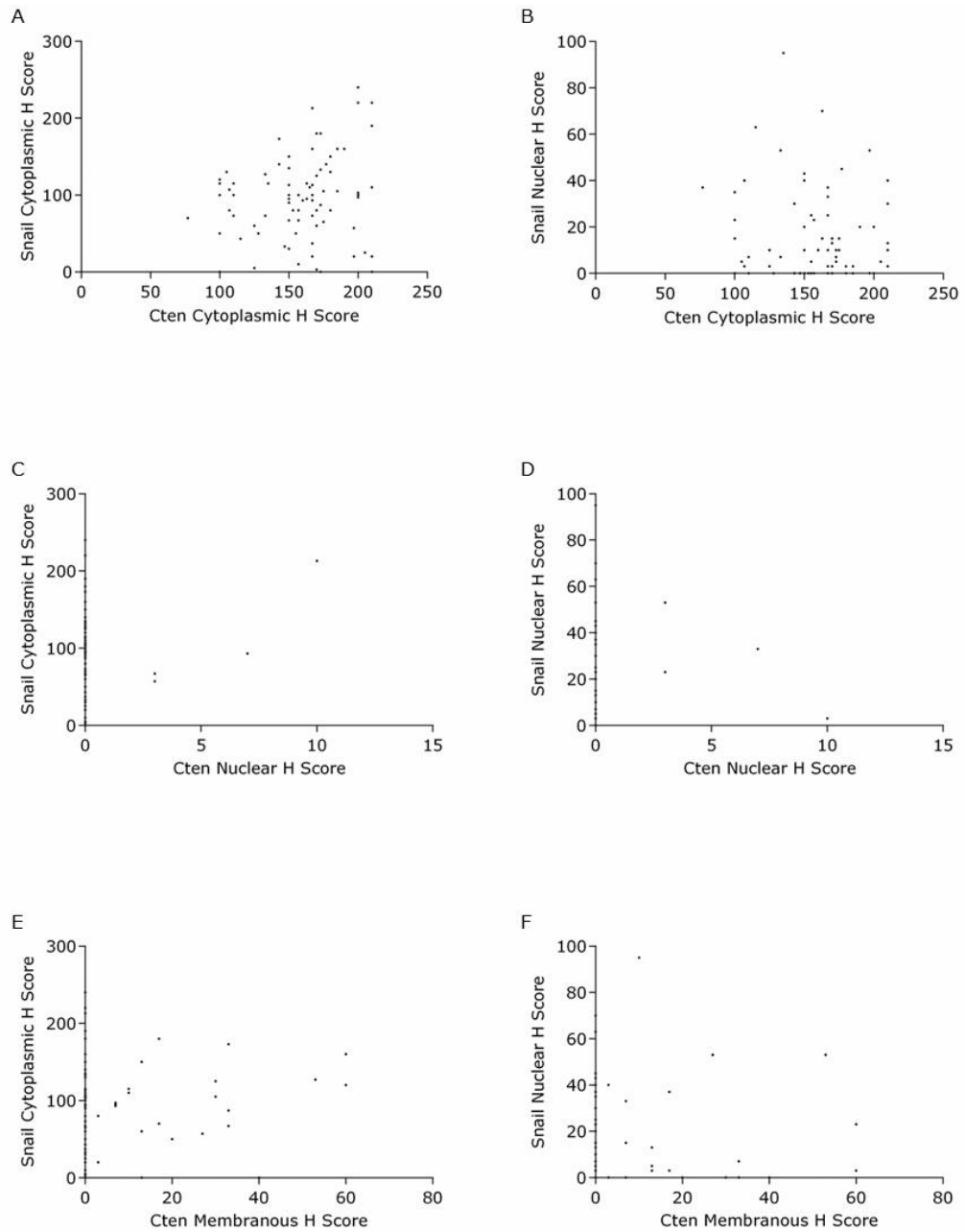
Figure 5-13*: The correlation of Cten and Snail staining. A) The graphs display the correlations of Cten cytoplasmic and Snail cytoplasmic H score, B) Cten cytoplasmic and Snail nuclear H score, C) Cten nuclear and Snail cytoplasmic H score, D) Cten nuclear and Snail nuclear H score, E) Cten membranous and Snail cytoplasmic H score and F) Cten membranous and Snail nuclear H score.*

	Cytoplasm Cten Staining		Nuclear Cten Staining		Membranous Cten Staining	
	r_s	P	r_s	P	r_s	P
Snail Cytoplasmic Staining	0.179	0.103	-0.001	0.996	0.022	0.843
Snail Nuclear Staining	-0.014	0.903	0.186	0.092	-0.005	0.964

Table 5-2: *The correlation of Cten and Snail staining of colorectal tumours (Spearman's rank).*

5.3. Discussion

Cten induces cell invasion and cell migration in most systems studied however knowledge of the underlying signalling mechanisms that promote this activity are sparse (Al-Ghamdi et al., 2011, Al-Ghamdi et al., 2013). Snail has been identified as a novel downstream target of Cten and signalling through Snail was responsible for the induction of cell migration and invasion mediated by Cten.

These results further implicate Cten as a regulator of EMT processes. However, usually molecular changes associated with the downregulation of epithelial marker E-cadherin are accompanied by the upregulation of mesenchymal marker N-cadherin but this was not the case following the manipulation of Cten expression in colorectal cell lines. It is possible that Cten promotes partial EMT (p-EMT) in which cells require some, but not all the characteristics of EMT. This may be accompanied by further molecular changes to promote full EMT (Leroy and Mostov, 2007). Since TGF-β is a master regulator of EMT and TGFβ also regulates Cten, it would be of interest to determine whether TGFβ signals through Cten to upregulate Snail and promote EMT processes (Xu et al., 2009, Peinado et al., 2003).

Cten was shown to prevent the degradation of Snail protein. Snail is often regulated at the protein level to ensure tight control over its transcriptional activity in response to external cues. Snail contains 2 Glycogen synthase kinase-3 beta (GSK3β) phosphorylation motifs, the status of which regulates Snail's cellular localisation and degradation. One of the phosphorylation sites is localised adjacent to a nuclear export sequence (NES) and regulates the export of Snail from the nucleus by increasing accessibility for Chromosomal maintenance 1 (CRM1) (also known as

Exportin) (Dominguez et al., 2003, Zhou et al., 2004). The second phosphorylation site overlaps a Beta-Transducin Repeat Containing E3 Ubiquitin Protein (β-Trcp) (also known as F-box/WD repeat-containing protein 1 (Fbxw1)) destruction box, a motif that is also present in β-catenin. Phosphorylation at this site is required for β-Trcp binding and phosphorylation thereby regulating β-Trcp mediated ubiquitination (Zhou et al., 2004). Phosphorylation of Snail by protein kinase D1 (PKD1) also causes the nuclear export of Snail (Zheng et al., 2014). Phsphorylations may also promote Snail nuclear retention. Both Large tumour suppressor 2 (LATS2) and p21 activated kinase (PAK1) phosphorylate Snail promoting its retention in the nucleus thereby increasing Snail activity, as does dephosporylation by C-terminal domain phosphatase 1 (SCP1) (Yang et al., 2005, Zhang et al., 2012, Wu et al., 2009). Further work needs to address how Cten is promoting the stabilisation of Snail protein. Snail nuclear localisation is dependent upon attachment to the ECM which suggests the involvement of focal adhesion signalling (Dominguez et al., 2003). It's possible that Cten could prevent Snail degradation by regulating its phosphorylation status and/or Snail's subsequent degradation via the ubiquitin proteasome pathway.

The localisation of Snail expression in colorectal tumours and normal colon was consistent with Snail function and role in cancer. Snail nuclear localisation was more prominent in the tumour where it is able to promote transcriptional changes to induce EMT whereas cytoplasmic localisation was more prominent in the normal colon. Others have investigated Snail in the colon and found an upregulation of expression in the tumour (Roy et al., 2005). Correlation of Cten and Snail staining was close to significance in both the nuclear and cytoplasmic compartments. Snail expression was not

associated with any of the clinicopathological features however others have found an association with lymph node metastasis (Fan et al., 2013). Reasons for the discrepancy between the data and previously published data were discussed previously and include the limited size of the data set, the scoring was not verified by a pathologist and additionally, TMA cores were taken from separate regions of the tumour (centre, luminal and invasive edge) which may dilute any signal for example, if Snail was only expressed at the invasive edge.

Cten has previously been shown to regulate FAK in CRC and it was hypothesised that Cten could signal to Snail downstream of FAK. However, although it was confirmed that Cten regulated Snail protein, forced expression of Cten was not associated with an increase in FAK, contradicting earlier reports from this lab (Al-Ghamdi et al., 2013). The reasons for this are not known however, this is only a preliminary result which requires further repetition. It is possible that as different batches of HCT116 cells were used, and cell lines can acquire changes over time, that this may affect cell signalling. Knockdown of FAK was however associated with a decrease in Snail protein suggesting positive regulation of Snail. This is a novel observation not previously reported however replication of this experiment was not performed due to time constraints and is necessary. Investigations into signalling downstream of Cten to ILK to promote Snail protein stability is also warranted.

Both Snail and Cten downregulate E-cadherin however, it is unlikely that Cten signals through Snail to downregulate E-cadherin. Cten was shown to downregulate E-cadherin at the protein level only and Snail is a transcriptional repressor of E-cadherin leading to change in message

levels. It is possible that in addition to Snail, Cten also regulates the stability of E-cadherin, promoting its membrane delocalisation and subsequent degradation and this should be investigated. The Src dependent activation of FAK has been shown to induce this cell activity to promote EMT whilst having no effect on Snail message (Cicchini et al., 2008). Snail regulates the expression of a number of other targets involved in EMT such as Occludin and Claudins (Ohkubo and Ozawa, 2004, Martinez-Estrada et al., 2006, Ikenouchi et al., 2003). It would be of interest to determine whether Cten has any downstream targets in common with Snail that could be mediating the increased migratory and invasive properties observed. Snail is also involved in other pathways besides regulating EMT. Snail regulates stem cell pathways which are linked to EMT pathways. (Hwang et al., 2014, Fan et al., 2012) Additionally, Snail plays a central role in cell metabolism (Dong et al., 2009, Haraguchi et al., 2013). Cten expression so far has not been linked to the regulation of metabolic activity but it is an avenue that could be explored.

Following further mechanistic data regarding the regulation of Snail by Cten, further work could investigate whether Cten signals through Snail to increase metastasis in animal models of cancer. All work previously has been performed using *in vitro* experiments and it would be an interesting next step to determine whether this signalling pathway is still relevant *in vivo*. Snail and Cten protein expression did not correlate in colorectal tumours however signalling mechanisms are complex and other signalling processes could be involved *in vivo*.

In summary, a novel Cten-Snail pathway has been discovered in colorectal cell lines, that acts to increase cell migration and invasion. This finding sheds further light on networks regulating EMT processes in cell motility. Further work could lead to the identification of novel targets against cancer metastasis.

6. Generation of a Cten Knockout Cell Line

6.1. Introduction

CRISPR-Cas9 technology is proving to be an efficient technique to genetically modify DNA and in the process is revolutionising molecular biology research. Using CRISPR-Cas9, frameshift gene knockout or targeted modifications, including specific nucleotide changes, gene activation/repression or insertion such as the addition of a protein tag are some of the possibilities that can be achieved using this technique. CRISPR-Cas9 technology quickly superseded previously used transcription activator-like effector nucleases (TALENs) and zinc finger nucleases (ZFNs) genome editing technologies. Since gaining popularity as a technique in molecular biology, modifications of the original CRISPR-Cas9 technique are arising including the paired nickase approach to improve target specificity and more recently, RNA-targeting Cas9 (RCas9) systems have been developed (Ran et al., 2013, Nelles et al., 2016). It may only be a matter of time until CRISPR-Cas9 technology can be used therapeutically.

The CRISPR technology takes advantage of a mechanism in the bacterial acquired immune response to protect against invading foreign bacteriophage and plasmid DNA. The technology exploits the type II CRISPR system in which foreign DNA is incorporated between CRISPR repeat sequences in the bacterial genome. Upon re-infection, the CRISPR RNA (crRNA) is able to target the invading foreign DNA through base pair complementation and cleavage occurs by the nuclease Cas9, thus eliminating the pending threat (Bikard and Marraffini, 2013).

In genome editing, Cas9 is directed to the target DNA site where a double strand break (DSB) is introduced, causing subsequent activation of the DNA damage response (DDR). Repair of DSBs via non-homologous end

joining (NHEJ) is error-prone and leads to the introduction of random indels which could cause a frameshift and subsequent gene knockout either by changing the resulting coding sequence or by the introduction of a premature stop codon. The use of a donor plasmid enables specific nucleotide editing by providing a template DNA sequence to promote DSB repair by homology directed repair (HDR), incorporating the gene modification (figure 6-1). As changes are made to the DNA sequence, modifications are inherited in the cell progeny (Wei et al., 2013).

Interrogation of Cten signalling has previously been achieved by manipulating Cten expression, either by forced expression of Cten using a plasmid vector or by knockdown using siRNA duplexes targeting Cten mRNA. To knockdown, short double stranded RNA oligonucleotides are introduced into the cell and cleaved by the RNAse II Dicer. Subsequent incorporation into the multiprotein RNAi induced silencing complex (RISC) guides the siRNA to target mRNA and by complementary base pairing can direct its degradation and inhibit its translation. Using siRNA to knockdown Cten has limitations in that as this technique operates at a post-transcriptional level and therefore the knockdown is only transient. Additionally, the protein expression often isn't completely lost and the degree of knockdown is not always consistent between experiments (Barrangou et al., 2015).

To overcome limitations of gene knockdown, CRISPR-Cas9 genome editing technology was used to create a Cten knockout cell line, to provide an alternative, or supplementary method to interrogate Cten signalling in CRC.
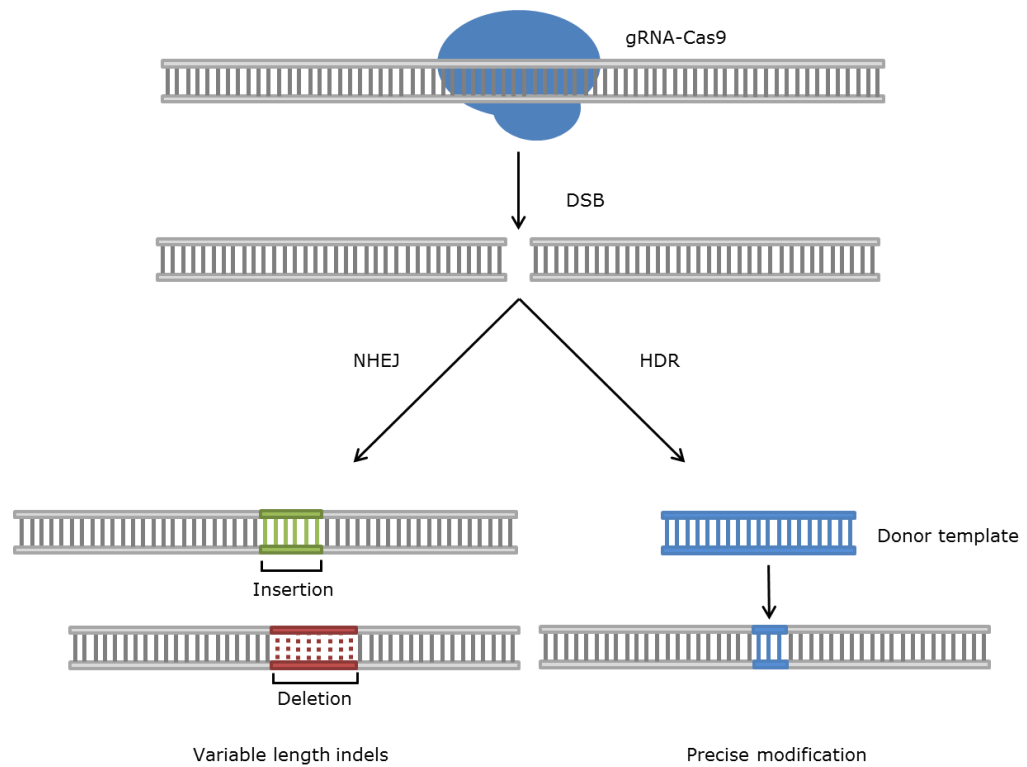
Figure 6-1*: The CRISPR-Cas9 system. CRISPR-Cas9 induced DSBs are repaired by either NHEJ or HDR. NHEJ is an error prone repair mechanism that induces random indels at the site of the DSB to generate products of variable length and sequence. HDR uses a donor plasmid to act as a template to repair the DSB. This repair mechanism is precise and is used to introduce targeted gene mutations.*

6.2. Results

6.2.1. Optimisation of CRISPR-Cas9 Construct Transfection

The generation of Cten knockout SW620 cells was achieved using CRISPR-Cas9 technology. The CRISPR-Cas9 construct comprised both the guide RNA (gRNA) to target Cten exon 3 (sequence CCGCCAGATCAAGGTGCCACGA) and the Cas9 gene to cleave the DNA at this target site (figure 6-2). The transfection of the CRISPR-Cas9 construct was optimised in SW620 and the number of cells expressing GFP (also contained within the construct) was determined by flow cytometry (figure 6-3). Comparable transfection efficiencies were achieved over the conditions in which the amount of construct and Lipofectamine 2000 transfection reagent were optimised. A condition using 4 µg of plasmid together with 5 µl of Lipofectamine gave the highest transfection efficiency (11.17%). These conditions were used for subsequent transfections.
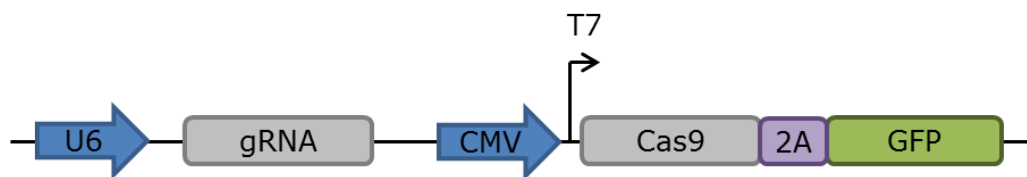
Figure 6-2: *The CRISPR-Cas9 plasmid format. The CRISPR-Cas9 construct (Sigma) comprised the gRNA sequence targeted to exon 3 of Cten downstream of the U6 promoter. The Cas9 gene was fused to GFP with a 2A peptide downstream of a CMV promoter.*
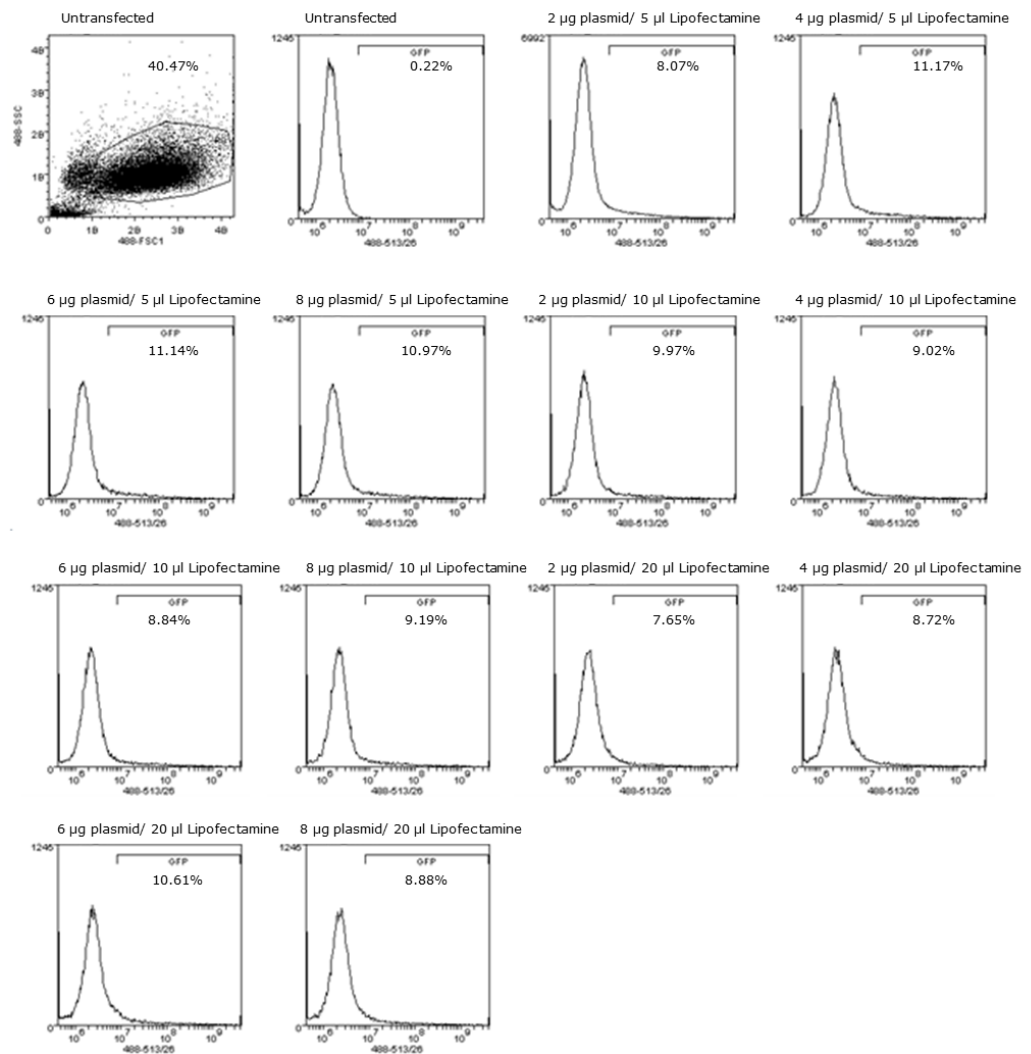
Figure 6-3: *Optimisation of the CRISPR-Cas9-GFP construct transfection. The percentage of GFP expressing SW620 cells was determined by flow cytometry.*

6.2.2. Confirmation of CRISPR-Cas9 Induced Mutation

Following the transfection of SW620 cells with the CRISPR-Cas9 construct, HRM was performed to determine whether this process had induced mutations at the target site in exon 3 of Cten. DNA was extracted from both CRISPR transfected and untransfected SW620 cells and PCR used to amplify the region around the CRISPR-Cas9 target site (figure 6-4). Agarose gel electrophoresis revealed bands corresponding to 333 bp as predicted for the amplification product. HRM analysis revealed a shift in the melting profile of the CRISPR-Cas9 treated SW620 cells compared to the untreated SW620 cells. A shift in the melting profile indicated a change in the DNA sequence and hence could suggest that mutations have been introduced into the Cten DNA sequence.
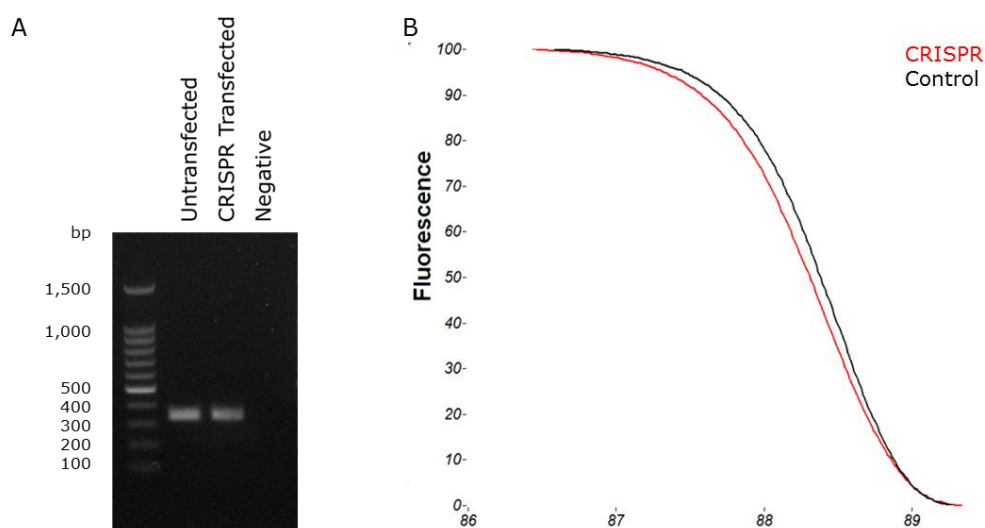
Figure 6-4: *Assessment of CRISPR-Cas9 induced mutation by HRM. (A) PCR amplification of a 333 bp region around the CRISPR target site in exon 3 of Cten for both CRISPR-Cas9 transfected and untransfected SW620 cells. (B) The active melt region from HRM analysis of CRISPR-Cas9 treated (red) and untreated (black) SW620 cells showed a shift in the melting profile.*

6.2.3. Establishment of Homogenous Cell Populations

The CRISPR-Cas9 construct, without a donor plasmid, induces random indels at the target site and hence it is likely that the transfected cells will display a range of mutations. In order to obtain a homogenous cell

population, GFP expressing cells were sorted following CRISPR-Cas9 construct transfection and clonal expansion of isolated single cells was performed (figure 6-5). A total of 384 isolated single CRISPR-Cas9 transfected cells were seeded into 96 well plates and of these, 20 established colony growth and were expanded to T75 flask stage.
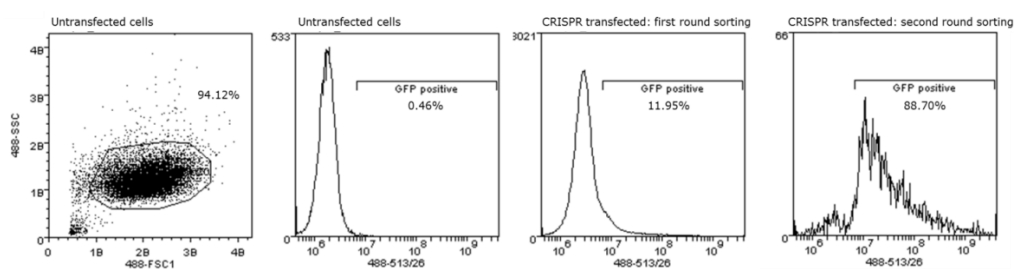
Figure 6-5: The isolation of single CRISPR-Cas9 transfected cells. CRISPR-Cas9 transfected SW620 cells were sorted based on the expression of GFP. Cells went through 2 rounds of sorting to ensure that only GFP positive cells were isolated.

6.2.4. CRISPR-Cas9 Induced Mutation of the *CTEN* gene

In order to create a gene knockout from the introduction of random indels, a frame shift was required to create a change in the downstream translated sequence which could introduce a premature stop codon. Following the clonal expansion of transfected cells, DNA was again extracted and the region around the Cten target site in exon 3 amplified. Purified plasmids isolated from single clones were screened by HRM to identify clonal cell populations that displayed a difference in melting profile

compared to untransfected SW620 cells (figure 6-6). Those melting profiles showing a difference of at least 4% from the untransfected SW620 cells were sequenced. To check for mutations on each allele separately, the amplified Cten sequence was inserted into a vector by TA cloning and following this, blue-white screening used to identify recombinants. The sequence of the clonal populations was subject to BLAST analysis (NCBI) to identify any difference in sequence between Cten in the CRISPR-Cas9 treated SW620 derived DNA and the Cten gene reference sequence (NC_000017.11) (figure 6-7). From the clonally expanded cell lines sequenced, 1 contained a mutation on both Cten alleles. The alleles from this cell population contained a 19 and 20 nucleotide deletion of the Cten sequence. Input of the resulting sequences into ORF Finder (NCBI) revealed that these sequences translated to 333 and 191 amino acid proteins respectively. Wt. Cten comprises 715 amino acids and therefore it can be confirmed that the truncated proteins were due to the introduction of premature stop codons.
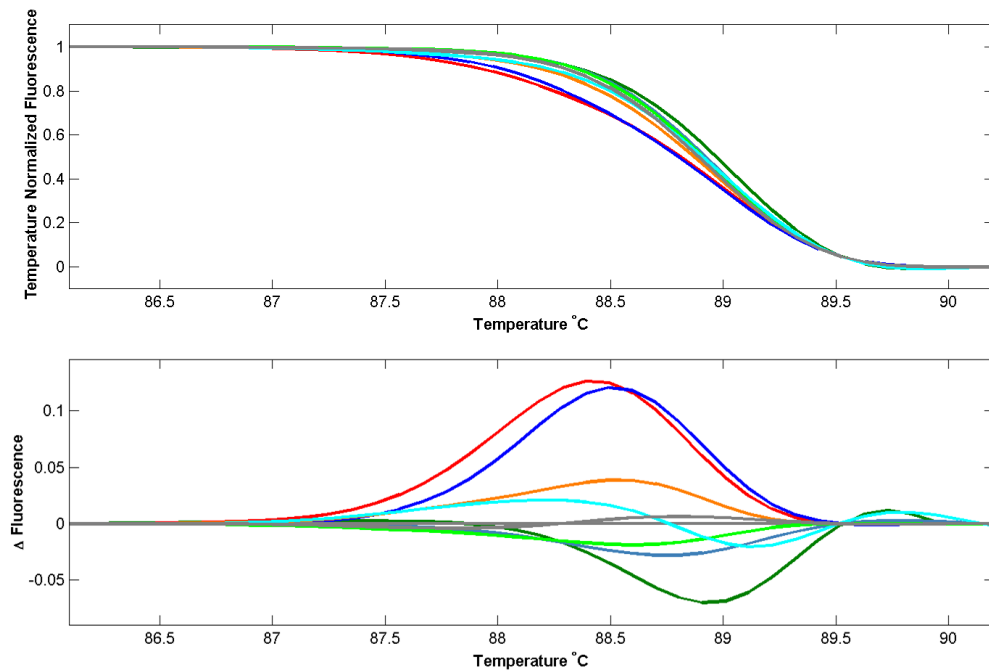
Figure 6-6*: Assessment of CRISPR-Cas9 induced mutation of clonal cell populations. The shifted melting curve (top) and difference plot (bottom) from HRM showed that CRISPR-Cas9 treated clonal SW620 cell populations display a difference in melting profile from untransfected SW620 cells (grey).*

A

Homo sapiens chromosome 17, GRCh38.p2 Primary Assembly
Sequence ID: ref|NC_000017.11| Length: 83257441 Number of Matches: 2

Range 1: 40488809 to 40489110 GenBank Graphics   ▼ Next Match ▲ Previous Match

Score	Expect	Identities	Gaps	Strand
455 bits(504)	4e-125	280/302(93%)	20/302(6%)	Plus/Minus

Features: tensin-4 isoform X1
           tensin-4 precursor

```
Query  6         TGGGCTCTc-tctctgggcctcagtgtcctcgtctctataaaagagggggacagaatga  64
                 ||||||||| |||||||||||||||||||||||||||||||||||||||||||||||||
Sbjct  40489110  TGGGCTCTCCTCTCTGGGCCTCAGTGTCCTCGTCTCTATAAAAGAGGGGGACAGAATGA  40489051

Query  65        ccttgaggatacttccagcctctctgttctatgagtcCAGGCTCCTGCATTTCACCAATG  124
                 |||||||||||||||||||||||||||||||||||||||||||||||||||||||||||
Sbjct  40489050  CCTTGAGGATACTTCCAGCCTCTCTGTTCTATGAGTCCAGGCTCCTGCATTTCACCAATG  40488991

Query  125       CTCTGCTTTTCTCCCCCAAAGACATAAAGTACATCGAGGTGA------------------  166
                 ||||||||||||||||||||||||||||||||||||||||||
Sbjct  40488990  CTCTGCTTTTCTCCCCCAAAGACATAAAGTACATCGAGGTGACCTCCGCCAGATCAAGGT  40488931

Query  167       -CCACGATGGCCCCCAGCACTGCTCCAGCCCCTCTGTCACCCCGCCCTTCGGCTCCCTTC  225
                  |||||||||||||||||||||||||||||||||||||||||||||||||||||||||||
Sbjct  40488930  GCCACGATGGCCCCCAGCACTGCTCCAGCCCCTCTGTCACCCCGCCCTTCGGCTCCCTTC  40488871

Query  226       GCAGTGGTGGCCTCCTCCTTTCCAGAGACGTCCCCCGAGAGACACGAAGCAGCAGTAAGG  285
                 ||||||||||||||||||||||||||||||||||||||||||||||||||||||||| ||
Sbjct  40488870  GCAGTGGTGGCCTCCTCCTTTCCAGAGACGTCCCCCGAGAGACACGAAGCAGCAGTGAGA  40488811

Query  286       GC  287
                 ||
Sbjct  40488810  GC  40488809
```

B Homo sapiens chromosome 17, GRCh38.p2 Primary Assembly
Sequence ID: ref|NC_000017.11| Length: 83257441 Number of Matches: 2

Range 1: 40488809 to 40489110 GenBank Graphics   ▼ Next Match ▲ Previous Match

Score	Expect	Identities	Gaps	Strand
452 bits(500)	5e-124	279/302(92%)	21/302(6%)	Plus/Minus

Features: tensin-4 isoform X1
           tensin-4 precursor

```
Query  9         TGGGCTCTc-tctctgggcctcagtgtcctcgtctctataaaagagggggacagaatga  67
                 ||||||||| |||||||||||||||||||||||||||||||||||||||||||||||||
Sbjct  40489110  TGGGCTCTCCTCTCTGGGCCTCAGTGTCCTCGTCTCTATAAAAGAGGGGGACAGAATGA  40489051

Query  68        ccttgaggatacttccagcctctctgttctatgagtcCAGGCTCCTGCATTTCACCAATG  127
                 |||||||||||||||||||||||||||||||||||||||||||||||||||||||||||
Sbjct  40489050  CCTTGAGGATACTTCCAGCCTCTCTGTTCTATGAGTCCAGGCTCCTGCATTTCACCAATG  40488991

Query  128       CTCTGCTTTTCTCCCCCAAAGACATAAAGTACATCGA--------------------GGT  167
                 ||||||||||||||||||||||||||||||||||||                    |||
Sbjct  40488990  CTCTGCTTTTCTCCCCCAAAGACATAAAGTACATCGAGGTGACCTCCGCCAGATCAAGGT  40488931

Query  168       GCCACGATGGCCCCCAGCACTGCTCCAGCCCCTCTGTCACCCCGCCCTTCGGCTCCCTTC  227
                 ||||||||||||||||||||||||||||||||||||||||||||||||||||||||||||
Sbjct  40488930  GCCACGATGGCCCCCAGCACTGCTCCAGCCCCTCTGTCACCCCGCCCTTCGGCTCCCTTC  40488871

Query  228       GCAGTGGTGGCCTCCTCCTTTCCAGAGACGTCCCCCGAGAGACACGAAGCAGCAGTAAGG  287
                 ||||||||||||||||||||||||||||||||||||||||||||||||||||||||| ||
Sbjct  40488870  GCAGTGGTGGCCTCCTCCTTTCCAGAGACGTCCCCCGAGAGACACGAAGCAGCAGTGAGA  40488811

Query  288       GC  289
                 ||
Sbjct  40488810  GC  40488809
```

Figure 6-7: BLAST analysis of CRISPR-Cas9 induced mutations. (A) BLAST analysis revealed a 19 nucleotide deletion in the DNA sequence derived from the CRISPR treated SW620 cells compared to the Cten gene reference sequence (NC_000017.11) (B) BLAST analysis revealed that the second allele contained a 20 nucleotide deletion of the Cten gene sequence.

6.2.5. Cten is Knocked Out at the Protein Level using CRISPR-Cas9 Genome Editing

Genome editing of SW620 cells was predicted to introduce a premature stop codon in the Cten amino acid sequence and hence result in loss of protein expression. To confirm that this was the case, a western blot was performed (figure 6-8). Protein expression was absent in the Cten knockout cell line even under long exposures whilst still present in the control cell line. This indicates that Cten was successfully knocked out in SW620 cells (SW620^{CtenKO}) using the CRISPR-cas9 technology.
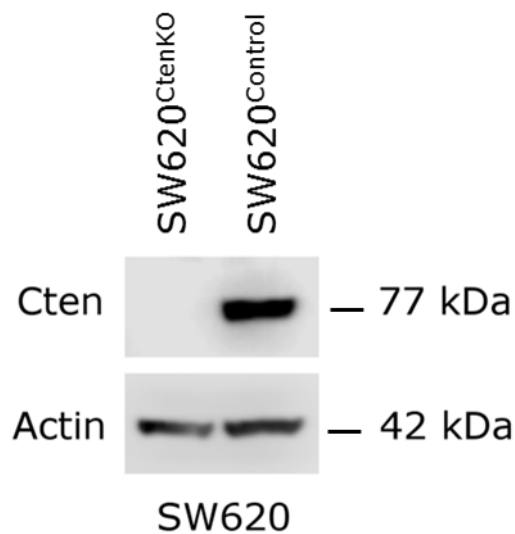
Figure 6-8*: CRISPR-Cas9 induced knockout of Cten protein. Cten protein was knocked out in CRISPR-Cas9 treated SW620 cells compared to the control cell line.*

6.2.6. Validation of the Targeting of Snail by Cten

The validation of Cten knockout on Cten downstream targets was next investigated. Cten was shown to regulate Snail protein expression using a dual approach of gene manipulation. Forced expression of Cten in low expressing cell lines HCT116 and Caco-2 was associated with an increase in Snail expression whereas siRNA knockdown of Cten in high expressing cell line SW620 was associated with a reduction in Cten expression. To validate this, Snail expression was investigated in SW620^CtenKO cells. SW620^CtenKO cells displayed lower Snail expression compared to SW620^Control cells that highly express Cten (figure 6-9). This corroborates with the findings shown using siRNA knockdown of Cten.
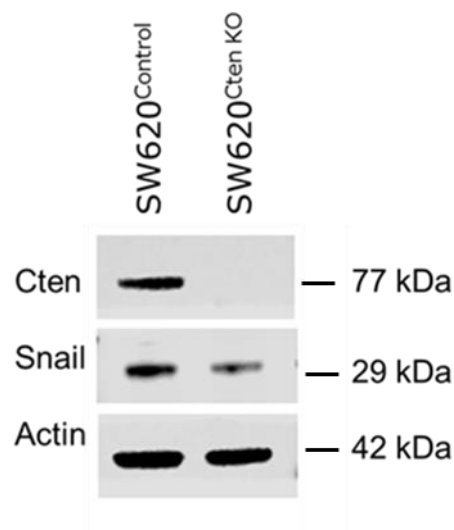
Figure 6-9*: Snail expression is reduced in SW620^CtenKO cells. Snail protein expression was decreased in SW620^CtenKO compared to SW620^Control cells that expressed Cten.*

6.3. Discussion

CRISPR-Cas9 technology is a useful tool for introducing genetic modifications. CRISPR-Cas9 was successfully employed to knockout Cten in the high expressing Cten cell line SW620, to provide validation of or an alternative to transient siRNA knockdown experiments.

Deletion was shown at the DNA level and consequent absence of expression shown at the protein level through the introduction of a frameshift mutation which gave rise to a premature stop codon on each Cten allele. It is possible that the truncated proteins are still expressed within the cell however, as the protein coding region of Cten begins in exon 2 and the CRISPR target site was in exon 3, this leaves only a small section of the Cten coding sequence remaining.

The CRISPR knockout cell line was used to validate siRNA knockdown experiments. Knockout of Cten in SW620 was associated with a reduction in Snail protein expression as previously demonstrated using siRNA. The reduction in Snail protein however was not as marked. It is possible that with long term loss of Cten, other pathways may compensate for this and adapt accordingly.

CRISPR-Cas9 is still a relatively new technology and the extent of off-target effects is currently unknown. This is however also a limitation when using siRNA knockdown as an alternative. There are a number of improvements to this method being described to help reduce the possibilities of this. One such method is the 'paired nickase' approach which uses 2 independent gRNA sequences to increase target specificity (Ran et al., 2013). However, to overcome any issues with knockdown and

knock out of expression, experiments are validated by forced expression experiments and therefore any issue with non-specific targeting should be eliminated.

The creation of a Cten knockout cell line also allows rescue experiments to be performed in which Cten can be restored following knockout and the functional relevance of this explored. It would be of interest to further use CRISPR to modify the *CTEN* gene to investigate the activity of Cten for example, the fluorescent labelling of Cten would allow its localisation to be studied following the manipulation of signalling pathways. In this way, endogenous Cten can be investigated rather than using ectopic expression of Cten.

In conclusion, CRISPR has proved to be an efficient technique to successfully manipulate Cten expression and consequently may allow the development of more complex *in vitro* models to study Cten signalling.

7. General Discussion

7.1.   Introduction

The overall aim of this thesis was to elucidate mechanisms of Cten signalling in CRC, in order to further understand the pathways involved in metastasis. This was investigated *in vitro* by the manipulation of cell signalling pathways to identify mediators of Cten signalling. Functional assays were performed to assess the relevance of such interactions and additionally, the protein expression of Cten and potential signalling targets was investigated in colorectal tumours. This study has made a number of novel observations regarding Cten signalling, the findings of which need to be consolidated and extended in the future.

7.2.   Cardinal Findings

7.2.1. Cten in the Nucleus has Increased Oncogenic Function but it is unlikely that Cten Regulates β-catenin Transcriptional Activity

Cten was previously found to be expressed in the nucleus and nuclear localisation of Cten was more prevalent in metastatic deposits than the primary tumour (Albasri et al., 2011a). Additionally, Cten was shown to bind to β-catenin in the nucleus, a component of the Wnt signalling pathway that is frequently upregulated in CRC (Liao et al., 2009). Considering this, it was hypothesised that Cten may have increased oncogenic function in the nucleus which could arise through the regulation of β-catenin activity and may promote the expression of CSC genes. Together it was hypothesised that these signalling mechanisms could promote CRC metastasis and induce cancer cell stemness.

The nuclear localisation of Cten in tissue sections was confirmed although, nuclear localisation was only present in 3% of the tumours investigated.

Additionally, nuclear expression was found to a similar extent in the normal colon as it was colorectal tumours. Whilst expression of nuclear Cten was previously shown to be upregulated in liver metastasis, it does not seem to be associated with the primary tumour. Cten, when forcibly expressed in the nucleus, gave enhanced cell migration and colony formation efficiency compared to wt. Cten. Investigations attempted to uncover signalling mechanisms that may give rise to this cell functional activity. It was confirmed that Cten in the nucleus did indeed bind to β-catenin and further to this, the interaction was shown to be mediated by the N-terminal region of Cten.

Most other Cten interacting proteins bind to Cten via the C-terminus. Integrin binding is most likely mediated via the PTB domain of Cten whilst DLC1 and c-Cbl bind to the SH2 domain of Cten (Cao et al., 2012, Hong et al., 2013). As far as we are aware, this is the first time that a protein has been identified to bind in the N-terminal region of Cten. Analysis of the Cten sequences reveals Serine rich regions in the N-terminal region with potential phosphorylation sites and it is possible that these could mediate signalling to other proteins. The other Tensins have the actin binding domain located at the N-terminus but their central regions do not show much homology and likely serve different roles (Lo and Lo, 2002).

The nuclear localisation of focal adhesion proteins is a common occurrence. Proteins often translocate to the nucleus and have roles such as acting as transcription factors or transcriptional regulators. ILK is a focal adhesion localised protein which following phosphorylation by P21 Protein (Cdc42/Rac)-Activated Kinase 1 (PAK1), translocates to the nucleus and transcriptionally represses CNKSR Family Member 3 (CNKSR3) (Acconcia et

al., 2007). Similarly, FAK translocates to the nucleus where it inactivates p53 signalling (Lim et al., 2008). Additionally, Paxillin localises to the nucleus where it regulates the activity of the androgen receptor (AR) in prostate cancer. Paxillin binds to and retains the AR in the nucleus thereby promoting its transcriptional activity. (Sen et al., 2012). Similar to Cten, Paxillin has no known NLS and its suggested possible that these proteins could shuttle to the nucleus with other NLS containing proteins (Lim, 2013). It was hypothesised that Cten may regulate the transcriptional activity of β-catenin in a similar way. Despite confirming that Cten does bind to β-catenin, Cten failed to induce (or repress) β-catenin transcriptional activity and furthermore, Cten did not help to retain β-catenin in the nucleus. The role Cten is serving in the nucleus whilst bound to β-catenin is at present unclear.

Cells that are able to undergo metastasis and known to display properties of stem cells (Brabletz et al., 2005). Since Cten expressing cells have greater migratory capabilities, it may be possible that Cten expression is linked to cell stemness. Ectopic expression of Cten however did not induce the expression of any of the CSC markers investigated, neither did Cten induce the transcriptional expression of any other targets when forcibly expressed in the nucleus. This work suggests that Cten in the nucleus does increase cell migration however, the signalling mechanisms inducing this are unclear. Further investigation into the molecular mechanisms involved is warranted.

7.2.2. Cten is Regulated by EGFR and Kras Signalling in CRC but a Tensin Switch does not Occur

It is of importance to try and elucidate the mechanisms that are regulating metastasis. Others have shown that Cten is regulated by EGFR signalling in breast cells. Signalling through this pathway induces a Tensin switch mechanism whereby increased Cten expression is associated with a decrease in the expression of Tensin 3. The Tensin switch promotes actin rearrangements and consequently increased cell motility (Katz et al., 2007). Additionally, downstream inactivation of DLC1 via Cten further regulates changes associated with cell motility through RhoA signalling (Cao et al., 2012). Since Cten is regulated by Kras signalling in CRC, it was hypothesised that the EGFR may signal upstream of this. This hypothesis, in addition to providing further understanding of signalling mechanisms contributing to metastasis in CRC, could also potentiate the use of Cten as a therapeutic target since it would lie downstream of EGFR-Kras signalling.

Cten was identified as a target of EGFR signalling in CRC cell lines and the regulation of Cten by Kras was also confirmed. EGFR and Kras commonly signal in the same pathway, but it is possible that the EGFR and Kras signal independently with regard to Cten expression. It is likely that EGFR signalling could regulate Cten via the PI3K and Stat3 pathways and additionally, other tyrosine kinases may feed into the Kras pathway to regulate Cten. This could be confirmed by manipulation of these signalling pathways.

EGFR was confirmed as a regulator, albeit a positive regulator and additionally, Kras was identified as a novel regulator of Tensin 3 expression. However, a Tensin switch did not occur either by EGFR or Kras

signalling. The first paper to propose a Tensin switch mechanism postulated that this regulated cell migration through differential actin binding of Tensin 3 and Cten. Since Cten does not contain an actin binding domain, displacement of Tensin 3 from integrin binding will induce loss of attachment of actin at focal adhesions. (Katz et al., 2007). Many proteins are in complex at focal adhesions directly binding actin, integrins or serving as adaptor proteins in between, maintaining a connection between the ECM and the cytoskeleton. Loss of Tensin 3 may not necessarily release the actin-integrin connection unless accompanied by additional molecular changes.

Later it was shown that the Tensin switch increased cell migration via DLC1 since Tensin 3 promotes DLC1 tumour suppressor activity and this is inhibited by Cten (Cao et al., 2012). However, in cancer, DLC1 is not widely expressed and this was confirmed in CRC cell lines. This may explain why a Tensin switch does not occur (Peng et al., 2013). It would be of interest to investigate whether Cten signalling to Tensin 3 is associated with a change in cell migration. The biological activity of Tensin 3 in cancer has before been studied in other tumour types. Tensin 3 was phosphorylated by Src and Tensin 3 knockdown reduced colony formation and cell migration in NSCLC and melanoma cell lines. Further to this, Tensin 3 promoted metastasis in a mouse breast cancer model. This would suggest that Tensin 3 has tumour promoting activity, which would be consistent with the findings of this study. The activity of Tensin 3 could be context dependent. In non-cancer cells where DLC1 is expressed, Tensin 3 may bind and inhibit cell motility whereas in tumour cells were Src activity is high, Tensin 3 may have tumour promoting activity. Interacting proteins may compete for binding to the SH2 domain (Qian et al., 2009).

Rho signalling is known to regulate pathways in a number of cellular processes that require cytoskeletal rearrangements. Signalling to downstream ROCK mediates focal adhesion signalling by regulating actin polymerisation and contraction (Olson and Sahai, 2009). The inactivation of DLC1 by Cten following EGF stimulation was postulated to induce RhoA activation and this was repressed by Tensin 3 (Cao et al., 2012). If the Tensin switch and DLC1 signalling do not play a prominent role in CRC, it would be of interest to determine whether Cten still regulates RhoA and the associated signalling pathways to induce actin remodelling via other mechanisms. Pathway analysis of differentially expressed genes following Cten forced expression revealed RhoA signalling, Rho-GDI signalling and Rho-GTPase family signalling pathways were significantly affected. Of the Rho family of proteins, RhoA has been most extensively studied however, expression profiling identified RhoB as a target of Cten signalling. Additionally, a number of other proteins involved in actin structural remodelling were identified as downstream targets of Cten and include Actin-related protein 2/3 complex subunit 1B (ARPC1B) and myosin 1B which are concerned with actin polymerisation and the formation of actin protrusions (Komaba and Coluccio, 2010, Volkmann et al., 2001). Confirmation and further investigation of these targets may identify novel mediators of Cten signalling.

Migration is a cyclic process comprising protrusion and attachment at the leading edge of the cell and detachment and retraction at the rear to allow movement of the cell body in the direction of cell migration. Consequently, active signalling pathways at the leading edge of the cell may be dissimilar to the cell rear to induce both actin protrusion and actomyosin contraction. It is worth considering this when investigating Cten signalling as assessing

the cell as a whole and independent of migration status may be over simplifying the process.

Cten's localisation in the stages of the focal adhesion life cycle, as far as it is known, has not been identified. Tensin 3 was found to be expressed mainly in fibrillar adhesions in human foreskin fibroblasts (Clark et al., 2010). These are formed in the final stages of focal adhesion maturation and maintain strong contact between the cell and ECM. Since there is no rapid attachment and detachment motion to the ECM, fibrillar adhesions are not generally associated with motile cells. It is surprising, therefore, that EGFR and Kras signalling, which are often upregulated in cancer, would induce Tensin 3 expression which is associated with fibrillar adhesions. Conversely, others have found that Tensin 3 localises to focal adhesions in a lung cell line (Cui et al., 2004). Knowledge of Tensin 3 expression in cancer and knowledge of signalling is sparse and further investigations regarding its role are needed to fully understand this.

It was of interest to determine the mechanisms of Cten signalling as it is possible that Cten could be a target for therapy in patients displaying a Kras mutation. Since it was shown that the EGFR could signal independently of Kras to increase Cten expression, this may have implications for its use as a therapeutic target for anti-EGFR resistant tumours. The role of Cten in CRC progression is gaining prominence and therapeutic inhibition may prove useful for the targeting of cell migration and invasion.

7.2.3. The Stabilisation of Snail Increases Tumourigenicity in the Colon

Cten is known to promote cell motility although in CRC it is unlikely that Cten induces cell motility through the Tensin switch mechanism. Additionally, Cten has previously been shown to induce cell motility by signalling to E-cadherin in CRC cell lines, the downregulation of which is a feature of EMT. EMT signalling plays a crucial role in metastasis to promote invasion and migration of tumour cells away from the primary tumour. Considering this, it was hypothesised that Cten may promote further molecular changes associated with EMT and as a consequence of this, induce cell motility in CRC cell lines.

Manipulation of Cten expression followed by western blotting for an EMT marker panel confirmed that Cten downregulated E-cadherin and in addition, identified Snail as a novel target of Cten signalling. This was identified using a dual approach of gene manipulation using both plasmid forced expression and siRNA knockdown reducing the possibility of experimental artefacts. Further to this, it was shown that Cten regulated the protein stability of Snail and this relationship was functionally relevant. A reduction in cell invasion, migration and colony formation efficiency were observed when cells were simultaneously transfected with a Cten expression construct together with Snail targeting siRNA, indicating that Cten regulates these functions in a Snail-dependent manner.

The stabilisation of Snail by Cten is a novel finding and further implicates Cten in EMT processes. However as Cten does not increase the transcriptional activity of E-cadherin, it is unlikely that a Cten-Snail-E-cadherin pathway exists. Although E-cadherin is a well described target of

Snail signalling, Snail also signals to other proteins independently of E-cadherin including tight junction proteins Caludin-1, Occludin and ZO-1. In addition to regulation at a transcriptional level, Snail also regulates expression at a post transcriptional level (Ohkubo and Ozawa, 2004). It was demonstrated that Cten regulates cell migration and invasion through Snail however downstream mediators of this effect have yet to be identified.

It is possible that Cten contributes to cell invasion and migration through focal adhesion signalling to promote actin structural rearrangements and also by the stabilisation of proteins involved in EMT. It seems Cten often regulates downstream targets at the protein level including E-cadherin, Snail and Tensin 3. Cten has been linked to the stabilisation of proteins through binding to c-Cbl, a RING finger E3 ubiquitin ligase that transfers ubiquitin from an E2 ubiquitin conjugating enzyme to the target protein. Following ubiquitination, the target protein is degraded by the proteasome. Cten prevents the degradation of EGFR in this way as a positive feedback mechanism to reinforce EGFR mediated signalling. The interaction with c-Cbl is mediated via the SH2 domain of Cten (Hong et al., 2013). c-Cbl has been linked to the degradation of other proteins including β-catenin, but not the ubiquitination of Snail (Shivanna et al., 2015). It is possible that Cten regulates EMT protein expression via other components of the ubiquitin proteasome pathway. Expression profiling identified a number of potential Cten targets involved in this pathway including Ubiquitin-conjugating enzyme E2R 2 (UBE2R2) which regulates β-TrCP substrate recognition in Snail and β-catenin degradation, Ubiquitin-conjugating enzyme E2D 4 (UBE2D4) and F-box and leucine-rich repeat protein 18 (FBXL18) and F-box protein 7 (FBXO27) which form part of the Skp, Cullin,

F-box containing (SCF) complex involved in substrate recognition (Semplici et al., 2002, Cardozo and Pagano, 2004).

Considering these findings, it would seem likely that Cten contributes to EMT processes and this could contribute to the effects of Cten mediated cell motility. Whether these pathways contribute to cell migration *in vivo* and CRC metastasis remains to be explored. Although *in vitro*, molecular changes associated with EMT have often been demonstrated, in different cancer models, the occurrence and relevance of EMT *in vivo* is debated. In breast cancer, for example, it is postulated that EMT may only act within specific subtypes with basal-like tumours associated with EMT marker expression (Sarrio et al., 2008). Furthermore, in mouse models of pancreatic and lung cancer, although EMT contributed to chemoresistance, it was not required by metastasising cells (Fischer et al., 2015, Zheng et al., 2015). However, EMT is complex and at present is not fully understood and hence these mouse models used may not fully recapitulate EMT processes in human cancer.

7.3. Final Conclusions

The activation of invasion and metastasis is one of the hallmarks of cancer that dictates malignant growth. Altered cell adhesion governed by changes in the expression of both cell-cell and cell-ECM adhesion molecules was described as central to this process (Hanahan and Weinberg, 2000). These events precede the adaptation of cells to a foreign environment and the establishment of macroscopic metastatic tumour development. Substantial advances have been made in recent years in an attempt to understand the molecular changes associated with the invasion-metastasis cascade

however, due the complexity of events it entails, the processes involved still lacks clear understanding.

 It is evident that Cten is emerging at the forefront as a regulator of cell adhesion and migration. It has been shown here that although Cten is regulated by EGFR and Kras signalling, cell motility does not appear to be regulated by a tensin switch mechanism in CRC. Further mechanisms as to how Cten contributes to cell motility through signalling to other focal adhesion localised proteins remains to be explored. Cten does however promote cell migration and invasion *in vitro* through the stabilisation of EMT proteins Snail and E-cadherin. How this is mediated downstream of Snail has yet to be determined. It has been confirmed that Cten does translocate to the nucleus in CRC and in this subcellular location Cten displays increased tumourigenicity. Mechanisms of this activity have yet to be elucidated however, it can be concluded that this is probably not mediated via Wnt signalling. A summary of the conclusions drawn from this thesis are depicted in figure 7-1.

The clinical significance of cancer metastasis cannot be understated, and further study of the underlying molecular mechanisms involved could ultimately provide a substantial benefit in cancer therapy. Since Cten signalling appears to be critical for invasion and migration *in vitro*, further clarification of Cten signalling may assist the drug discovery process. Cten may be a potential target for anti-metastatic therapy to repress EMT and consequently, cell invasion and migration. Firstly however, further pathway elucidation and validation *in vivo* is needed.
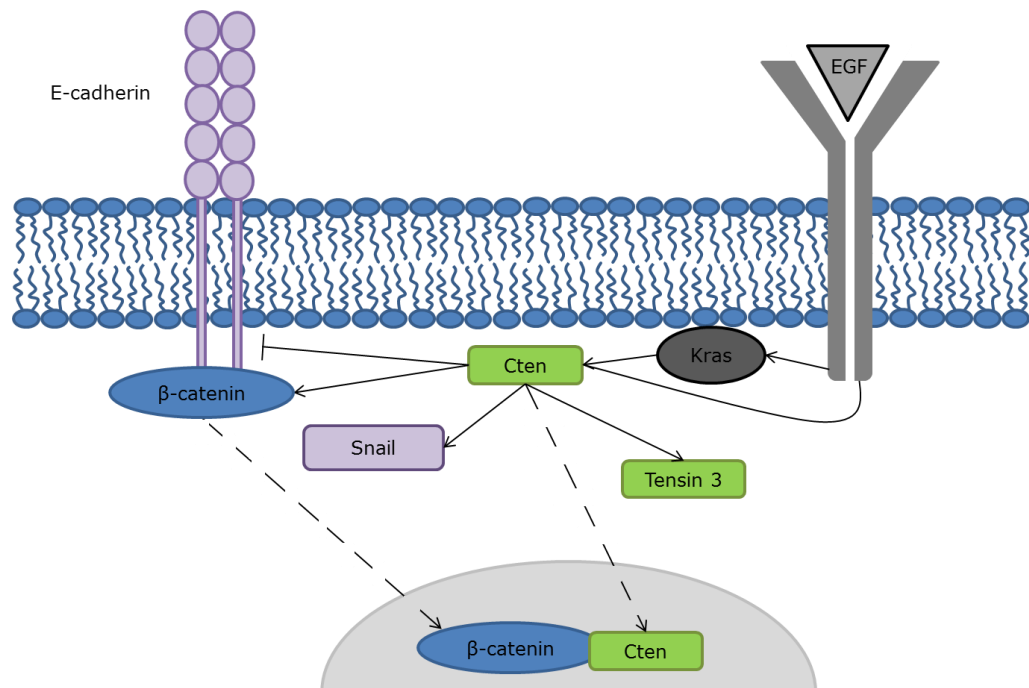
Figure 7-1: *A concluding diagrammatic representation of Cten signalling in CRC, determined from this thesis. Cten is regulated by both Kras and EGFR signalling but these could be independent events. Downstream, Cten stabilises both Snail and Tensin 3 proteins. Cten also translocates to the nucleus where it binds β-catenin via the N-terminal region.*

7.4.   Future Perspectives

The work presented here has demonstrated the role of Cten in EMT processes however, the comprehension of this Tensin family member would be enhanced with future study. This should include investigations into how Cten stabilises Snail protein. This could potentially be through the

regulation of Snail phosphorylation by GSK3β or through the regulation of the ubiquitin proteasome pathway. The EMT marker panel used in this study comprised only E-cadherin, N-cadherin, Vimentin and Snail. Many more proteins are involved in EMT and it would be interesting to determine whether Cten, in addition, regulates the expression of these proteins. In particular, it would be of interest to investigate whether Cten regulates Slug, which is in the same protein family as Snail.

Nuclear targeted Cten displays increased functional activity however, the underlying molecular mechanisms are unknown. Since no transcriptional targets were identified using the NLS-Cten construct for expression profiling, the identification of Cten binding proteins in the nucleus may give further indications to Cten's role in this subcellular localisation. This could be achieved using mass spectrometry techniques to identify any unknown proteins in complex with Cten. Investigations could also include the mechanisms of Cten translocation to the nucleus and whether Cten shuttles between the nuclear and cytoplasmic cell compartments.

A number of novel Cten downstream targets have potentially been identified by Affymetrix microarray expression profiling. Validation of these at the mRNA level by qRT-PCR and confirmation of these changes at the protein level is required. The identified genes are involved in a number of cell processes. Confirmation of downstream targets could potentially identify pathways that promote Cten mediated adhesion and migration but may also lead to the identification of novel Cten signalling pathways and functions.

This study has determined that Cten does not regulate cell adhesion and migration through a Tensin switch in CRC cell lines. However, since Cten is localised at focal adhesions, it is possible that Cten contributes to the turnover of focal adhesions and changes in actin structure through other mechanisms. Investigating whether Cten influences focal adhesion turnover, what stage of focal adhesion maturation Cten is involved in, where in the migrating cell it localises to and how these observations impact on actin structural rearrangements could all benefit the understanding of Cten signalling. Advances in live cell imaging are helping to understand focal adhesion dynamics. The manipulation of Cten signalling following the tagging of endogenous Cten with a fluorescent marker and the staining of actin in live cells may give further insights into the role of Cten in cell migration.

Throughout this study, Cten signalling has been investigated using CRC epithelial cell lines grown *in vitro* using standard culture techniques, including the culture of cells directly onto plastic (with the exception of the invasion assays in which cells are seeded on a basement membrane extract). However, this environment does not closely resemble those experienced *in vivo*. Cells *in vivo* grow on the ECM rather than plastic and considering that Cten is localised at focal adhesions it is certainly possible that interactions with the ECM could influence Cten signalling. The use of more physiologically relevant culture substrates, such as a coating of basement membrane on culture vessels, could be employed as a regular technique in an attempt to replicate the *in vivo* environment. Furthermore, the use of fibroblast conditioned media or epithelial/fibroblast co-cultures could be used to conserve the paracrine signalling experienced *in vivo*.

Thus, a range of approaches could be applied in order to create more complex culture conditions that, in return, may enable more relevant data on Cten function to be gathered.

8   References

ABDULLAH, L. N. & CHOW, E. K. 2013. Mechanisms of chemoresistance in cancer stem cells. *Clin Transl Med,* 2**,** 3.

ACCONCIA, F., BARNES, C. J., SINGH, R. R., TALUKDER, A. H. & KUMAR, R. 2007. Phosphorylation-dependent regulation of nuclear localization and functions of integrin-linked kinase. *Proc Natl Acad Sci U S A,* 104**,** 6782-7.

AL-GHAMDI, S., ALBASRI, A., CACHAT, J., IBRAHEM, S., MUHAMMAD, B. A., JACKSON, D., NATERI, A. S., KINDLE, K. B. & ILYAS, M. 2011. Cten Is Targeted by Kras Signalling to Regulate Cell Motility in the Colon and Pancreas. *PLoS One,* 6.

AL-GHAMDI, S., CACHAT, J., ALBASRI, A., AHMED, M., JACKSON, D., ZAITOUN, A., GUPPY, N., OTTO, W. R., ALISON, M. R., KINDLE, K. B. & ILYAS, M. 2013. C-terminal tensin-like gene functions as an oncogene and promotes cell motility in pancreatic cancer. *Pancreas,* 42**,** 135-40.

ALBASRI, A., AL-GHAMDI, S., FADHIL, W., ALESKANDARANY, M., LIAO, Y. C., JACKSON, D., LOBO, D. N., LO, S. H., KUMARI, R., DURRANT, L., WATSON, S., KINDLE, K. B. & ILYAS, M. 2011a. Cten signals through integrin-linked kinase (ILK) and may promote metastasis in colorectal cancer. *Oncogene,* 30**,** 2997-3002.

ALBASRI, A., ALESKANDARANY, M., BENHASOUNA, A., POWE, D. G., ELLIS, I. O., ILYAS, M. & GREEN, A. R. 2011b. CTEN (C-terminal tensin-like), a novel oncogene overexpressed in invasive breast carcinoma of poor prognosis. *Breast Cancer Research and Treatment,* 126**,** 47-54.

ALBASRI, A., FADHIL, W., SCHOLEFIELD, J. H., DURRANT, L. G. & ILYAS, M. 2014. Nuclear expression of phosphorylated focal adhesion kinase is associated with poor prognosis in human colorectal cancer. *Anticancer Res,* 34**,** 3969-74.

ALBASRI, A., SETH, R., JACKSON, D., BENHASOUNA, A., CROOK, S., NATERI, A. S., CHAPMAN, R. & ILYAS, M. 2009. C-terminal Tensin-like (CTEN) is an oncogene which alters cell motility possibly through repression of E-cadherin in colorectal cancer. *Journal of Pathology,* 218**,** 57-65.

ARMAGHANY, T., WILSON, J. D., CHU, Q. & MILLS, G. 2012. Genetic alterations in colorectal cancer. *Gastrointest Cancer Res,* 5**,** 19-27.

AVIZIENYTE, E., WYKE, A. W., JONES, R. J., MCLEAN, G. W., WESTHOFF, M. A., BRUNTON, V. G. & FRAME, M. C. 2002. Src-induced de-regulation of E-cadherin in colon cancer cells requires integrin signalling. *Nat Cell Biol,* 4**,** 632-8.

BARBIERI, I., PENSA, S., PANNELLINI, T., QUAGLINO, E., MARITANO, D., DEMARIA, M., VOSTER, A., TURKSON, J., CAVALLO, F., WATSON, C. J., PROVERO, P., MUSIANI, P. & POLI, V. 2010. Constitutively Active Stat3 Enhances Neu-Mediated Migration and Metastasis in Mammary Tumors via Upregulation of Cten. *Cancer Res,* 70**,** 2558-2567.

BARRANGOU, R., BIRMINGHAM, A., WIEMANN, S., BEIJERSBERGEN, R. L., HORNUNG, V. & SMITH, A. 2015. Advances in CRISPR-Cas9

genome engineering: lessons learned from RNA interference. *Nucleic Acids Res,* 43**,** 3407-19.

BELKIN, A. M. & STEPP, M. A. 2000. Integrins as receptors for laminins. *Microsc Res Tech,* 51**,** 280-301.

BENNETT, D. T., REECE, T. B., FOLEY, L. S., SJOBERG, A., MENG, X., FULLERTON, D. A. & WEYANT, M. J. 2015. C-terminal tensin-like protein mediates invasion of human lung cancer cells and is regulated by signal transducer and activator of transcription 3. *J Thorac Cardiovasc Surg,* 149**,** 369-75.

BIKARD, D. & MARRAFFINI, L. A. 2013. Control of gene expression by CRISPR-Cas systems. *F1000Prime Rep,* 5**,** 47.

BOLAND, C. R. & GOEL, A. 2010. Microsatellite instability in colorectal cancer. *Gastroenterology,* 138**,** 2073-2087 e3.

BRABLETZ, T., JUNG, A., REU, S., PORZNER, M., HLUBEK, F., KUNZ-SCHUGHART, L. A., KNUECHEL, R. & KIRCHNER, T. 2001. Variable beta-catenin expression in colorectal cancers indicates tumor progression driven by the tumor environment. *Proc Natl Acad Sci U S A,* 98**,** 10356-61.

BRABLETZ, T., JUNG, A., SPADERNA, S., HLUBEK, F. & KIRCHNER, T. 2005. Opinion: migrating cancer stem cells - an integrated concept of malignant tumour progression. *Nat Rev Cancer,* 5**,** 744-9.

BRAVO-CORDERO, J. J., HODGSON, L. & CONDEELIS, J. 2012. Directed cell invasion and migration during metastasis. *Curr Opin Cell Biol,* 24**,** 277-83.

BRAVOU, V., KLIRONOMOS, G., PAPADAKI, E., STEFANOU, D. & VARAKIS, J. 2003. Integrin-linked kinase (ILK) expression in human colon cancer. *Br J Cancer,* 89**,** 2340-1.

BRENNER, H., KLOOR, M. & POX, C. P. 2014. Colorectal cancer. *Lancet,* 383**,** 1490-502.

BRONNER, C. E., BAKER, S. M., MORRISON, P. T., WARREN, G., SMITH, L. G., LESCOE, M. K., KANE, M., EARABINO, C., LIPFORD, J., LINDBLOM, A. & ET AL. 1994. Mutation in the DNA mismatch repair gene homologue hMLH1 is associated with hereditary non-polyposis colon cancer. *Nature,* 368**,** 258-61.

BUNZ, F., HWANG, P. M., TORRANCE, C., WALDMAN, T., ZHANG, Y., DILLEHAY, L., WILLIAMS, J., LENGAUER, C., KINZLER, K. W. & VOGELSTEIN, B. 1999. Disruption of p53 in human cancer cells alters the responses to therapeutic agents. *J Clin Invest,* 104**,** 263-9.

CAMPBELL, I. D. & HUMPHRIES, M. J. 2011. Integrin structure, activation, and interactions. *Cold Spring Harb Perspect Biol,* 3.

CANO, A., PEREZ-MORENO, M. A., RODRIGO, I., LOCASCIO, A., BLANCO, M. J., DEL BARRIO, M. G., PORTILLO, F. & NIETO, M. A. 2000. The transcription factor snail controls epithelial-mesenchymal transitions by repressing E-cadherin expression. *Nat Cell Biol,* 2**,** 76-83.

CAO, X., VOSS, C., ZHAO, B., KANEKO, T. & LI, S. S. 2012. Differential regulation of the activity of deleted in liver cancer 1 (DLC1) by

tensins controls cell migration and transformation. *Proc Natl Acad Sci U S A,* 109**,** 1455-60.

CARDOZO, T. & PAGANO, M. 2004. The SCF ubiquitin ligase: insights into a molecular machine. *Nat Rev Mol Cell Biol,* 5**,** 739-51.

CENTER, M. M., JEMAL, A., SMITH, R. A. & WARD, E. 2009. Worldwide variations in colorectal cancer. *CA Cancer J Clin,* 59**,** 366-78.

CHAN, K. T., BENNIN, D. A. & HUTTENLOCHER, A. 2010. Regulation of adhesion dynamics by calpain-mediated proteolysis of focal adhesion kinase (FAK). *J Biol Chem,* 285**,** 11418-26.

CHAN, L. K., CHIU, Y. T., SZE, K. M. & NG, I. O. 2015. Tensin4 is up-regulated by EGF-induced ERK1/2 activity and promotes cell proliferation and migration in hepatocellular carcinoma. *Oncotarget,* 6**,** 20964-76.

CHAN, T. L., CURTIS, L. C., LEUNG, S. Y., FARRINGTON, S. M., HO, J. W., CHAN, A. S., LAM, P. W., TSE, C. W., DUNLOP, M. G., WYLLIE, A. H. & YUEN, S. T. 2001. Early-onset colorectal cancer with stable microsatellite DNA and near-diploid chromosomes. *Oncogene,* 20**,** 4871-6.

CHEN, H., DUNCAN, I. C., BOZORGCHAMI, H. & LO, S. H. 2002. Tensin1 and a previously undocumented family member, tensin2, positively regulate cell migration. *Proc Natl Acad Sci U S A,* 99**,** 733-8.

CHEN, H., ISHII, A., WONG, W. K., CHEN, L. B. & LO, S. H. 2000. Molecular characterization of human tensin. *Biochem J,* 351 Pt 2**,** 403-11.

CHEN, N. T., KUWABARA, Y., CONLEY, C., LIAO, Y. C., HONG, S. Y., CHEN, M., SHIH, Y. P., CHEN, H. W., HSIEH, F. & LO, S. H. 2013. Phylogenetic analysis, expression patterns, and transcriptional regulation of human CTEN gene. *Gene*.

CHRZANOWSKA-WODNICKA, M. & BURRIDGE, K. 1996. Rho-stimulated contractility drives the formation of stress fibers and focal adhesions. *J Cell Biol,* 133**,** 1403-15.

CHUANG, J. Z., LIN, D. C. & LIN, S. 1995. Molecular cloning, expression, and mapping of the high affinity actin-capping domain of chicken cardiac tensin. *J Cell Biol,* 128**,** 1095-109.

CICCHINI, C., LAUDADIO, I., CITARELLA, F., CORAZZARI, M., STEINDLER, C., CONIGLIARO, A., FANTONI, A., AMICONE, L. & TRIPODI, M. 2008. TGFbeta-induced EMT requires focal adhesion kinase (FAK) signaling. *Exp Cell Res,* 314**,** 143-52.

CLARK, K., HOWE, J. D., PULLAR, C. E., GREEN, J. A., ARTYM, V. V., YAMADA, K. M. & CRITCHLEY, D. R. 2010. Tensin 2 Modulates Cell Contractility in 3D Collagen Gels Through the RhoGAP DLC1. *Journal of Cellular Biochemistry,* 109**,** 808-817.

CUI, Y., LIAO, Y. C. & LO, S. H. 2004. Epidermal growth factor modulates tyrosine phosphorylation of a novel tensin family member, tensin3. *Mol Cancer Res,* 2**,** 225-32.

DAVIES, H., BIGNELL, G. R., COX, C., STEPHENS, P., EDKINS, S., CLEGG, S., TEAGUE, J., WOFFENDIN, H., GARNETT, M. J., BOTTOMLEY, W.,

DAVIS, N., DICKS, E., EWING, R., FLOYD, Y., GRAY, K., HALL, S., HAWES, R., HUGHES, J., KOSMIDOU, V., MENZIES, A., MOULD, C., PARKER, A., STEVENS, C., WATT, S., HOOPER, S., WILSON, R., JAYATILAKE, H., GUSTERSON, B. A., COOPER, C., SHIPLEY, J., HARGRAVE, D., PRITCHARD-JONES, K., MAITLAND, N., CHENEVIX-TRENCH, G., RIGGINS, G. J., BIGNER, D. D., PALMIERI, G., COSSU, A., FLANAGAN, A., NICHOLSON, A., HO, J. W., LEUNG, S. Y., YUEN, S. T., WEBER, B. L., SEIGLER, H. F., DARROW, T. L., PATERSON, H., MARAIS, R., MARSHALL, C. J., WOOSTER, R., STRATTON, M. R. & FUTREAL, P. A. 2002. Mutations of the BRAF gene in human cancer. *Nature,* 417**,** 949-54.

DAVIS, S., LU, M. L., LO, S. H., LIN, S., BUTLER, J. A., DRUKER, B. J., ROBERTS, T. M., AN, Q. & CHEN, L. B. 1991. Presence of an SH2 domain in the actin-binding protein tensin. *Science,* 252**,** 712-5.

DOMINGUEZ, D., MONTSERRAT-SENTIS, B., VIRGOS-SOLER, A., GUAITA, S., GRUESO, J., PORTA, M., PUIG, I., BAULIDA, J., FRANCI, C. & GARCIA DE HERREROS, A. 2003. Phosphorylation regulates the subcellular location and activity of the snail transcriptional repressor. *Mol Cell Biol,* 23**,** 5078-89.

DONG, J. M., LAU, L. S., NG, Y. W., LIM, L. & MANSER, E. 2009. Paxillin nuclear-cytoplasmic localization is regulated by phosphorylation of the LD4 motif: evidence that nuclear paxillin promotes cell proliferation. *Biochem J,* 418**,** 173-84.

EZRATTY, E. J., BERTAUX, C., MARCANTONIO, E. E. & GUNDERSEN, G. G. 2009. Clathrin mediates integrin endocytosis for focal adhesion disassembly in migrating cells. *J Cell Biol,* 187**,** 733-47.

EZRATTY, E. J., PARTRIDGE, M. A. & GUNDERSEN, G. G. 2005. Microtubule-induced focal adhesion disassembly is mediated by dynamin and focal adhesion kinase. *Nat Cell Biol,* 7**,** 581-90.

FAN, F., SAMUEL, S., EVANS, K. W., LU, J., XIA, L., ZHOU, Y., SCEUSI, E., TOZZI, F., YE, X. C., MANI, S. A. & ELLIS, L. M. 2012. Overexpression of snail induces epithelial-mesenchymal transition and a cancer stem cell-like phenotype in human colorectal cancer cells. *Cancer Med,* 1**,** 5-16.

FAN, X. J., WAN, X. B., YANG, Z. L., FU, X. H., HUANG, Y., CHEN, D. K., SONG, S. X., LIU, Q., XIAO, H. Y., WANG, L. & WANG, J. P. 2013. Snail promotes lymph node metastasis and Twist enhances tumor deposit formation through epithelial-mesenchymal transition in colorectal cancer. *Hum Pathol,* 44**,** 173-80.

FEARON, E. R. & VOGELSTEIN, B. 1990. A genetic model for colorectal tumorigenesis. *Cell,* 61**,** 759-67.

FERRARA, N., HILLAN, K. J., GERBER, H. P. & NOVOTNY, W. 2004. Discovery and development of bevacizumab, an anti-VEGF antibody for treating cancer. *Nat Rev Drug Discov,* 3**,** 391-400.

FISCHER, K. R., DURRANS, A., LEE, S., SHENG, J., LI, F., WONG, S. T., CHOI, H., EL RAYES, T., RYU, S., TROEGER, J., SCHWABE, R. F., VAHDAT, L. T., ALTORKI, N. K., MITTAL, V. & GAO, D. 2015. Epithelial-to-mesenchymal transition is not required for lung metastasis but contributes to chemoresistance. *Nature,* 527**,** 472-6.

FODDE, R. 2002. The APC gene in colorectal cancer. *Eur J Cancer,* 38**,** 867-71.

FRANKEN, N. A., RODERMOND, H. M., STAP, J., HAVEMAN, J. & VAN BREE, C. 2006. Clonogenic assay of cells in vitro. *Nat Protoc,* 1**,** 2315-9.

FUCHS, C., MITCHELL, E. P. & HOFF, P. M. 2006. Irinotecan in the treatment of colorectal cancer. *Cancer Treat Rev,* 32**,** 491-503.

FUKUMOTO, M., KURISU, S., YAMADA, T. & TAKENAWA, T. 2015. alpha-Actinin-4 enhances colorectal cancer cell invasion by suppressing focal adhesion maturation. *PLoS One,* 10**,** e0120616.

GRODEN, J., THLIVERIS, A., SAMOWITZ, W., CARLSON, M., GELBERT, L., ALBERTSEN, H., JOSLYN, G., STEVENS, J., SPIRIO, L., ROBERTSON, M. & ET AL. 1991. Identification and characterization of the familial adenomatous polyposis coli gene. *Cell,* 66**,** 589-600.

GUINNEY, J., DIENSTMANN, R., WANG, X., DE REYNIES, A., SCHLICKER, A., SONESON, C., MARISA, L., ROEPMAN, P., NYAMUNDANDA, G., ANGELINO, P., BOT, B. M., MORRIS, J. S., SIMON, I. M., GERSTER, S., FESSLER, E., DE SOUSA, E. M. F., MISSIAGLIA, E., RAMAY, H., BARRAS, D., HOMICSKO, K., MARU, D., MANYAM, G. C., BROOM, B., BOIGE, V., PEREZ-VILLAMIL, B., LADERAS, T., SALAZAR, R., GRAY, J. W., HANAHAN, D., TABERNERO, J., BERNARDS, R., FRIEND, S. H., LAURENT-PUIG, P., MEDEMA, J. P., SADANANDAM, A., WESSELS, L., DELORENZI, M., KOPETZ, S., VERMEULEN, L. & TEJPAR, S. 2015. The consensus molecular subtypes of colorectal cancer. *Nat Med,* 21**,** 1350-6.

HAFIZI, S., ALINDRI, F., KARLSSON, R. & DAHLBACK, B. 2002. Interaction of Axl receptor tyrosine kinase with C1-TEN, a novel C1 domain-containing protein with homology to tensin. *Biochem Biophys Res Commun,* 299**,** 793-800.

HANAHAN, D. & WEINBERG, R. A. 2000. The hallmarks of cancer. *Cell,* 100**,** 57-70.

HARAGUCHI, M., INDO, H. P., IWASAKI, Y., IWASHITA, Y., FUKUSHIGE, T., MAJIMA, H. J., IZUMO, K., HORIUCHI, M., KANEKURA, T., FURUKAWA, T. & OZAWA, M. 2013. Snail modulates cell metabolism in MDCK cells. *Biochem Biophys Res Commun,* 432**,** 618-25.

HERMANN, P. C., HUBER, S. L., HERRLER, T., AICHER, A., ELLWART, J. W., GUBA, M., BRUNS, C. J. & HEESCHEN, C. 2007. Distinct populations of cancer stem cells determine tumor growth and metastatic activity in human pancreatic cancer. *Cell Stem Cell,* 1**,** 313-23.

HOLLAND, S. J., PAN, A., FRANCI, C., HU, Y., CHANG, B., LI, W., DUAN, M., TORNEROS, A., YU, J., HECKRODT, T. J., ZHANG, J., DING, P., APATIRA, A., CHUA, J., BRANDT, R., PINE, P., GOFF, D., SINGH, R., PAYAN, D. G. & HITOSHI, Y. 2010. R428, a selective small molecule inhibitor of Axl kinase, blocks tumor spread and prolongs survival in models of metastatic breast cancer. *Cancer Res,* 70**,** 1544-54.

HONG, S. Y., SHIH, Y. P., LI, T., CARRAWAY, K. L., 3RD & LO, S. H. 2013. CTEN prolongs signaling by EGFR through reducing its ligand-induced degradation. *Cancer Res,* 73**,** 5266-76.

HOWARD, S., DEROO, T., FUJITA, Y. & ITASAKI, N. 2011. A positive role of cadherin in Wnt/beta-catenin signalling during epithelial-mesenchymal transition. *PLoS One,* 6**,** e23899.

HUNG, S.-Y., SHIH, Y.-P., CHEN, M. & LO, S. H. 2013. Up-Regulated Cten by FGF2 Contributes to FGF2-Mediated Cell Migration. *Molecular Carcinogenesis***,** n/a-n/a.

HUVENEERS, S., TRUONG, H., FASSLER, R., SONNENBERG, A. & DANEN, E. H. 2008. Binding of soluble fibronectin to integrin alpha5 beta1 - link to focal adhesion redistribution and contractile shape. *J Cell Sci,* 121**,** 2452-62.

HWANG, W. L., JIANG, J. K., YANG, S. H., HUANG, T. S., LAN, H. Y., TENG, H. W., YANG, C. Y., TSAI, Y. P., LIN, C. H., WANG, H. W. & YANG, M. H. 2014. MicroRNA-146a directs the symmetric division of Snail-dominant colorectal cancer stem cells. *Nature Cell Biology,* 16**,** 268-+.

IKENOUCHI, J., MATSUDA, M., FURUSE, M. & TSUKITA, S. 2003. Regulation of tight junctions during the epithelium-mesenchyme transition: direct repression of the gene expression of claudins/occludin by Snail. *J Cell Sci,* 116**,** 1959-67.

ILYAS, M., TOMLINSON, I. P., ROWAN, A., PIGNATELLI, M. & BODMER, W. F. 1997. Beta-catenin mutations in cell lines established from human colorectal cancers. *Proc Natl Acad Sci U S A,* 94**,** 10330-4.

JOHNSON, J. E., GIORGIONE, J. & NEWTON, A. C. 2000. The C1 and C2 domains of protein kinase C are independent membrane targeting modules, with specificity for phosphatidylserine conferred by the C1 domain. *Biochemistry,* 39**,** 11360-9.

KAPLAN, R. N., RIBA, R. D., ZACHAROULIS, S., BRAMLEY, A. H., VINCENT, L., COSTA, C., MACDONALD, D. D., JIN, D. K., SHIDO, K., KERNS, S. A., ZHU, Z., HICKLIN, D., WU, Y., PORT, J. L., ALTORKI, N., PORT, E. R., RUGGERO, D., SHMELKOV, S. V., JENSEN, K. K., RAFII, S. & LYDEN, D. 2005. VEGFR1-positive haematopoietic bone marrow progenitors initiate the pre-metastatic niche. *Nature,* 438**,** 820-7.

KATZ, M., AMIT, I., CITRI, A., SHAY, T., CARVALHO, S., LAVI, S., MILANEZI, F., LYASS, L., AMARIGLIO, N., JACOB-HIRSCH, J., BEN-CHETRIT, N., TARCIC, G., LINDZEN, M., AVRAHAM, R., LIAO, Y.-C., TRUSK, P., LYASS, A., RECHAVI, G., SPECTOR, N. L., LO, S. H., SCHMITT, F., BACUS, S. S. & YARDEN, Y. 2007. A reciprocal tensin-3-cten switch mediates EGF-driven mammary cell migration. *Nature Cell Biology,* 9**,** 961-U124.

KNIGHT, C. G., MORTON, L. F., PEACHEY, A. R., TUCKWELL, D. S., FARNDALE, R. W. & BARNES, M. J. 2000. The collagen-binding A-domains of integrins alpha(1)beta(1) and alpha(2)beta(1) recognize the same specific amino acid sequence, GFOGER, in native (triple-helical) collagens. *J Biol Chem,* 275**,** 35-40.

KOMABA, S. & COLUCCIO, L. M. 2010. Localization of myosin 1b to actin protrusions requires phosphoinositide binding. *J Biol Chem,* 285**,** 27686-93.

LAMOUILLE, S., XU, J. & DERYNCK, R. 2014. Molecular mechanisms of epithelial-mesenchymal transition. *Nat Rev Mol Cell Biol,* 15**,** 178-96.

LARK, A. L., LIVASY, C. A., CALVO, B., CASKEY, L., MOORE, D. T., YANG, X. & CANCE, W. G. 2003. Overexpression of focal adhesion kinase in primary colorectal carcinomas and colorectal liver metastases: immunohistochemistry and real-time PCR analyses. *Clin Cancer Res,* 9**,** 215-22.

LAWSON, C., LIM, S. T., URYU, S., CHEN, X. L., CALDERWOOD, D. A. & SCHLAEPFER, D. D. 2012. FAK promotes recruitment of talin to nascent adhesions to control cell motility. *J Cell Biol,* 196**,** 223-32.

LEACH, F. S., NICOLAIDES, N. C., PAPADOPOULOS, N., LIU, B., JEN, J., PARSONS, R., PELTOMAKI, P., SISTONEN, P., AALTONEN, L. A., NYSTROM-LAHTI, M. & ET AL. 1993. Mutations of a mutS homolog in hereditary nonpolyposis colorectal cancer. *Cell,* 75**,** 1215-25.

LEGATE, K. R. & FASSLER, R. 2009. Mechanisms that regulate adaptor binding to beta-integrin cytoplasmic tails. *J Cell Sci,* 122**,** 187-98.

LEROY, P. & MOSTOV, K. E. 2007. Slug is required for cell survival during partial epithelial-mesenchymal transition of HGF-induced tubulogenesis. *Mol Biol Cell,* 18**,** 1943-52.

LI, F., TIEDE, B., MASSAGUE, J. & KANG, Y. 2007. Beyond tumorigenesis: cancer stem cells in metastasis. *Cell Res,* 17**,** 3-14.

LI, Y., ROGOFF, H. A., KEATES, S., GAO, Y., MURIKIPUDI, S., MIKULE, K., LEGGETT, D., LI, W., PARDEE, A. B. & LI, C. J. 2015. Suppression of cancer relapse and metastasis by inhibiting cancer stemness. *Proc Natl Acad Sci U S A,* 112**,** 1839-44.

LIAO, Y.-C., CHEN, N.-T., SHIH, Y.-P., DONG, Y. & LO, S. H. 2009. Up-regulation of C-Terminal Tensin-like Molecule Promotes the Tumorigenicity of Colon Cancer through beta-Catenin. *Cancer Res,* 69**,** 4563-4566.

LIAO, Y.-C., SI, L., WHITE, R. W. D. & LO, S. H. 2007. The phosphotyrosine-independent interaction of DLC-1 and the SH2 domain of cten regulates focal adhesion localization and growth suppression activity of DLC-1. *Journal of Cell Biology,* 176**,** 43-49.

LIM, S. T. 2013. Nuclear FAK: a new mode of gene regulation from cellular adhesions. *Mol Cells,* 36**,** 1-6.

LIM, S. T., CHEN, X. L., LIM, Y., HANSON, D. A., VO, T. T., HOWERTON, K., LAROCQUE, N., FISHER, S. J., SCHLAEPFER, D. D. & ILIC, D. 2008. Nuclear FAK promotes cell proliferation and survival through FERM-enhanced p53 degradation. *Mol Cell,* 29**,** 9-22.

LO, S. H. 2006. Focal adhesions: what's new inside. *Dev Biol,* 294**,** 280-91.

LO, S. H. 2014. C-terminal tensin-like (CTEN): a promising biomarker and target for cancer. *Int J Biochem Cell Biol,* 51**,** 150-4.

LO, S. H., JANMEY, P. A., HARTWIG, J. H. & CHEN, L. B. 1994. INTERACTIONS OF TENSIN WITH ACTIN AND IDENTIFICATION OF ITS 3 DISTINCT ACTIN-BINDING DOMAINS. *Journal of Cell Biology,* 125**,** 1067-1075.

LO, S. H. & LO, T. B. 2002. Cten, a COOH-terminal tensin-like protein with prostate restricted expression, is down-regulated in prostate cancer. *Cancer Res,* 62**,** 4217-21.

LO, S. H., YU, Q. C., DEGENSTEIN, L., CHEN, L. B. & FUCHS, E. 1997. Progressive kidney degeneration in mice lacking tensin. *J Cell Biol,* 136**,** 1349-61.

LO, S. S., LO, S. H. & LO, S. H. 2005. Cleavage of cten by caspase-3 during apoptosis. *Oncogene,* 24**,** 4311-4.

LONGLEY, D. B., HARKIN, D. P. & JOHNSTON, P. G. 2003. 5-fluorouracil: mechanisms of action and clinical strategies. *Nat Rev Cancer,* 3**,** 330-8.

LU, Z., JIANG, G., BLUME-JENSEN, P. & HUNTER, T. 2001. Epidermal growth factor-induced tumor cell invasion and metastasis initiated by dephosphorylation and downregulation of focal adhesion kinase. *Mol Cell Biol,* 21**,** 4016-31.

MANI, S. A., GUO, W., LIAO, M. J., EATON, E. N., AYYANAN, A., ZHOU, A. Y., BROOKS, M., REINHARD, F., ZHANG, C. C., SHIPITSIN, M., CAMPBELL, L. L., POLYAK, K., BRISKEN, C., YANG, J. & WEINBERG, R. A. 2008. The epithelial-mesenchymal transition generates cells with properties of stem cells. *Cell,* 133**,** 704-15.

MARTINEZ-ESTRADA, O. M., CULLERES, A., SORIANO, F. X., PEINADO, H., BOLOS, V., MARTINEZ, F. O., REINA, M., CANO, A., FABRE, M. & VILARO, S. 2006. The transcription factors Slug and Snail act as repressors of Claudin-1 expression in epithelial cells. *Biochem J,* 394**,** 449-57.

MARTUSZEWSKA, D., LJUNGBERG, B., JOHANSSON, M., LANDBERG, G., OSLAKOVIC, C., DAHLBACK, B. & HAFIZI, S. 2009. Tensin3 is a negative regulator of cell migration and all four Tensin family members are downregulated in human kidney cancer. *PLoS One,* 4**,** e4350.

MCCLEVERTY, C. J., LIN, D. C. & LIDDINGTON, R. C. 2007. Structure of the PTB domain of tensin1 and a model for its recruitment to fibrillar adhesions. *Protein Sci,* 16**,** 1223-9.

MCLEAN, G. W., FINCHAM, V. J. & FRAME, M. C. 2000. v-Src induces tyrosine phosphorylation of focal adhesion kinase independently of tyrosine 397 and formation of a complex with Src. *J Biol Chem,* 275**,** 23333-9.

MCPHEE, T. R., MCDONALD, P. C., OLOUMI, A. & DEDHAR, S. 2008. Integrin-linked kinase regulates E-cadherin expression through PARP-1. *Dev Dyn,* 237**,** 2737-47.

MISALE, S., YAEGER, R., HOBOR, S., SCALA, E., JANAKIRAMAN, M., LISKA, D., VALTORTA, E., SCHIAVO, R., BUSCARINO, M., SIRAVEGNA, G., BENCARDINO, K., CERCEK, A., CHEN, C. T., VERONESE, S., ZANON, C., SARTORE-BIANCHI, A., GAMBACORTA, M., GALLICCHIO, M., VAKIANI, E., BOSCARO, V., MEDICO, E., WEISER, M., SIENA, S., DI NICOLANTONIO, F., SOLIT, D. & BARDELLI, A. 2012. Emergence of KRAS mutations and acquired resistance to anti-EGFR therapy in colorectal cancer. *Nature,* 486**,** 532-6.

MITRA, S. K. & SCHLAEPFER, D. D. 2006. Integrin-regulated FAK-Src signaling in normal and cancer cells. *Curr Opin Cell Biol,* 18**,** 516-23.

MONTAZER HAGHIGHI, M., RADPOUR, R., AGHAJANI, K., ZALI, N., MOLAEI, M. & ZALI, M. R. 2009. Four novel germline mutations in the MLH1 and PMS2 mismatch repair genes in patients with hereditary nonpolyposis colorectal cancer. *Int J Colorectal Dis,* 24**,** 885-93.

MUHARRAM, G., SAHGAL, P., KORPELA, T., DE FRANCESCHI, N., KAUKONEN, R., CLARK, K., TULASNE, D., CARPEN, O. & IVASKA, J. 2014. Tensin-4-Dependent MET Stabilization Is Essential for Survival and Proliferation in Carcinoma Cells. *Developmental Cell,* 29**,** 421-436.

MUKHERJEE, D. & ZHAO, J. 2013. The Role of chemokine receptor CXCR4 in breast cancer metastasis. *Am J Cancer Res,* 3**,** 46-57.

MURAKAMI, T., KAWADA, K., IWAMOTO, M., AKAGAMI, M., HIDA, K., NAKANISHI, Y., KANDA, K., KAWADA, M., SENO, H., TAKETO, M. M. & SAKAI, Y. 2013. The role of CXCR3 and CXCR4 in colorectal cancer metastasis. *Int J Cancer,* 132**,** 276-87.

MYERS, S. H., BRUNTON, V. G. & UNCITI-BROCETA, A. 2015. AXL Inhibitors in Cancer: A Medicinal Chemistry Perspective. *J Med Chem*.

NAYAL, A., WEBB, D. J. & HORWITZ, A. F. 2004. Talin: an emerging focal point of adhesion dynamics. *Curr Opin Cell Biol,* 16**,** 94-8.

NAZEMALHOSSEINI MOJARAD, E., KUPPEN, P. J., AGHDAEI, H. A. & ZALI, M. R. 2013. The CpG island methylator phenotype (CIMP) in colorectal cancer. *Gastroenterol Hepatol Bed Bench,* 6**,** 120-8.

NELLES, D. A., FANG, M. Y., O'CONNELL, M. R., XU, J. L., MARKMILLER, S. J., DOUDNA, J. A. & YEO, G. W. 2016. Programmable RNA Tracking in Live Cells with CRISPR/Cas9. *Cell*.

NG, I. O., LIANG, Z. D., CAO, L. & LEE, T. K. 2000. DLC-1 is deleted in primary hepatocellular carcinoma and exerts inhibitory effects on the proliferation of hepatoma cell lines with deleted DLC-1. *Cancer Res,* 60**,** 6581-4.

OCANA, O. H., CORCOLES, R., FABRA, A., MORENO-BUENO, G., ACLOQUE, H., VEGA, S., BARRALLO-GIMENO, A., CANO, A. & NIETO, M. A. 2012. Metastatic colonization requires the repression of the epithelial-mesenchymal transition inducer Prrx1. *Cancer Cell,* 22**,** 709-24.

OHKUBO, T. & OZAWA, M. 2004. The transcription factor Snail downregulates the tight junction components independently of E-cadherin downregulation. *J Cell Sci,* 117**,** 1675-85.

OKITA, K., ICHISAKA, T. & YAMANAKA, S. 2007. Generation of germline-competent induced pluripotent stem cells. *Nature,* 448**,** 313-7.

OLSON, M. F. & SAHAI, E. 2009. The actin cytoskeleton in cancer cell motility. *Clin Exp Metastasis,* 26**,** 273-87.

PAGET, S. 1889. The distribution of secondary growths in cancer of the breast. 1889. *Cancer Metastasis Rev,* 8**,** 98-101.

PALACIOS, F., TUSHIR, J. S., FUJITA, Y. & D'SOUZA-SCHOREY, C. 2005. Lysosomal targeting of E-cadherin: a unique mechanism for the down-regulation of cell-cell adhesion during epithelial to mesenchymal transitions. *Mol Cell Biol,* 25**,** 389-402.

PANG, R., LAW, W. L., CHU, A. C., POON, J. T., LAM, C. S., CHOW, A. K., NG, L., CHEUNG, L. W., LAN, X. R., LAN, H. Y., TAN, V. P., YAU, T. C., POON, R. T. & WONG, B. C. 2010. A subpopulation of CD26+ cancer stem cells with metastatic capacity in human colorectal cancer. *Cell Stem Cell,* 6**,** 603-15.

PARTRIDGE, M. A. & MARCANTONIO, E. E. 2006. Initiation of attachment and generation of mature focal adhesions by integrin-containing filopodia in cell spreading. *Mol Biol Cell,* 17**,** 4237-48.

PASAPERA, A. M., SCHNEIDER, I. C., RERICHA, E., SCHLAEPFER, D. D. & WATERMAN, C. M. 2010. Myosin II activity regulates vinculin recruitment to focal adhesions through FAK-mediated paxillin phosphorylation. *J Cell Biol,* 188**,** 877-90.

PEINADO, H., QUINTANILLA, M. & CANO, A. 2003. Transforming growth factor beta-1 induces snail transcription factor in epithelial cell lines: mechanisms for epithelial mesenchymal transitions. *J Biol Chem,* 278**,** 21113-23.

PENG, H., LONG, F., WU, Z., CHU, Y., LI, J., KUAI, R., ZHANG, J., KANG, Z., ZHANG, X. & GUAN, M. 2013. Downregulation of DLC-1 gene by promoter methylation during primary colorectal cancer progression. *Biomed Res Int,* 2013**,** 181384.

PERSTON, Y. 2011. Diagnosis and management of colorectal cancer. *Nurs Times,* 107**,** 16.

PROVENZANI, A., FRONZA, R., LORENI, F., PASCALE, A., AMADIO, M. & QUATTRONE, A. 2006. Global alterations in mRNA polysomal recruitment in a cell model of colorectal cancer progression to metastasis. *Carcinogenesis,* 27**,** 1323-33.

PROVENZANO, P. P., ELICEIRI, K. W., CAMPBELL, J. M., INMAN, D. R., WHITE, J. G. & KEELY, P. J. 2006. Collagen reorganization at the tumor-stromal interface facilitates local invasion. *BMC Med,* 4**,** 38.

QIAN, X. L., LI, G. R., ASMUSSEN, H. K., ASNAGHI, L., VASS, W. C., BRAVERMAN, R., YAMADA, K. M., POPESCU, N. C., PAPAGEORGE, A. G. & LOWY, D. R. 2007. Oncogenic inhibition by a deleted in liver cancer gene requires cooperation between tensin binding and Rho-specific GTPase-activating protein activities. *Proceedings of the National Academy of Sciences of the United States of America,* 104**,** 9012-9017.

QIAN, X. L., LI, G. R., VASS, W. C., PAPAGEORGE, A., WALKER, R. C., ASNAGHI, L., STEINBACH, P. J., TOSATO, G., HUNTER, K. & LOWY, D. R. 2009. The Tensin-3 Protein, Including its SH2 Domain, Is Phosphorylated by Src and Contributes to Tumorigenesis and Metastasis. *Cancer Cell,* 16**,** 246-258.

RAN, F. A., HSU, P. D., LIN, C. Y., GOOTENBERG, J. S., KONERMANN, S., TREVINO, A. E., SCOTT, D. A., INOUE, A., MATOBA, S., ZHANG, Y. & ZHANG, F. 2013. Double nicking by RNA-guided CRISPR Cas9 for enhanced genome editing specificity. *Cell,* 154**,** 1380-9.

ROTHENBERG, M. L. 2000. Efficacy of oxaliplatin in the treatment of colorectal cancer. *Oncology (Williston Park),* 14**,** 9-14.

ROY, H. K., SMYRK, T. C., KOETSIER, J., VICTOR, T. A. & WALI, R. K. 2005. The transcriptional repressor SNAIL is overexpressed in human colon cancer. *Dig Dis Sci,* 50**,** 42-6.

SALHAB, N., JONES, D. J., BOS, J. L., KINSELLA, A. & SCHOFIELD, P. F. 1989. Detection of ras gene alterations and ras proteins in colorectal cancer. *Dis Colon Rectum,* 32**,** 659-64.

SALTZ, L. B., COX, J. V., BLANKE, C., ROSEN, L. S., FEHRENBACHER, L., MOORE, M. J., MAROUN, J. A., ACKLAND, S. P., LOCKER, P. K., PIROTTA, N., ELFRING, G. L. & MILLER, L. L. 2000. Irinotecan plus fluorouracil and leucovorin for metastatic colorectal cancer. Irinotecan Study Group. *N Engl J Med,* 343**,** 905-14.

SARRIO, D., RODRIGUEZ-PINILLA, S. M., HARDISSON, D., CANO, A., MORENO-BUENO, G. & PALACIOS, J. 2008. Epithelial-mesenchymal transition in breast cancer relates to the basal-like phenotype. *Cancer Res,* 68**,** 989-97.

SASAKI, H., MORIYAMA, S., MIZUNO, K., YUKIUE, H., KONISHI, A., YANO, M., KAJI, M., FUKAI, I., KIRIYAMA, M., YAMAKAWA, Y. & FUJII, Y. 2003a. Cten mRNA expression was correlated with tumor progression in lung cancers. *Lung Cancer,* 40**,** 151-5.

SASAKI, H., YUKIUE, H., KOBAYASHI, Y., FUKAI, I. & FUJII, Y. 2003b. Cten mRNA expression is correlated with tumor progression in thymoma. *Tumour Biol,* 24**,** 271-4.

SCHATTON, T. & FRANK, M. H. 2010. The in vitro spheroid melanoma cell culture assay: cues on tumor initiation? *J Invest Dermatol,* 130**,** 1769-71.

SEMPLICI, F., MEGGIO, F., PINNA, L. A. & OLIVIERO, S. 2002. CK2-dependent phosphorylation of the E2 ubiquitin conjugating enzyme UBC3B induces its interaction with beta-TrCP and enhances beta-catenin degradation. *Oncogene,* 21**,** 3978-87.

SEN, A., DE CASTRO, I., DEFRANCO, D. B., DENG, F. M., MELAMED, J., KAPUR, P., RAJ, G. V., ROSSI, R. & HAMMES, S. R. 2012. Paxillin mediates extranuclear and intranuclear signaling in prostate cancer proliferation. *J Clin Invest,* 122**,** 2469-81.

SENG, T. J., LOW, J. S., LI, H., CUI, Y., GOH, H. K., WONG, M. L., SRIVASTAVA, G., SIDRANSKY, D., CALIFANO, J., STEENBERGEN, R. D., RHA, S. Y., TAN, J., HSIEH, W. S., AMBINDER, R. F., LIN, X., CHAN, A. T. & TAO, Q. 2007. The major 8p22 tumor suppressor DLC1 is frequently silenced by methylation in both endemic and sporadic nasopharyngeal, esophageal, and cervical carcinomas, and inhibits tumor cell colony formation. *Oncogene,* 26**,** 934-44.

SHIVANNA, S., HARROLD, I., SHASHAR, M., MEYER, R., KIANG, C., FRANCIS, J., ZHAO, Q., FENG, H., EDELMAN, E. R., RAHIMI, N. &

CHITALIA, V. C. 2015. The c-Cbl ubiquitin ligase regulates nuclear beta-catenin and angiogenesis by its tyrosine phosphorylation mediated through the Wnt signaling pathway. *J Biol Chem,* 290**,** 12537-46.

SJOESTROEM, C., KHOSRAVI, S., ZHANG, G., MARTINKA, M. & LI, G. 2013. C-terminal tensin-like protein is a novel prognostic marker for primary melanoma patients. *PLoS One,* 8**,** e80492.

SPANO, D., HECK, C., DE ANTONELLIS, P., CHRISTOFORI, G. & ZOLLO, M. 2012. Molecular networks that regulate cancer metastasis. *Semin Cancer Biol,* 22**,** 234-49.

TADDEI, M. L., GIANNONI, E., MORANDI, A., IPPOLITO, L., RAMAZZOTTI, M., CALLARI, M., GANDELLINI, P. & CHIARUGI, P. 2014. Mesenchymal to amoeboid transition is associated with stem-like features of melanoma cells. *Cell Commun Signal,* 12**,** 24.

TAN, C., COSTELLO, P., SANGHERA, J., DOMINGUEZ, D., BAULIDA, J., DE HERREROS, A. G. & DEDHAR, S. 2001. Inhibition of integrin linked kinase (ILK) suppresses beta-catenin-Lef/Tcf-dependent transcription and expression of the E-cadherin repressor, snail, in APC-/- human colon carcinoma cells. *Oncogene,* 20**,** 133-40.

THORPE, H., AKHLAQ, M., JACKSON, D., GHAMDI, S. A., STORR, S., MARTIN, S. & ILYAS, M. 2015. Multiple pathways regulate Cten in colorectal cancer without a Tensin switch. *Int J Exp Pathol,* 96**,** 362-9.

TOUTANT, M., COSTA, A., STUDLER, J. M., KADARE, G., CARNAUD, M. & GIRAULT, J. A. 2002. Alternative splicing controls the mechanisms of FAK autophosphorylation. *Mol Cell Biol,* 22**,** 7731-43.

TSAI, J. H., DONAHER, J. L., MURPHY, D. A., CHAU, S. & YANG, J. 2012. Spatiotemporal regulation of epithelial-mesenchymal transition is essential for squamous cell carcinoma metastasis. *Cancer Cell,* 22**,** 725-36.

UNIGENE DLC1 EST profile. NCBI http://www.ncbi.nlm.nih.gov/UniGene/ESTProfileViewer.cgi?uglist=Hs.134296. Date accessed: 23 May 2016.

UNIGENE TNS4 EST profile. NCBI http://www.ncbi.nlm.nih.gov/UniGene/ESTProfileViewer.cgi?uglist=Hs.438292. Date accessed: 23 May 2016.

VAUGHN, C. P., ZOBELL, S. D., FURTADO, L. V., BAKER, C. L. & SAMOWITZ, W. S. 2011. Frequency of KRAS, BRAF, and NRAS mutations in colorectal cancer. *Genes Chromosomes Cancer,* 50**,** 307-12.

VOGEL, C. & MARCOTTE, E. M. 2012. Insights into the regulation of protein abundance from proteomic and transcriptomic analyses. *Nature Reviews Genetics,* 13**,** 227-232.

VOLKMANN, N., AMANN, K. J., STOILOVA-MCPHIE, S., EGILE, C., WINTER, D. C., HAZELWOOD, L., HEUSER, J. E., LI, R., POLLARD, T. D. & HANEIN, D. 2001. Structure of Arp2/3 complex in its activated state and in actin filament branch junctions. *Science,* 293**,** 2456-9.

WEHRLE-HALLER, B. 2012. Structure and function of focal adhesions. *Curr Opin Cell Biol,* 24**,** 116-24.

WEI, C., LIU, J., YU, Z., ZHANG, B., GAO, G. & JIAO, R. 2013. TALEN or Cas9 - rapid, efficient and specific choices for genome modifications. *J Genet Genomics,* 40**,** 281-9.

WEIDNER, N. 2002. New paradigm for vessel intravasation by tumor cells. *Am J Pathol,* 160**,** 1937-9.

WESTHOFF, M. A., SERRELS, B., FINCHAM, V. J., FRAME, M. C. & CARRAGHER, N. O. 2004. SRC-mediated phosphorylation of focal adhesion kinase couples actin and adhesion dynamics to survival signaling. *Mol Cell Biol,* 24**,** 8113-33.

WORTHLEY, D. L. & LEGGETT, B. A. 2010. Colorectal cancer: molecular features and clinical opportunities. *Clin Biochem Rev,* 31**,** 31-8.

WU, Y., EVERS, B. M. & ZHOU, B. P. 2009. Small C-terminal domain phosphatase enhances snail activity through dephosphorylation. *J Biol Chem,* 284**,** 640-8.

XU, J., LAMOUILLE, S. & DERYNCK, R. 2009. TGF-beta-induced epithelial to mesenchymal transition. *Cell Res,* 19**,** 156-72.

YAMASHITA, M., HORIKOSHI, S., ASANUMA, K., TAKAHARA, H., SHIRATO, I. & TOMINO, Y. 2004. Tensin is potentially involved in extracellular matrix production in mesangial cells. *Histochem Cell Biol,* 121**,** 245-54.

YAN, Z., YIN, H., WANG, R., WU, D., SUN, W., LIU, B. & SU, Q. 2014. Overexpression of integrin-linked kinase (ILK) promotes migration and invasion of colorectal cancer cells by inducing epithelial-mesenchymal transition via NF-kappaB signaling. *Acta Histochem,* 116**,** 527-33.

YANG, Z., RAYALA, S., NGUYEN, D., VADLAMUDI, R. K., CHEN, S. & KUMAR, R. 2005. Pak1 phosphorylation of snail, a master regulator of epithelial-to-mesenchyme transition, modulates snail's subcellular localization and functions. *Cancer Res,* 65**,** 3179-84.

YE, Y., TIAN, H., LANGE, A. R., YEARSLEY, K., ROBERTSON, F. M. & BARSKY, S. H. 2013. The genesis and unique properties of the lymphovascular tumor embolus are because of calpain-regulated proteolysis of E-cadherin. *Oncogene,* 32**,** 1702-13.

YILMAZ, M. & CHRISTOFORI, G. 2010. Mechanisms of motility in metastasizing cells. *Mol Cancer Res,* 8**,** 629-42.

YOSHIGI, M., HOFFMAN, L. M., JENSEN, C. C., YOST, H. J. & BECKERLE, M. C. 2005. Mechanical force mobilizes zyxin from focal adhesions to actin filaments and regulates cytoskeletal reinforcement. *J Cell Biol,* 171**,** 209-15.

ZAIDEL-BAR, R., ITZKOVITZ, S., MA'AYAN, A., IYENGAR, R. & GEIGER, B. 2007. Functional atlas of the integrin adhesome. *Nat Cell Biol,* 9**,** 858-67.

ZHANG, K., RODRIGUEZ-AZNAR, E., YABUTA, N., OWEN, R. J., MINGOT, J. M., NOJIMA, H., NIETO, M. A. & LONGMORE, G. D. 2012. Lats2

kinase potentiates Snail1 activity by promoting nuclear retention upon phosphorylation. *EMBO J,* 31**,** 29-43.

ZHAO, Z., TAN, S. H., MACHIYAMA, H., KAWAUCHI, K., ARAKI, K., HIRATA, H. & SAWADA, Y. 2016. Association between tensin 1 and p130Cas at focal adhesions links actin inward flux to cell migration. *Biol Open*.

ZHENG, H., SHEN, M., ZHA, Y. L., LI, W., WEI, Y., BLANCO, M. A., REN, G., ZHOU, T., STORZ, P., WANG, H. Y. & KANG, Y. 2014. PKD1 phosphorylation-dependent degradation of SNAIL by SCF-FBXO11 regulates epithelial-mesenchymal transition and metastasis. *Cancer Cell,* 26**,** 358-73.

ZHENG, X., CARSTENS, J. L., KIM, J., SCHEIBLE, M., KAYE, J., SUGIMOTO, H., WU, C. C., LEBLEU, V. S. & KALLURI, R. 2015. Epithelial-to-mesenchymal transition is dispensable for metastasis but induces chemoresistance in pancreatic cancer. *Nature,* 527**,** 525-30.

ZHOU, B. P., DENG, J., XIA, W., XU, J., LI, Y. M., GUNDUZ, M. & HUNG, M. C. 2004. Dual regulation of Snail by GSK-3beta-mediated phosphorylation in control of epithelial-mesenchymal transition. *Nat Cell Biol,* 6**,** 931-40.

9   Appendices

9.1   Cell Line Mutation Profiling

Cell Line	*KRAS* Exon 2	*KRAS* Exon 4	*BRAF* Exon 11	*BRAF* Exon 15	*PIK3CA* Exon 20	*PTEN* Exon 3	*TP53* Exon 6
HCT116	Mutant	Wt.	Wt.	Wt.	Mutant	Wt.	Wt.
RKO	Wt.	Wt.	Wt.	Mutant	Mutant	Wt.	Wt.
C32	Wt.	Wt.	Wt.	Wt.	Wt.	Wt.	Wt.
CACO2	Wt.	Wt.	Wt.	Wt.	Wt.	Wt.	Mutant
SW480	Mutant	Wt.	Wt.	Wt.	Wt.	Wt.	Wt.
SW620	Mutant	Wt.	Wt.	Wt.	Wt.	Wt.	Wt.
DLD1	Mutant	Wt.	Wt.	Wt.	Wt.	Wt.	Wt.

Table 9-1: The mutation status of CRC cell lines for commonly mutated genes in CRC.
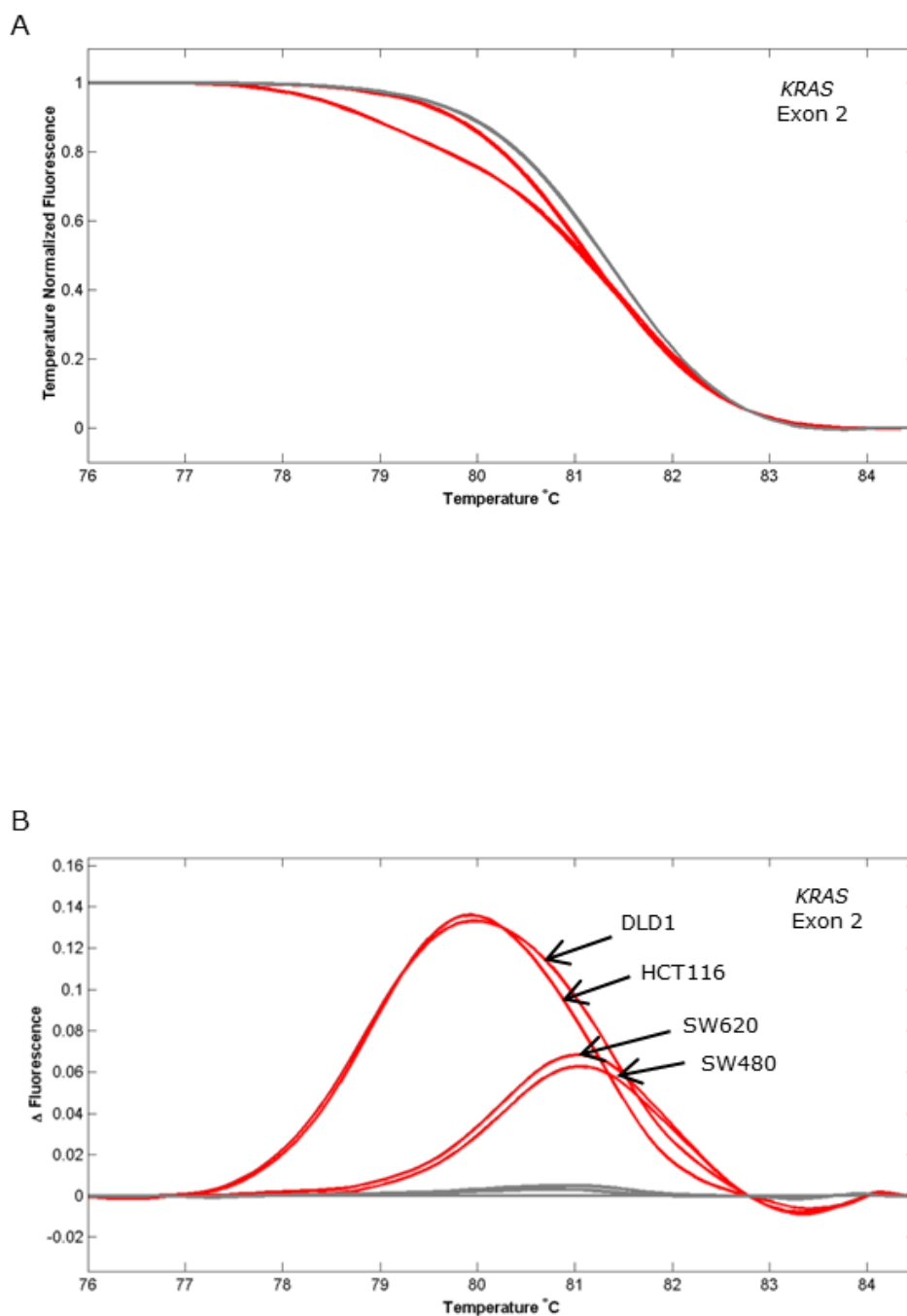
Figure 9-1: The screening of CRC cell lines for a mutation in KRAS exon 2.
A) KRAS exon 2 shifted melting curve for HCT116, Caco-2, RKO, DLD1,
C32 SW480 and SW620. B) The difference plot for Kras exon 2 revealed
that DLD1, HCT116, SW620 and SW480 displayed a mutation in this exon.
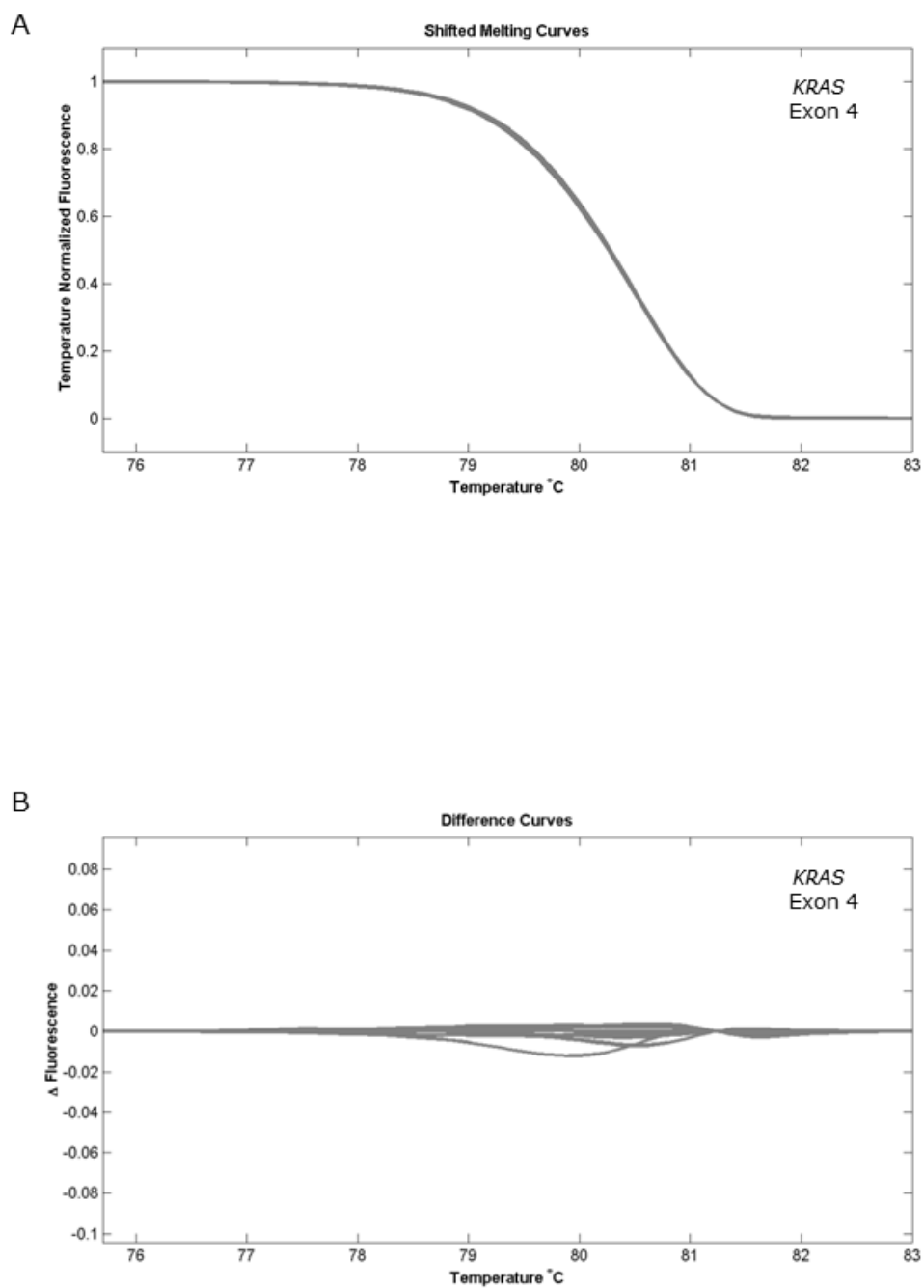
Figure 9-2: *The screening of CRC cell lines for a mutation in KRAS exon 4. A) KRAS exon 4 shifted melting curve for HCT116, Caco-2, RKO, DLD1, C32 SW480 and SW620. B) The difference plot for Kras exon 4 revealed that all cell lines were wt. for this exon*.
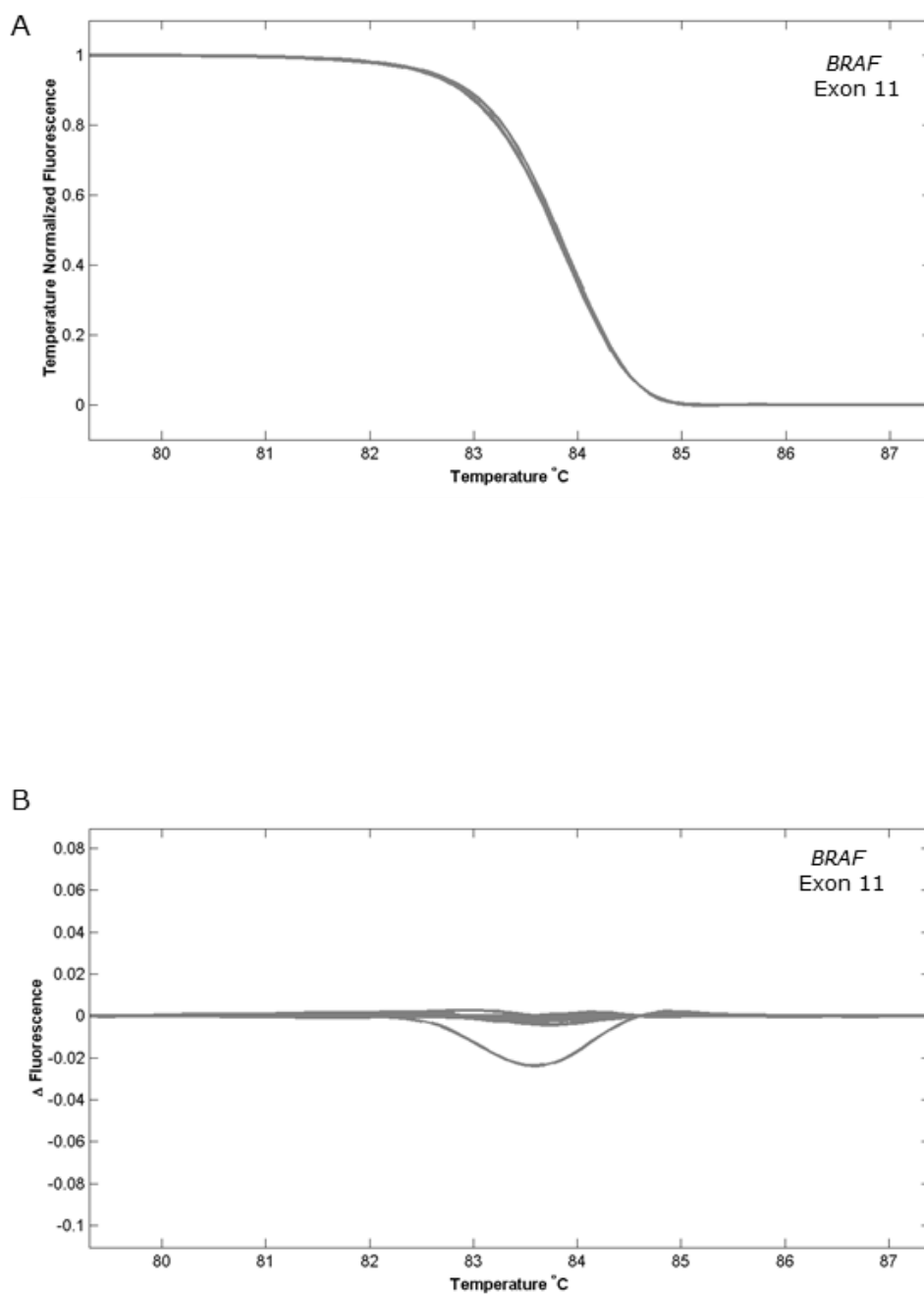
Figure 9-3: *The screening of CRC cell lines for a mutation in BRAF exon 11. A) BRAF exon 11 shifted melting curve for HCT116, Caco-2, RKO, DLD1, C32 SW480 and SW620. B) The difference plot for BRAF exon 11 revealed that all cell lines were wt. for this exon.*
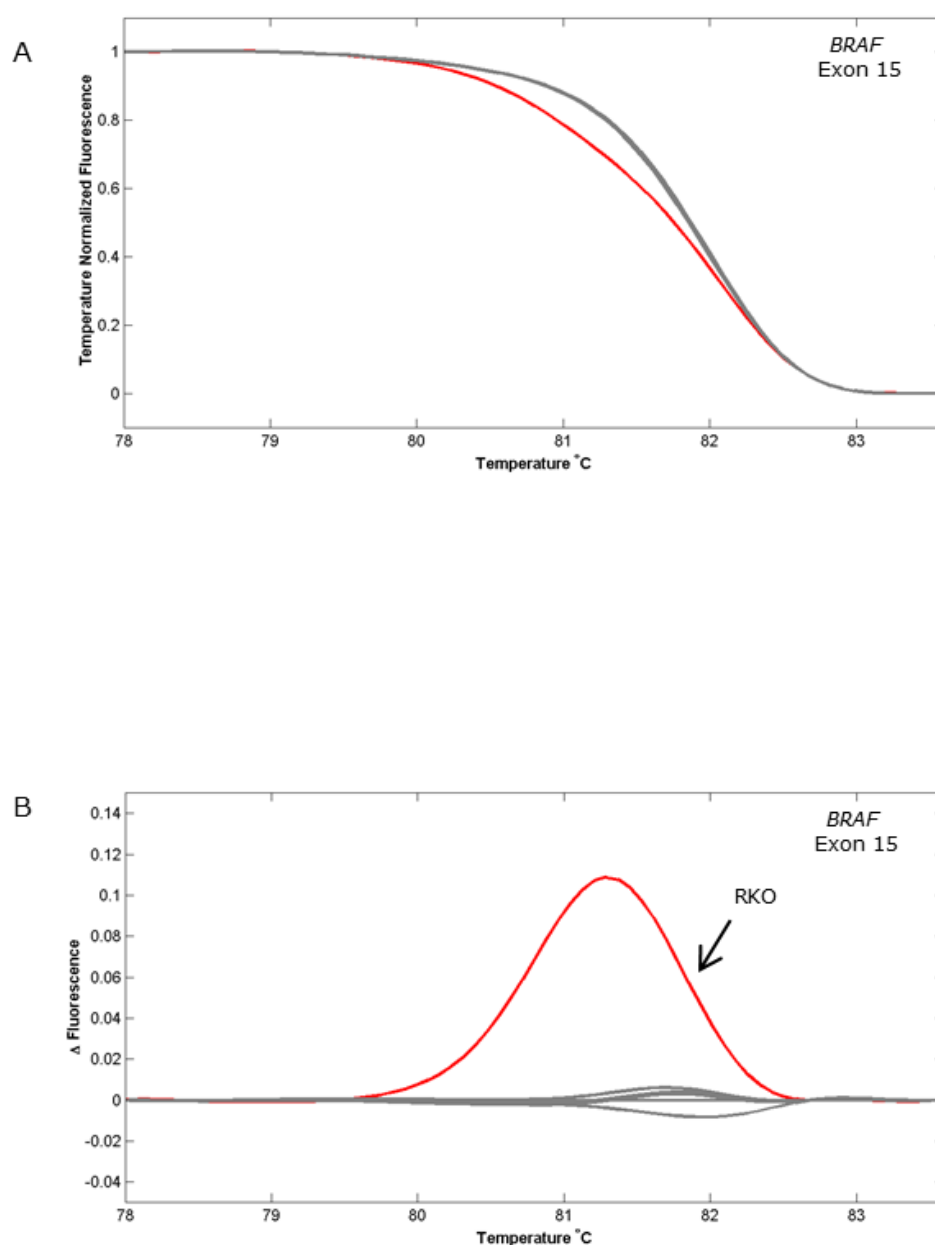
Figure 9-4: *The screening of CRC cell lines for a mutation in BRAF exon 15. A) BRAF exon 15 shifted melting curve for HCT116, Caco-2, RKO, DLD1, C32 SW480 and SW620. B) The difference plot for BRAF exon 15 revealed that only RKO displayed a mutation in this exon.*
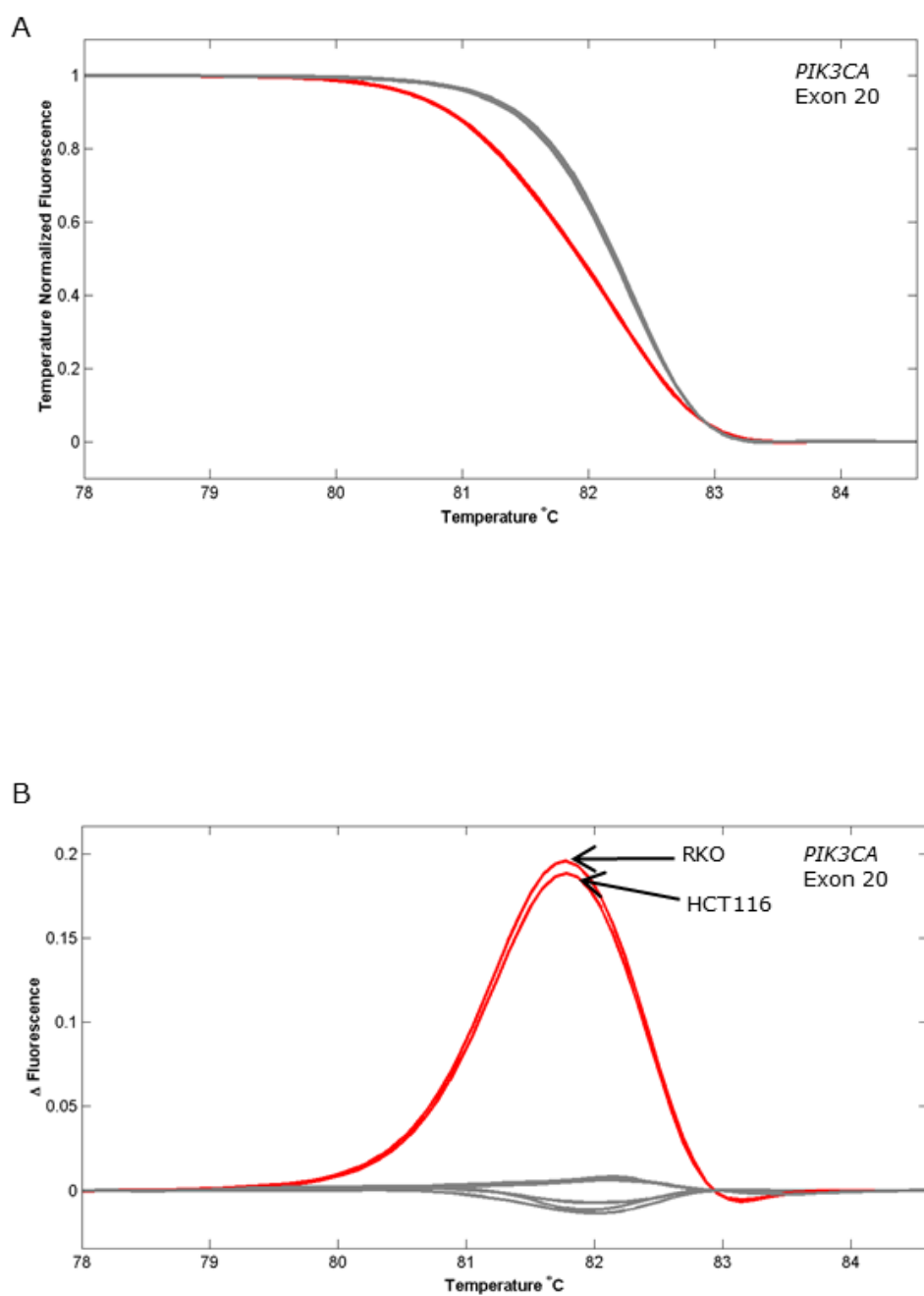
Figure 9-5: The screening of CRC cell lines for a mutation in PIK3CA exon 20. A) PIK3CA exon 20 shifted melting curve for HCT116, Caco-2, RKO, DLD1, C32 SW480 and SW620. B) The difference plot for PIK3CA exon 20 revealed that HCT116 and RKO displayed a mutation in this exon.
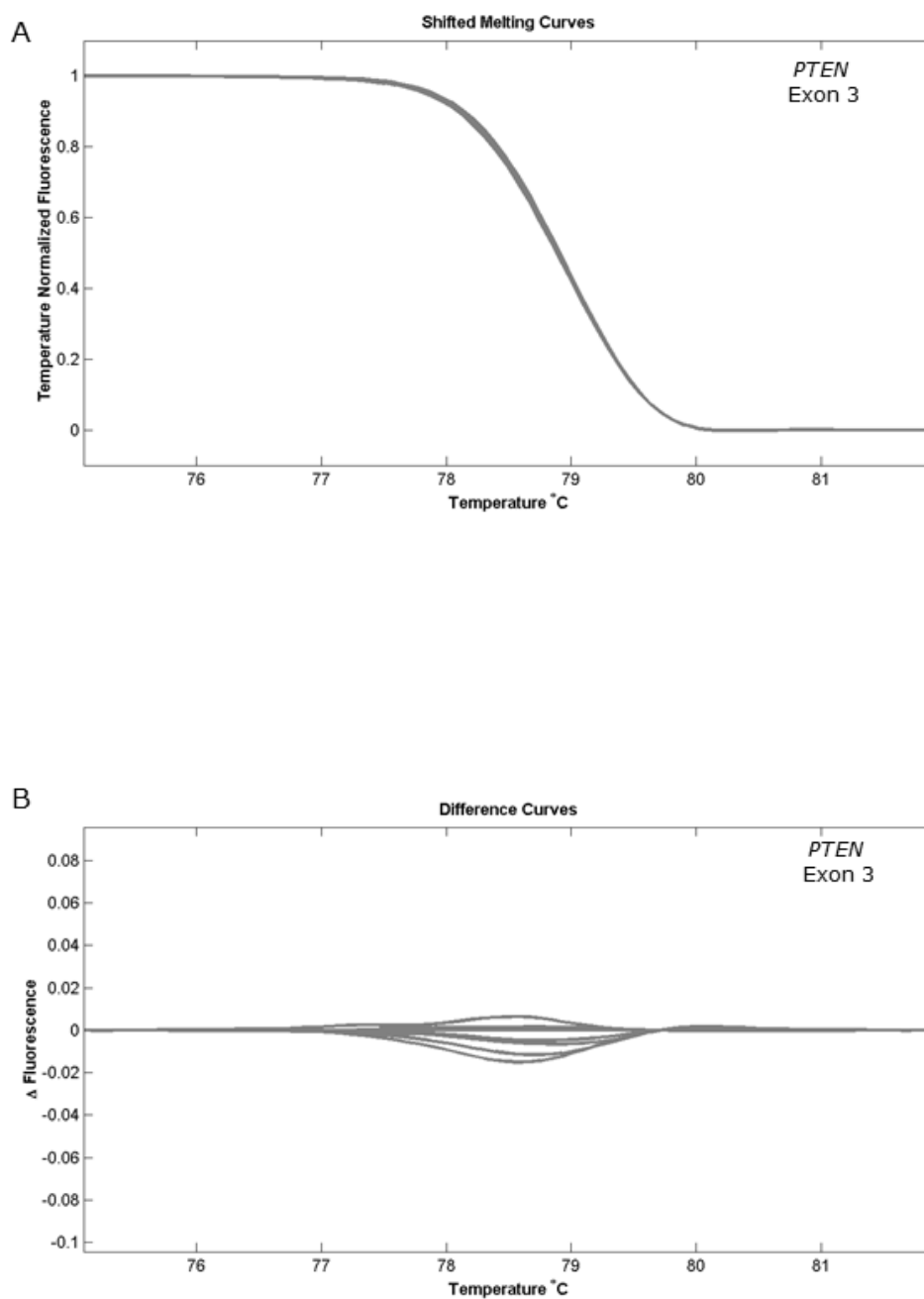
Figure 9-6: *The screening of CRC cell lines for a mutation in PTEN exon 3.*

A) PTEN exon 3 shifted melting curve for HCT116, Caco-2, RKO, DLD1, C32

SW480 and SW620. B) The difference plot for PTEN exon 3 revealed that

all cell lines were wt. for this exon.
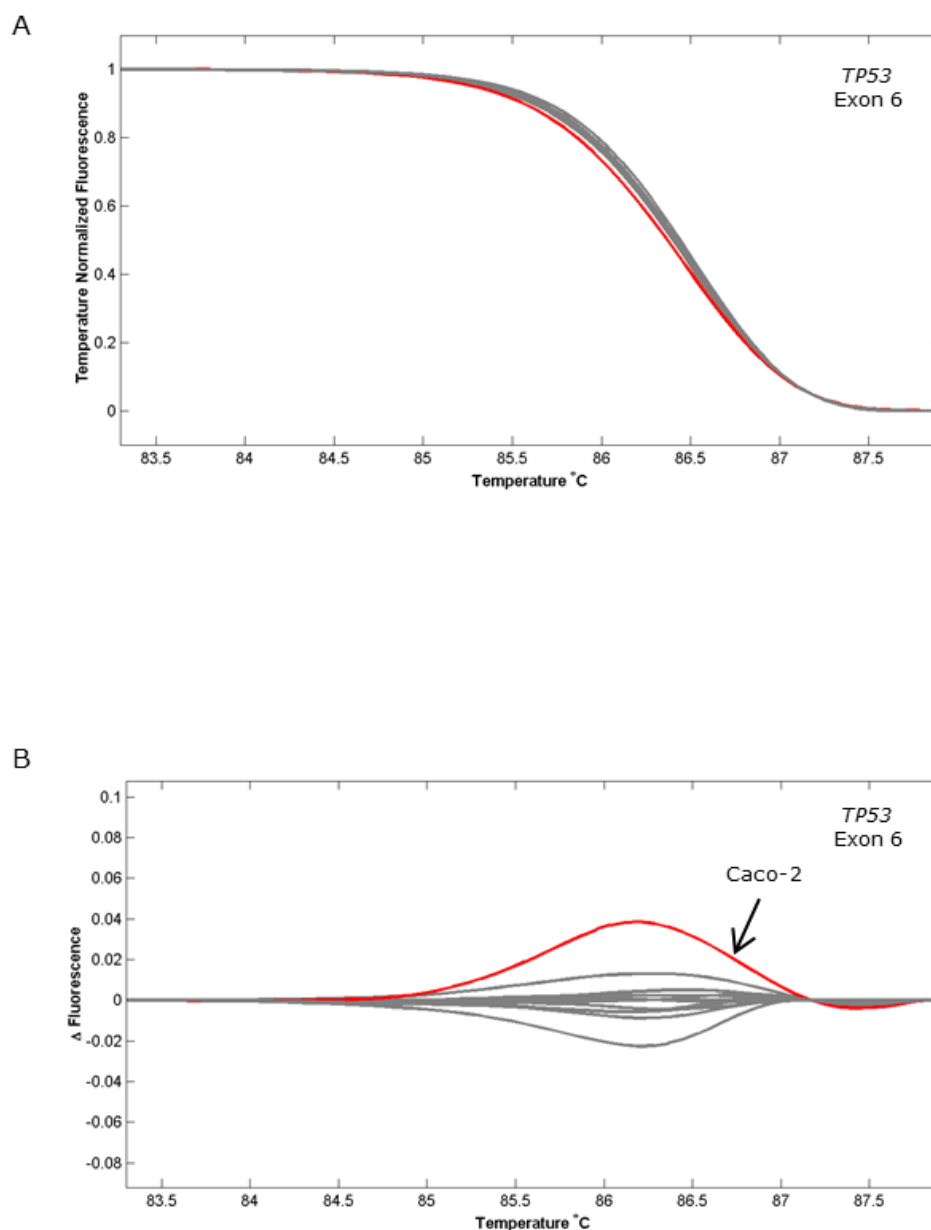
Figure 9-7*: The screening of CRC cell lines for a mutation in TP53 exon 6.*

A) TP53 exon 6 shifted melting curve for HCT116, Caco-2, RKO, DLD1, C32

SW480 and SW620. B) The difference plot for TP53 exon 6 revealed that

only Caco-2 displayed a mutation in this exon.

9.2   Expression profiling differentially expressed genes

Gene Symbol	Gene Title	p-value	Fold Change
C22orf34	chromosome 22 open reading frame 34	4.35E-11	2.374
RAB5A	RAB5A, member RAS oncogene family	3.40E-10	21.422
PRIM1	primase, DNA, polypeptide 1 (49kDa)	4.18E-10	5.570
TES	testis derived transcript (3 LIM domains)	9.95E-10	8.153
CLN6	ceroid-lipofuscinosis, neuronal 6, late infantile, variant	1.03E-09	-8.174
DEFB129	defensin, beta 129	1.24E-09	68.318
---	---	2.94E-09	2.562
SUPT6H	suppressor of Ty 6 homolog (S. cerevisiae)	3.46E-09	29.598
---	---	4.01E-09	118.962
DNAH6	dynein, axonemal, heavy chain 6	4.42E-09	-5.504
ZSCAN21	zinc finger and SCAN domain containing 21	5.32E-09	3.205
SCGB2A2	secretoglobin, family 2A, member 2	5.36E-09	9.788
KRT18	keratin 18	7.55E-09	2.273
LOC339874	hypothetical LOC339874	7.63E-09	-3.408
SFRS18	splicing factor, arginine/serine-rich 18	8.89E-09	25.165
---	---	1.19E-08	9.285
---	---	1.26E-08	12.298
ARPC1B	actin related protein 2/3 complex, subunit 1B, 41kDa	1.37E-08	-2.178
SLC28A2	solute carrier family 28 (sodium-coupled nucleoside transporter), member 2	1.59E-08	-10.350
NLGN4X	neuroligin 4, X-linked	1.93E-08	38.750
UBE2D4	ubiquitin-conjugating enzyme E2D 4 (putative)	2.25E-08	-2.924
CELA3A	chymotrypsin-like elastase family, member 3A	3.11E-08	-2.769
EPHA2	EPH receptor A2	4.16E-08	2.019
---	---	4.17E-08	6.399
TMEM160	transmembrane protein 160	5.10E-08	5.215
---	---	5.32E-08	-14.329
NCRNA00258	non-protein coding RNA 258	6.74E-08	6.485
ZBED5	zinc finger, BED-type containing 5	7.92E-08	-3.168

---	---	1.05E-07	11.726
ZNF765	zinc finger protein 765	1.13E-07	2.139
FLJ35946	hypothetical protein FLJ35946	1.16E-07	24.044
FLJ34208	hypothetical LOC401106	1.16E-07	4.360
---	---	1.23E-07	8.912
LCLAT1	lysocardiolipin acyltransferase 1	1.24E-07	6.586
RAB21	RAB21, member RAS oncogene family	1.26E-07	3.557
PLA2G2E	phospholipase A2, group IIE	1.30E-07	-3.577
C14orf34	chromosome 14 open reading frame 34	1.36E-07	4.186
TMEM87A	transmembrane protein 87A	1.81E-07	4.112
---	---	1.87E-07	-3.315
NEU2	sialidase 2 (cytosolic sialidase)	1.93E-07	9.327
ZNF765	zinc finger protein 765	2.01E-07	2.165
DDX50	DEAD (Asp-Glu-Ala-Asp) box polypeptide 50	2.04E-07	2.659
EPS15	epidermal growth factor receptor pathway substrate 15	2.17E-07	5.395
TAS2R13	taste receptor, type 2, member 13	2.44E-07	2.485
CELA3A	chymotrypsin-like elastase family, member 3A	2.67E-07	-2.713
MAGEA2 /// MAGEA2B	melanoma antigen family A, 2 /// melanoma antigen family A, 2B	2.93E-07	4.191
FEM1A	Fem-1 homolog a (C. elegans)	3.13E-07	7.610
FBXL18	F-box and leucine-rich repeat protein 18	3.82E-07	-3.716
TFCP2L1	transcription factor CP2-like 1	3.95E-07	-4.213
CEP170 /// CEP170P1	centrosomal protein 170kDa /// centrosomal protein 170kDa pseudogene 1	4.33E-07	6.329
MYO1B	myosin IB	4.52E-07	-3.088
NASP	Nuclear autoantigenic sperm protein (histone-binding)	4.60E-07	12.136
PAX5	paired box 5	4.75E-07	5.104
FAM82A1	family with sequence similarity 82, member A1	5.21E-07	-7.764
GTPBP3	GTP binding protein 3 (mitochondrial)	5.38E-07	2.744
---	---	5.53E-07	-3.813
GADD45GIP1	Growth arrest and DNA-damage-inducible, gamma interacting protein 1	5.73E-07	7.518
TFF2	trefoil factor 2	6.00E-07	-4.666

LOC643201	centrosomal protein 192kDa pseudogene	6.03E-07	6.335
PMS2P11	postmeiotic segregation increased 2 pseudogene 11	6.78E-07	-2.478
NCOA3	Nuclear receptor coactivator 3	7.12E-07	-3.695
THOC4	THO complex 4	7.35E-07	-3.276
---	---	7.38E-07	-2.178
RNF17	ring finger protein 17	7.38E-07	2.476
---	---	7.77E-07	14.907
RPA1	replication protein A1, 70kDa	8.16E-07	2.847
---	---	8.87E-07	13.318
GAL3ST3	galactose-3-O-sulfotransferase 3	9.13E-07	2.129
---	---	9.14E-07	-2.640
SRSF1	serine/arginine-rich splicing factor 1	9.38E-07	2.722
---	---	9.88E-07	8.608
GNG12	guanine nucleotide binding protein (G protein), gamma 12	9.94E-07	2.473
TMBIM6	transmembrane BAX inhibitor motif containing 6	1.05E-06	2.183
RPS16	ribosomal protein S16	1.11E-06	2.006
KIAA2026	KIAA2026	1.21E-06	-3.618
PRSS33	protease, serine, 33	1.22E-06	-4.053
GAP43	growth associated protein 43	1.25E-06	-10.945
PHC3	polyhomeotic homolog 3 (Drosophila)	1.27E-06	9.117
---	---	1.28E-06	2.231
DNAJC15	DnaJ (Hsp40) homolog, subfamily C, member 15	1.28E-06	5.638
MTHFR	methylenetetrahydrofolate reductase (NAD(P)H)	1.30E-06	14.212
C1orf105	chromosome 1 open reading frame 105	1.32E-06	-3.050
TPMT	thiopurine S-methyltransferase	1.33E-06	3.419
CCDC90B	coiled-coil domain containing 90B	1.43E-06	2.386
---	---	1.55E-06	3.916
SLMAP	sarcolemma associated protein	1.58E-06	11.044
YY1	YY1 transcription factor	1.60E-06	2.444
ALG14	Asparagine-linked glycosylation 14 homolog (S. cerevisiae)	1.74E-06	3.219
TPTE2P1	Transmembrane phosphoinositide 3-phosphatase and tensin homolog 2 pseudogene 1	1.84E-06	6.784

ALDH1A2	aldehyde dehydrogenase 1 family, member A2	1.94E-06	5.289
---	---	2.04E-06	-4.884
---	---	2.12E-06	-10.500
ACOT9	acyl-CoA thioesterase 9	2.19E-06	2.583
OR2H2	olfactory receptor, family 2, subfamily H, member 2	2.24E-06	-2.888
CBWD1 /// CBWD2 /// CBWD3 /// CBWD5 /// CBWD6 /// CBWD7 /// LOC100507355	COBW domain containing 1 /// COBW domain containing 2 /// COBW domain containing 3 ///	2.27E-06	2.035
NOSTRIN	nitric oxide synthase trafficker	2.30E-06	-11.442
---	---	2.41E-06	3.819
HERPUD1	homocysteine-inducible, endoplasmic reticulum stress-inducible, ubiquitin-like domain m	2.66E-06	2.238
TROVE2	TROVE domain family, member 2	2.67E-06	2.384
PTPRN2	protein tyrosine phosphatase, receptor type, N polypeptide 2	2.72E-06	2.471
MND1	meiotic nuclear divisions 1 homolog (S. cerevisiae)	2.78E-06	3.085
ZNF548	zinc finger protein 548	2.92E-06	-3.106
LMBRD1	LMBR1 domain containing 1	2.94E-06	2.770
KIR3DL1 /// KIR3DL2 /// LOC727787	killer cell immunoglobulin-like receptor, three domains, long cytoplasmic tail, 1 /// k	3.04E-06	-2.763
ANKRD17	ankyrin repeat domain 17	3.19E-06	2.797
LOC100287483	transcription elongation factor B (SIII), polypeptide 1 pseudogene	3.33E-06	2.533
FBXL5	F-box and leucine-rich repeat protein 5	3.44E-06	2.231
GMPS	guanine monphosphate synthetase	3.52E-06	2.614
SRP54	signal recognition particle 54kDa	3.54E-06	2.474
ARMC10	armadillo repeat containing 10	3.86E-06	-2.039
NGFRAP1	nerve growth factor receptor (TNFRSF16) associated protein 1	4.05E-06	2.153
KIR3DL1 /// KIR3DL2 /// LOC727787	killer cell immunoglobulin-like receptor, three domains, long cytoplasmic tail, 1 /// k	4.33E-06	-5.783
EDA2R	ectodysplasin A2 receptor	4.36E-06	3.104

H2AFJ	H2A histone family, member J	4.39E-06	-2.582
TM9SF4	transmembrane 9 superfamily protein member 4	4.53E-06	-8.039
MAP4K5	mitogen-activated protein kinase kinase kinase kinase 5	4.58E-06	6.896
NCLN	nicalin	4.62E-06	-2.472
ECH1	enoyl CoA hydratase 1, peroxisomal	4.75E-06	3.107
UBE2D4	ubiquitin-conjugating enzyme E2D 4 (putative)	5.22E-06	-3.398
XPO7	exportin 7	5.35E-06	-2.086
FBXL18	F-box and leucine-rich repeat protein 18	5.38E-06	-3.921
RYK	RYK receptor-like tyrosine kinase	5.41E-06	2.405
PALM2	paralemmin 2	5.88E-06	3.341
---	---	6.02E-06	-2.177
APBB2	amyloid beta (A4) precursor protein-binding, family B, member 2	6.11E-06	-2.421
DNAJC22	DnaJ (Hsp40) homolog, subfamily C, member 22	6.41E-06	-4.169
MTERFD2	MTERF domain containing 2	6.65E-06	-2.419
---	---	6.81E-06	2.304
LARP6	La ribonucleoprotein domain family, member 6	7.10E-06	4.506
CENPT	centromere protein T	7.60E-06	-4.572
NUFIP2	nuclear fragile X mental retardation protein interacting protein 2	7.61E-06	2.085
LOC100505818 /// MLLT4	afadin-like /// myeloid/lymphoid or mixed-lineage leukemia (trithorax homolog, Drosophi	7.72E-06	-3.031
SPOP	speckle-type POZ protein	7.88E-06	2.190
SMARCA4	SWI/SNF related, matrix associated, actin dependent regulator of chromatin, subfamily a	8.07E-06	2.068
---	---	8.34E-06	8.072
IGFBP7	insulin-like growth factor binding protein 7	8.54E-06	13.298
KLK2	kallikrein-related peptidase 2	8.93E-06	-2.952
SPAG11A	sperm associated antigen 11A	9.15E-06	-2.328
SP110	SP110 nuclear body protein	9.24E-06	-2.424
C21orf89	chromosome 21 open reading frame 89	9.89E-06	-2.299
QDPR	quinoid dihydropteridine reductase	9.93E-06	-2.601

ZMYND8	zinc finger, MYND-type containing 8	1.06E-05	6.175
C16orf79	chromosome 16 open reading frame 79	1.07E-05	-2.228
C14orf164	chromosome 14 open reading frame 164	1.10E-05	-2.164
TSC2	tuberous sclerosis 2	1.33E-05	-2.328
LSG1	large subunit GTPase 1 homolog (S. cerevisiae)	1.35E-05	3.079
---	---	1.45E-05	-2.357
---	---	1.49E-05	2.199
GFM1	G elongation factor, mitochondrial 1	1.51E-05	2.143
SEMA5B	sema domain, seven thrombospondin repeats (type 1 and type 1-like), transmembrane domai	1.74E-05	2.410
FTH1	ferritin, heavy polypeptide 1	1.75E-05	3.073
CLIP4	CAP-GLY domain containing linker protein family, member 4	1.75E-05	2.562
NR1I2	nuclear receptor subfamily 1, group I, member 2	1.80E-05	5.177
SLC2A11	solute carrier family 2 (facilitated glucose transporter), member 11	1.85E-05	3.049
EPS8L2	EPS8-like 2	1.85E-05	2.403
COPB1	coatomer protein complex, subunit beta 1	1.85E-05	2.112
MFAP3	microfibrillar-associated protein 3	1.92E-05	7.246
CKAP4	cytoskeleton-associated protein 4	2.15E-05	8.351
GLG1	golgi glycoprotein 1	2.17E-05	2.350
---	---	2.18E-05	-3.227
LRIG2	leucine-rich repeats and immunoglobulin-like domains 2	2.18E-05	2.776
---	---	2.19E-05	-2.684
SEC63	SEC63 homolog (S. cerevisiae)	2.34E-05	2.068
PSMD13	proteasome (prosome, macropain) 26S subunit, non-ATPase, 13	2.46E-05	2.250
UQCC	ubiquinol-cytochrome c reductase complex chaperone	2.71E-05	2.554
GDEP	gene differentially expressed in prostate	2.73E-05	2.882
---	---	2.76E-05	4.854
OTUB1	OTU domain, ubiquitin aldehyde binding 1	2.77E-05	2.399
OR13C4	olfactory receptor, family 13,	2.92E-05	6.896

	subfamily C, member 4		
CEACAM21	carcinoembryonic antigen-related cell adhesion molecule 21	3.10E-05	2.519
---	---	3.13E-05	2.408
KIR3DL1 /// KIR3DL2 /// LOC727787	killer cell immunoglobulin-like receptor, three domains, long cytoplasmic tail, 1 /// k	3.13E-05	-7.372
RASA4 /// RASA4P	RAS p21 protein activator 4 /// RAS p21 protein activator 4 pseudogene	3.14E-05	2.991
CTBP1	C-terminal binding protein 1	3.17E-05	3.814
LUC7L3	LUC7-like 3 (S. cerevisiae)	3.49E-05	2.047
EGR1	early growth response 1	3.58E-05	2.576
H2AFJ	H2A histone family, member J	3.74E-05	-3.366
SP110	SP110 nuclear body protein	3.75E-05	-2.737
RBM15	RNA binding motif protein 15	3.81E-05	3.104
---	---	3.95E-05	-2.796
LOC645249	hypothetical LOC645249	4.10E-05	3.289
CREB3L1	cAMP responsive element binding protein 3-like 1	4.19E-05	6.062
NDUFAF2	NADH dehydrogenase (ubiquinone) 1 alpha subcomplex, assembly factor 2	4.37E-05	2.012
GPCPD1	glycerophosphocholine phosphodiesterase GDE1 homolog (S. cerevisiae)	4.39E-05	-2.659
LSM4	LSM4 homolog, U6 small nuclear RNA associated (S. cerevisiae)	4.41E-05	-3.239
SLC12A4	Solute carrier family 12 (potassium/chloride transporters), member 4	4.53E-05	2.423
---	---	4.57E-05	6.686
GMIP	GEM interacting protein	4.58E-05	-2.063
SCRT1	scratch homolog 1, zinc finger protein (Drosophila)	4.84E-05	-12.317
RRN3	RRN3 RNA polymerase I transcription factor homolog (S. cerevisiae)	4.95E-05	3.195
CSNK1E	casein kinase 1, epsilon	5.14E-05	2.044
ARCN1	archain 1	5.21E-05	-2.117
PKD1L2	polycystic kidney disease 1-like 2	5.30E-05	-3.142
FAM92A1	family with sequence similarity 92, member A1	5.30E-05	2.759
ADAM29	ADAM metallopeptidase domain 29	5.49E-05	-2.207
CTAGE9	CTAGE family, member 9	5.71E-05	3.431
GOLGA2	golgin A2	5.75E-05	2.755

FAM71B	family with sequence similarity 71, member B	6.12E-05	-2.449
NAP1L5	nucleosome assembly protein 1-like 5	6.37E-05	2.115
---	---	6.49E-05	-3.195
MARCKS	myristoylated alanine-rich protein kinase C substrate	6.49E-05	-3.580
GNRHR	gonadotropin-releasing hormone receptor	7.10E-05	5.110
PIGX	phosphatidylinositol glycan anchor biosynthesis, class X	7.36E-05	-2.467
TSNARE1	t-SNARE domain containing 1	7.60E-05	-2.186
C20orf196	chromosome 20 open reading frame 196	8.32E-05	2.255
NSA2	NSA2 ribosome biogenesis homolog (S. cerevisiae)	8.61E-05	-2.329
TOMM20	translocase of outer mitochondrial membrane 20 homolog (yeast)	8.90E-05	2.225
TBP	TATA box binding protein	9.05E-05	-2.444
ADPRHL1	ADP-ribosylhydrolase like 1	9.20E-05	4.751
C17orf58	chromosome 17 open reading frame 58	9.42E-05	2.006
BDNF	brain-derived neurotrophic factor	9.64E-05	2.753
CTDSP2	CTD (carboxy-terminal domain, RNA polymerase II, polypeptide A) small phosphatase 2	9.78E-05	3.262
LOC100129722	hypothetical LOC100129722	9.84E-05	-2.505
C4orf35	chromosome 4 open reading frame 35	9.85E-05	-3.404
PURA	purine-rich element binding protein A	0.000107159	2.300
SH2B3	SH2B adaptor protein 3	0.000107947	-3.737
FBXO27	F-box protein 27	0.000108663	-3.671
LOC100506165	hypothetical LOC100506165	0.000109983	2.096
LOC284912	hypothetical LOC284912	0.000110913	-2.500
LOC100128176	hypothetical protein LOC100128176	0.000111603	-3.383
CC2D2A	coiled-coil and C2 domain containing 2A	0.000116392	-5.802
TACO1	translational activator of mitochondrially encoded cytochrome c oxidase I	0.000118597	-2.425
SHMT2	serine hydroxymethyltransferase 2 (mitochondrial)	0.000123585	-2.118
CWF19L1	CWF19-like 1, cell cycle control (S. pombe)	0.000125018	2.172
RCN1	reticulocalbin 1, EF-hand	0.000126642	-2.348

	calcium binding domain		
LOC10013431 7 /// LOC284412	hypothetical LOC100134317 /// hypothetical LOC284412	0.000131332	4.616
SRCAP	Snf2-related CREBBP activator protein	0.000132105	-2.000
DDX3Y	DEAD (Asp-Glu-Ala-Asp) box polypeptide 3, Y-linked	0.000137696	2.419
---	---	0.00014098	-2.423
SLC46A2	solute carrier family 46, member 2	0.000147631	-2.872
C14orf37	chromosome 14 open reading frame 37	0.000147986	2.459
DEFB124	defensin, beta 124	0.000148694	-2.892
LOC10028874 5	Hypothetical protein LOC100288745	0.00015408	2.081
OCLN	occludin	0.00015546	2.488
QKI	quaking homolog, KH domain RNA binding (mouse)	0.00015596	4.612
---	---	0.000162306	-3.623
---	---	0.000171998	-5.014
UBE2R2	ubiquitin-conjugating enzyme E2R 2	0.000173081	2.065
---	---	0.000177242	2.435
---	---	0.000179871	-5.256
---	---	0.000181685	2.772
PPP2R5A	protein phosphatase 2, regulatory subunit B', alpha	0.000186861	-2.051
KIR3DL1 /// KIR3DL2 /// LOC727787	killer cell immunoglobulin-like receptor, three domains, long cytoplasmic tail, 1 /// k	0.000191051	-2.355
---	---	0.000193299	4.419
PAK2	p21 protein (Cdc42/Rac)-activated kinase 2	0.00019359	2.018
BCOR	BCL6 corepressor	0.00019647	-2.785
C15orf39	chromosome 15 open reading frame 39	0.000210463	2.515
LOC10012807 9	Hypothetical protein LOC100128079	0.000214814	2.509
KLHL11	kelch-like 11 (Drosophila)	0.000215484	-2.558
INO80D	INO80 complex subunit D	0.00022435	2.043
---	---	0.000229555	2.128
GGCX	gamma-glutamyl carboxylase	0.000237888	2.319
---	---	0.000242838	2.793
ADCY1	adenylate cyclase 1 (brain)	0.000245995	6.734
SERPINE1	serpin peptidase inhibitor, clade E (nexin, plasminogen activator inhibitor type 1), me	0.000248086	-3.108

CLEC4C	C-type lectin domain family 4, member C	0.000248142	2.957
MTA2	metastasis associated 1 family, member 2	0.000251756	3.008
BMPR1A	bone morphogenetic protein receptor, type IA	0.000254652	2.436
---	---	0.000261217	-4.574
---	---	0.000262724	-5.285
PLIN5	perilipin 5	0.000264111	2.662
ARHGAP17	Rho GTPase activating protein 17	0.00026494	2.566
PHF7	PHD finger protein 7	0.000265994	-2.032
CD46	CD46 molecule, complement regulatory protein	0.000270348	3.292
---	---	0.000271464	4.144
---	---	0.000271715	5.383
TAPBP	TAP binding protein (tapasin)	0.000272708	-3.048
NADSYN1	NAD synthetase 1	0.000292395	2.218
FARP1	FERM, RhoGEF (ARHGEF) and pleckstrin domain protein 1 (chondrocyte-derived)	0.000296812	-2.004
APOOL	apolipoprotein O-like	0.000301929	2.298
NUP98	nucleoporin 98kDa	0.000303371	-3.119
PLA2G16	phospholipase A2, group XVI	0.000305549	3.218
FLVCR2	feline leukemia virus subgroup C cellular receptor family, member 2	0.00030773	-2.305
TRAF1	TNF receptor-associated factor 1	0.000320281	4.833
RDX	radixin	0.000334686	-2.856
TGM5	transglutaminase 5	0.000337534	-3.568
ASB2	ankyrin repeat and SOCS box-containing 2	0.00033841	2.519
---	---	0.000355112	-2.276
---	---	0.000356235	2.799
---	---	0.000356931	-2.365
---	---	0.000364586	-2.101
B4GALT5	UDP-Gal:betaGlcNAc beta 1,4- galactosyltransferase, polypeptide 5	0.000369749	2.134
RMND5A	required for meiotic nuclear division 5 homolog A (S. cerevisiae)	0.000378958	2.659
LOC100129427	hypothetical LOC100129427	0.000383709	-2.105
SSFA2	Sperm specific antigen 2	0.000385409	3.132
---	---	0.000386526	2.832
---	---	0.000386536	6.528
KCNS2	potassium voltage-gated	0.0003891	2.594

	channel, delayed-rectifier, subfamily S, member 2		
RNASEH1	Ribonuclease H1	0.000394355	3.045
---	---	0.000405817	3.097
LOC338667	hypothetical protein LOC338667	0.000406379	-3.310
C10orf81	chromosome 10 open reading frame 81	0.000415318	2.420
APP	amyloid beta (A4) precursor protein	0.000423078	2.460
TTLL11	tubulin tyrosine ligase-like family, member 11	0.000424228	6.688
AXL	AXL receptor tyrosine kinase	0.000436862	-2.284
---	---	0.000446108	2.493
ADD3	adducin 3 (gamma)	0.000451926	2.301
GOSR2	golgi SNAP receptor complex member 2	0.000476196	2.273
DLX4	distal-less homeobox 4	0.000477819	2.428
NSMAF	neutral sphingomyelinase (N-SMase) activation associated factor	0.0004811	-2.627
---	---	0.000484486	4.576
---	---	0.000485678	2.126
YEATS2	YEATS domain containing 2	0.00049167	2.741
---	---	0.00049388	-6.065
---	---	0.000501764	-6.352
BSND	Bartter syndrome, infantile, with sensorineural deafness (Barttin)	0.000506114	2.031
---	---	0.000506279	2.102
C1orf156	chromosome 1 open reading frame 156	0.000506612	2.439
FAM9C	family with sequence similarity 9, member C	0.000518259	-2.045
CNKSR3	CNKSR family member 3	0.000523468	2.394
ARMC8	armadillo repeat containing 8	0.000533413	-2.274
CAPZA1	capping protein (actin filament) muscle Z-line, alpha 1	0.000535909	2.168
---	---	0.000536198	-2.038
STX16	syntaxin 16	0.000536339	-3.289
ALKBH7	alkB, alkylation repair homolog 7 (E. coli)	0.000570776	2.938
---	---	0.000575586	2.030
---	---	0.000579974	2.108
TMEM17	transmembrane protein 17	0.000584939	3.231
SFRP4	secreted frizzled-related protein 4	0.000585799	2.182
ERO1L	ERO1-like (S. cerevisiae)	0.000589523	2.267
---	---	0.000594597	3.983

KDM5A	lysine (K)-specific demethylase 5A	0.000596193	-2.043
SPRED1	sprouty-related, EVH1 domain containing 1	0.000601675	-2.110
RHOB	ras homolog gene family, member B	0.000617572	2.077
SULF2	sulfatase 2	0.000620825	-3.417
MSI2	musashi homolog 2 (Drosophila)	0.00062601	2.266
---	---	0.000632733	-2.301
VRK3	vaccinia related kinase 3	0.00063838	-2.986
TMEM128	transmembrane protein 128	0.00064248	3.164
FBXO33	F-box protein 33	0.000661169	2.390
LPAR3	lysophosphatidic acid receptor 3	0.000665671	2.278
VWA3A	von Willebrand factor A domain containing 3A	0.00067169	2.655
LIMK2	LIM domain kinase 2	0.0006739	2.193
NOVA2	neuro-oncological ventral antigen 2	0.000674307	-2.525
MGC45922	hypothetical LOC284365	0.000683045	2.551

Table 9-2: *Differentially expressed genes HCT116 Cten vs. empty vector. Microarray gene expression profiling differentially expressed genes between Cten and empty vector transfected HCT116 cells (>2-fold, p<0.05).*

Gene Symbol	Gene Title	p	Fold Change
NLGN4X	neuroligin 4, X-linked	1.62E-07	-20.508
THOC4	THO complex 4	1.07E-06	3.144
ZSCAN21	zinc finger and SCAN domain containing 21	1.50E-06	-2.009
KIAA2026	KIAA2026	2.40E-06	3.334
GADD45GIP1	Growth arrest and DNA-damage-inducible, gamma interacting protein 1	3.25E-06	-5.531
GTPBP3	GTP binding protein 3 (mitochondrial)	4.76E-06	-2.269
PLA2G2E	phospholipase A2, group IIE	7.02E-06	2.396
MYO1B	myosin IB	7.14E-06	2.376

Table 9-3: *Differentially expressed genes HCT116 NLS-Cten vs. Cten.*

Microarray gene expression profiling differentially expressed genes

between NLS-Cten and Cten transfected HCT116 cells (>2-fold, p<0.05).

Gene Symbol	Gene Title	P	Fold Change
FHAD1	forkhead-associated (FHA) phosphopeptide binding domain 1	1.19E-08	-2.214
C14orf34	chromosome 14 open reading frame 34	2.86E-08	5.160
LARP6	La ribonucleoprotein domain family, member 6	4.66E-08	11.160
SLC28A2	solute carrier family 28 (sodium-coupled nucleoside transporter), member 2	5.62E-08	-8.070
TES	testis derived transcript (3 LIM domains)	1.49E-07	3.846
SCGB2A2	secretoglobin, family 2A, member 2	1.82E-07	5.281
---	---	2.13E-07	28.527
DEFB129	defensin, beta 129	2.31E-07	14.228
PRIM1	primase, DNA, polypeptide 1 (49kDa)	3.00E-07	2.609
SUPT6H	suppressor of Ty 6 homolog (S. cerevisiae)	6.21E-07	8.363
---	---	7.35E-07	-8.105
RAP1A	RAP1A, member of RAS oncogene family	1.00E-06	-2.947
HPDL	4-hydroxyphenylpyruvate dioxygenase-like	1.08E-06	-2.106
NLGN4X	neuroligin 4, X-linked	1.11E-06	12.506
PLA2G2E	phospholipase A2, group IIE	1.31E-06	-2.798
---	---	2.75E-06	3.863
RAB5A	RAB5A, member RAS oncogene family	3.15E-06	3.843
CLN6	ceroid-lipofuscinosis, neuronal 6, late infantile, variant	3.48E-06	-2.733
---	---	8.07E-06	5.116
---	---	9.08E-06	-2.778
---	---	1.18E-05	4.118
---	---	1.52E-05	-3.671
CEP170 /// CEP170P1	centrosomal protein 170kDa /// centrosomal protein 170kDa pseudogene 1	2.36E-05	3.487
NEU2	sialidase 2 (cytosolic sialidase)	2.46E-05	4.042
GAP43	growth associated protein 43	2.50E-05	-5.918
---	---	2.68E-05	-7.723
TSPAN5	tetraspanin 5	3.35E-05	-2.076
PRKCH	protein kinase C, eta	3.52E-05	-6.306
FLJ34208	hypothetical LOC401106	3.77E-05	2.318
HAVCR2	hepatitis A virus cellular receptor 2	3.78E-05	-2.006
SLC46A2	solute carrier family 46, member 2	4.76E-05	-3.305

Table 9-4*: Differentially expressed genes RKO Cten vs. empty vector. Microarray gene expression profiling differentially expressed genes between Cten and empty vector transfected RKO cells (>2-fold, p<0.05).*

Gene Symbol	Gene Title	P	Fold Change
NLGN4X	neuroligin 4, X-linked	2.13E-06	-10.7276
---	---	2.21E-06	-2.00805

Table 9-5: *Differentially expressed genes RKO NLS-Cten vs. Cten. Microarray gene expression profiling differentially expressed genes between NLS-Cten and Cten transfected RKO cells (>2-fold, p<0.05).*

Gene Symbol	Gene Title	HCT116 Fold Change	RKO Fold Change
C14orf34	chromosome 14 open reading frame 34	4.18565	5.19592
LARP6	La ribonucleoprotein domain family, member 6	4.50633	11.1601
SLC28A2	solute carrier family 28 (sodium-coupled nucleoside transporter), member 2	-10.3504	-8.0695
TES	testis derived transcript (3 LIM domains)	8.15302	3.84614
SCGB2A2	secretoglobin, family 2A, member 2	9.78797	5.2816
---	---	118.962	28.5269
DEFB129	defensin, beta 129	68.3176	14.2278
PRIM1	primase, DNA, polypeptide 1 (49kDa)	5.56956	2.60943
SUPT6H	suppressor of Ty 6 homolog (S. cerevisiae)	29.598	8.36304
---	---	-14.3285	-8.1051
NLGN4X	neuroligin 4, X-linked	38.7495	12.5056
PLA2G2E	phospholipase A2, group IIE	-3.57728	-2.79833
---	---	9.28453	3.8633
RAB5A	RAB5A, member RAS oncogene family	21.4215	3.84287
CLN6	ceroid-lipofuscinosis, neuronal 6, late infantile, variant	-8.17389	-2.7334
---	---	11.7262	5.11592
---	---	-3.81319	-2.7779
---	---	8.91223	4.11794
---	---	-4.88433	-3.67067
CEP170 /// CEP170P1	centrosomal protein 170kDa /// centrosomal protein 170kDa pseudogene 1	6.3291	3.4868
NEU2	sialidase 2 (cytosolic sialidase)	9.32727	4.0423
GAP43	growth associated protein 43	-10.9453	-5.91768
---	---	-5.25649	-7.72255
FLJ34208	hypothetical LOC401106	4.36028	2.31831
SLC46A2	solute carrier family 46, member 2	-2.87195	-3.30508

Table 9-6*: Differentially expressed genes in HCT116 and RKO. Microarray gene expression profiling differentially expressed genes between Cten and empty vector transfected cells common to both HCT116 and RKO (>2-fold, p<0.05).*